Physical and Mathematical Aspects of Solute Transport in Continuous Arterio-Venous Hemodiafiltration

fysische en mathematische aspecten van solute transport
in continue arterio-veneuze hemodiafiltratie

(with a summary in Dutch)

PROEFSCHRIFT

Ter verkrijging van de graad van Doctor aan
de Erasmus Universiteit Rotterdam op gezag van
de Rector Magnificus

Prof. Dr P.W.C. Akkermans M.A.

en volgens het besluit van het College voor Promoties.
De openbare verdediging zal plaatsvinden op
woensdag 26 maart 1997 om 11.45 uur.

door

Emin Akçahüseyin

geboren te Burdur-Güney, Turkije

PROMOTIECOMMISIE

Promotor : Prof. Dr. M.A.D.H. Schalekamp

Overige leden : Prof. Dr. Ir. C. Ince
Prof. Dr. R.M. Heethaar
Prof. Dr. W. Weimar
Dr. Ir. W.A. van Duyl (tevens co-promotor)

to my parents and children

CONTENTS   page

INTRODUCTION TO CONTINUOUS ARTERIO-VENOUS HEMODIAFILTRATION (CAVHD)

1.1 INTRODUCTION

The kidney is an organ of vital importance in the human body. Its main function is to maintain and regulate the composition of solutes in the blood plasma, and indirectly also that of the interstitial and intracellular fluid.

A total loss of the kidney function within hours or days is called acute renal failure (ARF), which often results from sepsis, a clinical syndrome accompanied also by massive edema, circulatory insufficiency, respiratory failure and sometimes neurological damage [1,2]. Acute renal failure and the associated water overload are common problems in critically ill patients and contribute significantly to mortality. It may be secondary to among other things such as hypotension, hypovolemia, trauma, drugs and disseminated intravascular coagulation. It may occur also in patients with multiple-organ failure. The resultant inability to remove toxic metabolites or to correct acid-base and electrolyte abnormalities is commonly associated with a fluid overload, with or without pulmonary edema, and an increase in interstitial water with a consequent reduction in tissue perfusion. Such patients are often hemodynamically unstable and characterized by a high catabolic rate [3,4]. The combination of low or unstable blood pressure and edema makes it quite difficult to judge how much fluid should be withdrawn safely [4]. Therefore, they need intensive dialysis and ultrafiltration treatment. However, the combination of ultrafiltration and intermittent hemodialysis (IHD) frequently leads to hypotension and neurological deterioration and may further jeopardize kidney function [5]. Furthermore, rapid correction of the acidosis together with the rise of inflammatory mediators that result from the blood-membrane interaction may aggravate respiratory failure [6-11]. Consequently, in many patients with ARF 'conventional' form of hemodialysis and ultrafiltration techniques was contraindicated. Therefore, to treat patients with such complicated ARF a different form of dialysis therapy was needed with the following attributes [3,12,13]:

- efficient removal of toxic metabolites presumably responsible for the uremic syndrome,
- correction of the patient's electrolyte abnormalities such as sodium for the treatment or prevention of hypotension and potassium for the treatment or prevention of hyperkalemia,
- correction of acid-base status by administering buffer-anions to control metabolic acidosis,

- correction of patient's fluid balance by removing the excess body water and replacing the ultra filtrate with a clean substitution fluid,
- the ability freely to administer the parenteral nutrition and other hyper alimentation solutions,
- the ability to start the treatment anytime,
- gradual treatment so as to avoid sudden disturbances in the delicate equilibrium and fluid status of the patient.

During the last decade, on considering these attributes, impressive advances have been made for the treatment of such complicated ARF in critically ill patients. This has led to the increased use of continuous renal replacement techniques in the intensive care unit as opposed to the use of intermittent hemodialysis and peritoneal dialysis [12,14]. Continuous arterio-venous hemodiafiltration (CAVHD) is one of the continuous renal replacement techniques, which nowadays has become a widely used renal replacement therapy [3,13,15, 16].

1.2 HISTORICAL DEVELOPMENT OF CAVHD

It was first demonstrated in 1913 that the dialysis of blood could remove small solutes that are normally excreted in urine [17]. The first dialysis machine was developed by Kollf [18] in 1946. Its surface area was large enough to be beneficial in treatment of patients with kidney failure. Later in the 1960's, blood access devices were developed, which allowed hemodialysis to be employed for the treatment of chronically in patients with permanent loss of kidney function (chronic renal failure: CRF). In the early years of dialysis, patients were treated for 8 to 12 hours, two to three times a week. As early as 1960, Scribner et al [19] introduced a technique of continuous hemodialysis without the use of a blood pump, for the treatment of ARF. In 1964 however, the drawback of this development became clear when Peterson et al [20] observed acute encephalopathy during dialysis treatment. They explained this by the rapid fall in the solute plasma concentration due to diffusion, leading to osmotic disequilibrium between plasma water and the brain tissue. Further, hemodialysis was refined by using controlled ultrafiltration, by bicarbonate as a buffer substitute rather than acetate, by high or variable sodium concentrations in dialysate and by cooler-temperature dialysate [21-24]. By virtue of these developments, most patients with CRF can now adequately be treated by IHD in two or three sessions of 4 to 5 hours a week. In subsequent years IHD became standard for the treatment of acute or chronic renal failure in critically ill patients. However, dialysis induced hypotension and vascular instability together with sharp fluctuations in the plasma osmolality, pH and intravascular fluid volume, make the IHD poorly tolerated in unstable patients.

In 1967, Henderson et al [25] described the so-called pump-driven hemofiltration technique,

where venous blood is pumped from the patient through an artificial kidney and subsequently back to the patient. By a hydrostatic pressure gradient across a semi-permeable membrane (cut-off point: 40.000 Daltons) an ultrafiltrate is produced from plasma water. Solute mass transport is based on convection. The intravascular volume is preserved by replacing the ultrafiltrate with a substitution fluid that has an electrolyte composition similar to that of the plasma. With hemofiltration the efficiency of the removal of urea was lower but disequilibrium was seldom seen and blood pressure was more stable. For hemofiltration, new highly permeable membranes were developed, which allowed passage of water and solutes of up to several thousand Daltons at very low pressures. Moreover, Babb et al [26] pointed out that the so-called 'middle molecules', which were believed to contribute to the uremic syndrome, were removed more efficiently with this technique. This middle molecule hypothesis also led to the development of peritoneal dialysis techniques. For the treatment of patients with complicated ARF, peritoneal dialysis is usually better tolerated but may be contraindicated by intra-abdominal pathology, infection, technical difficulties or respiratory compromise [27-31].

In 1977, Kramer et al [32] described a technique, called continuous arterio-venous hemofiltration (CAVH), which enables the control of uremia in critically ill patients with ARF without cardiovascular stability associated with conventional IHD. He used a small hemofilter and connected it to catheters in the femoral artery and vein to obtain a spontaneous blood flow driven by the arterial blood pressure of the patient only. To control the rate of fluid loss, he administered a substitution fluid. When small highly permeable hemofilters became generally available, many dialysis physicians relied on CAVH for the treatment of critically ill patients with ARF. In spite of very low blood pressures (50-70 mmHg), the gradual fluid withdrawal (10-14 l/day) was very well tolerated by these patients [33,34]. As far as the treatment of uremia was concerned, the CAVH treatment proved to have limited to low urea clearance. The solute transport in CAVH occurs by convection and limited by the rate of ultrafiltrate production. When the rate of urea generation exceeds the rate of urea removal, a steady-state BUN level is not achieved. This may take place because of 1) high urea generation due to catabolism (For the highly catabolic patients, the rate of ultrafiltration was seldom enough to provide adequate clearance of uremic solutes (7-10 ml/min).) and/or 2) inadequate rate of ultrafiltration flow, particularly in hypotensive patients. It was particularly these hypotensive and unstable patients who needed a continuous form of renal therapy. If the patient were more stable, then a traditional form of IHD could be implemented. Indeed, it was common practice for patients on CAVH to have IHD treatment as well until several adaptations of the CAVH technique were suggested.

Kaplan et al [35] suggested the application of a suction pump (usually 150-200 mmHg) to the ultrafiltrate compartment to increase the ultrafiltration flow rate. However an increased

filtration fraction (sometimes exceeding 50%) may favor hemofilter clotting despite adequate heparinization. Both Wendon et al [36] and Kaplan et al [37] relied on pumped veno-venous hemofiltration to increase blood flow rates (100-300 ml/min) through the hemofilter and so to increase the ultrafiltration flow rate. With this technique an ultrafiltration flow rate of up to 50 l/day and an urea clearance of 34 ml/min may be produced. Further, Kaplan et al [38] proved the enhancement of the efficiency of CAVH by infusing the substitution fluid in the arterial line (predilution), rather than in the venous line (postdilution). Infusing replacement fluid to the blood within the extracorporeal circuit via the arterial line just before the blood inlet port of the hemofilter (predilution) reduces the blood viscosity, hematocrit and plasma protein concentration and increases the flow and hydrostatic pressure across the membrane. In addition, predilution increases the availability of urea for convective transport by favoring its movement from the erythrocyte. All of this will increase the ultrafiltration flow rate [38,39]. Ronco et al [40] suggested additional dialysis with the same dialyzer. He first used a dialysate flow rate of 20 l/h for 2 hours a day and reasoned that at a high dialysate pressure no ultrafiltration would take place. The method was, of course, soon abandoned because of the considerable risk of 'back filtration'. Meanwhile Geronemus et al [41] suggested continuous hemodialysis rather than hemofiltration. At a dialysate flow rate of 1-2 l/h adequate clearance of urea was easily obtained. Unfortunately their dialyzer provided very low ultrafiltration flow rate. Later they suggested the use of highly permeable membranes.

In 1984, Geronemus et al [42] described the technique of continuous arterio-venous hemodiafiltration (CAVHD). They emphasized the role of dialysate flow in the enhancement of solute clearance by diffusion. Infusing a dialysate solution through the filtrate/dialysate compartment of the hemofilter counter-current to the blood flow enhances the solute transport by diffusion. At that time, Van Geelen and Vincent [15,16] in the intensive care unit of Erasmus University Hospital in Rotterdam were pioneering the technique of CAVHD and they aimed for the combination of convective and diffusive transport. Solute transport by both diffusion and convection provides a higher clearance of urea (with a dialysate flow rate of 1 l/h up to 25 ml/min against 10 ml/min in CAVH). Without removing large volumes of ultrafiltrate CAVHD has more effective control of uraemia than the CAVH alone. Increasing the dialysate flow rate up to 3 l/h may further increase the urea clearance up to 50 ml/min [43]. The dialysate flow rate (up to 4-5 l/h) is considerably less than the rate of patient's blood flow through the hemofilter. Complete equilibration of small solutes should occur between blood and dialysate if the blood flow rate is higher than the dialysate flow rate [44]. CAVHD combines the advantages of CAVH and slow hemodialysis, and may be performed by intensive care unit staff without the need for dialysis machines and trained dialysis nurses. The technique of CAVHD was soon to become the first choice treatment of acute renal failure in the intensive care setting [3,4,15,16,44-46].

1.3 PHYSICAL PRINCIPLES OF SOLUTE TRANSPORT IN CAVHD

Continuous arterio-venous *hemodiafiltration* is the combination of continuous arterio-venous *hemofiltration* with slow *hemodialysis*. In CAVHD, solute transport occurs simultaneously by combined effects of dialysis and hemofiltration.
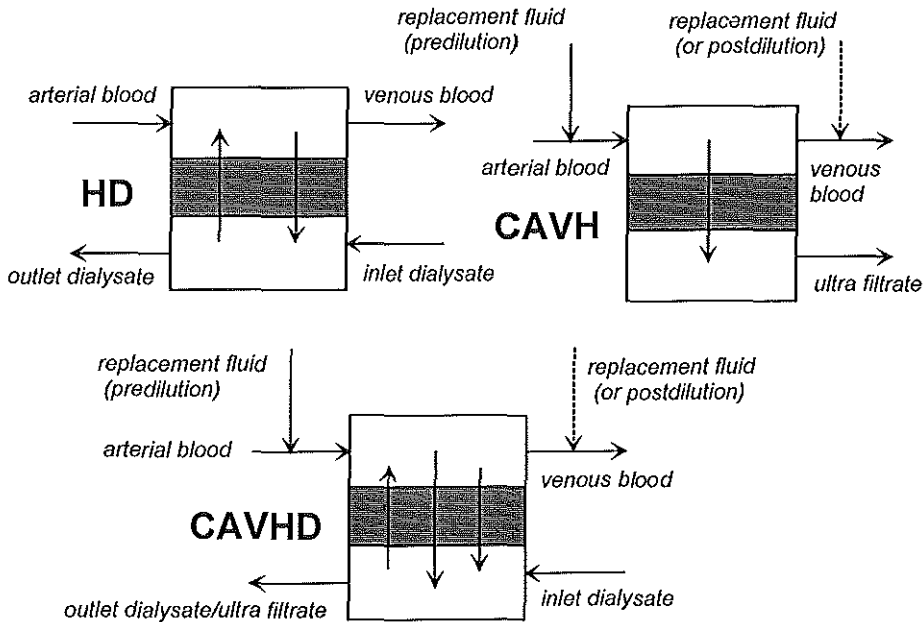
Figure 1.1: Principles of the conventional intermittent hemodialysis, continuous arterio-venous hemofiltration and continuous arterio-venous hemodiafiltration.

In Figure 1.1, the physical principles of CAVHD, CAVH and conventional hemodialysis are depicted. With CAVH, blood is led through a flat sheet or a capillary hemofilter. The hemofilter consists of a blood and an ultrafiltrate compartment, which is separated by a membrane. The membrane is permeable to solutes of up to several thousand Daltons. Blood flow is driven from the difference between the patient's arterial and venous systemic pressures. Transmembrane pressure difference (TMP) across the hemofilter membrane results in the movement of plasma water from blood into the filtrate compartment. As water moves across the hemofilter membrane, it "drags" solutes such as urea and creatinine, with it. This process is called *ultrafiltration* for water and *convection* for solute transport. Filtered water together with non-protein bound solutes with low and middle molecular weights (MW) is called ultrafiltrate. Thus, the composition of ultrafiltrate is similar to that of the plasma water. The quantity of solute movement by convection depends on molecular size, membrane hydraulic permeability, TMP and the rate of ultrafiltration flow. For solutes that are far below the

molecular 'cut-off' of the membrane, the rate of ultrafiltration alone determines the convective mass transport rate.

The ratio of solute concentration in ultrafiltrate to that in the plasma water retained is called *solute sieving coefficient*. The sieving coefficient depends on the particular membrane (diameter of a membrane pore), the molecular size and protein-binding properties of the solute. Sieving coefficient of uraemic solutes such as urea and creatinine equals one and that of the blood cells and proteins equals zero. Proteins and blood cells are too large to cross the membrane and remain within the blood compartment and return through the venous end of hemofilter to the systemic circulation. Cations such as sodium and potassium have a sieving coefficient of slightly less than one and anions have values greater than one. This is caused by the fact that the negatively charged proteins attract cations, resulting in a decreased transmembrane movement, and repel anions, causing to an increased transmembrane movement (Gibbs-Donnan effect).

Ultrafiltration does not affect the concentration of solute in plasma water. To inhibit coagulation heparin is added continuously to the blood when it enters the extracorporeal circuit. To prevent the patient from too volume depleted because of large amounts of plasma water removed as ultrafiltrate (10-15 l/day), a substitution fluid is administered to the blood either before the blood inlet port or after the blood outlet port of the hemofilter. Replacement of the ultrafiltrate with a clean substitution fluid decreases the concentration of both solutes and proteins in plasma water, decreases the hematocrit and blood viscosity, and increases the rate of blood flow and hydrostatic pressure across the hemofilter membrane by dilutional effects.

In contrast to CAVH, in hemodialysis, diffusive transport is the major principle underlying blood purification, especially for the elimination of substances in the low molecular weight range, e.g. of urea and creatinine. Diffusion is a passive and rapid transport process. Transmembrane concentration gradient, thus the driving force for the solute diffusion across the membrane causes the solutes to diffuse from plasma water through the hemofilter membrane into the dialysate fluid that has an ideal plasma water composition and provides the osmotic gradient for diffusion. By running the dialysate fluid through the filtrate/dialysate compartment of the hemofilter counter-currently to the blood flow, solute transport by convection is enhanced by diffusion. The rate of diffusive mass transport is mainly determined by the molecular size of solute, the type of particular membrane (surface area, diffusive permeability) and the rate of dialysate flow. Solutes with a small MW such as urea (60 Daltons) and creatinine (113 Daltons) are removed by diffusion (dialysis), whereas for solutes with a MW greater than 500 Daltons diffusion is less efficient and their removal occurs predominantly by convection (hemofiltration).

1.4 AIM AND OUTLINE OF THE THESIS

Continuous arterio-venous hemodiafiltration (CAVHD) has become a widely used renal replacement therapy for patients with acute renal failure (ARF). It is a new intensive care method of complete renal replacement therapy in the critically ill and unstable kidney patient. Despite impressive advances in the intensive care hemodialysis therapy, many investigators have studied the CAVHD as a continuous renal therapy only from the clinical point of view. In 1984 Van Geelen and Vincent [15,16] in their first experiments with CAVHD, stressed the importance of simultaneous convective and diffusive solute transport. Nevertheless, there was then virtually no insight in both the determinants of solute and volume transport and the relationships between the hemofilter characteristics and operational and clinical conditions in CAVHD. For example, it was not known to what extent the CAVHD treatment had influence on the disappearance rate of drugs and how slow the dialysate flow rate in the presence of ultrafiltration must be to be able to control the patient's uraemic state. Therefore, a study was begun of the physical and mathematical aspects of solute and volume transport in CAVHD, so as to be able to optimize the CAVHD treatment.

The aim of this thesis is to investigate the determinants of blood, ultrafiltration and dialysate flow rates on the uraemic solute and drugs clearance, to describe the physical transport processes in CAVHD, to formulate the physical relationships between hemofilter characteristics and operational quantities, and to access the efficacy of CAVHD compared to IHD as far as its side-effects such as hypotension are concerned. This thesis is also to be beneficial in the sense of the fact that the dialysis physician should have a functional knowledge of the physical principles involved during treatment with a hemofilter. Such knowledge allows him to more accurately predict the results of therapy and to optimize the treatment protocol. In addition, he must interpret manufacturers' specifications and critically evaluate new devices offered for CAVHD. In order to follow the important physical concepts involved a certain amount of mathematical manipulation is required, but more rigorous mathematical and clinical engineering treatments are reduced to the expressions of clinical importance, such as solute clearance.

Outline of the thesis

In **Chapter 2**, the latest developments about the problems encountered in intermittent hemodialysis are reviewed from a literature study. Further, the indications and contraindications of CAVHD treatment, clinical equipment and its preparation are outlined.

In **Chapter 3**, an analysis of determinants of blood and ultrafiltration flow rates is done by comparing the clinical observations with the theoretical prediction. In patients treated with

CAVHD, serial measurements of blood flow rate, blood pressure and ultrafiltration rate were performed, so as to estimate the hemofilter resistance to blood flow and its hydraulic permeability. The aim of these studies was to examine the feasibility of predicting hemofilter performance under clinical conditions.

In **Chapter 4**, the results of resistance to blood flow and membrane permeability index measured in a laboratory setting are given. In laboratory setting, for some CAVH(D) capillary hemofilters, the resistance to flow was measured with fluid solutions of different viscosity. The hemofilters were perfused with saline, sucrose solution, pig blood and human blood as perfusion fluid. The effect of hemofilter resistance on the hydraulic performance (ultrafiltration) was also investigated by measuring the membrane permeability index and the resistance to (human) blood flow simultaneously over a survival time of about 220 hours. The aim of these studies was to examine the feasibility of predicting the hemofilter performance under laboratory conditions.

In **Chapter 5**, a general description of solute and volume transport in CAVHD is given. Existing models of conventional hemodialysis are not likely to be useful for the analysis of solute transport in CAVHD, since the solute transport in CAVHD differs from that in intermittent hemodialysis and hemodiafiltration in several respects. In view of the shortcomings of previous models, we developed a new mathematical model of CAVHD. This model takes into account the variation of concentration in the blood and dialysate boundary layers as well as inside the membrane in the presence of simultaneous diffusive and convective solute transports. The model equations require numerical solutions.

In **Chapter 6**, analytical solutions to uraemic solute and volume transport in CAVHD are presented to calculate the diffusive mass transfer coefficient (K_d) for a solute when blood, filtrate and dialysate flow rates and solute concentrations are known. We made some assumptions. Then, we introduced analytical solutions to solute and volume transport in CAVHD, so as to obtain expressions of the overall diffusive mass transfer coefficient, depending on the ultrafiltration volume flux profiles under the following conditions:

- K_o for zero ultrafiltration volume flux ($J_v=0$),
- K_a for a constant (mean) volume flux ($J_v=J_a=Q_f/S$), and
- K_d for a linear decreasing volume flux ($J_v=\alpha+\beta x$).

Further we derived expressions of solute clearance in relation to the overall mass transfer coefficients K_o, K_a and K_d. By virtue of the expressions of the overall mass transfer coefficients related to solute clearance, the model is well suited for the analysis of solute transport by simultaneous convection and diffusion in CAVHD. This was the first detailed

analytical mathematical analysis of solute and volume transport in CAVHD and can easily be implemented in any spreadsheet program.

In **Chapter 7**, the model is applied to clinical data obtained with 0.6 m^2 AN-69 capillary hemofilters. The model equations governing the overall mass transfer coefficients (K_o, K_d and K_a) are evaluated by applying them to data of urea clearance measurements. Our model is a useful addition to the existing models of hemodiafiltration, especially because it allows calculation of the diffusive mass transfer coefficient from the clinical data of CAVHD. It may be used both as a means to further our insight in the determinants of solute transport in CAVHD and to adjust clinical settings, e.g. dialysate flow rate, based on the predicted clearance of uraemic solutes.

In **Chapter 8**, we studied the determinants of uraemic solute clearance in CAVHD. Clearance and its diffusive and convective components of uraemic solutes such as urea, creatinine and phosphate were determined in the region of relative low dialysate flow rates (Q_{di}) at varying blood (Q_{bi}) and ultrafiltration flow rates (Q_f). The degree of conditions in which blood-dialysate solute equilibrium can be achieved was investigated. The diffusive permeability coefficients ($K_s=SK_d$) of urea and phosphate were related to diffusive permeability coefficient of creatinine. Further, by running a simple sensitivity analysis on the overall diffusive permeability coefficient, we analyzed the dependence of K_s on the flow rates and on the strength of concentration driving force at the blood inlet of the hemofilter. The sensitivity analysis provides information about the reliability of predicting the K_s from flow rates and solute concentrations.

In **Chapter 9**, we describe a numerical computational method for solving the equations governing the mass balance in Chapter 5. The method was applied to the clearance data of uraemic solutes and some antibiotic drugs up to 1500 Daltons and to the data of hemofilter hydraulic condition measured during CAVHD, so as to determine the relative weighting factors of blood (f_b) and dialysate (f_d) solute concentrations contributing the convective uraemic solute transport and the resistances (R_b+R_m and R_d) to diffusion from the overall diffusive mass transfer coefficient (K_d) within the operational limits of CAVHD. Depending on the hemofilter hydraulic condition (MI) and the dialysate flow rates (Q_{di}), the resistance (R_b+R_m) of blood and membrane and the resistance (R_d) of dialysate to diffusion were determined by Wilson's plots. Further, by making use of the capillary pore theory, the diffusive permeation coefficients (K_s) of some antibiotic drugs were related to that of the creatinine so as to predict the clearance of antibiotic drugs from the clearance of creatinine under the same operational conditions and hemofilter characteristics (a prediction model). Predicting the clearance of drugs from the clearance of creatinine is sufficiently accurate to be used in the clinic.

In **Chapter 10**, a simulation study was performed to investigate the effect of dialysis duration, the rate of urea removal, the flow rate of ultrafiltration and the dialysate sodium concentration on the fluid shift, which occurs during intermittent hemodialysis or hemodiafiltration therapy. Hereby we determined quantitatively the necessary sodium concentration in the dialysate solution to diminish the intercompartmental fluid shift in the presence of ultrafiltration. We concluded that CAVHD is a better alternative technique for the treatment of patients with serious hemodynamic instability than the intermittent hemodialysis or hemodiafiltration.

1.5 REFERENCES

[1]. Steinhausen M, Parekh N. Principles of acute renal failure. Proceedings of 9th international congress of nephrology. Ed. Robinson RR. Springer Verlag New York 1984 page 702-710.

[2]. Cameron JS. Acute renal failure in the intensive care unit today. Intensive Care Medicine 1986; 12: 64-70.

[3]. Dickson DM, Brown EA, Kox W. Continuous arteriovenous hemodialysis (CAVHD): A new method of complete renal replacement therapy in the critically ill patient. Intensive Care World 1088; 5(3): 78-80.

[4]. Vincent HH, Vos MC. The use of continuous arteriovenous hemodiafiltration in multiple organ failure patients. Applied Cardiopulmonary Pathophysiology 1991; 4: 109-116.

[5]. Myers BD, Moran SM. Mechanism of disease. Hemodynamically mediated acute renal failure. New England Journal of Medicine 1986; 314: 97-105.

[6]. Sherman RA. The pathophysiologic basis for hemodialysis-related hypotension. Seminars in dialysis 1988; 1: 136-142.

[7]. Henrich WL, Woodard TD, Blachley JD, Gomez-Sanchez C, Pettinger W, Cronin RE. Role of plasma osmolality in blood pressure stability after dialysis and ultrafiltration. Kidney International 1980; 18: 480-488

[8]. Port FK, Johnson WJ, Klass DW. Prevention of dialysis disequilibrium syndrome by using of high sodium concentration in the dialysate. Kidney International 1973; 3: 327-333.

[9]. Keshaviah P, Shapiro FL, A critical examination of dialysis-induced hypotension. Am J Kidney Dis 1982; 2: 58.

[10]. Henderson LW. Symptomatic hypotension during hemodialysis. Kidney International 1980; 17: 571-576.

[11]. de Broe MA, Heyrman RM, De Backer WA, Verpooten GA, Vermeire PA. Pathogenesis of dialysis-induced hypoxemia: A short overview. Kidney Int 1988; 33 (supp 24): S 57-61.

[12]. Lauer A, Saccagi A, Ronco C, Belledonne M, Glabman S, Bosch J. Continuous arteriovenous hemofiltration in the critically ill patient. Annals of internal medicine 1983; 99: 455-460.

[13]. Vos MC. Continuous Arteriovenous Hemodiafiltration [PhD Thesis]. Erasmus University Rotterdam. Uitgeverij Eburn, Delft, 1993.

[14]. Barlett RH, Bosch J, Geronymus R, Paganini EP, Ronco C, Swartz R. Continuous arterio-venous hemofiltration for acute renal failure. Trans ASAIO 1988; 34: 67-77.

[15]. Vincent HH, Van Geelen JA. Continuous arteriovenous hemofiltration (CAVH) and

hemodiafiltration (CAVHD) in the critically ill. Experience with the AN-69 plate filter. Int Symp on Acute Renal Replacement Therapy, Boca Raton, Florida, March 1987 (Abstract).

[16]. Van Geelen JA, Vincent HH, Schalekamp MADH. Continuous arteriovenous haemofiltration and haemodiafiltration in acute renal failure. Nephrol Dial transplant 1988; 2: 181-186.

[17]. Drukker WA. Hemodialysis, a historical review. In Replacement of renal function by dialysis. Sec ed. 1986 Martinus Nijhoff Publishers Dordrecht. Ed. Drukker WA. chapter 2, page 3-52.

[18]. Klinkmann H. Historical overview of renal failure therapy- A homage to Nils Alwall. Contrib Nephrol 1990; 78: 1-23.

[19]. Scribner BH, Caner JEZ, Bun R, Quinton W. The technique of continuous hemodialysis. Trans ASAIO 1960; 6: 88-103.

[20]. Peterson HdeC, Swanson AG. Acute encephalopathy occurring during hemodialysis. Archives in internal Medicine 1964; 113:877-880.

[21]. Leunissen KML, Hoorntje SJ, Fiers HA. Acetate versus bicarbonate hemodialysis in critically ill patients. Nephron 1986; 42: 145-151.

[22]. Po CL, Afolabi M, Raja RM. The role of sequential ultrafiltration and varying dialysate sodium on vascular stability during hemodialysis. ASAIO J 1993; 30: M798-M800.

[23]. Henrich WL, Woodard TD, McPaul JJ. The chronic efficacy and safety of high sodium dialysate. Am J Kidney Dis 1982; 2: 349-354.

[24. Agarwal R, Jost C, Khair-El-Din T, Victor R, Grayburn P, Henrich WL. 35°C dialysis increases peripheral resistance and improves hemodynamic stability in uremic patients. JASN 1992; 3: 351-357.

[25]. Henderson LW, Besarab A, Michaels, Bluemle LW. Blood purification by ultrafiltration and fluid replacement (diafiltration). Trans Am Soc Artif Intern Organs 1967; 13: 216-226.

[26]. Babb AL, Popovich RP, Cristopher TG, Scribner BH. The genesis of the square meter-hour hypothesis. Trans Am Soc Artif Intern Organs 1971; 17: 81.

[27]. Nolph KD. Peritoneal dialysis for acute renal failure. Trans ASAIO 1988; 34: 54-55.

[28]. Schreiber M. Peritoneal dialysis for acute renal failure. In: Paganini EP, ed. Acute continuous renal replacement therapy. Boston, Martin Nijhof Publishing. 1986: 269-282.

[29]. Nolph KD, Sorkin M. Peritoneal dialysis for acute renal failure. In: Massry SG, Glasssock RJ (eds.). Textbook of Nephrology. Baltimore, Williams & Wilkins, 1990; 439-458.

[30]. Firmat J, Zucchini A. Peritoneal dialysis for acute renal failure. Contrib Nephrol 1979; 17: 33-40.

[31]. Nasrullah M, Shikora S, McMohan M. Peritoneal dialysis for acute renal failure: Overfeeding resulting from dextrose absorbed during dialysis. Crit Care Med 1990; 18: 29-31.

[32]. Kramer P, Wigger W, Rieger J, Matthaei D, Scheler F. Arteriovenous haemofiltration: A new and simple method for treatment of over-hydrated patients resistant to diuretics. Klin Wschr 1977; 55: 1121-1122.

[33]. Kramer P, Seegers A, De Vivie D, Trautmann M, Scheler F. Therapeutic potential of hemofiltration. Clinical Nephrology 1979; 11: 145-149.

[34]. Kramer P, Kaufhold G, Grone HJ. Management of anuric intensive care patients with arteriovenous hemofiltration. Int J Artif Organs 1980; 3: 255-230.

[35]. Kaplan AA, Longnecker RE, Folkert VW. Suction-assisted continuous arteriovenous hemofiltration. Trans Am Soc Artif Intern Organs 1983; 29: 408-413.

[36].   Wendon J, Smithies M, Sheppard M, Bullen K, Tinker J, Bihari D. Continuous high volume veno-venous haemofiltration in acute renal failure. Intensive Care Med 1989; 15; 358-363.

[37].   Kaplan AA, Longnecker RE, Folkert VW. Continuous arteriovenous hemofiltration. A report of six months' experience. Annals of Internal Medicine 1984; 100: 358-367.

[38].   Kaplan AA. Predilution versus postdilution for continuous arteriovenous hemofiltration. Trans ASAIO 1985; 31: 28-32.

[39].   Golper TA. Continuous arteriovenous hemofiltration in acute renal failure. Am J Kidney Dis 1985; 6: 373-386.

[40].   Ronco C, Brendolan A, Braganti L, Chiaramonte S, Fabris A, Ferriani M, Dell'Aquila R, Milan M, La Greca G. Arteriovenous hemodiafiltration associated with continuous arteriovenous hemofiltration: A combined therapy for acute renal failure in the hypercatabolic patient. Blood Purif 1987: 5: 33-40.

[41].   Geronemus R, Schneider N. Continuous arteriovenous hemodialysis: A new modality for treatment of acute renal failure. Trans ASAIO 1984; 30: 610-613.

[42].   Geronemus R, Schneider N. Further studies with continuous arteriovenous hemodialysis (CAVHD) in acute renal failure (ARF). Abstract Trans ASAIO 1985; 14: 54.

[43].   Bonnardeaux A, Pichette V, Quimet D, Geadah D, Habel F, Cardinal J. Solute clearances with high dialysate flow rates and glucose absorption from the dialysate in continuous arteriovenous hemodialysis. Am J Kidney Dis 1992; 19: 31-38.

[44].   Sigler MH, Teehan BP. Solute transport in continuous hemodialysis: A new treatment modality for acute renal failure. Kidney Int 1987; 32: 562-571.

[45].   Raja R, Kramer M, Goldstein S, Caruana R, Lerner A. Comparison of continuous arteriovenous hemofiltration and continuous arteriovenous dialysis in critically ill patients. Trans Am Soc Artif Intern Organs 1986; 32: 435-436.

[46].   Stevens PE, Riley B, Davies SP, Gower PE, Brown EA, Kox W. Continuous arteriovenous hemodialysis in critically ill patients. The Lancet 1988; 16: 150-152.

CONTINUOUS ARTERIO-VENOUS HEMODIAFILTRATION
An overview of clinical practice and equipment

2.1 INTRODUCTION

Intermittent hemodialysis (IHD) is a form of renal replacement therapy, which was developed for the treatment of patients with chronic renal failure. Patients are dialyzed 2 or 3 times a week, for 3 to 6 hours per dialysis session. In these few hours, solute clearance (the solute removal rate per inlet solute concentration in units of ml/min) has to be high to tide over the interdialytic time interval. The high clearances are obtained by a large surface area, a blood flow rate of Q_{ba}=200 to 300 ml/min and a dialysate flow rate of Q_{di}=500 ml/min. During dialysis, plasma water is withdrawn to an amount adjusted to the interdialytic body weight-gain (BWG) of the patient. Acute renal failure (ARF) is a potentially reversible condition. After acute tubular necrosis, if the patient's general condition improves, one may expect recovery of kidney function after a period of two to six weeks [1]. In the period of these two to six weeks, the clinical condition of critically ill patient is frequently complicated by multiple organ failure with hemodynamic, respiratory or neurological instability. Treating such a patient with intermittent machine hemodialysis is not tolerated. In this chapter we give a short overview of the clinical problems encountered during the treatment of patients with ARF with intermittent hemodialysis, with emphasis on the possible consequences for critically ill patients. From literature, we review the indications and possible contraindications and finally the guidelines of initiating the clinical equipment of a CAVHD system.

2.2 CLINICAL PROBLEMS WITH INTERMITTENT HEMODIALYSIS

Dialysis-induced hypotension

In IHD therapy, the most frequent complication is *dialysis-induced hypotension* [2]. Clinical studies show that rapid fluid removal during dialysis often leads to arterial hypotension. In the early years of hemodialysis, this was attributed to hypovolemia caused by a fluid removal rate that exceeds the rate of fluid mobilization from the interstitial space [3]. However, in 1978, Bergström et al [4] showed that rapid fluid removal was better tolerated if it were done without simultaneous dialysis. During simultaneous hemodialysis and hemofiltration, removal of water was easier to perform than during hemodialysis alone [5,6]. Furthermore, it was proved that even with isovolemic hemodialysis a reduction in blood pressure could be observed [7], suggesting that solute transport during dialysis interferes with the mechanisms of blood pressure control and therefore contributes to the side effects of the dialysis treatment. Some investigators explained this phenomenon by stating that:
• 	The rapid fall in plasma osmolality causes a fluid shift from the extracellular into the

    intracellular compartment, the so-called disequilibrium syndrome [4,8,9]. This internal fluid shift together with external fluid removal by ultrafiltration decreases intravascular volume [10].

- The response of the autonomic nervous system alters during dialysis treatment [11,12] because of either the autonomic neuropathy or the fall in plasma osmolality.

- Sodium concentration in the dialysate solution is not optimal. Schultze et al [13] have demonstrated that when using a dialysate containing sodium of 126 mmol/l, the patient's mean arterial blood pressure (MAP) dropped 30 mmHg and plasma prostaglandins (PGE_2) and plasma renin activity rose significantly in comparison with a dialysate containing sodium of 140 mmol/l. By using the dialysate containing sodium of 140 mmol/l, the drop in blood pressure was only 13 mmHg. On the other hand, the finding that sodium balance is identical during hemofiltration (HF) and hemodialysis argues against prostaglandins playing an important role in vascular stability during HF.

- Interacting the blood with membrane leads to complement activation, which probably through the production of arachidonic acid metabolites, causes vasodilatation [13,14-16].

- In a simulation study we also analyzed the influence of dialysate sodium concentration, the rate and amount of ultrafiltration, duration of a dialysis session and urea clearance on the transcellular fluid shift during treatment with modeled dialysis sessions of 1 to 8 hours. The simulation results showed that the magnitude of fluid shift from extracellular into the intracellular fluid compartment decreases with slow dialysis, high sodium concentration in the dialysate fluid, low rate and amount of ultrafiltration and low rates of urea removal (See Chapter 10).

Usually, the risk of dialysis-induced hypotension poses no severe restrictions to the treatment of patients with chronic renal failure. In hemodynamically unstable patients, however, the risk of hypotension with IHD is often unacceptable. In these patients, even with slow dialysis at a blood flow rate of 180 ml/min, a recirculating dialysate stream and an ultrafiltration flow rate of only 200-300 ml/h, hypotension frequently occurs [17].

Hypoxemia

Hypoxemia is another complication of IHD therapy. This can be explained by several causes: In using the acetate buffered dialysate, the loss of CO_2 into the dialysate and a decreased respiratory quotient that results from acetate metabolism will both lead to an insufficient respiratory drive and hypoventilation [18,19]. A rapid increase in blood pH may cause hypoventilation, also with bicarbonate buffered dialysate [18]. The membrane bioincompatibility gives rise to the secretion of inflammatory mediators that may lead to pulmonary

vasoconstriction [16,20-22]. By using dialysate solution containing bicarbonate and more biocompatible membranes (such as AN-69, polysulfone) rather than cuprophane, these ventilatory problems may largely be prevented [20,22].

Neurological damage

IHD may cause *neurological deterioration*. Patients may become unconscious as a result of uremic encephalopathy itself. The patient's uraemic state also has a predisposition to the development of seizures [23]. Hemodialysis may, paradoxically, impair the neurological condition as a result of sudden changes in pH and osmolality. Kennedy et al [24] and La Greca et al [25] have shown that during dialysis urea levels in cerebrospinal fluid decreased more slowly than those in plasma. Arieff et al [26] show that in uremic dogs rapid dialysis causes brain edema and seizures. Slow dialysis, although resulting in a similar reduction in urea concentration, was not associated with brain edema. The brain edema was caused by a fluid shift resulting from an osmotic disequilibrium between plasma and cerebrospinal fluid. Interestingly, it could be shown that the change in osmolality did not result from changes in urea concentration alone. The authors suggested that another, as yet undefined, osmotically active solute is present in the brain, creating an osmotic gradient between brain tissue and plasma. In a clinical study, Port et al [27] demonstrated that the first dialysis treatment caused disturbances in the electroencephalogram in virtually all patients and subjective symptoms of disequilibrium in most of them. He compared two groups of patients, one with a normal dialysate sodium concentration and one with an increased dialysate sodium concentration in order to prevent the fall in plasma osmolality. He found that by this intervention, neurological problems could be prevented. Davenport et al [28] showed that, in case of hepatic encephalopathy cerebral perfusion pressure falls during intermittent hemofiltration treatment but not during CAVH.

In conclusion, rapid removal of solutes and fluids in intermittent hemodialysis has some disadvantages. These are indications that, in order to prevent neurological complications of dialysis, one should aim for slower solute transport rates. Therefore, in patients with neurological problems, continuous treatment methods are to be preferred. In general, these problems do not impede the treatment of chronic renal failure patients. With acute renal failure patients, however, hemodynamic, neurologic and/or respiratory instability, inherent to the cause of the renal failure, are the most frequent problems encountered. These problems call for a more gentle approach, i.e. by continuous methods, such as CAVH or CAVHD.

2.3 INDICATIONS FOR CAVHD

In section 2.2, it was stated that the patients with ARF must be treated with a more gentle

approach, such as CAVHD. In the University Hospital Rotterdam, the official indications for CAVHD are cases of renal failure complicated by circulatory, respiratory or neurological instability, and cases of renal failure in which daily dialysis treatment would be needed. In general, patients treated by CAVHD are patients who have had major surgery or patients with sepsis and multiple organ failure, including renal failure [1].

Circulatory instability

The single and most important reason for treating patients with CAVHD is the renal failure in combination with circulatory instability. The combination of low or unstable blood pressure and edema makes it quite difficult to judge how much fluid can be withdrawn safely. In case of a compromised myocardial function, the vascular refilling rate during ultrafiltration will be very slow. If such patients would be treated with IHD, this would lead to osmotic disequilibrium by which vascular refilling is further impaired (See Chapter 10). With CAVHD, due to the low rates of uraemic solute removal, osmotic disequilibrium is prevented [29] and fluid removal occurs more gradually. Indeed, several studies have shown improved vascular stability during treatment with CAVHD [30-34].

Respiratory failure

(Threatening) respiratory failure due to fluid overload alone is not necessarily an indication to use continuous instead of intermittent techniques. These patients are best treated with ultrafiltration. However, if a patient with renal failure is weaned from the ventilator with difficulty, CAVHD is to be preferred over IHD. The latter may lead to a diminished respiratory drive and may lead to pulmonary vasoconstriction. The latter phenomenon is attributed to bioincompatibility of the membrane [35,36]. In CAVHD only the more biocompatible synthetic membranes are used. Moreover, by the longer duration of use, protein adsorption to the membrane minimizes any bioincompatibility effects [37-39].

Neurological instability

Neurological instability is another indication for CAVHD. Neurological disturbances during IHD arise from an osmotic disequilibrium between blood and cerebrospinal fluid [40-42]. Again, with CAVHD, by the lower rate of solute removal, osmotic disequilibrium is prevented. This was borne out by the study of Davenport et al [43], who showed that in patients with hepatic encephalopathy cerebral perfusion pressure fell after intermittent hemofiltration but was preserved during treatment with CAVH.

Need for daily dialysis treatment

Another indication to choose continuous instead of intermittent treatments is the need for daily dialysis treatment. Patients with ARF, especially those with sepsis, are in a hyper

metabolic state with fever, an increased cardiac output and an increased resting energy expenditure [44]. Therefore, there is an increased demand of both energy and proteins. The positive cumulative caloric balance is associated with improved overall survival [44-46]. To obtain a positive caloric balance, patients often receive total parenteral nutrition, which may be complicated by very high rates of urea production and fluid overload. Until recently, this necessitated daily hemodialysis and ultrafiltration. Nowadays these problems are easily managed by CAVHD [47-50]. Indeed, patients with multiple organ failure treated by CAVH, show a positive energy balance and higher survival rates compared to patients treated by intermittent methods [51]. Compared to IHD, the rate of uremic solute removal is lower in CAVHD, but at usual dialysate flow rates the total removal per day is similar. Furthermore, intermittent therapies carry the risk of fluid overload in the period between two treatments. This risk is avoided by CAVHD. With both treatment modalities one-should realize that amino acids are removed to a certain extent [52-56] but the rate of removal is small when compared to the rate of administration. Another example of a situation, which used to be dealt with by daily intense dialysis treatment, is kidney transplantation in a patient with primary hyper oxaluria. In these patients plasma oxalate levels should be kept below 20 μmol/l [57] until the graft functions well. This is virtually impossible with intermittent treatment. With CAVHD, at a dialysate flow rate of approximately 4-5 l/h, however, a constant plasma oxalate clearance of 40-50 ml/min can be obtained, which suffices to control hyperoxalemia.
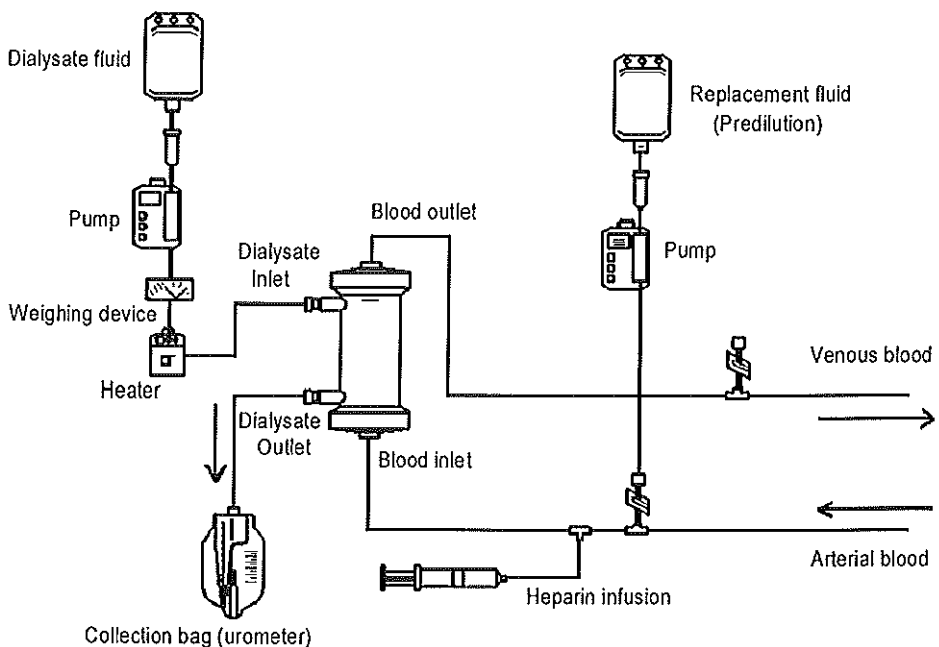
Multiple organ failure ...
It has been hypothesized that continuous techniques can effectively remove inflammatory mediators associated with sepsis, the adult respirator distress syndrome (ARDS) and multiple organ failure [58,59]. This prompted Paganini et al [60] to study the effect of CAVH in patients with ARDS who had no renal failure. In that study, a beneficial effect on the course of ARDS could not be demonstrated. It is likely, however, that for most peptides endogenous clearances are much faster than their removal by CAVH or CAVHD. Therefore current research still focuses on the precise pathophysiological mechanisms involved in the multiple organ failure syndrome. The trend is to look for ways to more selectively remove or neutralize the key pathogenetic factors by affinity columns or specific antibodies or drugs.

Logistic problems
Logistic indications for treatment with CAVHD are especially justified if frequent dialysis treatment would interfere with other aspects of patient care and if the arterial blood access poses no particular problem. Frequent and prolonged investigations or operations can proceed without disconnecting the hemofilter.

2.4 CONTRAINDICATIONS

In general view, CAVHD is contraindicated only if the extracorporeal circuit interferes with the mobilization of the patient or because of problems with the arterial blood access. Thus, when a patient, who has been treated with CAVHD recovers, one tends to continue the treatment by IHD [63]. In case of problems with arterial blood access, the use of pumped veno-venous hemodiafiltration should be considered. The main disadvantage of the pumped technique is that in this case more specialized personnel is needed to watch this system. Moreover, if the pump is equipped with all the necessary alarms and safeguards, this implies that the pump is frequently interrupted which may lead to clotting of the system.

Dialysate fluid

Replacement fluid
(Predilution)

Pump

Blood outlet

Dialysate
Inlet

Pump

Weighing device

Venous blood

Heater

Dialysate
Outlet

Blood inlet

Arterial blood

Heparin infusion

Collection bag (urometer)

Figure 2.1: A schematic representation of a CAVHD system [63].

2.5 CLINICAL EQUIPMENT OF CAVHD

The extracorporeal circuit used for CAVHD is shown in Figure 2.1. The patient is connected via a flexible tubing from the arterial access to the arterial port of the hemofilter. Blood from the arterial line circulates through the hemofilter, and returns to the patient from the venous

port. Blood pumps are not required. Heparin is infused into the arterial line. Dialysate is administered either by gravity or infusion pump counter-current to blood flow. Dialysate and additional ultrafiltrate are collected in a graduated ultrafiltration or dialysate collection bag. A substitution fluid is administered into the arterial line (predilution) or into the venous line (postdilution). A list of the necessary equipment for CAVHD is given below:

- catheters for arterial and venous access (and the disposables used for their introduction),
- a small surface high-flux hemofilter,
- arterial/venous blood tubing set with at least an entrance port in the arterial blood line for heparin administration and preferably an additional arterial and/or venous port for administration of substitution fluid,
- ultrafiltration line, infusion line for substitution fluid, infusion line for dialysate fluid,
- graduated ultrafiltration collection bag or urometer,
- heparin pump,
- pump for substitution fluid, which can deliver up to 1000 ml/h
- dialysate pump which can deliver up to approximately 5 l/h,
- weighing device, dialysate heater,
- heparin, substitution fluid, dialysate fluid,
- two liters of rinsing fluid: NaCl 0.9%, containing heparin 5000 U/l.

Blood access catheters

Vascular access is achieved by means of an arterial shunt, either via femoral artery and vein catheters inserted percutaneously with a Seldinger wire technique or surgical insertion of a Scribner forearm or leg shunt [64]. In CAVHD, blood flows spontaneously. Low blood flow rates may lead to excessive hemoconcentration and to early clotting of the hemofilter. Therefore, Geronemus and others [61-65] prefer the use of low resistance femoral catheters which allow high blood flow rates [66], but have reported occasional problems with bleeding and hematoma formation at the site of insertion. Reported complications of arterial cannulation include dissection, thrombosis, false aneurysm formation, fistula formation, infection, and superficial or retroperitoneal bleeding. However, Kramer et al [67] have demonstrated that these complications were considerably reduced when specially designed short catheters were used exclusively. CAVH-catheters are best placed in the femoral artery and vein. These vessels are usually wide enough to accommodate the catheters and the introduction procedure is simple. If the femoral vessels cannot be used, one may consider using the axillary or brachial artery and the jugular or subclavian vein for access. If a patient has a vascular prothesis of the femoral artery located less than 20 cm above the groin, the use of the femoral artery can be hazardous. Sometimes, due to extensive arteriosclerosis, cannulation of the femoral artery is impossible. In such cases, the axillary or brachial artery

or, if blood pressure is high enough, a Scribner shunt may be used as an alternative vascular access. Scribner shunts may be placed in the lower leg or in the forearm. In recent series, with the use of special CAVH-catheters, the incidence of damage to the femoral artery was reported to be 2% [1,68]. Furthermore, in a retrospective analysis, Swann et al [69] found no evidence for either sepsis or increased morbidity related to catheter infections.

Hemofilter
For CAVHD one needs a small surface highly permeable hemofilter with a low resistance to blood flow. High flux characteristics usually coincide with good biocompatibility [70].
For optimal function a high diffusive permeability is also required. Protein adsorption to the membrane surface causes a decrease of membrane permeability in time. In view of the long duration of use, obviously, protein adsorption is undesirable. The typical hemofilter used for CAVH or CAVHD has short capillaries with a diameter of between 220 and 280 μm and a membrane surface area of between 0.16 and 0.7 m^2. In CAVH high-flux membranes are used in order to obtain adequate convective clearance. In CAVHD clearance occurs more by diffusion than by convection. The rate of ultrafiltration must still be high enough to be able to withdraw several liters of fluid per day. When using a high flux membrane, a total membrane surface area of 0.6 m^2 is enough to obtain an ultrafiltration rate of 300 to 1000 ml/min. A much larger membrane surface area is undesirable for two reasons: 1) It leads to an excessive ultrafiltrate production and thereby necessitates substitution infusion rates that are above the range of the intravenous infusion pumps that are generally available. 2) It implies more extensive contact between blood and membrane material and, hence, a greater risk of clotting.

The life span of each hemofilter is limited by a reduction in efficiency over a period of continuous use or by clotting of the extracorporeal circuit. The hydraulic efficiency of the hemofilter may be monitored by regular comparisons of the membrane hydraulic permeability coefficient or ultrafiltration coefficient, which we call the hydraulic permeability index. Also regular monitoring the diffusive mass transfer coefficient of urea will reflect the diffusive performance of the hemofilter during the treatment. If the membrane permeability becomes poor, as reflected by an ultrafiltration rate or less than 200 ml/h, the hemofilter may be changed. The average life span of a non-clotting hemofilter is about 2 days but may be as long as 5 days [62].

Dialysate fluid
In CAVHD sterile dialysate is necessary in order to prevent back-transport of possible contaminants, such as pyrogen, from dialysate to blood [71-73]. It is easiest to use a commercially available hemofiltration substitution fluid as dialysate fluid, which come in bags

of up to 5 liters. Dialysate fluid for peritoneal dialysis is less suitable for use in CAVHD, mainly because of its low sodium content and high content of glucose (See Table 2.1). After a few days of treatment with CAVHD at a dialysate flow rate of 1 l/h, Vos [63] reported that they have frequently encountered hypokalemia, hypophosphatemia and alkalosis. In their view therefore, the composition of an ideal dialysate solution should be so as to prevent electrolyte derangements during the stable phase of CAVHD treatment. At the start of treatment, when serum potassium and phosphate are high and bicarbonate is low, the same dialysate fluid may still be used albeit at a higher dialysate flow rate. They would not advocate the use of a range of different dialysate solutions, both because it is impractical and because it offers no guarantee that individual modifications or supplementation are no longer needed. Until recently, all solutions contained either lactate or acetate as a buffer substitute, since the addition of bicarbonate would be precluded because of precipitation with calcium and magnesium. Presently, we use for dialysate a fluid to which bicarbonate is added just before use. When used within 24 hours, precipitation of calcium carbonate is negligible. With bicarbonate containing fluids, the possible harmful effects of acetate and the inconvenience of spurious elevation of blood lactate is eliminated. Furthermore, Jenkins et al [74] have demonstrated that in children on CAVHD who have persistent metabolic acidosis, changing from lactate-buffered dialysate to bicarbonate-buffered dialysate considerably improves the metabolic acidosis.

Table 2.1: Composition of fluids which can be used for dialysate fluid in CAVHD (mmol/l) [63]

Dialysate fluid	Na^+	K^+	Ca^{2+}	Mg^{2+}	Cl^-	Lact	Ac^-	$HCO3^-$	Glucose
Fres. HF11	140	1	1.63	0.75	101	45.0	0	0	10.9
Fres. HF21	135	2	1.88	0.75	109	33.8	0	0	8.3
Fres. HF02	140	0	2.00	1.00	111	0	35	0	0
Schiwa SH-44 HEP	140	2	1.75	0.50	112	2.9	0	31.4	5.6
Schiwa SH-35 HEP	140	0	1.75	0.50	110	2.9	0	31.4	5.6
Schiwa SH-36 HEP	140	4	1.75	0.50	114	2.9	0	39.7	5.6
Schiwa SH-41 HEP	141	0	0	0.72	108	0	0	34.3	5.6
Hospal L0	140	0	1.75	0.75	100	45.0	0	0	0
Hospal L2	142	2	2.00	0.75	110	40.0	0	0	0
Hospal LG4D	140	4	2.00	0.75	110	40.0	0	0	6.1
Gambro Hemofiltrasol 21	140	1	1.60	0.75	100	45.0	0	0	11.1
Gambro Hemofiltrasol 22	140	0	1.60	0.75	100	45.0	0	0	11.1
Gambro Hemofiltrasol 23	140	1	1.80	0.75	100	45.0	0	0	11.1

Substitution fluid

For substitution fluid one may use simple Ringer's lactate. In case of hyponatremia, the addition of 1 gr NaCl to 500 ml of Ringer's lactate so as to increase its sodium concentration to 180 mmol/l (in case of predilution) will correct the hyponatremia. Alternatively, if the patient is no longer acidotic, one might consider the use of isotonic saline for substitution fluid. Substitution can be given either by infusing the fluid on the arterial line (predilution) or on the venous line of the hemofilter (postdilution). Predilution has several advantages [75,76]. By predilution the hematocrit and the plasma protein concentration are decreased, which leads to a decrease of the blood viscosity and an increase of blood flow rate. The flow rate of the substitution fluid must be adjusted hourly to the rate of ultrafiltration so as to achieve the desired fluid balance.

Pumps and weighing devices

For safety reasons the use of a pump in the blood line is not advised. If one were to use a pump in the blood line, this would at least necessitate the use of a bubble trap and a device for monitoring the pressure in the arterial blood line, immediately after the pump (in order to detect clotting of the hemofilter) and preferably also in the venous blood line. One might also argue that the extracorporeal system ought to be supervised by a renal nurse. For pumping dialysate fluid, a special pump, that may deliver up to 3-5 l/h, is useful but a simple screw clamp will also do. As dialysis fluid comes in big bags, it is necessary to use a weighing device to check the amount of dialysate delivered every hour. The total amount of ultrafiltrate plus spent dialysate may be measured either by weighing or by using a calibrated container. When substitution fluid is given into the arterial line ('predilution'), an infusion pump, has to be used because of the high pressure. In view of the high ultrafiltration flow rate that occurs in the first few hours, this pump must be able to deliver up to 1000 ml/h.

Anticoagulation and clotting

The main determinant of clotting in CAVHD is blood flow or the lack thereof. In CAVHD, one deals with an extracorporeal system with low pressures and low blood flow rates. The interruption of flow by kinking of lines or catheters promotes clotting. Cooling of the blood in the connecting lines also increases viscosity and reduces the blood flow. It is therefore important to obtain a blood flow rate at all times as high as possible. For this reason, the use of low resistance circuit is beneficial. The main determinant of the level of anticoagulation necessary is the presence or absence of clotting of blood in the extracorporeal circuit. Clotting may be suspected if there is sharp fall in the ultrafiltration flow rate or if the blood lines become dark. The most useful policy against the clotting is to give the patient a bolus dose of 500 units per hour of heparin prior to connection to the extracorporeal circuit. Thereafter, between 500 and 1000 units/hour of heparin is infused via a syringe pump into the arterial

line proximal to the hemofilter. The dose may be changed to between 250 and 750 U/h as clinically indicated. When platelet counts comes below $20 \cdot 10^9/l$, no heparin is needed at all. One might consider regional heparinization, i.e. heparin in the arterial line and protamine in the venous line [77]. Recently Mehta et al [78,79] have published a scheme for citrate anticoagulation in CAVHD.

2.6 PRIMING AND INITIATING CAVHD SYSTEM

It is extremely important to properly prime the hemofilter for CAVHD. The purpose of priming a hemofilter is to purge all air and, with some hemofilters, glycerine, which is used to prevent dehydration of the membrane. The hemofilter is primed from blood side as well as from the dialysate side if it is necessary. On the blood side, the priming is accomplished via a gravity flow of 2 l saline containing 5000 or 10000 U/l of heparin [61,62]. The dialysate side is primed via the gravity flow of the dialysate fluid. Here follows a complete description of priming procedure [63]:

- Attach the blood lines and the ultrafiltrate line to the hemofilter. The ultrafiltrate outlet has to be situated on the arterial site of the hemofilter.
- Place the hemofilter in a holder in the upright position, the venous port at the top.
- Connect the proximal end of the arterial line to the rinsing fluid bag and the distal end of the venous line to an empty sterile bag.
- Clamp the ultrafiltrate line and run 1 to 1½ liters of heparinized saline through the blood lines and through the hemofilter under gravity flow.
- Make sure that side ports have been rinsed as well and that all air has been eliminated.
- Then unclamp the ultrafiltrate line and clamp the venous line.
- Run ½ liter of heparinized saline through the system. Hereby forced ultrafiltration will occur and glycerine is rinsed out of the pores of the membrane.
- Finally unclamp the venous line and rinse the rest of the fluid through the system.

After priming, the pumps, heater, urometer, heparin, substitution fluid and dialysate fluid are connected to the system and the hemofilter, filled with rinsing fluid, is connected to the catheters. After connecting the catheters, the hemofilter is placed in a vertical position at a level of the patient, about 50 cm above the ultrafiltrate/dialysate container in order to get a negative pressure in the dialysate compartment and thereby enhance the rate of ultrafiltration. It is customary to position the hemofilter with the dialysate outlet up, in order to make sure that any air in the dialysate compartment leaves the compartment immediately. There should be no direct contact between the sterile dialysate exit port and the container in which ultrafiltrate and dialysate are collected. The hemofilter is left in place as long as it functions well. If ultrafiltration rate falls below 200 ml/h, and kinking of the catheters or blood lines has

been excluded, the hemofilter is replaced. If the patient must be transported, it is easiest to temporarily disconnect the dialysate infusion line and fix the hemofilter onto the leg of the patient.

2.7 REFERENCES

[1]. Vincent HH, Vos MC. The use of continuous arteriovenous hemodiafiltration in multiple organ failure patients Applied Cardiopulmonary Pathophysiology 1991; 4: 109-116.

[2]. Rosa AA, Fryd DS, Kjellstrand CM. Dialysis symptoms and stabilization in long-term dialysis. Arch Int Med 1980; 140: 804-807.

[3]. Maher JF, Schreiner GE. Hazards and complications of dialysis. The New England Journal of Medicine 1965; 12: 370-377.

[4]. Bergström J. Ultrafiltration without dialysis fir removal of fluid and solutes in uremia. Clinical Nephrology 1978; 4: 156-164.

[5]. Leber HW, Wizemann V, Goubeaud G, Rawer P, Schutterle G. Hemodiafiltration: A new alternative to hemofiltration and conventional hemodialysis. Artif Organs 1987; 2: 150-153.

[6]. Leber HW, Wizemann V, Goubeaud G, Rawer P, Schutterle G. Simultaneous hemofiltration/hemodialysis an effective alternative to hemofiltration and conventional hemodialysis in the treatment of uremic patients. Clinical Nephrology 1978; 9: 115-121.

[7]. Wehle B, Asaba H, Castenfors J, Fürst P, Gunnarsson B, Shaldon S, Bergström J. Hemodynamic changes during sequential ultrafiltration and dialysis. Kidney Int 1979; 15: 411-418.

[8]. Henrich WL, Woodard TD, Blachley JD, Gomez-Sanchez C, Pettinger W, Cronin RE. Role of plasma osmolality in blood pressure stability after dialysis and ultrafiltration. Kidney Int 1980; 18: 480-488.

[9]. Sherman RA. The pathophysiologic basis for hemodialysis-related hypotension. Seminars in dialysis 1988; 1: 136-142.

[10]. van Stone, Bauer J, Carey J. The effect of dialysate sodium concentration on body fluid distribution during hemodialysis. Trans Am Soc Artif Intern Organs 1980; 26: 383-386.

[11]. Baldamus CA, Ernst W, Koch KM. Sympathetic and hemodynamic response to volume removal during different forms of renal replacement therapy. Nephron 1982; 31: 324-332.

[12]. Maeda K, Fujita Y, Shinzato T, Morita H, Kobayakawa H, Takai I. Mechanism of dialysis-induced hypotension. Trans Am Soc Artif Intern Organs 1989; 35: 245-247.

[13]. Schultze G, Maiga M, Neumayer HH, Wagner K, Keller F, Molzahn M, Nigam S. Prostaglandin E_2 promotes hypotension on low-sodium hemodialysis. Nephron 1984; 37: 250-256.

[14]. Shaldon S, Deschodt G, Branger B, Granolleras C, Baldamus CA, Koch KM, Lysaght MJ, Dinarello CA. Haemodialysis hypotension: The interleukin hypothesis restated. Proceedings EDTA-ERA 1985; 22: 229-243.

[15]. Basile C, Drüecke T. Dialysis membrane biocompatibility. Nephron 1989; 52: 113-118.

[16]. Hakim RM, Breilatt J, Lazarus M, Port F. Complement activation and hypersensitivity

reactions to dialysis membranes. N Engl J Med 1984; 311: 878-882.

[17].   van Geelen JA, Woittiez AJJ, Schalekamp MADH. Bicarbonate versus acetate hemodialysis in ventilated patients. Clin Nephrol 1987; 28: 130-133.

[18].   De Broe MA, Heyrman RM, De Backer WA, Verpooten GA, Vermeire PA. Pathogenesis of dialysis-induced hypoxemia: A short overview. Kidney Int 1988; 33 (supp 24): S 57-61.

[19].   Blanchet F, Kanfer A, Cramer E. Benyahia A, Georges R, Mery J-P, Amiel C. Relative contribution of intrinsic lung dysfunction and hypoventilation to hypoxemia during hemodialysis. Kidney Int 1984; 26: 430-435.

[20].   Kolb G, Fischer W, Schoenemann H, Bathke K, Hoeffken H, Mueller T, Lange H, Joseph K, Havemann K. Effects of cuprophan, hemophan, and polysulfone membranes on the oxidative metabolism, degranulation reaction enzyme release and pulmonary sequestration of granulocytes. Contrib Nephrol (Basel) 1989; 74: 10-21.

[21].   Henderson LW, Chenoweth D. Biocompatibility of artificial organs: an overview. Blood Purif 1987; 5: 100-111.

[22].   De Backer WA, Verpooten GA, Borgonjon DJ, Vermeire PJ, Lins RR, De Broe ME. Hypoxemia during hemodialysis: effects of different membranes and dialysate compositions. Kidney Int 1983; 23: 738-743.

[23].   Tyler H. Neurologic disorders in renal failure. A Journal of medicine. 1968; 44: 734-748.

[24].   Kennedy AC, Linton AL, Eaton JC. Urea levels in cerebrospinal fluid after haemodialysis. The Lancet 1962; 24: 410-411.

[25].   La Greca G, Biasioli S, Borin D, Brendolam A, Chiaramonte S, Fabris A, Feriani M, Ronco C. Dialytic encephalopathy. Contrib. Nephrol. 1985; 45: 9-28.

[26].   Arieff AI, Massry SG, Barrientos A, Kleeman CR. Brain water and electrolyte metabolism in uremia: Effects of slow and rapid dialysis. Kidney Int 1973; 4: 177-187.

[27].   Port FK, Johnson WJ, Klass Dw. Prevention of dialysis disequilibrium syndrome by use of high sodium concentration in the dialysate. Kidney Int 1973; 3: 327-333.

[28].   Davenport A, Will EJ, Davison AM. Early changes in intracranial pressure during haemofiltration treatment in patients with grade 4 hepatic encephalopathy and acute oliguric renal failure. Nephrol Dial Transplant 1990; 5: 192-198.

[29].   Twardowski ZJ, Nolph KD. Blood purification in acute renal failure. Annals of Internal Medicine 1984; 100: 447-449.

[30].   Kohen JA, Whitley KY, Kjellstrand CM. Continuous arteriovenous hemofiltration: A comparison with hemodialysis in acute renal failure. Trans Am Soc Artif Intern Organs 1985; 31: 196-173.

[31].   Tam PYW, Huraib S, Mahan B, LeBlanc D, Lunski CA, Holtzer C, Doyle CE, Vas SI, Uldall PR. Slow continuous hemodialysis for the management of complicated acute renal failure in an intensive care unit. Clinical Nephrology 1988; 30: 79-85.

[32].   Paganini EP, Suhoza K, Swann S, Golding L, Nakamoto S. Continuous renal replacement therapy in patients with acute renal dysfunction undergoing intraaortic balloon pump and/or left ventricular device support. Trans Am Soc Artif Intern Organs 1986; 32; 414-417.

[33].   Kaplan AA, Longnecker RE, Folkert VW. Continuous arteriovenous hemofiltration. A report of six months' experience. Annals of Internal Medicine 1984; 100: 358-367.

[34].   Paganini EP, O'Hara P, Nakamoto S. Slow continuous ultrafiltration in hemodialysis resistant

oliguric acute renal failure patients. Trans Am Soc Artif Intern Organs 1984; 30: 173-177.

[35]. Hakim RM, Breilatt J, Lazarus M, Port F. Complement activation and hypersensitivity reactions to dialysis membranes. N Engl J Med 1984; 311: 878-882.

[36]. De Backer WA, Verpooten GA, Borgonjon DJ, Vermeire PJ, Lins RR, De Broe ME. Hypoxemia during hemodialysis: effects of different membranes and dialysate compositions. Kidney Int 1983; 23: 738-743.

[37]. Kuwahara T, Markert M, Wauters JP. Protein adsorption on dialyzer membranes influences their biocompatibility properties. Contrib Nephrol (Basel) 1989; 74: 53-57.

[38]. Kuwahara T, Markert M, Wauters JP. Modulations of leukopenia, thrombocytopenia and protein adsorption of 3 hemodialyzer membranes. A comparison of dialyzer reprocessing techniques. Kidney Int. 1987; 32: 434-435.

[39]. Chenoweth DE, Cheung AK, Ward DM, Henderson L. Anaphylatoxin formation during hemodialysis: Comparison of new and re-used dialyzers. Kidney Int 1983: 24: 770-774.

[40]. Port KF, Johnson WJ, Klass DW. Prevention of dialysis disequilibrium syndrome by use of high sodium concentration in the dialysate. Kidney Int 1973; 3: 327-333.

[41]. Peterson HC, Swanson AG. Acute encephalopathy occurring during hemodialysis. Archives of internal medicine 1964; 113: 877-880.

[42]. La Greca G, Biasioli S, Borin D, Brendolam A, Chiaramonte S, Fabris A, Feriani M, Ronco C. Dialytic encephalopathy. Contrib. Nephrol. 1985; 45: 9-28.

[43]. Davenport A, Will EJ, Davison AM. Early changes in intracranial pressure during haemofiltration treatment in patients with grade 4 hepatic encephalopathy and acute oliguric renal failure. Nephrol Dial Transplant 1990; 5: 192-198.

[44]. Shizgal HM, Martin MF. Caloric requirement of the critically ill septic patient. Critical Care Medicine. 1988; 16: 312-317.

[45]. Mault JR, Bartlett RH, Dechert RE, Clark SF, Swartz RD. Starvation: a major contribution to mortality in acute renal failure? Trans Am Soc Artif Organs 1983; 29: 390-393.

[46]. Mault JR, Kresowik TF, Dechert RE, Arnoldi DK, Swartz RD, Bartlett RH. Continuous arteriovenous hemofiltration: The answer to starvation in acute renal failure? Trans Am Soc Artif Organs 1984; 30: 203-205.

[47]. Raja R, Kramer M, Goldstein S, Caruana R, Lerner A. Comparison of continuous arteriovenous hemofiltration and continuous arteriovenous dialysis in critically ill patients. Trans Am Soc Artif Intern Organs 1986; 32: 435-436.

[48]. Stevens PE, Riley B, Davies SP, Gower PE, Brown EA, Kox W. Continuous arteriovenous hemodialysis in critically ill patients. The Lancet 1988; 16: 150-152.

[49]. Maher ER, Hart L, Levy D, Scoble JE, Baillod RA, Sweny P, Varghese Z, Moorhead JF. Comparison of continuous arteriovenous haemofiltration and hemodialysis in acute renal failure. The Lancet 1988; 16: 129.

[50]. Keshaviah PR. Technical aspects of continuous and intermittent therapies. Trans Am Soc Artif Intern Organs 1988; 34: 61-62.

[51]. Bartlett RH, Mault JR, Dechert RE, Palmer J, Swartz D, Port FK. Continuous arteriovenous hemofiltration: Improved survival in surgical acute renal failure? Surgery 1986; 100: 400-408.

[52]. Chanard J, Toupance O, Gillery P, Lavaud S. Evaluation of protein loss during hemofiltration. Kidney Int. 1988; 33 suppl.24: 114-116.

[53].   Wolfson M, Jones MR, Kopple JD. Amino acid loss during hemodialysis with infusion of amino acids and glucose. Kidney Int 1982; 21: 500-506.

[54].   Paganini EP, Flaque J, Whitman G, Nakamoto S. Amino acid balance in patients with oliguric acute renal failure undergoing slow continuous ultrafiltration (SCUF). Trans Am Soc Artif Intern Organs 1982; 28: 615-620.

[55].   Davenport A, Roberts NB. Amino acid losses during haemofiltration. Blood Purif 1989; 7: 192-196.

[56].   Davenport A, Roberts NB. Amino acid losses during continuous high-flux hemofiltration in the critically ill patient. Critical Care Medicine. 1989; 17: 1010-1014.

[57].   Scheinman JI. Therapy for primary hyperoxaluria. Kidney Int 1991; 40: 389-399.

[58].   Wolner E. Continuous arteriovenous hemofiltration. Applications other than for renal failure. In: Paganini E, ed. Acute continuous renal replacement therapy, Martinus Nijhoff Publishing. 1986: 283-292.

[59].   Coraim FJ Coraim HP, Ebermann R, Stellwag FM. Acute respiratory failure after cardiac failure: Clinical experience with the application of continuous arteriovenous hemofiltration. Critical Care Medicine 1986; 14: 714-718.

[60].   Cosentino F, Paganini E, Lockrem J, Bosworth C, Stoller J, Wiedemann H. Continuous arterio-venous hemofiltration (CAVH) in the adult respiratory distress syndrome: a randomized controlled trial Intensivbehandlung 1990; 15: 103-104 (Abstract).

[61].   Geronemus R, Scheider N. Continuous Arteriovenous Hemodialysis - Clinical Experience in Acute Continuous Renal Replacement Therapy. Paganini EP (ed), Martinus Nijhorff. Boston, 1986, p 255.

[62].   van Geelen JA, Vincent HH and Schalekamp MADH. Continuous Arteriovenous Haemofiltration and Haemodiafiltration in Acute Renal Failure. Nephrol Dial Transplant 1988; 2; 181-186.

[63].   Vos MC."Continuous Arteriovenous Hemodiafiltration". Uitgeverij Eburn, Delft, 1993 (Erasmus University Rotterdam Ph.D. Thesis).

[64].   Dickson DM, Brown EA, Kox W. Continuous Arteriovenous Hemodialysis (CAVHD): A new method of complete renal replacement therapy in critically ill patient. Intensive Care World 1988; 5; 3; 78 - 80.

[65].   Sigler MH, Teehan BP, van Valkenburg D. Solute transport in continuous hemodialysis. Kidney Int 1987; 32; 562- 567.

[66].   Kaplan AA, Longnecker RE, Folkert VW. Continuous Arteriovenous Hemofiltration: A report of six months experience. Annals if Internal Medicine 1983; 99; 455-460.

[67].   Kramer P, Bohler J, Kehr A, Grone HJ, Schrader J, Matthaei D, Scheler F. Intensive care potential of continuous arteriovenous hemofiltration. Trans Am Soc Artif Intern Organs 1982; 28: 28-32

[68].   Olbricht CJ. Continuous arteriovenous hemofiltration- The control of azotemia in acute renal failure. In: acute continuous renal replacement therapy. 1986, Martinus Nijhoff Publishing. Ed. E. Paganini.

[69].   Swann S. Paganini E. The practical technical aspects of slow continuous ultrafiltration (SCUF) and continuous arteriovenous hemofiltration (CAVH). Developments in Nephrology, Acute continuous renal replacement therapy. Ed. Paganini EP, Martinus Nijhoff Publishing, Boston

1986; 13: 51-77.

[70]. Lysaght MJ. Hemodialysis membranes in transition. Contr. Nephrol. 1988: 61; 1-17.

[71]. Golper TA, Leone M. Back transport of dialysate solutes during in vitro continuous arteriovenous hemodialysis. Blood Purif 1989; 7: 223-229.

[72]. Baurmeister U, Vienken J, Daum V. High-flux dialysis membranes: Endotoxin transfer by back filtration can be a problem. Nephrol Dial Transplant 1989; 4 Suppl: 89-93.

[73]. Kolmos HJ. Hygienic problems in dialysis. Danish medical bulletin 1985; 32: 338-361.

[74]. Jenkins RD, Jackson E, Kuhn R, Funk J. Benefit of bicarbonate dialysis during CAVHD. Trans Am Soc Artif Intern Organs 1990; 36: M465-466.

[75]. Kaplan AA. The predilution mode for continuous arteriovenous hemofiltration. Chapter 9, page 143-172. Developments in Nephrology, Acute continuous renal replacement therapy. Ed. Paganini EP, Martinus Nijhoff Publishing, Boston 1986.

[76]. Kaplan AA. Predilution versus postdilution for continuous arteriovenous hemofiltration. Trans Am Soc Artif Intern Organs 1985; 31: 28-32.

[77]. Kaplan AA, Petrillo R. Regional heparinization for continuous arterio-venous hemofiltration. Trans Am Soc Artif Intern Organs 1987; 33: 312-315.

[78]. Mehta RL, McDonald BR, Aguilar M, Ward DM. Regional citrate anticoagulation for continuous arteriovenous hemodialysis in critically ill patients. Kidney Int 1990; 38: 976-981.

[79]. Mehta R, McDonald BR. Regional citrate anticoagulation for continuous arteriovenous hemodiafiltration. Contrib Nephrol 1991; 93: 210-214.

DETERMINANTS OF BLOOD AND ULTRAFILTRATION FLOW RATES: Clinical observations and theoretical predictions

3.1 INTRODUCTION

Continuous arterio-venous hemofiltration (CAVH) and hemodiafiltration (CAVHD) are used in intensive care units for the treatment of patients with acute renal failure. Both techniques are based on spontaneous blood flow and spontaneous ultrafiltration. CAVHD works by achieving arterial and venous vascular access, and perfusing a small hemofilter taking the benefit of the patient's arterial blood pressure instead of a blood pump. At a rate depending on the desired overall fluid balance, substitution fluid is infused [1]. Many nephrologists feel that CAVH(D) is the optimal form of renal replacement therapy in critically ill patients. However, failure of the technique may occur due to an inadequate blood flow rate, leading to excessive hemoconcentration and clotting. It is therefore important to obtain an adequate rate of blood flow through the hemofilter, so as to minimize the risk of excessive hemoconcentration and clotting.

Theoretically, blood and ultrafiltration flow rates may be predicted on the basis of geometry of the extracorporeal circuit, membrane characteristics and blood viscosity. In their *in vitro* simulation and mathematical model of CAVH, Pallone et al [2] reported that they were able to predict the hemofilter performance in a laboratory setting. The resistance to blood flow was in good agreement with their model predictions. However, Olbricht et al [3] found in a clinical study that the resistance to blood flow was 3 times higher than expected.

The aim of the present study was to examine the feasibility of predicting hemofilter performance under clinical conditions. In patients who were treated with CAVHD, serial measurements of blood flow rate, blood pressures and ultrafiltration rate were performed so as to estimate the hemofilter resistance (R_f) to blood flow and its hydraulic permeability index (MI). The resistance of each component of the extracorporeal circuit was predicted from their geometry and blood viscosity and then compared with the measured values. The blood and ultrafiltration flow rates were recorded during the whole CAVHD treatment in order to observe the time courses of MI and R_f. The hemofilter resistance to blood flow was also measured in a laboratory setting (See Chapter 4). Clinical and laboratory data were then compared with the theoretical predictions.

3.2 RESISTANCE TO BLOOD FLOW

The extracorporeal circuit of CAVHD consists of components of arterial blood access (catheter and tubing), hemofilter and venous blood access (tubing and catheter). In the

following, the variables and constants relating to arterial access, hemofilter and venous access are denoted by the subscripts aa, f and va respectively. The blood flow rate (Q_{be}) circulating through the extracorporeal circuit depends on the intra-arterial (P_{ia}) and intra-venous (P_{iv}) blood pressures and undergoes a total resistance (R_t):

$$Q_{be} = \frac{P_{ia} - P_{iv}}{R_t} \tag{3.1}$$

in which the intra-arterial pressure (P_{ia}) is taken to be equal to the mean arterial pressure (MAP), measured from the femoral artery and the intra-venous pressure (P_{iv}) is taken as the mean venous pressure (MVP), measured from the femoral vein.

Observed resistance of the extracorporeal circuit to blood flow
The total resistance (R_t) is the sum of R_{aa}, R_f and R_{va}, each representing the resistance of the arterial access, the hemofilter and the venous access respectively:

$$R_t = R_{aa} + R_f + R_{va} \tag{3.2}$$

To calculate the total resistance (R_t) in mmHg per ml/min, the individual resistances of the extracorporeal circuit have to be calculated on dividing the pressure drop across the component by the blood flow rate:

$$R_f = \frac{P_{bi} - P_{bo}}{Q_{ba} + Q_{pred} - \frac{1}{2}Q_f} \tag{3.3}$$

$$R_{aa} = \frac{P_{ia} - P_{bi}}{Q_{ba}} \tag{3.4}$$

$$R_{va} = \frac{P_{bo} - P_{iv}}{Q_{ba} + Q_{pred} - Q_f} \tag{3.5}$$

in which P_{bi} [mmHg] is the prefilter-, P_{bo} [mmHg] the postfilter hydrostatic blood pressure, Q_{ba} [ml/min] the arterial blood flow rate, Q_{pred} [ml/min] the infusion rate of substitution fluid and Q_f [ml/min] the flow rate of ultrafiltration.

Predicting the blood flow rate circulating in the extracorporeal circuit
In the previous equations, the blood flow rate (Q_{ba}) entering the extracorporeal circuit is assumed to be measured. However, in most clinical applications Q_{ba} is not measured and must be estimated from the overall circuit resistance ($R_{t,p}$) and the blood viscosity. Under the conditions of our study, with shear rates of 150 to 400 sec^{-1}, blood may be regarded as a Newtonian fluid [4]. Furthermore, within the fibers and channels the blood flow is laminar. Therefore, we also calculated the resistance to blood flow from the geometry of each

component using the Poiseuille law. The total circuit resistance to blood flow is predicted as:

$$R_{t,p} = R_{aa,p} + R_{f,p} + R_{va,p} \tag{3.6}$$

where $R_{aa,p}$, $R_{f,p}$ and $R_{va,p}$ represent respectively the resistance of the arterial access components, the hemofilter and the venous access components, which are predicted from manufacturers' specifications and blood viscosity. Resistance of the arterial access ($R_{aa,p}$) is calculated from [2]:

$$R_{aa,p} = \frac{128}{\pi} \sum_j (\frac{\eta_{aa} L_{aa}}{d_{aa}^4})_j \tag{3.7}$$

where the sum is over the number (j) of arterial access components with L_{aa} [m] the length, d_{aa}[m] the internal diameter and η_{aa} [mmHg min] the blood viscosity in the arterial access. The resistance to blood flow ($R_{f,p}$) for a capillary hemofilter is calculated from:

$$R_{f,p} = \frac{64 (\eta_{bi} + \eta_{bo}) L_f}{\pi N d_f^4} \tag{3.8}$$

where L_f [m] is the length of fibers, N the number of fibers, d_f [μm] the internal diameter of a fiber, η_{bi} and η_{bo} [mmHg min] the blood viscosity at the blood inlet and outlet respectively. For a plate hemofilter the $R_{f,p}$ is calculated from:

$$R_{f,p} = \frac{3 (\eta_{bi} + \eta_{bo}) L_c}{4 N_c w_c h_{bc}^3} \tag{3.9}$$

where L_c [m] is the length of blood channels, N_c the number of blood channels, w_c the blood channel width and h_{bc} [m] the blood channel half-height [5]. Resistance of the venous access ($R_{va,p}$) is calculated as:

$$R_{va,p} = \frac{128}{\pi} \sum_j (\frac{\eta_{bo} L_{va}}{d_{va}^4})_j \tag{3.10}$$

where the sum is over the number (j) of venous access components with L_{va} [m] the length, d_{va} [m] the internal diameter and η_{bo} [mmHg min] the blood viscosity at the blood outlet of the hemofilter that equals the blood viscosity in the venous access (η_{va}) in case of predilution.

Normalized resistance to blood flow
Parameters like the length, internal diameter, number of fibers or channels, channel width, channel half-height and membrane total surface area of the circuit components are mostly determined from manufacturers' specifications. From these specifications it is possible to calculate the individual circuit resistances to the blood flow and compare them with the observed resistances. We therefore defined normalized resistance to the blood flow ($R_{n,i}$[10^5/ml] on dividing the observed resistance (R_i) by the predicted blood viscosity (η_i):

$$R_{n,i} = \frac{R_i}{\eta_i} \tag{3.11}$$

where the subscript i represents the subscript aa for the arterial access, the subscript f for the hemofilter and the subscript va for the venous access. The normalized resistance to blood flow is the same as the resistance calculated from the geometry.

Predicting the blood viscosity

The blood viscosity (η_b) depends on plasma protein concentration (C_p), hematocrit (Ht) and temperature (T). In narrow tubes blood viscosity may decrease according to the Fahreaeus-Lindqvist effect. With a diameter of 200 to 240 µm, however, the decrease in blood viscosity is less than 5% and may therefore be neglected [6]. We calculated the blood viscosity from an empirical formula as described by Pallone et al [7]:

$$\eta_b = 1.449 \, \eta_{b,37} \, e^{2.303 \cdot y(T)} \tag{3.12}$$

where $\eta_{b,37}$ is the blood viscosity at $37\,^{\circ}$C and the constant 1.449 represents the ratio of water viscosity at $20\,^{\circ}$C to that at $37\,^{\circ}$C. The term $y(T)$ represents:

$$y(T) = \frac{1.327 \cdot (20 - T) - 0.00105 \cdot (T - 20)^2}{T + 105} \tag{3.13}$$

in a range of $20 \leq T \leq 100\,^{\circ}$C. The blood viscosity at $37\,^{\circ}$C is given by

$$\eta_{b,37} = \eta_{p,37} (1 + 2.5Ht + 0.0735Ht^2) \tag{3.14}$$

The plasma viscosity at $37\,^{\circ}$C is given by:

$$\eta_{p,37} = \eta_{w,37} + (\eta_{pn} - \eta_{w,37}) \frac{C_p}{C_{pn}} \tag{3.15}$$

where the water viscosity ($\eta_{w,37}$) at $37\,^{\circ}$C is 0.864x10^{-7} mm Hg·min. The normal plasma viscosity (η_{pn}) is 1.54x10^{-7} mm Hg·min at a plasma protein concentration of $C_{pn}=7$ g/dl. The values of η_{aa}, η_{bi} and η_{bo}, representing the blood viscosity in the arterial access, the hemofilter blood inlet and the hemofilter blood outlet respectively are calculated from the boundary values of hematocrit and protein concentration (Ht_i, Ht_o, C_{pi}, C_{po}). Blood viscosity in the arterial access (η_{aa}) is calculated from eq.(3.12) by substituting arterial hematocrit (Ht_a) in eq.(3.14) and arterial plasma protein concentration (C_{pa}) in eq.(3.15) and a blood temperature of 37°C in the patient in eq.(3.13). The blood temperature in the extracorporeal circuit has to be measured. Blood viscosity (η_{bi}) at the blood inlet is calculated from eq.(3.12) by substituting the plasma protein concentration (C_{pi}) at the blood inlet in eq.(3.15) and the hematocrit at the blood inlet (Ht_i) in eq.(3.14) from:

$$C_{pi} = \frac{(1 - Ht_a) C_{pa} Q_{ba}}{(1 - Ht_a) Q_{ba} + Q_{pred}} \tag{3.16}$$

$$Ht_i = \frac{Ht_a Q_{ba}}{Q_{ba} + Q_{pred}} \tag{3.17}$$

Likewise, the blood viscosity (η_{bo}) at the blood outlet is calculated from eq.(3.12) by substituting the plasma protein concentration at the blood outlet (C_{po}) in eq.(3.15) and the hematocrit at the blood outlet (Ht_o) in eq.(3.14) from:

$$C_{po} = \frac{(1 - Ht_a) C_{pa} Q_{ba}}{(1 - Ht_a) Q_{ba} + Q_{pred} - Q_f} \tag{3.18}$$

$$Ht_o = \frac{Ht_a Q_{ba}}{Q_{ba} + Q_{pred} - Q_f} \tag{3.19}$$

Observed resistance versus predicted resistance

From a theoretical point of view, the observed resistance must be equal to the resistance calculated from the circuit geometry and blood viscosity. In practice however, because of uncalculated pressure losses, geometrical differences, and the way of calculating the blood viscosity, the predicted resistance of each circuit component differs from the measured resistance. The ratio of the measured resistance (R_i) to the predicted resistance ($R_{i,p}$) is denoted with α_i:

$$\alpha_i = \frac{R_i}{R_{i,p}} \tag{3.20}$$

where the subscript i represents the subscript aa for the arterial access, the subscript f for the hemofilter and the subscript va for the venous access.

3.3 MEMBRANE HYDRAULIC PERMEABILITY INDEX (MI)

Membrane hydraulic permeability index (MI, [ml/h·mmHg]) or the ultrafiltration coefficient is used to indicate the hydraulic performance of the hemofilter during a CAVHD treatment. We defined the membrane permeability index as the product of the hydraulic permeability coefficient (L_p, [ml/(m²·min·mmHg)]) and the total surface area of the membrane (S, [m²]). MI is calculated from the measured rate of ultrafiltration flow and the mean transmembrane pressure difference (TMP$_m$, [mmHg]) as:

$$MI = 60 L_p S = \frac{60 Q_f}{TMP_m} \tag{3.21}$$

Clinical observations and theoretical predictions

The membrane hydraulic permeability coefficient (L_p) is calculated from eq.(3.21) as:

$$L_p = \frac{Q_f}{S \cdot TMP_m} \qquad (3.22)$$

The mean transmembrane pressure difference (TMP_m) was calculated as:

$$TMP_m = \frac{1}{2}(P_{bi} + P_{bo}) - P_d - \Pi_{pm} \qquad (3.23)$$

where P_d [mmHg], the pressure midway in the ultrafiltration /dialysate compartment, was calculated from the height of the fluid column (h_c) in the ultrafiltration line:

$$P_d = \frac{h_c}{1.36} \qquad (3.24)$$

where 1.36 is a conversion factor from cmH_2O to mmHg. Further, Π_{pm}, representing the mean oncotic pressure caused by the plasma proteins, is calculated according to the equation of Landis and Pappenheimer [8]:

$$\Pi_{pm} = 2.1\,C_{pm} + 0.16\,C_{pm}^2 + 0.009\,C_{pm}^3 \qquad (3.25)$$

where C_{pm} [g/dl] is the mean concentration of plasma proteins:

$$C_{pm} = \frac{1}{2}(C_{pi} + C_{po}) \qquad (3.26)$$

with the protein concentration at the blood inlet (C_{pi}) and that at the blood outlet (C_{po}). The Bernouilli effects were thus neglected. Equation (3.25) had previously been found to fit experimental data closely over the range 0 to 25% of protein [9,10]. When we compared the measured values with the calculated, the difference was always less than 5 mmHg [11].

3.4 METHODS

### Clinical protocol and measurements
In this study we determined the resistance to blood flow of the extracorporeal device as well as the hydraulic permeability of the hemofilter membrane in intensive care patients treated with CAVHD. Twenty patients were treated with CAVHD for acute renal failure and sepsis and/or circulatory or neurological instability (See Table 3.1). The CAVHD circuit was installed as depicted in Figure 3.1 (for details, see Chapter 2). A hemofiltration substitution solution (HF-11, Fresenius, Germany) was used as dialysate fluid. For both vascular and venous blood access we used:
- CAVH-catheters 11.4 cm long with an internal diameter of 2.7 mm (M8CAVH4, Medcomp) in the femoral vessels, Shaldon catheters 15 cm long with an internal diameter of 2.3 mm, and Scribner shunts,
- arterial standard polyvinylcholoride (PVC) tubing 0.9 m long with an internal diameter of 4.36 mm, venous standard PVC tubing 1 m long.

Three types of hemofilters were used (See also Table 4.1 in Chapter 4):

- a polyacrylonitrilic (AN-69) plate hemofilter (15 compartments, length 26.8 cm, width 6.7 cm, channel height $200+0.26 \cdot TMP_m$ µm, membrane surface 0.43 m^2; SCU/CAVHD, Hospal, France),
- a polyacrylonitrilic (AN-69) capillary hemofilter (6000 fibers, total length 15 cm, including 2 cm within potting, internal diameter of fibers 240 µm, and 220 µm within potting, membrane surface 0.6 m^2; Multiflow-60, Hospal, France) and
- a polysulfone (PS) capillary hemofilter (4600 fibers, total fiber length 8.5 cm, internal diameter of fibers 200 µm, membrane surface 0.23 m^2; Spiraflo HFT02, Sorin Biomedica, Italy); all specifications according to manufacturers.
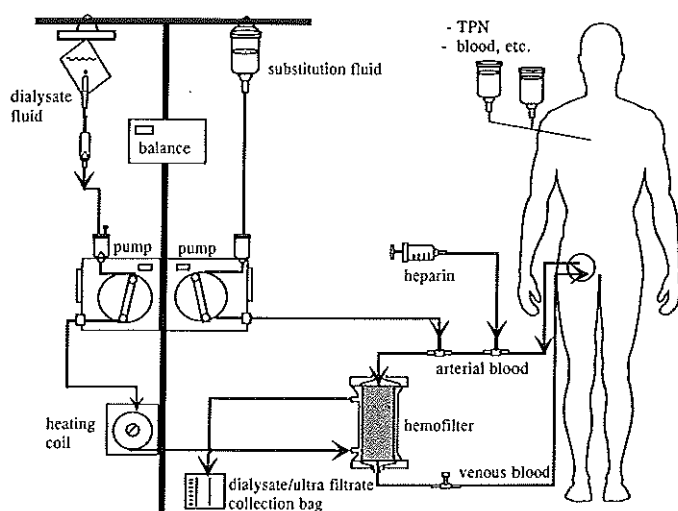
Figure 3.1: A schematic representation of a CAVHD system.

Hemofilters were prepared by rinsing the blood compartment with 2 liters of saline containing heparin 5000 U/l, allowing filtration to take place. Hemofilters were placed in the upright position, with the ultrafiltrate outlet up. Ultrafiltrate column height was about 60 cm. Standard anticoagulation consisted of heparin 500 U/h, infused into the arterial line of the hemofilter. No loading dose of heparin was given. No protamine was used. Three patients received no heparin because of excessive bleeding, thrombocytopenia or hepatic failure and coagulation disorders. Ringer's lactate as substitution fluid was infused into the arterial line (predilution). The amount of substitution fluid was adjusted hourly to the net ultrafiltration flow rate. Reasons for hemofilter replacement were clotting of the hemofilter or an ultrafiltration flow rate <200 ml/h. Furthermore, hemofilters were removed when dialysis was

no longer necessary or when clinical improvement allowed mobilization to treat the patient further with the conventional intermittent hemodialysis. Average hemofilter 'survival' time was 3 days.

Electronic pressure transducers were connected to the arterial and the venous lines to measure the pre-(P_{bi}, [mmHg]) and postfilter (P_{bo}, [mmHg]) hydraulic pressures. Both pressures were measured using the same pressure transducer. In the patients, we also measured intra-arterial (P_{ia},[mmHg]) and intra-venous (P_{iv}, [mmHg]) pressures by the same pressure transducers after clamping the line for 10 seconds. Blood flow rate through the arterial catheter (Q_{ba}, [ml/min]) before perfusing the predilution fluid was determined in duplicate by measuring the time required for an air bubble displacement over 13 ml of tubing. The flow rate of substitution fluid (Q_{pred},[ml/min]) was measured by weighing device. Arterial hematocrit (Ht_a) and plasma protein concentration (C_{pa}, [g/dl]) were measured to calculate the blood viscosity (η_b, [mmHg·min]) and the oncotic pressure (Π_p,[mmHg]). Ultrafiltration flow rate (Q_f, [ml/min]) was determined by timed collection of ultrafiltrate from the ultrafiltrate line over five minutes after switching off the dialysate pump.

In a separate study we took blood samples for viscosity measurements from 10 patients, aged 38 to 66 years, who had been treated in the intensive care department for at least three days. Viscosity measurements were performed using an apparatus that measures the flow rate of blood at 37°C through a glass capillary with a known resistance. The internal diameter of the capillary is 1.05 mm and the velocity is approximately 30 mm/sec, yielding shear rates similar to those within the fibers of the hemofilters.

3.5 RESULTS

Statistics
The clinical data are presented as means ± 1 S.D. The time dependent decrease of hemofilter permeability was analyzed by regression analysis. Previous experiments showed that a good fit was obtained by linear regression of the membrane index (MI) or hydraulic permeability (L_p) as a logarithmic function of treatment time (t, [hours]) [1]. This regression analysis was performed for each individual hemofilter. An approximately equal number of data points were obtained before and after 12 h of use. Slopes and extrapolated values at 12 h of use were compared by Wilcoxon's Rank test (see Table 3.5).

Resistance to blood flow
Causes of renal failure and the mean arterial blood pressure values (MAP) on starting CAVHD treatment are given in Table 3.1. The mean arterial pressure was below 70 mmHg in a third of the patients. Hematocrit and plasma protein concentration were determined to

calculate the blood viscosity at $37\,^{\circ}$C from different patients according to eq.(3.12). The component resistances R_{aa}, R_f and R_{va} were calculated from the measured pressure differences and the blood flow rates according to eq.(3.4), eq.(3.3) and eq.(3.5) respectively. In Table 3.2, the values of measured resistance (values as means $\pm$SD) are given for the different components of the extracorporeal circuit.

Table 3.1: Patient characteristics [11]. MAP: Mean arterial pressure on starting the CAVHD treatment.

Age	Cause of renal failure	MAP	Age	Cause	MAP
41	sepsis, hepatoreal syndrome	107	44	cardiogenic shock	58
59	sepsis, rapidly progressive glomerulonephritis	70	71	cardiogenic shock	69
60	rapidly progressive glomerulonephritis	107	64	cardiogenic shock	78
70	rapidly progressive glomerulonephritis	75	52	cardiogenic shock	67
29	thrombotic thrombocytopenic purpura	120	34	sepsis	66
25	trauma, shock, rhabdomyolyis	115	75	sepsis	96
62	sepsis, interstitial nephritis	64	64	sepsis	68
61	open hart surgery, shock	65	30	sepsis	105
49	tumor infiltration in the kidney	135	69	Sepsis	84
68	aortic surgery	108	64	legionella nephritis	106

On starting the CAVHD treatments, the CAVH-catheters had a resistance to blood flow of only 0.10 mmHg/(ml/min), while for the Shaldon catheters 0.16 mmHg per ml/min and for the Scribner shunt this value was 0.36 mmHg per ml/min. The average hemofilter resistance to blood flow was between 0.24 and 0.35 mmHg per ml/min. Using CAVH-catheters, the overall resistance (R_t) during CAVHD treatment was approximately 0.45 to 0.55 mmHg/(ml/min). This resulted in blood flow rates of 164$\pm$59 ml/min (range 63-284 ml/min). In Table 3.2, the observed resistances were compared with the resistances predicted from the component geometry and calculated blood viscosity. The values of the resistance of the circuit components we observed were two to three times higher than the values calculated from the circuit geometry and blood viscosity. With the CAVH catheters+tubing and the AN-69 capillary hemofilter, as can be seen from the ratios (α_i) of the observed resistances to the predicted resistances in Table 3.2, the ratio of the total observed resistance to the total predicted resistance ($R_t/R_{t,p}$=2.45) results in an overestimation of the blood flow rate (Q_{bx} in eq.(3.1)) by 145%. The discrepancy between the observed and predicted values of circuit resistance to blood flow may partly be explained by underestimation of blood viscosity. To determine the blood viscosity in the hemofilter, we measured the actual blood viscosity from the blood samples of 10 intensive care patients. Actual blood viscosity was measured at $37\,^{\circ}$C and at shear rates similar to those in the hemofilter and it ranged from 2.27×10^{-7} to 3.17×10^{-7} mmHg·min. This was 1.43 times (range 12.-1.5) higher than those calculated by eq.(3.12).

Clinical observations and theoretical predictions

Thus, the measured blood viscosity (See Table 3.3) was 1.43 times higher than the value calculated according to Pallone et al [7]. After correcting the blood viscosity by a factor of 1.43, the size ($R_t/R_{t,p}$=1.70) of the overestimation was 70%.

Table 3.2: Observed and predicted resistances to blood flow in mmHg·min/ml of the circuit components at the start of CAVHD treatment of different patients. $R_{n,i}$ [10^5/ml] is the resistance calculated from geometry. ( )$^+$: Values after being corrected with 1.43 for the predicted blood viscosity. ^{1}: Polysulfone

components of the extracorporeal circuit		observed resistance	predicted resistance	$R_{n,1}$	obs./pre. α_i	n
arterial access	tubing			1.0		
	CAVH catheter + tubing	0.10 ± 0.04	0.05±0.01	1.9	2.0 (1.4)$^+$	39
	Schribner shunt + tubing	0.36 ± 0.07				6
	Shaldons catheter + tubing	0.16 ± 0.05	0.08±0.01	3.2	1.9 (1.3)	6
filter	AN-69 plate hemofilter	0.25 ± 0.06	0.09±0.01	3.1	2.8 (1.9)	16
	AN-69 capillary hemofilter	0.24 ± 0.11	0.08±0.02	3.1	2.9 (2)	17
	^{1}PS capillary hemofilter	0.35 ± 0.14	0.14±0.01	4.7	2.4 (1.7)	17
venous access	tubing			1.1		
	tubing + CAVH catheter	0.10 ± 0.04	0.05±0.01	2.0	1.9 (1.3)	39
	tubing + Schribner shunt	0.36 ± 0.13				6
	tubing + Shaldons catheter	0.16 ± 0.05	0.09±0.01	3.3	1.9 (1.3)	6

Table 3.3: Blood viscosity measurements [11].

Nr.	Ht	C_p [g/l]	η_b[10^{-7} mmHg·min]	obs./pred.
1	0.21	55	2.84	1.33
2	0.31	49	3.55	1.49
3	0.25	55	2.66	1.17
4	0.21	53	3.23	1.54
5	0.26	36	3.06	1.53
6	0.33	45	3.69	1.55
7	0.3	75	3.93	1.41
8	0.34	54	3.96	1.54
9	0.26	54	3.05	1.33
10	0.24	56	3.11	1.38
average±SD	0.27±0.05	53.2±9.3	3.31± 0.43	1.43± 0.12

Hemofilter resistance to blood flow during the CAVHD treatment

Figure 3.2 shows the resistance to blood flow for an AN-69 capillary hemofilter during the treatment of one patient. Generally, there was no appreciable change in the hemofilter

resistance with time. In a few cases, a sudden increase in the resistance to blood flow heralded clotting of the hemofilter. A few hours before the hemofilter had become clotted completely, a sharp drop in the blood flow rate was observed.
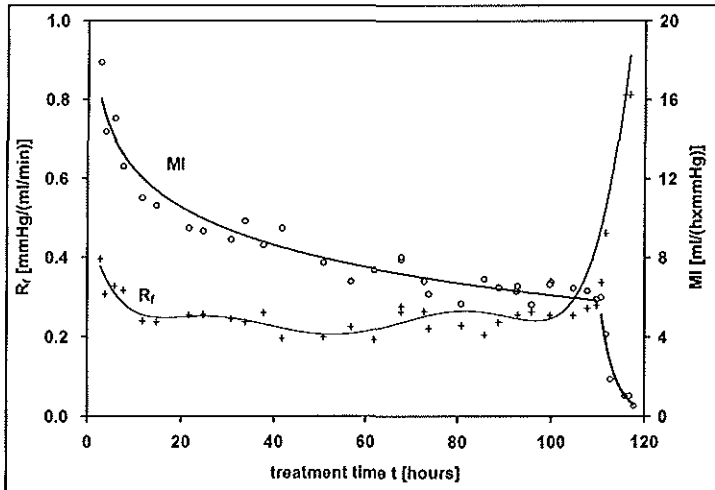
Figure 3.2: Recording the hydraulic permeability index (MI) and the hemofilter resistance (R_f) to the blood flow.

The average hemofilter resistance to blood flow was between 0.24 and 0.35 mmHg·min/ml. To compare the measured resistance of an AN-69 capillary hemofilter with the predicted values during the treatment, hematocrit and plasma protein concentrations were determined to calculate the blood viscosity at $37°C$ from four different patients. In Table 3.4, the observed and predicted values of the resistances of extracorporeal circuit are shown under different conditions, where the observed values of hemofilter resistance (R_f) higher than 0.4 mmHg/(ml/min) were not taken into account because of clotting. We found that the ratio of measured averaged resistance to that of predicted average resistance varied per patient. The average individual correction factors were calculated as $\alpha_a = 1.0$ for the arterial access, $\alpha_v = 0.9$ for the venous access and $\alpha_f = 2.8$ for the hemofilter. The average ratio $R_t/R_{t,p}$ was 1.5, resulting in 50% overestimation of the blood flow rate ($Q_{ba} = 297$ ml/min). The over-estimation of blood flow rate is mostly resulted from the underestimation of blood viscosity in the hemofilter. After correcting the blood viscosity by a factor of 1.43, the size ($R_t/R_{t,p} = 1.06$) of the overestimation was 6%. From the measurements of hemofilter resistance, recorded from different patients during about 5 days at arbitrarily chosen time intervals (See Figure 3.3), the correction factor ($\alpha_f/1.43 = R_f/R_{f,p}$) was determined in relation to various hemofilter resistance (R_f). We found that α_f is related to R_f according to the regression equation: $\alpha_f/1.43 = R_f/R_{f,p} = R_f/0.09$ ($R^2 = 0.96$, n=50) for $0.04 \leq R_f \leq 0.6$ mmHg·min/ml. From

this regression equation follows that the average value of the predicted hemofilter resistance was $R_{f,p}$ =0.09 mmHg·min/ml.

Table 3.4: Predicted and measured resistances to the blood flow from different patients with an extracorporeal circuit consisting of the CAVH catheters+tubing for both the arterial and venous access components and the AN-69 capillary hemofilter. Resistances are all in [mmHg per blood flow rate of 100 ml/min]. n (number of data points) = 4 for each patient.

| Patient nr. →	1	2	3	4	average
Q_{ha} [ml/min]	154.9±4.9	294.5±33.2	152.1±10.1	192.4±35.5	198.5±20.9
Q_f [ml/min]	10.4±2.7	14.1±2.4	8.4±3.2	9.3±2.3	10.6±2.4
Q_{pred} [ml/min]	10.8±2.9	14.3±2.8	6.3±2.9	4.0±0.8	8.9±2.4
C_{pa} [g/l]	56.6±7.3	47.0±5.3	81.7±0.3	67.6±3.4	63.2±4.1
Ht_a	0.25±0.05	0.26±0.05	0.23±0.02	0.32±0.01	0.27±0.03
P_{ia} [mmHg]	62.3±1.5	93.2±17.2	80.0±1.4	93.0±16.8	82.1±9.2
$R_{aa,p}$	8.31±0.79	7.80±0.83	9.30±0.30	9.78±0.32	8.80±0.56
R_{aa}	6.39±1.76	6.48±0.80	12.54±0.17	9.72±2.10	8.78±1.21
$R_{va,p}$	8.29±0.78	7.81±0.84	9.44±0.32	10.13±0.56	8.92±0.63
R_{va}	7.25±1.47	6.41±0.74	10.15±3.45	8.33±1.18	8.04±1.71
$R_{f,p}$	6.88±0.59	6.54±0.69	7.85±0.20	8.42±0.37	7.42±0.46
R_f	16.57±3.14	16.96±2.55	24.37±1.56	25.25±4.28	20.99±2.90
$\alpha_a = R_{aa}/R_{aa,p}$	0.77	0.83	1.35	0.99	1.00 (0.70)[+]
$\alpha_v = R_{va}/R_{va,p}$	0.87	0.82	1.08	0.82	0.90 (0.64)[+]
$\alpha_f = R_f/R_{f,p}$	2.41	2.59	3.10	3.00	2.83 (1.98)[+]
$\alpha_t = R_t/R_{t,g}$					1.50 (1.06)[+]
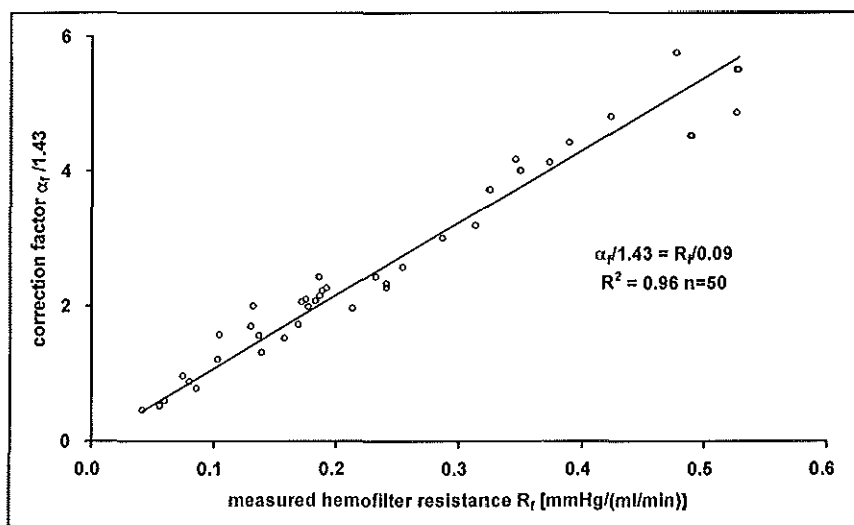
Figure 3.3: Correction factor ($\alpha_f / 1.43$) in relation to the observed hemofilter resistance (R_f).

From Tables 3.2 and 3.4 and Figure 3.3 can be seen that in CAVHD the method of predicting the hemofilter resistance to blood flow from the geometry and from the calculated blood viscosity from hematocrit, plasma protein concentration and temperature is not reliable. This is partly due to an underestimation of blood viscosity (1.43 times the measured blood viscosity), partly due to the fiber swelling and may be due to the protein adhesion on the membrane during the prolonged use of hemofilter and clotting.

Decline of ultrafiltration flow rate and membrane index over time

In Figure 3.4, the rate of ultrafiltration flow (Q_f) and the rate of replacement fluid infusion (Q_{pred}) are shown during the treatment. From Figure 3.4, it is apparent that ultrafiltration flow rate decreased over the treatment time (t) as:

$$Q_f(t) = 15 - 2.1\ln(t) \tag{3.27}$$

for t≤115 hours (R^2=0.95, n=31), while blood flow rate and mean transmembrane pressure difference (TMP_m) remained constant (See Figure 3.5). This shows that the membrane hydraulic permeability index (MI) decreased in time.
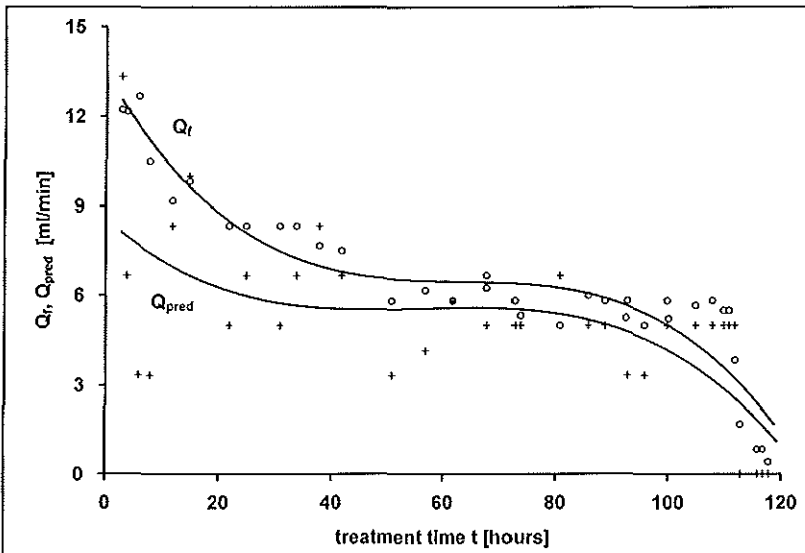

Figure 3.4: Recording the infusion rate of substitution fluid (Q_{pred}) and the rate of ultrafiltration flow (Q_f), which was measured by timed collection.

In Figure 3.2, the membrane hydraulic permeability index (MI) and the hemofilter resistance to blood flow are shown. The MI decreased over the treatment time according to:

$$MI(t) = 18.8 - 2.8\ln(t) \tag{3.28}$$

Clinical observations and theoretical predictions

for $t \leq 115$ hours ($R^2=0.94$, n=31), while the resistance remained constant (24 mmHg per 100 ml/min) until the hemofilter had become clotted. When the ultrafiltration flow rate was less than 5 ml/min, the hemofilter resistance showed an increase indicating that the hemofilter had become clotted. After a few hours, the hemofilter was completely clotted and eventually replaced with a new one.
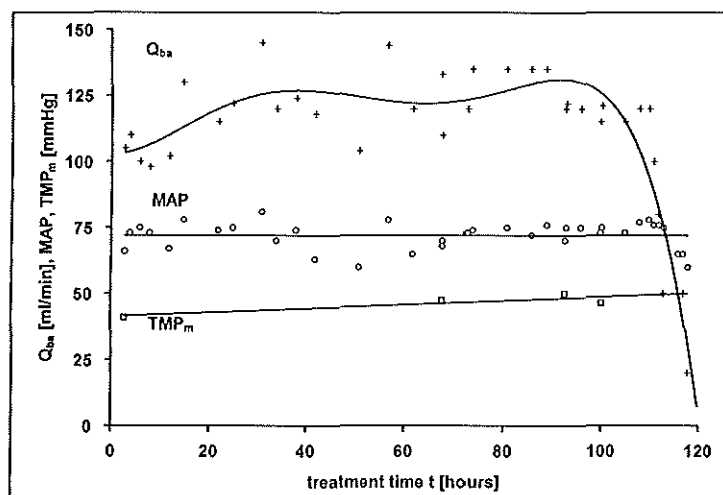
Figure 3.5: Recording the patient's arterial blood flow rate (Q_{ba}), mean arterial pressure (MAP) and hemofilter mean transmembrane pressure (TMP_m) during a CAVHD treatment of 120 hours.

Figure 3.2 shows that the membrane index MI was not affected by the hemofilter resistance until the hemofilter had become clotted. The survival time of this hemofilter was 5 days or less than 5 days due to early clotting of the hemofilter or other technical failures.

Decreasing the MI in time is presumably due to the decrease in the hydraulic permeability coefficient (L_p). This phenomenon has also been demonstrated by others [1,9,12]. It has been shown that during continued use of a membrane, a decline in the hydraulic permeability occurs because of protein adhesion [10,13]. In Figure 3.6, the average rate of decline of L_p with three different hemofilters is shown. Hydraulic permeability of both the AN-69 membranes was less than that of the polysulfone membrane (See Table 3.5). The decline in L_p was least apparent with a small polysulfone capillary hemofilter. The rate of the decrease in L_p was faster with the plate hemofilter than with the capillary hemofilter. In Table 3.5, the hydraulic permeability coefficients of three types of hemofilters are shown in units of cm/(min·mmHg) after interpolation for $t \geq 12h$.

Table 3.5: Hydraulic permeability coefficient (L_p, [cm/(min mmHg)])
of three types of hemofilters [11]. [1] : Value obtained by interpolation,
[2] : Slope b in the formula $L_p(t)=a-b\ln(t)$.

AN-69 capillary hemofilters		AN-69 plate hemofilters		PS capillary hemofilters	
L_p^1after 12h	slope[2]	L_p^1after 12h	slope[2]	L_p^1after 12h	slope[2]
2.69	0.39	2.81	0.67	6.47	0.55
3.66	1.55	0.56	1.62	5.94	1.30
2.57	0.60	5.70	1.79	4.11	0.05
2.14	0.34	2.34	0.84	6.27	0.70
2.90	0.73	2.26	1.05	4.50	1.27
2.60	0.98	2.87	2.01	6.53	0.53
2.81	0.87	2.02	1.53		
		2.97	1.26		
		3.35	1.05		
		2.85	1.10		
		3.23	1.08		
		0.92	1.03		
		1.71	2.53		
average: 2.77	0.72	2.58	1.35	5.03	0.69

The average L_p-values of 2.77 and 2.58 for the AN-69 hemofilters were both lower than the value of 5.03 for the polysulfone (PS) hemofilter ($p<0.01$). The slopes 0.72 and 0.69 for the capillary filters were both lower than the slope of 1.35 for the plate hemofilter ($p<0.05$).
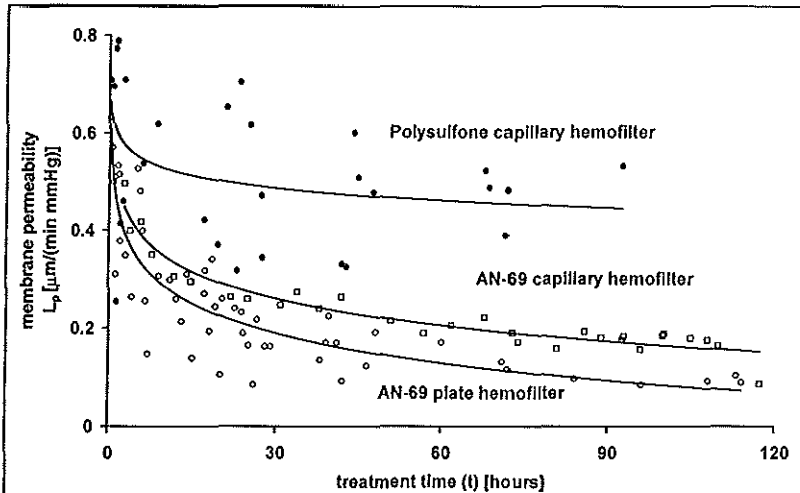
Figure 3.6: Membrane hydraulic permeability coefficient L_p with treatment time (t).

3.6 DISCUSSION AND CONCLUSION

Blood flow rate

Pallone and Peterson have shown that, for capillary and flat plate hemofilters, the resistance to flow may be predicted from the hemofilter geometry [2,7]. Their prediction was based on Poiseuille's law. In their calculations it was assumed that blood behaves as a Newtonian fluid and that the blood flow through the hemofilter is laminar. Furthermore, they used data from the literature that allow the calculation of blood viscosity from hematocrit, protein concentration and temperature. In our study we used the same methods. We found that the hemofilter resistance to flow was two to three times higher than the predicted value. A similar finding has recently been reported for a number of other hemofilters [3]. To explain this discrepancy we considered clotting of fibers, underestimation of blood viscosity as we have shown in this chapter, turbulent flow and/or additional pressure losses due to the sudden changes in the blood path diameter and deviations of the internal diameter of the fibers. To determine the effect of these factors on the observed hemofilter resistance to the blood flow, we decided to measure the resistance of a number of different hemofilters in a laboratory setting (See Chapter 4). The measured circuit resistance to blood flow showed a discrepancy when we predicted it from manufacturers' specifications and blood viscosity. The discrepancy between the predicted and the actual hemofilter resistance was partly due to an underestimation of blood viscosity and partly due to an increased resistance in the hemofilter as a result of, probably, a small decrease in the fiber diameter. Also, small pressure losses along the extracorporeal circuit due to deviations from ideal cylindric geometry (constriction and widening in the hemofilter potting and access components) contribute to the discrepancy. Clearly, the blood viscosity which is estimated according to Pallone's expression, eq.(3.12), has to be corrected by a factor 1.43 per each mmHg/(ml/min) of the hemofilter resistance.

Estimating the blood flow rate from patients output such as arterio-venous pressure difference, protein concentration, hematocrit and hemofilter manufacturer specification is not reliable, as far as the hemofilter is concerned. Ideally, the blood flow rate should be measured continuously. It is technically feasible to measure blood flow by means of the echo-Doppler principle, using a flow probe around the blood line, but the necessary equipment is not yet widely available. As an alternative, injecting a 0.3 ml air bubble into the blood line may help to determine the blood flow rate. In the laboratory setting, we have measured the blood flow rate by using the echo-Doppler principle as well (See Chapter 4.).

Ultrafiltration flow

The fall in the ultrafiltration flow rate over time may be explained both by changes in the membrane permeability, presumably resulting from protein adsorption to the membrane, and by a fall in the available membrane surface area, e.g. due to unsuspected clotting of fibers. For reasons given above, unsuspected clotting of fibers is unlikely to occur under clinical

conditions. Therefore, the decrease in membrane permeability with time is more likely to be due to ongoing protein adsorption. We should note that according to Jenkins et al [12] the hemofilter hydraulic permeability may decline even after contact with water alone. To our knowledge, however, others have not reproduced this finding. For the AN-69 capillary hemofilter we did not observe a fall in the hydraulic permeability coefficient (L_p) between 1 and 48 hours of saline perfusion, but we did observe a fall in L_p with plasma and blood (See Chapter 4). During continuous treatments the net ultrafiltrate production is measured every hour and the substitution infusion rate is adjusted accordingly. A sufficient net ultrafiltration rate is an easy indication that the system functions well. A very low ultrafiltration flow rate may be an indication that blood flow has stopped due to clotting at the venous end of the hemofilter. When the rate of ultrafiltration has become less than 200 ml/h or when clotting of the hemofilter has occurred, the hemofilter must be replace. If the catheters are flushed, changing of hemofilters may generally be deferred so as to take place during working hours.

Clinical implications
In critically ill patients, in whom CAVH(D) is indicated, blood pressure tends to be low. A low resistance to blood flow of the extracorporeal circuit is therefore mandatory. In this respect CAVH catheters are clearly to be preferred to Scribner shunts. The use of a Scribner shunt instead of catheters doubled the overall resistance of the extracorporeal system. In our view, Scribner shunts should be regarded as unsuitable for CAVH(D). The resistance to blood flow of the hemofilters studied was low enough to ensure an adequate blood flow rate in most cases. To obtain a reasonably accurate prediction of blood flow rate under clinical conditions, data of hemofilter resistance and a more accurate estimation of blood viscosity in a laboratory setting were needed. With regard to the three hemofilters studied, the ultrafiltration rate was always high enough for correction of over-hydration. On the other hand, because of the time dependent fall in membrane permeability, the ultrafiltration flow rate will soon become too low for adequate solute removal through convection alone. In case of CAVH this necessitates frequent changes of the hemofilters. In case of CAVHD the fall in ultrafiltration flow rate will result in a fall of solute removal by convection and also by diffusion since the number of membrane pores, with which the rate of solute removal by diffusion increases, will be decreased due to the same factors influencing the fall in the ultrafiltration flow rate.

Feasibility of predicting hemofilter performance
The feasibility of continuous therapies such CAVH and CAVHD depends strongly on the hemofilter performance that may fail due to technical failures, usually because of inadequate blood flow. Inadequate low rates of blood flow can lead to excessive hemoconcentration that in turn results in an increase in the hemofilter resistance, causing early clotting of the hemofilter. Estimating the adequate blood flow rate to achieve a desired rate of patient's fluid loss and toxin clearance depends not only on the patient's output but also on the

mathematical modeling that describes the solute and fluid transport across the hemofilter. Apparently, predicting the blood flow rate from manufacturer specifications is not reliable and has to be measured continuously. When this model is applied for predicting the blood flow rate, the correction factor 1.43 for the blood viscosity has to be taken into account.

3.7 REFERENCES

[1].   Van Geelen JA, Vincent HH, Schalekamp MADH. Continuous arterio-venous haemofiltration and haemodiafiltration in acute renal failure. Nephr Dial Transpl 1988; 2: 181-186.

[2].   Pallone TL, Petersen J. Continuous arteriovenous hemofiltration: An in vitro simulation and mathematical model. Kidney Int 1988; 33: 685-698.

[3].   Olbricht CJ, Haubitz M, Häbel U, Frei U, Koch K-M. Continuous arteriovenous hemofiltration: In vivo functional characteristics and its dependence on vascular access and filter design. Nephron 1990; 55: 49-57.

[4].   Merrill EW, Pelletier GA. Viscosity of human blood: Transition from Newtonian to non-Newtonian. J Appl Physiol 1967; 23: 178-82.

[5].   Min-Shing Lih M. Transport phenomena in medicine and biology. J Wiley & Sons, New York 1975 (Ed.)

[6].   Gaehtgens P. Flow of blood through narrow capillaries: Rheological mechanisms determining capillary hematocrit and apparent viscosity. Biorheology 1980; 17: 183-89.

[7].   Pallone TL, Hyver S, Petersen J. The simulation of continuous arteriovenous hemodialysis with a mathematical model. Kidney Int 1989; 35: 125-133.

[8].   Landis EM, Pappenheimer JR. Exchange of substances through the capillary wall. In Handbook of Physiology. Circulation, (vol II chapt 29), Washington, D.C., Am Physiol Soc, 1963 pp 962-1034.

[9].   Sigler MH, Teehan BP, van Valkenburg D. Solute transport in continuous hemodialysis. Kidney Int 1987; 32; 562- 567.

[10].   Colton CK, Henderson LW, Ford CA, Lysaght MJ. Kinetics of hemofiltration. I. In vitro transport characteristics of a hollow fiber blood ultrafilter. Journal of Laboratory and Clinical Medicine 1975; 3; 355-371.

[11].   Vincent HH, Akcahuseyin E, Vos MC, van Ittersum JF, van Duyl WA, Schalekamp MADH. Determinants of blood flow and ultrafiltration in continuous arteriovenous haemodiafiltration: Theoretical predictions and laboratory and clinical observations. Nephrology Dialysis Transplantation 1990; 5; 1031-1037.

[12].   Jenkins RD, Kuhn RJ, Funk JE. Permeability decay in CAVH hemofilters. Trans Am Soc Artif Intern Organs 1988; 34: 590-93.

[13].   Bosch T, Schmidt B, Santleben W, Gurland HJ. Effect of protein adsorption on diffusive and convective transport through polysulphone membranes. Contrib Nephrol 1985; 46; 14-22.

DETERMINANTS OF BLOOD AND ULTRAFILTRATION FLOW RATES: Laboratory observations and theoretical predictions

<div align="right">

Chapter 4
</div>

4.1 INTRODUCTION

Patients with acute renal failure treated with continuous arterio-venous hemodiafiltration (CAVHD) are characterized with their circulatory instability, leading to low and/or unstable blood pressures. The combination of a low and unstable blood pressure makes it quite difficult to judge how much fluid can be withdrawn safely. Besides this, failure of the technique may occur because of an inadequate blood flow rate, leading to excessive hemoconcentration and clotting. In Chapter 3 we introduced a methodology [1] to predict the blood flow rate under different clinical conditions and hemofilter characteristics. We related the blood flow rate to the resistance exerted by the extracorporeal circuit, based on geometry and blood viscosity. With three kinds of hemofilters (AN-69 capillary, AN-69 plate and PS capillary), we showed that the observed hemofilter resistance to blood flow was about 3 times greater as that calculated from geometry and predicted blood viscosity (See Chapter 3). Also the resistance was showed to remain constant during the whole treatment time until the hemofilter began to clot. To obtain a reasonably accurate prediction of blood flow rate under clinical conditions, a more accurate estimation of the hemofilter resistance to blood flow in a laboratory setting was needed.

In this chapter, the resistance to flow was measured with fluid solutions of different viscosity for some CAVH(D) capillary hemofilters (See Table 4.1). The hemofilters were perfused with saline, sucrose solution and pig blood as perfusion fluid. The viscosity values of saline and sucrose solutions were taken from published data and that of the pig blood was measured. Using the viscosity values provided, we compared the resistance of each hemofilter with the theoretical predictions. The effect of hemofilter resistance on the hydraulic performance (ultrafiltration) was also investigated by measuring the membrane permeability index (MI) and the resistance to (human) blood flow simultaneously over a survival time of about 220 hours.

4.2 METHODS

Predicting hemofilter resistance from housing and membrane geometry
A typical capillary hemofilter is schematically depicted in Figure 4.1. Although the hollow fibers seem like a bundle of horizontal straight tubes lying parallel to each other, they differ very much from the straight tube configuration. However, in many studies it has been assumed that a hollow fiber can be considered as a straight porous tube configuration. In flow systems, such as the capillary hemofilters encountered in both *in vitro* and *in vivo* studies, the

pressure drop results mainly from the friction of the flowing fluid with the surface of tubing and to some extent from some additional irregularities such as bends, valves, fittings, bifurcation, sudden expansions and constrictions.
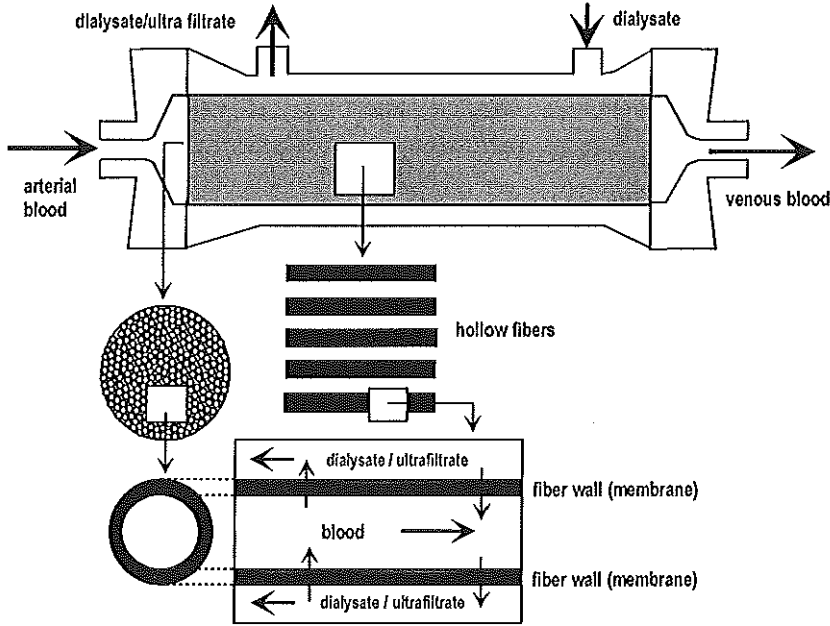
Figure 4.1: A schematic representation of an idealized capillary hemofilter configuration.

For a steady flow of incompressible fluid in horizontal tubes with irregularities, the pressure loss is calculated as [2]:

$$\Delta P_b = \rho \sum_i (f_f \frac{1}{2} v_m^2 4 \frac{L}{d})_i + \rho \sum_j (\frac{1}{2} v_m^2 e_v)_j \qquad (4.1)$$

where ρ is density of the fluid, f_f the friction factor, v_m the average longitudinal velocity of the flowing fluid, L the length of a segment, d the internal diameter, e_v the friction loss factor of the irregularity. The first term on the right-hand side of eq.(4.1) represents the pressure loss due to friction forces of i straight tube sections, the second term represents the pressure loss due to j irregularities. The average velocity, assuming a parabolic velocity profile, is calculated from the fluid flow rate (Q_b) dividing by the cross-sectional area of the tubing:

$$v_m = \frac{4 Q_b}{\pi d^2} \qquad (4.2)$$

The friction factor f_f depends on the Reynold number (R_e). For a laminar flow ($R_e < 2100$):

$$f_f = 16R_e^{-1} \tag{4.3}$$

and for a turbulent flow ($R_e > 2100$):

$$f_f = 0.0791R_e^{-0.25} \tag{4.4}$$

The Reynold number is given by:

$$R_e = dv_m \frac{\rho}{\eta} \tag{4.5}$$

where η is the fluid viscosity. The values of e_v for some obstacles can be found in standard handbooks and texts [3-4]. For a sudden expansion:

$$e_v = (1 - \frac{S_s}{S_b})^2 \tag{4.6}$$

and for a sudden constriction:

$$e_v = 0.45(1 - \frac{S_s}{S_b}) \tag{4.7}$$

where S_s and S_b are the cross-sectional areas of narrow and wide parts of tubing respectively. Substitution of eqs.(4.2), (4.3) and (4.5) in the first term on the right-hand side of eq.(4.1) yields the Hagen-Poiseuille's relationship:

$$\rho \sum_i (f_f \frac{1}{2} v_m^2 4 \frac{L}{d})_i = R_{fp} Q_b \tag{4.8}$$

with

$$R_{fp} = \sum_i (\frac{128\eta L}{N\pi d^4})_i \tag{4.9}$$

where N is the number of tubes (fibers) lying in parallel and R_{fp} is the resistance due to friction forces only, called the Poiseuille's resistance to the flowing fluid in a straight tubing. On substituting eq.(4.2) in the second term of the right-hand side of eq.(4.1) and dividing by Q_b, we find the resistance to flowing fluid due to irregularities:

$$\sum_j (\frac{8 \rho e_v}{\pi^2 d^4})_j Q_b = hQ_b \tag{4.10}$$

The total resistance to flowing fluid becomes:

$$R_f = R_{fp} + hQ_b \tag{4.11}$$

where R_{fp} is the Poiseuille's resistance for laminar flow and has to be considered as the resistance to flowing fluid without irregularities. hQ_b is the resistance because of the irregularities and flow rate. According to eq.(4.11), the resistance to flowing fluid varies with a fluid flow rate (Q_b) with the variation coefficient (h), representing the change in R_f per unit

Laboratory observations and theoretical predictions

flow rate (slope). Eq.(4.11) is valid for laminar flow. For turbulent flow, the total resistance can be derived on the same way as eq.(4.11) using the friction factor f_f in eq.(4.4).

Laboratory protocol

Using saline as perfusion fluid, we first tested the method of calculating the resistance to flow by measuring the flow rate and pressure drop over a 1.52 m long glass tubing with an inner diameter of 4.1 mm and also for a 2.23 m long standard polyvinyl chloride (PVC) blood tubing with an inner diameter of 4.36 mm. Then the resistance of some CAVH(D) capillary hemofilters (See Tables 4.1 and 4.2) were studied at different flow rates.
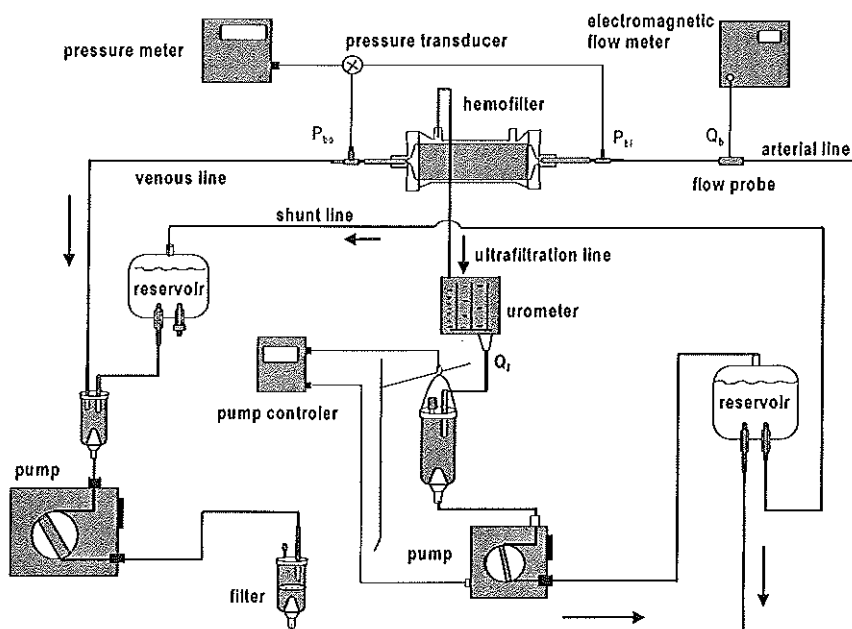
Figure 4.2: Experimental set-up to measure the hemofilter permeability index (MI) and resistance to flow (R_f).

The resistance of AN-69 capillary hemofilters was determined also with sucrose solution and pig blood as perfusion fluid. Eight AN-69 capillary hemofilters were used. They were all first perfused with saline, then two hemofilter were perfused with a sucrose solution and three hemofilters were perfused with pig blood (see Table 4.2 for further specifications). Hemofilters were prepared by rinsing the blood compartment with 2 l of saline containing heparin 5000 U/l, allowing filtration to take place. After that, the dialysate compartment was closed. Blood tubing with an inner diameter of 4.3 mm, containing side ports was used and adjusted so we could measure the pressure in the perfusion fluid 2 cm before and after the hemofilter. An

electromagnetic flow probe was inserted in the tubing so that mean flow rate could be measured continuously. Flow rates were measured also by an ultrasound Doppler velocity meter and by water column height. The experiments were performed at room temperature, with the experimental set-up shown in Figure 4.2. Hemofilters were in the horizontal position. A Rhodial[R] or Belco[R] blood pump was used to generate pulsatile flow rates from 50 to 600 ml/min. The hemofilter resistance to flow was thus measured at different flow rates. Furthermore, with all three solutions we once changed the set-up to create an open circuit with a container at a variable height, in which gravity generated a constant flow through the hemofilter and the pump was used to return the fluid to the container. Values of viscosity for the saline and sucrose solutions were taken from published tables [5]. The viscosity of pig blood with a hematocrit value of 0.23-0.26 was measured at room temperature with a Viscomat viscosity meter.

Further, the hemofilter resistance (R_f) and membrane permeability index (MI) of an "AN-69" capillary hemofilter were recorded during about 220 hours under laboratory conditions, with an experimental set-up as is shown in Figure 4.2. From arterial line, the plasma protein concentrations were measured to determine the transmembrane pressure difference (TMP). To keep the hematocrit value constant during the experimentation, the ultrafiltrate was recirculated into the arterial line by using a blood pump. A specially designed electronic circuit was used to regulate the blood pump controlling the amount of ultrafiltrate to be recirculated into the arterial line. Ultrafiltration flow rate was determined by timed collection. The pre- and postfilter pressures were measured with the same pressure transducers.

4.3 RESULTS

Resistance to flow

We plotted measured resistance of hemofilters and tubing against flow rates. Linear regression analyses were used to calculate the slope (h) and the Poiseuille resistance (R_{fp}) at a zero slope or at a zero flow rate (Q_b) according to eq.(4.11). The slopes were also calculated from eq.(4.10). The results of resistance measurements are given in Table 4.2, Figure 4.3 and Figure 4.4. For both glass and PVC tubing with saline as perfusion fluid, the resistance to a light pulsatile flow was in accordance with that predicted according to Poiseuille's law (with a relative error less than 10%). The flow rates at which turbulence may occur were calculated from eq.(4.2) and eq.(4.5). In a laminar flow region ($R_e < 2100$), an average value of the resistance (R_f) was calculated over the flow rates.

Under the same laboratory conditions using saline as perfusion fluid, the resistances (R_f) of six hemofilters from five different manufacturers were measured and compared with the values calculated from eq.(4.9). For all the hemofilters, the observed values were higher (up

to 50%) than the calculated values. To explain this discrepancy, we measured the diameters of many arbitrarily chosen fibers (of the Hospal AN-69 hemofilter). From one fiber only, at least 10 diameters along the fiber length were measured. In total 308 of diameters were measured. Based on the results of the diameter measurements, the resistance was calculated again (See Table 4.2). The difference between the calculated and observed values of R_f was 2%. Only for Hospal AN-69 hemofilter, the resistance increased slightly with the flow rate. The calculated slopes (the variation in R_f per 100 ml/min) were different from those obtained from the regression analysis. The calculated slope of Asahi 23320 hemofilter only was in good agreement with the observed value.

Table 4.1: Manufacturer data of CAVH(D) capillary hemofilters and calculated resistance to flow for blood, sucrose solution (or pig blood) and saline as perfusion fluid. [1] : wet condition, [2] : calculated from measured resistance.

hemofilter	type	d_m	d_f	L_r	N	S	R_{fp} blood	R_{fp} sucrose	R_{fp} saline
Hospal Multiflow-60	AN-69	50	[1]240	15	6	0.6	10.7	8.6	3.8
Amicon D-20	PS	75	250	12.7	5	0.4	9.3	7.4	3.3
Amicon D-30	PS	75	250	21.2	5	0.7	15.5	12.4	5.5
Gambro FH 22	PA	60	215	4.1	2.1	0.16	44.8	35.8	16.0
Gambro FH 66	PA	60	215	17.2	6.2	0.59	18.5	14.8	6.6
Fresenius A-V 400	PS	35	220	25.5	4.5	0.7	34.5	27.6	12.3
Sorin HFT 02	PS	40	200	12.0	4.6	0.24	20.3	16.3	7.3
Renaflo HF250	PS	40	280	14.0	2.8	0.25	11.6	9.3	4.1
Renaflo HF500	PS	40	280	21.5	3.35	0.5	14.9	11.9	5.3
Asahi APF-03	PAN	35	250	18.5	3.4	0.39	19.9	15.9	7.1
Asahi APF-6	PAN	35	250	18.5	6.4	0.6	10.6	8.4	3.8
Asahi 23320	PAN	-	200	22	6.5	[2]0.86	30.2	24.1	10.8
Asahi 24527	PAN	-	200	22	6.5	[2]0.86	30.2	24.1	10.8

AN-69: Acrylonitrile-69, PS: Polysulfone, PA: Polyamide, PAN: Polyacylonitrile, d_m: fiber wall thickness [μm], d_f: fiber internal diameter [μm], L_r: fiber length [m], N: number of fibers [x10^3], S: effective membrane surface area [m^2], R_{fp} [mmHg/(100 ml/min)]: resistance to flow calculated from Hagen-Poiseuille's relationship.

Viscosity [mmHg min]: $3.5 \cdot 10^{-7}$ (blood wth Ht=0.25)

$2.8 \cdot 10^{-7}$ (sucrose or pig blood with Ht=0.23-0.26)

$1.2 \cdot 10^{-7}$ (saline)

Table 4.2: Resistance to fluid flow for tubing and some capillary hemofilters.
R_f [mmHg/(100 ml/min)]= R_{fp} + h Q_b, with h (slope) in units of % per 100 ml/min.

tubing hemofilter	perfusion fluid	calculated resistance		measured resistance			$R_f(h=0)/R_{fp}$
		R_{fp}	h	R_f (h=0)	[3]R_f	h	
glass tubing	saline	2.27	0.0	1.92	2.20±0.46	0.05	0.86
PVC tubing		3.15	0.0	3.16	3.44±0.21	0.04	1.00
Hospal AN-69		3.97	1.55	5.42	5.87±0.25	4.1	1.37
"		[1]4.06					1.33
"		[2]5.54					0.98
Sorin HFT02		7.4	0.9	8.44	8.44±0.15	0.0	1.14
Asahi 23320	saline	10.92	0.6	14.03	13.87±0.24	0.7	1.28
Asahi 24527		10.92	0.6	12.27	12.03±0.26	0.1	1.12
Renaflo HF 250		4.01	1.6	5.74	5.76±0.16	0.4	1.43
Diafilter 30		13.41	0.5	20.21	20.57±0.49	1.2	1.51
8x AN-69 filters	saline	3.9	1.55	[4]5.5±0.9		[4]7.2±1.8	1.41
2x AN-69 filters	sucrose	9.1		13.2±2.0		5.0±0.1	1.45
3x AN-69 filters	pig blood	9.1		23.3±1.2		0.5±0.8	2.56

$\eta = 1.25 \cdot 10^{-7}$ mmHg min (for saline),

$\eta = 2.80 \cdot 10^{-7}$ mmHg min (for sucrose solution and pig blood with Ht=0.23 - 0.26).

[1]: fiber diameter 220 μm in the potting (L=2 cm) and 240 μm in a fiber block (L=13 cm)

[2]: fiber diameter 231.6 μm (n=52) in the potting and 217.4 μm (n=266) in a fiber block measured in a separate study (8-10% less than the manufacturer specification),

[3]: average value over the flow rates in a laminar flow region (See Figure 4.4),

[4]: average value over the number of hemofilters used

From the measurements of resistance to flow of a number of Hospal AN-69 capillary hemofilters with saline (8 hemofilters) and sucrose solution (2 hemofilters) we observed that both with saline and with the sucrose solution, the resistance was 40% higher than the values calculated according to manufacturer specifications. Similar values were obtained with either pulsatile or constant flows. The resistance rose slightly with increasing flow rates. With pig blood with Ht=0.23-0.26, the resistance to flow was 156% higher than the calculated value, and it did not increase with the flow rates (See Figure 4.4).

Permeability index

Perfusing the AN-69 capillary hemofilters with saline, plasma and human blood, we studied the time courses of the hemofilter resistance, $R_f(t)$, and the membrane permeability index, MI(t) (known as ultrafiltration coefficient). Three AN-69 capillary hemofilters were used.
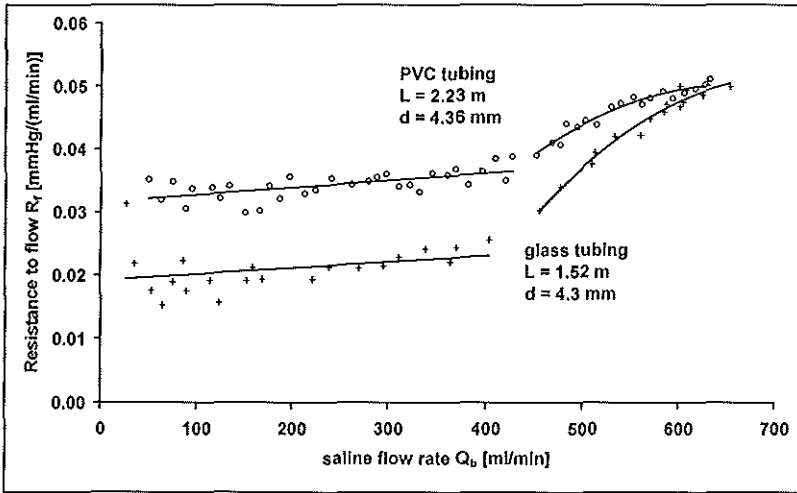
Figure 4.3: Resistance to flow, measured over a standard PVC tubing and a glass tubing, in relation to flow rate. Turbulent flow occurs at Q_b = 426 ml/min for glass tubing and at Q_b = 432 ml/min for PVC tubing.
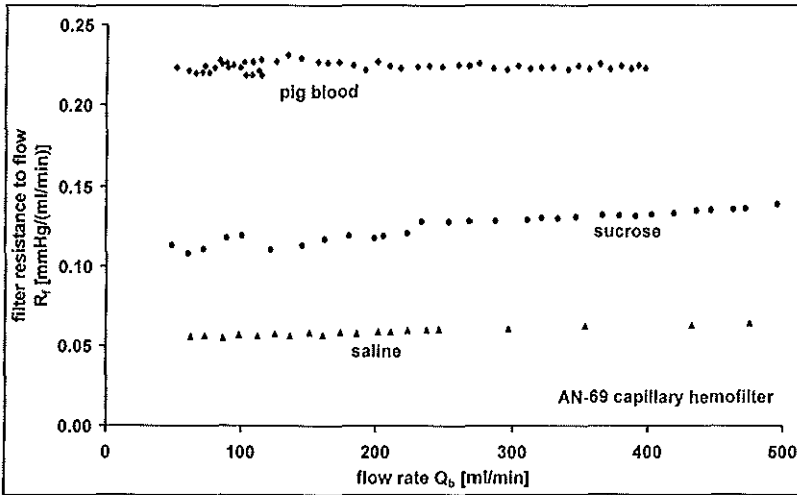
Figure 4.4: Resistance to flow of AN-69 capillary hemofilter, using saline, sucrose and pig blood.

One hemofilter was perfused with saline during about 140 hours. Neither a decrease in MI nor an increase in R_f was observed. A second hemofilter, perfused with plasma showed a decrease in MI between 1 and 51 hours according to the following regression equation:

$$MI(t) = 12.4 - 1.1\ln(t) \qquad (4.12)$$

with ($R^2 =0.75$, n=109). A third hemofilter, perfused with human blood showed a decrease in MI between 1 and 140 hours according to the following regression equation:

$$MI(t) = 16.7 - 2.1\ln(t) \tag{4.13}$$

with ($R^2 =0.74$, n= 210). In Figure 4.5, the recorded MI and R_f observations during about 220 hours experimentation were shown. Up to about 140 hours of human blood perfusion, the R_f was about 0.16±0.01 mmHg·min/ml. Afterwards, the R_f increased up to 0.6 mmHg·min/ml within 20 hours. The sudden increase of R_f was an indication of clotting. Within hours was the hemofilter completely clotted. We also observed a similar sudden increase of R_f under clinical conditions, see Chapter 3.
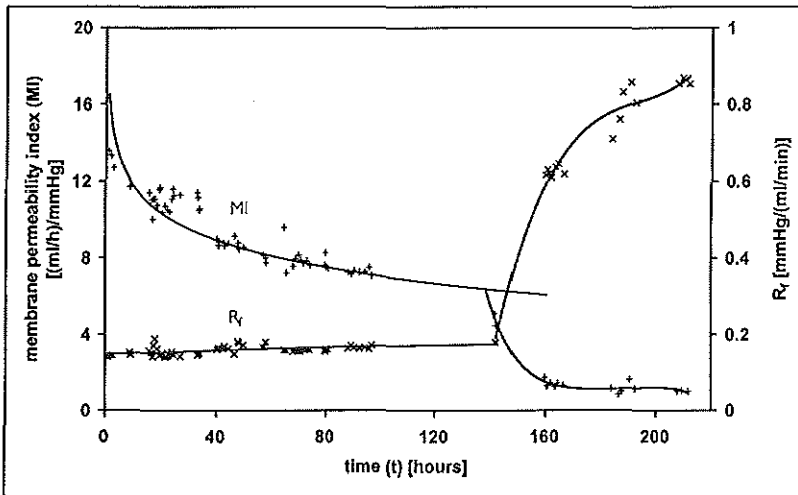
Figure 4.5: Membrane permeability index (MI) and the filter resistance (R_f) of an AN-69 capillary hemofilter, perfused with human blood (Ht=0.25-0.3) in relation to time (t).

4.4 DISCUSSION AND CONCLUSION

Laboratory measurements showed that the resistance of tubing was in accordance with the calculated value, which argues against gross methodological mistakes. The resistance of the hemofilter, perfused with saline or a sucrose solution, was 40% higher than expected. Furthermore, it was to some extent flow dependent, suggesting that turbulence does occur, most likely at the hemofilter inlet. However, this can hardly explain why the extrapolated resistance at a virtually zero flow rate was increased with 40%. Also, when we applied Bernouilli's law (See Eq.(4.10)) to estimate the pressure drop that results from the sudden change in diameter at the hemofilter in- and outlet [6], we calculated a pressure drop of far less than 1 mmHg. On the other hand, a 40% increase in R_f would be explained if the fiber

diameter would be a mere 8-10% lower than the given value. When hemofilters were perfused with pig blood, the discrepancy between the observed and predicted resistance was 156%, which rose to a suspicion that the pig blood viscosity measured in laboratory was not the same with that in the hemofilter . With human blood, the R_f was 0.16 mmHg·min/ml when a high dose of heparin prevented clotting. This argues against a significant contribution of clotting of fibers to the hemofilter resistance. The predicted value of R_f with human blood was 0.08 mmHg ·min/ml (in Chapter 3). On the other hand, comparison of actual blood viscosity with the value calculated according to eq.(3.17) confirmed our suspicion that we had grossly underestimated blood viscosity (Chapter 3). With blood, the R_f no longer seemed flow dependent, probably showing that the higher viscosity of blood diminishes turbulence. If the blood flow rate would be predicted by just combining this laboratory data on hemofilter resistance during blood perfusion with a more accurate estimation of blood viscosity (considering the correction factor of 1.43) and a fiber diameter 8-10% less than the specified, the flow rate would be overestimated by only 20%. It should be noted that according to Jenkins et al [7] the hemofilter hydraulic permeability may fall even after contact with water alone. To our knowledge, however, this finding was not reproduced by others. For the AN-69 capillary hemofilter we did not observe a fall in hydraulic permeability between 1 and 150 hours of saline perfusion (data not shown). The resistance to flow of the hemofilters studied was low enough to ensure an adequate blood flow rate commonly. By using laboratory data on hemofilter resistance and a more accurate estimate of blood viscosity, a reasonably accurate prediction of a blood flow rate under clinical conditions is feasible.

4.5 REFERENCES

[1]. Vincent HH, Akcahuseyin E, Vos MC, van Ittersum JF, van Duyl WA, Schalekamp MADH. Determinants of blood flow and ultrafiltration in continuous arteriovenous haemodiafiltration: Theoretical predictions and laboratory and clinical observations. Nephrology Dialysis Transplantation 1990; 5; 1031-1037.

[2]. Min-Shing Lih M. Transport phenomena in medicine and biology. J Wiley & Sons, New York 1975 (Ed.), p.328

[3]. Bird RB, Stewart WE and Lightfoot EN. *Transport Phenomena*. Wiley: New York, 1960. p.217

[4]. Smiht JM, Stammers E, Janssen LPBM. *Physicshe Transportverschijuselen* I. Delftse Uitgevers Maatschappij, Delft, 1984, Holland. p.47

[5]. Sohen HA and Harte EA. (Eds.). Handbook of biochemistry. Selected data for molecular biology. The Chemical Rubber Co. Cleveland, Ohio, 1968.

[6]. Gaehtgens P. Flow of blood through narrow capillaries: Rheological mechanisms determining capillary hematocrit and apparent viscosity. Biorheology 1980; 17: 183-89.

[7]. Jenkins RD, Kuhn RJ, Funk JE. Permeability decay in CAVH hemofilters. Trans Am Soc Artif Intern Organs 1988; 34: 590-93.

SOLUTE AND VOLUME TRANSPORT IN CONTINUOUS ARTERIO-VENOUS HEMODIAFILTRATION

5.1 INTRODUCTION

Continuous arterio-venous hemodiafiltration (CAVHD) is characterized by the use of a small surface highly permeable hemofilter, spontaneous blood flow and spontaneous ultrafiltration. Solutes are removed by simultaneous convection, i.e., plasma water is removed together with all dissolved molecules that can pass through the membrane pores, and by diffusion [1,2]. CAVHD is a combination of continuous arteriovenous hemofiltration (CAVH) with slow hemodialysis, but it differs from CAVH, conventional intermittent hemodialysis and intermittent hemodiafiltration in several respects:

1)   With CAVH, solute transport occurs by convection and it is limited by the amount of ultra filtrate production. The patient's blood is pressed into hollow fibers with a highly permeable membrane. As a result of pressure difference across the membrane, fluid is lost from the plasma and it becomes a part of the ultra filtrate. In hemodialysis, diffusive transport is the major principle underlying blood purification, especially for the elimination of substances in the low molecular weight range, e.g., of urea and of creatinine. In CAVHD, however, the solute transport occurs both by convection and by diffusion simultaneously. Both processes have an influence on one another [3]. Ultrafiltration leads to an increased solute concentration in the dialysate side of the hemofilter and thereby decreases diffusion. Dialysis lowers the solute concentration in plasma water and thereby decreases the amount of solute that is removed by ultrafiltration. The ultrafiltration is due to the difference between spontaneous physiological blood pressure and the pressure on the dialysate side as a result of flows.

2)   Since the CAVHD treatment is a slow and continuous process, the rate of dialysate flow (up to 60 ml/min) is lower than it is in conventional hemodialysis (500 ml/min). Dialysate flow rates (10-60 ml/min) are very low compared to the blood flow rates (50-350 ml/min) and, consequently, the change in dialysate solute concentration over the length of the hemofilter cannot be taken to be linear, as in conventional models of dialysis [4]. The dialysate flow rates that are used in CAVHD might be too low for optimal distribution of dialysate over the dialysate compartment. With low dialysate flow rates, the resistance to diffusion exerted by the dialysate compartment may be much higher than in conventional hemodialysis.

3)   The diffusive performance of a CAVHD hemofilter is determined mostly by its overall diffusive mass transfer coefficient (K_d). In mathematical analysis of solute transport by

combined convection and diffusion, the overall (diffusive) permeability (K_d) is defined as the ratio of the solute flux (J_s) to the solute concentration gradient ($\Delta C = C_w - C_d$) when ultrafiltration volume flux (J_v) vanishes [5]. This corresponds to the overall mass transfer coefficient (K_o) used for conventional hemodialysis. The K_d of a dialyzer used for conventional hemodialysis or hemodiafiltration for a specific solute is calculated not only at zero-ultrafiltration, but also with standard values of blood (200 ml/min) and dialysate flow rates (500 ml/min). This is due to a lower rate of ultrafiltrate production ($\approx$5 ml/min for hemodialysis and $\approx$50-60 ml/min for intermittent hemodiafiltration) than the dialysate flow rates (500 ml/min). In CAVHD however, the blood flow is spontaneous and the ultrafiltration flow rates are no longer negligibly low as compared with the dialysate flow rates. It is then questionable whether the value of K_o, usually obtained at negligible ultrafiltration and at high dialysate flow rates, is valid in the conventional range of ultra filtrate production (up to 20 ml/min) as it is in CAVHD.

4) In contrast to intermittent hemodialysis (4-5 hours in a week), CAVHD is a continuous technique. With prolonged use of the hemofilter, deterioration of the membrane is likely not only to decrease the rate of ultrafiltration but also to impair diffusive performance [6].

CAVHD is a new renal replacement technique. Insight into the determinants of solute clearance is needed to determine the optimal flow rates. Also, data on drug clearance are needed. For some drugs dose adaptations may be necessary [7]. For this and the above reasons, existing models of hemodialysis and hemofiltration are not likely to be useful for the analysis of solute transport in CAVHD. Therefore, we need a mathematical model that could be used to analyze solute transport by CAVHD.

Previous models of solute transport by hemodialysis and hemodiafiltration
In the mathematical model of conventional hemodialysis, as published by Sargent and Gotch [4], a linear change in the solute concentration over the length of the dialyzer is assumed. Convective transport is neglected. Thus the rate of solute transport depends on the difference between the concentration in blood and that in dialysate and on the overall mass transfer coefficient of diffusion (K_o). By using this model, one may calculate the length-averaged K_o from the total solute transport and the log-mean concentration difference over the membrane. In CAVHD, the contribution of convective transport is relatively great. Also, because of the ratio of blood and dialysate flow rates, a curvilinear decrease of blood solute concentration over the length of the hemofilter is to be expected.

Rose et al [8] published a one dimensional model of simultaneous hemodialysis and

ultrafiltration. In their model, which they developed for intermittent hemodialysis, the analysis of solute transport was based on the assumption that the ultrafiltration volume flux is constant along the membrane, which corresponds to a situation when the ultrafiltration is proportional to the transmembrane pressure difference. The overall mass transfer coefficient was determined by clearance measurements at zero-ultrafiltration, hence the effect of ultrafiltration on the overall diffusive mass transfer coefficient was neglected. The overall mass transfer coefficient of diffusion is the inverse of the total resistance to diffusion, which consists of the resistance to diffusion of the blood compartment, that of the membrane and that of the dialysate compartment [9]. In conventional dialysis the bigger part of the resistance to diffusion is exerted by the blood compartment and the membrane. According to Grimsrud and Babb [10], the resistance to diffusion in the dialysate compartment approaches zero at a fast and turbulent dialysate flow. Accordingly, they developed a model of solute transport in which the resistance to diffusion of the dialysate compartment was neglected. Also in their model, ultrafiltration rate was taken to be zero. In CAVHD, this approach is not valid because of the low dialysate flow rate and the relatively high rate of ultrafiltration.

In his mathematical analysis of combined convection and diffusion, Sigdell [11] gave expressions for the overall diffusive permeability (K_d) with ultrafiltration and (K_o) without ultrafiltration, noting that the ultrafiltration reduces the effective diffusive permeability due to reduction of the concentration gradient (ΔC), but at the same time adds even more through convection. His expressions are valid for the operational limits of conventional hemodialysis ($Q_f \ll Q_{bi} \ll Q_{di}$).

Sigler et al [12] first described solute clearance by CAVHD in patients. They did not discern the local solute transport by convection from that by diffusion and the study does not provide any insight into the determinants of diffusive transport. Pallone et al [13] studied solute transport by CAVHD in a laboratory setting. They presented a model in which they defined the local solute flux by convection and by diffusion. These fluxes were then integrated over the length of the hemofilter to calculated the solute clearance. With their model, they could calculate the curvilinear change in solute concentration along the hemofilter. Since their model did not provide an analytical expression of K_d, the K_d was determined by using curve-fitting techniques. They did not recognize the influence of differences in the dialysate flow rate on K_d (See Chapter 7). Jaffrin et al [14] published a mathematical model of combined convection and diffusion, to be applied to intermittent hemodiafiltration, which is a pump-driven hemodiafiltration technique. They expressed K_d as a function of the resistance of diffusion in blood, in membrane and in dialysate. These values are, however, not readily available. They determined the proper mass transfer coefficient (K_d) by making use of K_o from the clearance measurements at zero-ultrafiltration and curve fitting techniques.

In view of the shortcomings of the above models, we developed a new model of CAVHD. In the present chapter, we first define a general model of CAVHD that can easily be implemented in any spreadsheet program or programmed in any higher programming language. Then, with some simplifications (Chapter 6), we analytically solve the model equations, so as to provide expressions of K_d depending on the local behavior of ultrafiltration volume flux, as a function of blood, filtrate and dialysate flow rates and solute concentrations. By virtue of this expression of K_d, the model is well suited for the analysis of diffusive transport in CAVHD.

5.2 MATHEMATICAL MODEL OF CAVHD

Model description
In Figure 5.1, a schematic representation of a CAVHD flow system is shown. Blood from the arterial line flows inside the fibers (blood compartment) to the venous line. Blood enters the hemofilter at x=0 (blood inlet) and leaves it at $x=L_f$ (blood outlet). The dialysate fluid flows counter currently outside the fibers (dialysate compartment). Dialysate enters the hemofilter at $x=L_f$ dialysate inlet) and leaves at x=0 (dialysate outlet). The dialysate and blood compartments are separated by the fiber wall (membrane)
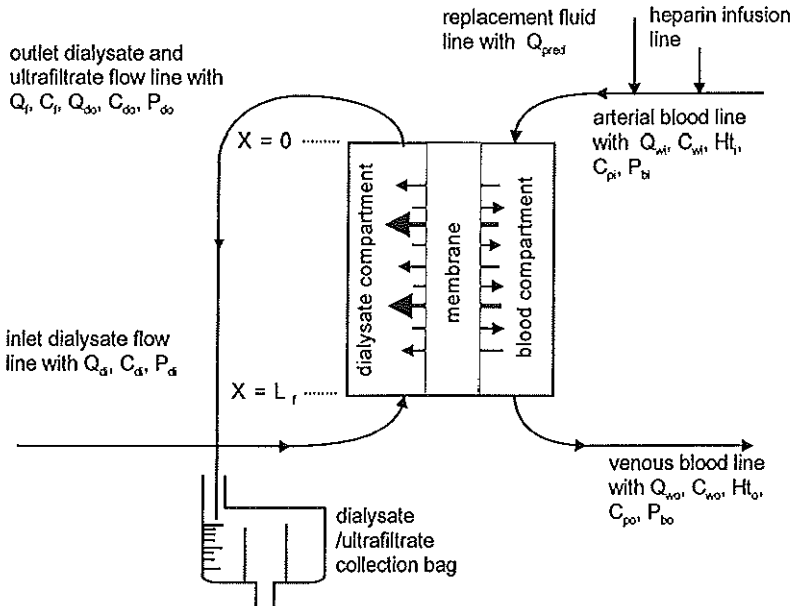
Figure 5.1: Schematic representation of CAVHD flow system.

The hemofilter is characterized by a small surface, highly permeable membrane and consists

of N number of hollow fibers each with an effective length (L_f) and internal radius (r_f) and its surface area ($S=2N\pi r_f L_f$) is equal to the sum of the filtering surfaces of all the fibers. In Table 5.1, the boundary definitions and variables of the model equations are shown.

Table 5.1: The boundary conditions of model variables for counter-current operation.

variables	$x = 0$	x	$x = L_f$
blood flow rate	Q_{bi}	Q_b	Q_{bo}
plasma water flow rate	Q_{wi}	Q_w	Q_{wo}
dialysate flow rate	Q_{do}	Q_d	Q_{di}
solute concentration in plasma water	C_{wi}	C_w	C_{wo}
solute concentration in dialysate	C_{do}	C_d	$C_{di}=0$
plasma protein concentration	C_{pi}	C_p	C_{po}
blood pressure	P_{bi}	P_b	P_{bo}
hematocrit	Ht_i	Ht	Ht_o
blood viscosity	η_{bi}	η_b	η_{bo}
dialysate pressure	P_{do}	P_d	P_{di}
oncotic pressure	Π_{pi}	Π_p	Π_{po}

notations for radial solute concentrations	
$r \leq 0$, blood bulk	$C_w(0)=C_w$
$0 \leq r \leq d_b$, blood boundary layer	$C_w(r)$
$r=r_d$, blood-membrane interface	C_{wm}
$d_b \leq r \leq d_m$, membrane	$C_m(r)$
$r=d_m$, membrane-dialysate interface	C_{md}
$d_m \leq r \leq d_d$, dialysate boundary layer	$C_d(r)$
$r \geq d_d$, dialysate bulk	$C_d(r_d)=C_d$

Input variables

The mathematical model requires the following input variables, which can all be obtained from either clinical measurements or manufacturers' specifications:

- arterial blood flow rate (Q_{ba}),
- dialysate inlet flow rate (Q_{di}),
- ultrafiltration flow rate (Q_f),
- infusion rate of substitution (predilution) fluid (Q_{pred}),
- arterial hematocrit (Ht_a),
- arterial plasma protein concentration (C_{pa}),
- temperature (T),
- solute concentration in the arterial blood plasma (C_{pl}),
- solute concentration in the dialysate/ultra filtrate outlet (C_{do}),
- solute concentration in filtrate (C_f),
- total membrane surface area (S),
- length of the hemofilter (membrane) (L_t),
- diffusive mass transfer coefficient (K_d) that follows from the model calculations,
- non-protein-bound fraction of the solute (F_f),
- sieving coefficient (γ) that is the fraction of the solute mass that passes through the membrane during ultrafiltration,
- pre- and postfilter hydrostatic blood pressures (P_{bi} and P_{bo}), dialysate pressure (P_d) or the height of hemofilter ultrafiltration line (h_c).

From these input values of the variables we calculated the local solute concentrations, the local flow rates in both blood and dialysate compartments over the length of the hemofilter and thereby, the convective (Cl_c) and diffusive (Cl_d) contributions to the total solute clearance (Cl).

Assumptions

The derivation of the mathematical model is based on the following major assumptions:

1) All of the hollow fibers in the hemofilter behave as a single capillary tube.
2) The permeability coefficients are constant along the hemofilter length.
3) Solute sieving coefficient is constant along the hemofilter length.
4) The flow rates and concentrations are time-independent for a given set of measurements (steady-state)

5.3 EQUATIONS NEEDED FOR MATHEMATICAL SIMULATION

Our mathematical model is based on the standard equations for continuity and mass balance of transmembrane volume and solute transport. The expressions for transmembrane volume and solute flux are combined with overall balances to obtain results in terms of the solute clearance. The model describes the flux of a solute from plasma water to dialysate by simultaneous convection and diffusion during countercurrent hemodiafiltration. The solute

concentration at the dialysate inlet is taken to be zero. As can be seen from Figure 5.2, the fiber wall (membrane) and a very thin concentration boundary layer at each side of the fiber wall may be considered as a virtual membrane. No concentration jell-layer forming is considered. Here, we briefly describe the equations and techniques required to provide mathematical simulation of solute and volume transport in CAVHD:

- Pressure-flow relations
- Ultrafiltration or transmembrane volume flux,
- Overall solute mass balance,
- Transmembrane solute mass flux,
- Solute clearance,
- Approximations and analytical solutions (See Chapter 6),
- Computational techniques (See Chapter 9).

Pressure - flow relationships

At the beginning of the fibers (hemofilter blood inlet), where they arise from the arterial line, the blood pressure, which tends to force the plasma water and small solutes out of the fibers to the dialysate side, considerably exceeds the sum of the opposing pressures. As the blood flows toward the venous line there is a gradual decrease in the effective ultrafiltration pressure (TMP). As a result, the blood flow rate decreases down the hemofilter length. Because of the continuity the dialysate flow rate increases. The decrease in blood flow (Q_b) or in plasma water flow rate (Q_v) and the increase in dialysate flow rate (Q_d) over a differential length dx (an annular segment of the hollow fiber wall of length dx lying at a distance x from the beginning of the fiber) may be expressed in the differential form by the following continuity equations:

$$\frac{dQ_b}{dx} = \frac{dQ_w}{dx} = -\frac{dQ_d}{dx} = -w J_v \tag{5.1}$$

where J_v is the ultrafiltration volume flux (density), w is the ratio of total membrane surface area (S) to the fiber length (L_f), which corresponds to the width of the hemofilter:

$$w \equiv \frac{S}{L_f} = 2\pi r_f N \tag{5.2}$$

where r_f is the internal radius of a fiber and N is the number of fibers.

Ultrafiltration volume flux

The ultrafiltration volume flux (density) depends on the hydraulic permeability (L_p) and the local transmembrane pressure difference (TMP):

$$J_v = L_p TMP \tag{5.3}$$

The local transmembrane pressure difference is given by Starling's law:

$$TMP = P_b - P_d - \Pi_p \tag{5.4}$$

with P_b, P_d and Π_p each representing the local blood hydrostatic pressure, dialysate pressure and oncotic pressure respectively. To determine the blood hydrostatic pressure (P_b) over the length of the hemofilter in eq.(5.4), the Poiseuille's law is used in differential form:

$$\frac{dP_b}{dx} = -\frac{R_f}{L_f}\eta_b Q_b \tag{5.5}$$

where R_f is the hemofilter resistance to the blood flow (See eq.(3.3) and eq.(3.8)) and η_b is the local blood viscosity, calculated from an empirical formula (See eq.(3.12)) as described by Pallone et al [13,16].To determine the local blood viscosity in the hemofilter, the blood viscosity in eq.(5.5) has to be evaluated at each point (x) along the hemofilter length by relating hematocrit (Ht) and plasma protein concentration (C_p) to the local blood flow rate (Q_b) as:

$$Ht = \frac{Ht_i Q_{bi}}{Q_b} \tag{5.6}$$

$$C_p = \frac{C_{pi} Q_{bi}(1 - Ht_i)}{Q_b(1 - Ht)} \tag{5.7}$$

where Ht_i, Q_{bi} and C_{pi} are the hematocrit, blood flow rate and plasma protein concentration at the hemofilter blood inlet. The dialysate fluid flows in the opposite direction to the blood flow. Because of flow resistance in the dialysate compartment the pressure rises with the axial position (x). However, since the dialysate flow rate is small compared to the blood flow rates, the dialysate pressure drop is small and can be neglected. Therefore, the pressure (P_d, [mmHg]) midway on the dialysate compartment can be calculated from the height of the fluid column in the ultra filtrate line according to eq.(3.24). Oncotic pressure is given by a third order polynomial from the protein concentration according to eq.(3.25) of Landis-Pappenheimer's empirical formula [16]. The CAVHD hemofilter membrane is essentially impermeable to the plasma proteins and they only contribute a transmembrane oncotic pressure difference. Since the filtration of plasma water increases the concentration of the plasma proteins, the net oncotic pressure increases down the fibre axis. Since the plasma proteins cannot pass the membrane, the local values of protein concentration can be derived from the overall protein mass balance, namely eq.(5.7).

Overall solute mass balance

The mass balance for a particular solute over a differential length (dx) of the hemofilter implies that the mass removal from blood compartment is equal to the mass gain into the dialysate compartment. A mass balance for a particular solute may be written as a differential

mass transfer rate from the blood side ($Q_w C_w$) or from the dialysate side ($Q_d C_d$),:

$$\frac{d(Q_w C_w)}{dx} = -\frac{d(Q_d C_d)}{dx} = -w J_s \tag{5.8}$$

where J_s represents the transmembrane local solute mass flux (density), C_w and C_d are local solute bulk concentrations in plasma water and dialysate respectively. Integrating the sum of both mass transfer rates in eq.(5.8) over a distance from 0 to x, we obtain the overall mass balance:

$$\int_o^x \frac{d}{dy}(Q_w C_w + Q_d C_d) dy = 0 \tag{5.9}$$

where y is a dummy variable. Consequently:

$$Q_w C_w + Q_d C_d = Q_{wi} C_{wi} - Q_{do} C_{do} \equiv \Delta M \tag{5.10}$$

which means that the solute mass transport rate from the blood compartment into the dialysate compartment is the same everywhere along the hemofilter length and equals to ΔM.
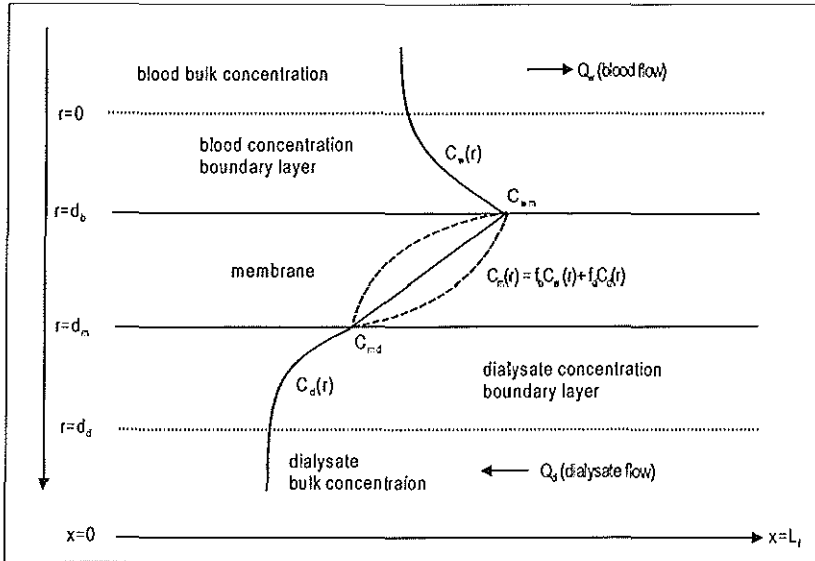
Figure 5.2: Radial concentration profiles in blood, membrane and dialysate compartments. See Section "Transmembrane solute mass flux".

Solute mass flux

Transmembrane solute mass flux
The local radial behavior of the solute flux (J_s) at some point (r) in the membrane can be

described by the equation:

$$J_s = \gamma J_v C_m(r) - D_m \frac{\partial C_m(r)}{\partial r} \tag{5.11}$$

where J_v is the local ultrafiltration volume flux, $C_m(r)$ is the radial solute concentration in the membrane, D_m is an effective diffusion coefficient in the membrane and γ is the convective transport (sieving) coefficient which is assumed to be independent of r. The continuity relation:

$$\frac{\partial C_m(r)}{\partial t} = -\frac{\partial J_v}{\partial r} \tag{5.12}$$

combined with the steady-state condition (assuming that a steady-state solute transport is achieved):

$$\frac{\partial C_m(r)}{\partial t} = 0 \tag{5.13}$$

leads to the differential equation:

$$\frac{\partial^2 C_m(r)}{\partial r^2} - \gamma \frac{J_v}{D_m} \frac{\partial C_m(r)}{\partial r} = 0 \tag{5.14}$$

which has the solution for the radial solute concentration ($C_m(r)$) for $d_b \le r \le d_m$:

$$C_m(r) = \frac{J_s}{J_v} + (C_{wm} - \frac{J_s}{J_v}) e^{\gamma \frac{J_v}{D_m} r} \tag{5.15}$$

where C_{wm} is the solute concentration at the blood-membrane interface (at $r=d_b$ with d_b representing the thickness of the blood concentration boundary layer). Integrating eq.(5.11) over d_m, we find the net local solute flux in terms of interface concentrations:

$$J_s = \frac{\gamma J_v}{e^{\theta_m} - 1} (C_{wm} e^{\theta_m} - C_{md}) \tag{5.16}$$

in which C_{md} is the solute concentration at the membrane-dialysate interface (at $r=d_d$ with d_d representing the thickness of the dialysate concentration boundary layer) and

$$\theta_m = \gamma J_v \frac{d_m}{D_m} = \gamma J_v R_m = \gamma \frac{J_v}{P_m} \tag{5.17}$$

is the membrane Péclet number with $1/P_m = R_m = d_m/D_m$ representing the resistance of membrane to diffusion. The reciprocal of R_m represents the membrane diffusive permeability (P_m). Eq.(5.16) expresses the net solute flux (J_s) across the membrane in terms of the solute concentration (C_{wm}) at the blood-membrane and the solute concentration (C_{md}) at the membrane-dialysate interface [17,18] (See Figure 5.1 and Figure 5.2) by simultaneous convection and diffusion.

To incorporate eq.(5.16) into an overall description of solute transport during CAVHD, the

solute flux has to be expressed in terms of bulk solute concentrations. In general, these bulk solute concentrations will not be equal to the interface concentrations due to an unstirred concentration layer in the blood region and due to an unstirred concentration layer in the dialysate region. The interface solute concentrations can be related to the bulk concentrations by using thin film theory used by Jaffrin et al [14].

Solute flux from blood bulk to blood-membrane interface
The local behavior of the solute flux at some point (r) in the blood concentration boundary layer can be described by the equation:

$$J_s = J_v C_w(r) - D_b \frac{\partial C_w(r)}{\partial r} \tag{5.18}$$

where $C_w(r)$ is the radial solute concentration in the blood boundary layer, D_b is the effective diffusion coefficient in the blood boundary layer. The continuity relation combined with the steady-state condition leads to the differential equation

$$\frac{\partial^2 C_w(r)}{\partial r^2} - \frac{J_v}{D_b} \frac{\partial C_w(r)}{\partial r} = 0 \tag{5.19}$$

The solution for the radial solute concentration ($C_w(r)$) for $0 \leq r \leq d_b$ is:

$$C_w(r) = \frac{J_s}{J_v} + (C_w(0) - \frac{J_s}{J_v}) e^{\frac{J_v}{D_b} r} \tag{5.20}$$

where $C_w(0)$ is the solute concentration at r=0 (the blood bulk). The solute concentration at the blood-membrane interface (C_{wm}) at $r=r_b$ follows from eq.(5.20):

$$C_{wm} = \frac{J_s}{J_v} + (C_w(0) - \frac{J_s}{J_v}) e^{\theta_b} \tag{5.21}$$

in which

$$\theta_b = J_v \frac{d_b}{D_b} = J_v R_b \tag{5.22}$$

is the Péclet number of blood boundary layer with $R_b = d_b/D_b$ representing the resistance of blood boundary layer to diffusion.

Solute flux from membrane-dialysate interface to dialysate bulk
The local behavior of the solute flux at some point (r) in the dialysate boundary concentration layer can be described by the equation

$$J_s = J_v C_d(r) - D_d \frac{\partial C_d(r)}{\partial r} \tag{5.23}$$

where $C_d(r)$ is the radial solute concentration in the dialysate boundary layer, D_d is an

effective solute diffusion coefficient in the dialysate boundary layer. The continuity relation combined with the steady-state condition leads to the differential equation

$$\frac{\partial^2 C_d(r)}{\partial r^2} - \frac{J_v}{D_d}\frac{\partial C_d(r)}{\partial r} = 0 \tag{5.24}$$

The solution for the radial solute concentration ($C_d(r)$) for $d_m \leq r \leq d_d$ is:

$$C_d(r) = \frac{J_s}{J_v} + (C_{md} - \frac{J_s}{J_v})e^{\frac{J_v}{D_d}r} \tag{5.25}$$

The solute concentration at the membrane-dialysate interface (C_{md}) at $r=d_m$ follows from eq.(5.25):

$$C_{md} = \frac{J_s}{J_v} + (C_d(r_d) - \frac{J_s}{J_v})e^{-\theta_d} \tag{5.26}$$

in which $C_d(r_d)$ is the solute concentration at $r=r_d$ (the dialysate bulk) and

$$\theta_d = J_v\frac{d_d}{D_d} = J_v R_d \tag{5.27}$$

is the Péclet number of dialysate boundary layer with $R_d = d_d/D_d$ representing the resistance of dialysate boundary layer to diffusion.

Solute flux from blood bulk to dialysate bulk

Substitution of eq.(5.26) and eq.(5.21) in eq.(5.16) yields the net solute mass flux from blood bulk to dialysate bulk:

$$J_s = \gamma \lambda J_v (e^{\theta_t}C_w - C_d) \tag{5.28}$$

where $C_w=C_w(0)$ and $C_d=C_d(d_d)$ represent the solute bulk concentrations in (blood) plasma water and in dialysate respectively and λ represents:

$$\lambda = \frac{1}{(1 - \gamma)e^{\theta_d}(e^{\theta_m} - 1) + \gamma(e^{\theta_t} - 1)} \tag{5.29}$$

with θ_t defined as:

$$\theta_t = J_v(R_b + \frac{\gamma}{P_m} + R_d) = \theta_b + \theta_m + \theta_d \tag{5.30}$$

For $\gamma=1$ as can be seen from eq.(5.30), the total resistance (R_{td}) to diffusive solute transport becomes equal to the sum of resistances of the membrane, the blood and dialysate concentration boundary layers:

$$\frac{1}{K_d} = R_{td} = R_b + \frac{1}{P_m} + R_d \tag{5.31}$$

where (K_d) represents an overall diffusive mass transfer or permeability coefficient. Given the

overall mass transfer coefficient (K_d) for an arbitrary solute, an observed Péclet number can be defined:

$$\theta_o = \frac{\gamma J_v}{K_d} \tag{5.32}$$

For $\gamma=1$, the theoretical total Péclet number (θ_t) equals the observed Péclet number (θ_o). Transmembrane solute flux in eq.(5.28) can be separated into the convective and diffusive components explicitly:

$$J_s = \gamma J_v (f_b C_w + f_d C_d) + K_d (C_w - C_d) \tag{5.33}$$

with

$$f_b = e^{\theta_t}\lambda - \frac{1}{\theta_o} \tag{5.34}$$

$$f_d = -\lambda + \frac{1}{\theta_o} \tag{5.35}$$

where f_b and f_d are the factors describing the relative weighting of blood and dialysate concentrations in the evaluation of the concentration of solute which is dragged by plasma water into the dialysate region or by dialysate fluid into the blood region in case of a back filtration.

The second term on the right hand side of eq.(5.33) is the diffusive component and the first term is the convective component. As stated by Zydney [19] however, the division of solute flux (J_s) in eq.(5.28) into separate convective and diffusive contributions as in eq.(5.33) is somewhat misleading. It must be remembered that the convective flow alters the concentration profiles due to interaction between the convective and diffusive components. Also the effect of the convective flow on the concentration gradient is a function of the volume flux (J_v) which in turn varies with the axial position along the hemofilter length.

Solute sieving coefficient

The solute dragged along by the plasma water flowing through the membrane can be reduced by a hindrance factor called as the sieving coefficient of the solute, i.e. the ratio of solute concentration in ultra filtrate to that in plasma water. In CAVHD, an apparent sieving coefficient is calculated as:

$$\gamma = \frac{2 C_f}{C_{wi} + C_{wo}} \tag{5.36}$$

with C_f is the concentration of non protein bound solute that passes through the membrane during ultrafiltration at zero dialysate flow rate. For practical clinical purposes, the unbound

free fraction of uraemic solutes and therapeutic drugs (administered to sick ICU patients), equals the ratio of solute concentration in the ultra filtrate to the mean solute concentration in plasma water in the hemofilter, thus the solute sieving coefficient. During clinical use, for uraemic solutes of up to at least 1000 Daltons, the apparent sieving coefficient is one. Therefore the apparent sieving coefficient is equal to the free fraction of solutes which are bound to plasma proteins [7].

Solute clearance

In clinical conventional hemodialysis, the ratio of the rate of solute mass removal to its concentration at the blood inlet is called clearance (Cl) or clearance rate. It is calculated from the macroscopic (overall) mass balance equations and measured either from dialysate side or blood side of the hemofilter [12].

Depending on the profile of ultrafiltration volume flux (J_v), when solute sieving coefficient (γ) and the overall diffusive mass transfer coefficient (K_d) are known, the total clearance can be obtained, in moles per unit of time, by integrating eq.(5.28) over the membrane length and dividing by C_{wi}:

$$Cl = \frac{w}{C_{wi}} \int_0^L \lambda J_v (C_w e^{\theta_t} - C_d) dx \qquad (5.37)$$

To express the clearance as the contributions of convective and diffusive transport separately one can use the solute flux expression from eq.(5.33) in eq.(5.37). Separating the first and the second terms on the right hand side of eq.(5.33) into convective (Cl_c) and diffusive (Cl_d) components [13], we define:

$$Cl_c = \frac{\gamma w}{C_{wi}} \int_o^{L_f} J_v (f_b C_w + f_d C_d) dx \qquad (5.38)$$

$$Cl_d = \frac{w K_d}{C_{wi}} \int_o^{L_f} (C_w - C_d) dx \qquad (5.39)$$

In order to determine the solute clearance from eq.(5.37) or eqs.(5.38-5.39), the local flow rates, the solute concentrations, the solute sieving coefficient, the overall diffusive mass transfer coefficient (or the individual resistances to diffusion) are required to be known. Equations governing the local flow and concentration profiles can be solved by using numerical integration methods or, instead, can be solved directly from the continuity equations by using numerical differentiation techniques [20].

5.4 DISCUSSION AND CONCLUSION

This model takes into account the variation of concentration in the blood and dialysate

boundary layers as well as inside the membrane in the presence of simultaneous diffusive and convective solute transports. The drawback of this model is that it requires an estimation of blood, dialysate, and membrane resistance and not just their sum to determine the solute clearance in CAVHD. The boundary layer thickness (d_b) of blood side and that (d_d) for the dialysate side are not known. Precise values of R_b, R_d and $1/P_m$ can hardly be obtained from clinical data. To some extend, the d_b and d_d may be calculated from inner and outer diameters of the hemofilter fibers as described by Sigdell [11]. However, Sigdell's expressions are related to the dry or wet state condition of membrane only, not to the operating hemofilter membrane index (MI) which decreases with time (See Chapter 3). Therefore, depending on the membrane condition (MI) and the dialysate flow rate (Q_{di}) and the precise values of R_b, R_d and $1/P_m$ have to be determined in *in vitro* studies. Also, use of numerical models is time-consuming. We therefore decided to make some simplifications in the modeling of solute transport in CAVHD, so as to obtain the overall diffusive mass transfer coefficient (K_d) from clinical data (See Chapter 6) at first and then to analyze the resistances R_b, R_d and $1/P_m$ under different operational and clinical conditions (See Chapter 9).

5.5 REFERENCES

[1]. van Geelen JA, Vincent HH, Schalekamp MADH. Continuous arteriovenous haemofiltration and haemodiafiltration in acute renal failure. Nephrol Dial Transpl 1988; 2: 181-186.

[2]. Geronemus R, Schneider N. Continuous arteriovenous hemodialysis: A new modality for treatment of acute renal failure. Trans Am Soc Artif Intern Organs 1984; 30: 610-613.

[3]. Husted FC, Nolph KD, Vitale FC, Maher JF. Detrimental effects of ultrafiltration on diffusion in coils. J. Lab. Clin. Med. 1976; 3: 435-442.

[4]. Sargent JA, Gotch FA. Principles and biophysics of dialysis. In: Drukker W, Parsons FM, Maher JF. Replacement of renal function by dialysis. Martinus Nijhoff Medical Division Publ, The Hague, 1978.

[5]. Kedem O and Katchalsky A, Thermodynamic Analysis of Permeability of Biological Membranes to Non-electrolytes, Biochimica et Biophysica Act., (1958) Vol:27 pp.229-249.

[6]. Vincent HH, Akcahuseyin E, Vos MC, van Ittersum FJ, van Duyl WA, Schalekamp MADH: Determinants of blood flow and ultrafiltration in continuous arteriovenous hemodiafiltration: Theoretical predictions and laboratory and clinical observations. Nephrology Dialysis Transplantation, (1990), 5, pp.1031-1037.

[7]. Vos MC, 'Continuous Arteriovenous Hemodiafiltration', Uitgeverij Eburn, Delft, 1993 (Erasmus University Rotterdam PhD Thesis).

[8]. Rose SM, Uvelli DA, Babb AL. A one dimensional mathematical model of transmembrane diffusional and convective mass transfer in a hemodialyser. ASME paper no. 73-WA/510-514.

[9]. Colton CK, Lowrie EG. Hemodialysis,: Physical principles and technical considerations, in: The Kidney, second edition 1981; 2: 2425-2489.

[10]. Grimsrud L, Babb AL. Velocity and concentration profiles for laminar flow of a Newtonian

fluid in a dialyzer. Chem Eng Progr Symp Ser no 66 1966; 62: 20-31.

[11]. Sigdel J.E., Calculation of Diffusive and Convective Mass Transfer, The International Journal of Artificial Organs, (1982) Vol:5 pp.361-372.

[12]. Sigler MH, Teehan BP. Solute transport in continuous hemodialysis: A new treatment for acute renal failure. Kidney International 1987; 32: 562-571.

[13]. Pallone TL, Hyver S, Peterson J. The simulation of continuous arteriovenous hemodialysis with a mathematical model. Kidney Int 1989; 35: 125-33.

[14]. Jaffrin MY, Ding L, Laurent JM. Simultaneous convective and diffusive mass transfer in a hemodialyser. Journal of Biomedical Engineering, (1990) Vol:112 pp.212-219.

[15]. Pallone T.L. and Pettersen J., Continuous Arteriovenous Hemofiltration: An in vitro Simulation and Mathematical Model, Kidney International, (1988) Vol:33 pp.685-698.

[16]. Landis EM, Pappenheimer JR. Exchange of substances through the capillary wall, in: Handbook of Physiology. Circulation. Washington, Am Physiol Soc 1963, sect 2, vol II, chapt 29, p 962-1034.

[17]. Levitt DG. General continuum analysis of transport through pores. I. Proof of Onsager's reciprocity postulate for uniform pores. Biophys J 1975; 15: 533-51.

[18]. Villarroel F., Klein E., Holland F., Solute Flux in Hemodialysis and Hemofiltration Membranes, Trans. Am. Soc. Artif. Intern. Organs., (1977) Vol:22 pp.225-233.

[19]. Zydney L.A., Bulk Mass Transport Limitations during High-Flux Hemodialysis, Artif. Organs. (1993) Vol. 17, No: 11, pp. 919 - 924.

[20]. Gear C.W.: Numerical Initial Value Problems in Ordinary Differential Equations. Englewood Cliffs, New Jersey, Printice-Hall, (1971).

ANALYTICAL SOLUTIONS TO SOLUTE TRANSPORT IN CONTINUOUS ARTERIO-VENOUS HEMODIAFILTRATION

6.1 INTRODUCTION

In Chapter 5, a mathematical model of solute and volume transport in continuous arterio-venous hemodiafiltration (CAVHD) was introduced. The model takes into account the variation of concentration in the blood and dialysate boundary layers as well as inside the membrane in the presence of simultaneous diffusive and convective solute transports. The drawback of that model is that it requires an estimate of blood, dialysate, and membrane resistance and not just their sum to determine the solute clearance in CAVHD. However, the boundary layer thickness (d_b) of blood side and that (d_d) of the dialysate side are not known. Precise values of R_b, R_d and $1/P_m$ can hardly be obtained from clinical data. Also, the use of numerical models is time-consuming. We therefore decided to make some simplifications in the modeling of solute transport in CAVHD so as to obtain the overall diffusive mass transfer coefficient (K_d) from clinical data under different operational and clinical conditions. The drawback of mathematical models of others [1-2] was that also in the presence of remarkably high ultrafiltration flow rates, overall mass transfer coefficient (K_d) of a dialyzer is calculated first at zero-ultrafiltration with standard blood (200 ml/min) and dialysate flow rates (500 ml/min) and then determined by means of the curve-fitting techniques. That of course resulted from the mass balance errors in their calculations when they calculated the overall mass transfer coefficient (K_d) of a dialyzer at zero ultrafiltration in a flowing system where the ultra-filtration was indeed not negligibly small. In CAVHD, the dialysate flow rates are low compared to the rates of ultrafiltration flows, making the dialysis treatment as slow as possible. Therefore, the overall mass transfer coefficient of a CAVHD hemofilter has to be calculated in the presence of ultrafiltration.

In this chapter, analytical solutions to solute and volume transport in CAVHD are presented in order to calculate the diffusive mass transfer coefficient (K_d) for a solute when blood, filtrate and dialysate flow rates and solute concentrations are known. We therefore made simplifications in eq.(5.3) and eq.(5.33), each representing the ultrafiltration volume flux (J_v) and solute mass flux (J_s) respectively. In the following sections, we introduce analytical solutions to solute and volume transport in CAVHD, so as to obtain expressions of the overall diffusive mass transfer coefficient, depending on ultrafiltration volume flux under the following conditions:
- K_o for zero ultrafiltration volume flux ($J_v=0$),
- K_a for a constant, mean volume flux ($J_v=J_a=Q_f/S$),
- K_d for a linear decreasing volume flux ($J_v=\alpha + \beta x$).

The overall mass transfer coefficients (K_o, K_a and K_d) are derived from the equations governing the overall mass balance.

6.2 MATHEMATICAL MODEL

Model description and assumptions

This mathematical analysis of CAVHD is valid primarily for a hollow fiber dialyzer or hemofilter, but with some minor modifications also for parallel plate dialyzer. See Chapter 5, Section 5.2 for the model description and Table 5.1 for the definition of boundary conditions. The derivation of the mathematical model is based on the following assumptions:

1)   All fibers behave equal. Hence the effective surface area of the hemofilter $S=2N\pi r_i L_f$ with r_r the inner radius and L_f the effective hemofilter length.

2)   The hydraulic and diffusive permeability (L_p and K_d) are constant along the filter length.

3)   The solute concentration in the blood (C_w) and in the dialysate (C_d) are "mixing-cup" concentrations [1]. This avoids the mathematical complexity of partial differential equations describing the concentration boundary layers and concentration polarization. This is also because we measure the average solute concentrations from arterial blood and from dialysate line connecting to the collection bag (see Figure 5.1), not directly from the blood bulk inside the fibers and from the dialysate bulk outside the fibers.

4)   The flow rates and concentrations are time-independent during measurements (steady-state).

5)   The transmembrane pressure gradient decreases linearly with increasing longitudinal distance (x).

6)   The sieving coefficient is one (for solutes such as urea, creatinine and phosphate). The sieving coefficient is a constant ($0 \leq \gamma \leq 1$), depending on the relative size of the membrane passing molecules and the membrane pores. It indicates the fraction of the solute that ultrafiltration drags through membrane.

Solute mass flux

Generally, mathematical analysis of solute transport by combined convection and diffusion in clinical hemodialysis is based on the following solute flux equation:

$$J_s = \gamma J_v (f_b C_w + f_d C_d) + K_d (C_w - C_d) \tag{6.1}$$

where J_s is local solute mass flux, C_w and C_d are local "mixing-cup" solute concentrations in blood and dialysate compartments, γ is sieving coefficient, K_d is the overall diffusive mass transfer coefficient representing the reciprocal of the overall resistance to diffusive solute

transport. Further, the f_b and f_d are factors describing the relative weighting of blood and dialysate concentrations in the contribution to the convective solute removal. Eq.(6.1) provides a rigorous expression for the solute flux for arbitrary values of the transmembrane volume flux J_v along the hemofilter length. In the limit of very high J_v, the convective weighting factors become $f_b=1$ and $f_d=0$, and consequently, independent from the solute sieving coefficient, eq.(6.1) becomes equal to:

$$J_s = J_v C_w \tag{6.2}$$

In the limit of zero transmembrane volume flux ($J_v=0$), eq.(6.1) reduces to:

$$J_s = K_o (C_w - C_d) \tag{6.3}$$

where the solute flux is governed by the diffusion only and the overall diffusive permeability (K_o) is determined at zero ultrafiltration. For low and moderate ultrafiltration volume flux (for small Péclet numbers, $\gamma J_v / K_d \ll 1$), the (length averaged) weighting factors are equal to $f_b=f_d\approx0.5$ [2,3] (See Figure 6.1). Therefore, for $\gamma=1$, eq.(6.1) becomes:

$$J_s = J_v \frac{C_w + C_d}{2} + K_d (C_w - C_d) \tag{6.4}$$

The condition $\gamma J_v / K_d \ll 1$ is verified in hemodiafiltration for most solutes with sieving coefficient $\gamma=1$ [2].
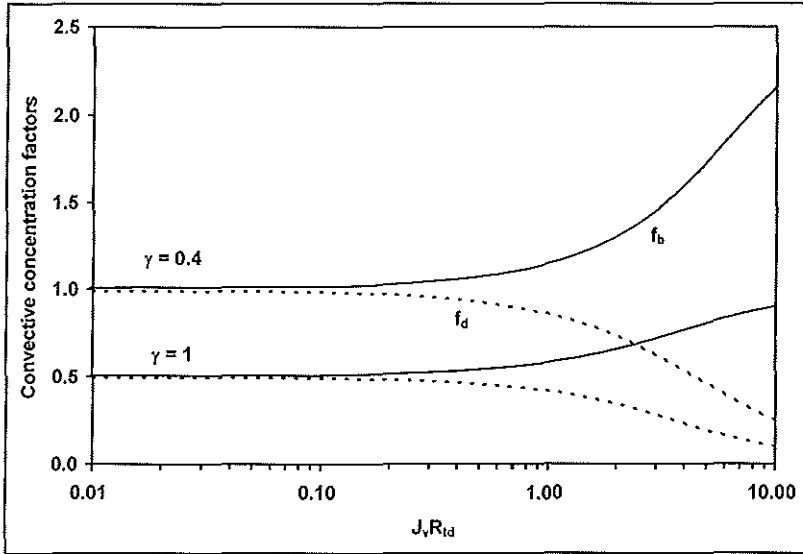
Figure 6.1: Theoretical convective concentration factors f_b and f_d (dashed lines) calculated from eq.(5.34) and eq.(5.35) respectively as a function of total Péclet number $\theta_t=\gamma J_v / K_d=\gamma J_v R_{td}$ for sieving coefficient $\gamma=1$ and $\gamma=0.4$ [19].

Pressure -flow relationships

At the beginning of the fibers (x=0, blood inlet), the blood pressure (P_{bi}) exceeds the sum of the opposing hydrostatic dialysate pressure (P_{do}) and oncotic pressure of the plasma proteins (Π_{pi}). Since the filtration of plasma water makes the concentration of the plasma proteins (C_p) to increase, the net oncotic pressure increases down the fiber axis. From the blood inlet to the end of the fibers (x=L_f, blood outlet) there is a gradual decrease in the effective ultrafiltration pressure. This decrease is due partly to the fall in hydrostatic blood pressure, which occurs because of the resistance to flow through the capillary fibers, and partly to the rise in oncotic pressure. Dialysis fluid flows in the opposite direction to the blood flow. Due to flow resistance in the dialysate compartment the pressure rises with the axial position (x).The most general formulation of ultrafiltration or transmembrane volume flux (J_v) for simultaneous convection and diffusion is given by Sigdell [4]. In fact, Sigdell's formulation was intended for intermittent hemodialysis or hemodiafiltration, not for CAVHD. After some minor modifications in the original expression, we rewrite Sigdell's formulation as for our conventional symbols (See reference [4] and the appendix for a detailed derivation of eq.(6.5)):

$$J_v = L_p TMP_i Cosh(x a_1) - \sqrt{\frac{L_p}{a_2} \frac{(\Delta P_b^e - \Delta P_d)}{L_f}} Sinh(x a_1) \tag{6.5}$$

where L_p is the hydraulic permeability, TMP_i is the transmembrane pressure difference at the hemofilter blood inlet, ΔP_b^e is the total pressure drop along the hemofilter length on the blood side, ΔP_d is the pressure drop along the hemofilter length on the dialysate side of the membrane, a_1 and a_2 are constants, x is the axial position of the hemofilter. Transmembrane pressure difference at the hemofilter blood inlet (TMP_i) is given by:

$$TMP_i = P_{bi} - P_{do} - \Pi_{pi} \tag{6.6}$$

with P_{bi}, P_{do} and Π_{pi}, each representing the hydrostatic blood pressure, dialysate pressure and oncotic pressure respectively at the hemofilter blood inlet (x=0). Pressure drop along the hemofilter length on the blood side of the membrane (ΔP_b^e) is given by:

$$\Delta P_b^e = P_{bi} - P_{bo} - \Pi_{pi} + \Pi_{po} \tag{6.7}$$

with P_{bo} and Π_{po}, each representing the hydrostatic blood pressure and oncotic pressure at the blood outlet (x=L_f). Oncotic pressure Π_{pi} and Π_{po} are calculated from a third order polynomial from the protein concentrations according to eqs.(3.16.-3.18), the Landis-Pappenheimer's empirical formula [5]. In eq.(6.5), the constants a_1 and a_2 represent:

$$a_1 = \mp \sqrt{L_p a_2} \tag{6.8}$$

$$a_2 = \frac{1}{L_f} (\frac{\Delta P_b^e}{Q_{bi}} - \frac{\Delta P_d}{Q_{do}}) \tag{6.9}$$

where Q_{bi} and Q_{do} represent the blood flow rate at the blood inlet and the dialysate flow rate at the dialysate outlet respectively. For $a_1 < 0$, direction of ultrafiltration flow is backwards, indicating the process of back filtration. In CAVHD, the ultrafiltration volume flux (J_v) is moderate. It is controlled by membrane hydraulic permeability (L_p) and local transmembrane (or ultrafiltration) pressure (TMP). Colton et al [6] has proved that at low transmembrane pressure differences (up to 200 mmHg), the J_v is proportional to the product of TMP and L_p, while, at high TMP's, the ultrafiltration volume flux reaches a limit, at which the concentration polarization takes place. Since in CAVHD, the observed TMP is up to 80 mmHg, we can assume that the ultrafiltration volume flux varies linearly with the hemofilter length. For small values of a_1's (See Appendix), eq.(6.5) can be approximated by:

$$J_v = \alpha + \beta x \tag{6.10}$$

with

$$\alpha = L_p TMP_i \tag{6.11}$$

$$\beta = -\frac{L_p}{L_f}(\Delta P_b^e - \Delta P_d) \tag{6.12}$$

Pressure drop along the hemofilter length on the dialysate side of the membrane (ΔP_d) is given by:

$$\Delta P_d = P_{do} - P_{di} \approx 0 \tag{6.13}$$

with P_{di} representing the hydrostatic pressure at the dialysate inlet ($x=L_f$). The dialysate fluid flows in the opposite direction to the blood flow. Due to flow resistance in the dialysate compartment the pressure rises with the axial position (x). But, since the dialysate flow rate is small compared to the blood flow rates, the dialysate pressure drop (ΔP_d) is small and can be neglected. Therefore, the pressure (P_d, [mmHg]) midway on the dialysate compartment can be calculated from the height of the fluid column in the ultra filtrate line (h_c, [cm]) according to $P_d = -h_c/1.36$.

Local flow rates

On integrating eq.(5.1) from 0 to x using eq.(6.10), we find the local plasma water flow rate:

$$Q_w = Q_{wi} - w(\alpha x + \frac{\beta}{2} x^2) \tag{6.14}$$

where Q_{wi} is the flow rate of plasma water at the blood inlet (x=0). Similarly, one can obtain the equation for local dialysate flow rate (Q_d):

$$Q_d = w(\alpha x + \frac{\beta}{2} x^2) - Q_{do} \tag{6.15}$$

where Q_{do} is the flow rates of dialysate at x=0. See Table 5.1 for the definition of the boundary conditions.

Net ultrafiltration flow rate
The total ultrafiltration rate (Q_f) is the value of the cumulative flow rate at x=L_f which follows from integrating the second term on the right-hand side of eq.(6.14):

$$Q_f = Q_{wi} - Q_{wo} = Q_{do} - Q_{di} = SL_p TMP_m \qquad (6.16)$$

where Q_{wo} and Q_{di} are respectively the flow rates of plasma water and dialysate at x=L_f and TMP_m the mean transmembrane pressure difference:

$$TMP_m = \frac{1}{2}(P_{bi} + P_{bo}) - P_d - \frac{1}{2}(\Pi_{pi} + \Pi_{po}) \qquad (6.17)$$

The hydraulic permeability L_p, expressing the ultrafiltration coefficient per unit of membrane surface area, can be calculated from eq.(6.16) and eq.(6.17).

Solute mass balance
The mass balance for a particular solute over a differential length (dx) of the hemofilter implies that the mass removal from the blood compartment is equal to the mass gain into the dialysate compartment. Using eq.(5.1) and eq.(6.10), we substitute eq.(6.4) in eq.(5.8) and get:

$$\frac{dC_w}{dx} = w\left(\frac{J_v}{2} - K_d\right)\frac{(C_w - C_d)}{Q_w} \qquad (6.18)$$

$$\frac{dC_d}{dx} = w\left(\frac{J_v}{2} + K_d\right)\frac{(C_w - C_d)}{Q_d} \qquad (6.19)$$

Eq.(6.18) and eq.(6.19) can be solved analytically for C_w and C_d, using eq.(6.10) and eq.(6.4).

Concentration profiles
On integrating the difference {dC_w/dx - dC_d/dx} from eqs.(6.18-6.19) over a differential length (dx) of the hemofilter we obtain:

$$C_w - C_d = (C_{wi} - C_{do})e^{I + K_d(I_1 - I_2)} \qquad (6.20)$$

where C_{wi} and C_{do} are respectively the plasma water and dialysate solute concentrations at x=0 and variables I, I_1 and I_2 represent:

$$I = \frac{1}{2}\ln\left(\frac{Q_{wi}Q_{do}}{Q_w(-Q_d)}\right) \qquad (6.21)$$

$$I_1 = \int_0^x \frac{dy}{-\frac{\beta}{2}y^2 + \alpha y - \frac{Q_{wi}}{w}} \qquad (6.22)$$

$$I_2 = \int_0^x \frac{dy}{-\dfrac{\beta}{2}y^2 + \alpha y - \dfrac{Q_{do}}{w}}$$

(6.23)

Defining the discriminant q_k:

$$q_k = \alpha^2 + 2\beta \frac{Q_k}{w}$$

(6.24)

where if $k=1$, $q_k=q_1$, $Q_k=Q_{wi}$ yielding I_1 and if $k=2$, $q_k=q_2$, $Q_k=Q_{do}$ yielding I_2. The solutions to eqs.(6.22-6.23) are to be found in standard reference books [7]:

for $q_k>0$:

$$I_k = \frac{\ln\left|\dfrac{\beta x + \alpha - \sqrt{q_k}}{\beta x + \alpha + \sqrt{q_k}}\right| - \ln\left|\dfrac{\alpha - \sqrt{q_k}}{\alpha + \sqrt{q_k}}\right|}{\sqrt{q_k}}$$

(6.25)

for $q_k<0$:

$$I_k = \frac{\arctan(\dfrac{\beta x + \alpha}{\sqrt{-q_k}}) - \arctan(\dfrac{\alpha}{\sqrt{-q_k}})}{\dfrac{\sqrt{-q_k}}{2}}$$

(6.26)

for $q_k=0$:

$$I_k = \frac{2}{\alpha}(1 - \frac{\alpha}{\alpha + \beta x})$$

(6.27)

Multiplication of eq.(6.20) by Q_w and subtraction of the resulting expression from eq.(5.13) yields:

$$C_w = \frac{\Delta M + Q_d(C_{wi} - C_{do})e^{1 + K_d(I_1 - I_2)}}{Q_{wi} - Q_{do}}$$

(6.28)

where ΔM is given by eq.(5.10). In a similar way, multiplication of eq.(6.20) by Q_d and addition of the resulting expression to eq.(5.10) yields:

$$C_d = \frac{\Delta M - Q_w(C_{wi} - C_{do})e^{1 + K_d(I_1 - I_2)}}{Q_{wi} - Q_{do}}$$

(6.29)

To solve the concentration equations (6.28-6.29), one needs to know the mass transfer coefficient (K_d). Detailed description and derivations of eqs.(6.14-6.18) can be found elsewhere [8].

Concentration profiles at zero ultrafiltration volume flux
In the limit of $J_v=0$, the solute transport occurs only by diffusion. The flow rate of the plasma

water ($Q_{wi}=Q_{wo}$) and that of the dialysate ($Q_{do}=Q_{di}$) do not vary with the distance along the hemofilter length. Consequently, eqs.(6.28-6.29), representing the concentration profiles on both blood and dialysate side of the membrane become:

$$C_w = \frac{\Delta M - Q_{di}(C_{wi} - C_{do})\, e^{-\frac{wK_o}{Q_{wi}}(1 - \frac{Q_{wi}}{Q_{di}})}}{Q_{wi} - Q_{di}} \tag{6.30}$$

$$C_d = \frac{\Delta M - Q_{bi}(C_{wi} - C_{do})\, e^{-\frac{wK_o}{Q_{wi}}(1 - \frac{Q_{wi}}{Q_{di}})}}{Q_{wi} - Q_{di}} \tag{6.31}$$

Flow rates and concentration profiles for a constant volume flux profile

In most clinical applications however, the ultrafiltration volume flux is assumed to be constant along the hemofilter length and calculated from the net rate of ultrafiltration flow, using eq.(6.16):

$$J_a = \frac{Q_f}{S} = L_p\, TMP_m \tag{6.32}$$

With J_a as given by eq.(6.32), the flow profiles from eqs.(6.14-6.15) become:

$$Q_w = Q_{wi} - w\, x\, J_a \tag{6.33}$$

$$Q_d = w\, x\, J_a - Q_{do} \tag{6.34}$$

The boundary values of eqs.(6.33-6.34) at $x=L$ give the net total ultrafiltration flow. Using the mean, constant $J_v=J_a$ in eq.(6.20), the concentration gradient can be written:

$$C_w - C_d = (C_{wi} - C_{do})[\frac{Q_w}{Q_{wi}}]^{\frac{K_a}{J_a} - \frac{1}{2}} \cdot [\frac{Q_{do}}{-Q_d}]^{\frac{K_a}{J_a} - \frac{1}{2}} \tag{6.35}$$

Multiplication of eq.(6.35) by Q_w and subtraction of the resulting expression from eq.(5.10) yields:

$$C_w = \frac{\Delta M - Q_{do}(C_{wi} - C_{do})\, F(x)^{\frac{K_a}{J_a} - \frac{1}{2}}}{Q_{wi} - Q_{do}} \tag{6.36}$$

In a similar way, multiplication of eq.(6.35) by Q_d and addition of the resulting expression to eq.(5.10) yields

$$C_d = \frac{\Delta M - Q_{wi}(C_{wi} - C_{do})\, F(x)^{\frac{K_a}{J_a} + \frac{1}{2}}}{Q_{wi} - Q_{do}} \tag{6.37}$$

with

$$F(x) \equiv (1 - \frac{Q_f}{Q_{wi}} \frac{x}{L_f})(1 - \frac{Q_f}{Q_{do}} \frac{x}{L_f})^{-1} \tag{6.38}$$

Detailed description and derivations of eqs.(6.32-6.38) can be found elsewhere [9,10].

Clearance and overall mass transfer coefficient

In clinical hemodialysis, solute clearance (Cl) is defined as the ratio of the amount of solute removed per unit of time to its concentration at the blood inlet, with the assumption that solute concentration at the dialysate inlet (C_{di}) is zero. It is calculated from the flow rates and measured solute concentrations from either blood or dialysate compartment as:

$$Cl = Q_{wi}(1 - \frac{C_{wo}}{C_{wi}}) + Q_f \frac{C_{wo}}{C_{wi}} = Q_{di} \frac{C_{do}}{C_{wi}} + Q_f \frac{C_{do}}{C_{wi}} \tag{6.39}$$

where C_{wo} is the solute concentration at the blood outlet. In their evaluation of CAVHD, Sigler et al [11] and others [12,13] used eq.(6.39) to separate solute clearance into estimates of diffusive and convective components. We designate these as Cl_D and Cl_C respectively:

$$Cl = Cl_D + Cl_C \tag{6.40}$$

with:

$$Cl_D = Q_{wi}(1 - \frac{C_{wo}}{C_{wi}}) = Q_{di} \frac{C_{do}}{C_{wi}} \tag{6.41}$$

$$Cl_C = Q_f(1 - \frac{Cl_D}{Q_{wi}}) = Cl_D \frac{Q_f}{Q_{di}} \tag{6.42}$$

However, the Cl_D in eq.(6.41) is a hypothetical clearance that would produce the same concentration at the outlet of the hemofilter without ultrafiltration (Q_f=0). Thus, Cl_D is not the clearance measured at zero-ultrafiltration for the same blood and dialysate flow rates. Therefore it may not be regarded as the contribution to dialysis to the overall clearance and eq.(6.41) may not be used to predict the diffusive performance in CAVHD, unless the outgoing dialysate solute concentration (C_{do}) is measured at Q_f=0. In conventional hemodialysis, since the convective component (Cl_C) is practically zero, the solute clearance is mainly by diffusion (Cl=Cl_D for Q_f=0). However, we are interested in CAVHD where the volume flux (J_v) decreases along the membrane length as given by eq.(6.5) or by eq.(6.10). This means that the condition of zero net ultrafiltration (Q_f=0) is not necessarily combined with the condition of J_v=0, but for example with the case of J_v>0 in the first half and J_v<0 in the second half (back filtration) of the hemofilter. Therefore, in case of CAVHD, Cl_D and Cl_C in eq.(6.40) are not rigorously defined in terms of true diffusive and convective clearances. For J_v=0 and consequently for Q_f=0, Cl_D represents pure diffusive clearance.

For an ultrafiltration volume flux profile, as given by eq.(6.10), clearance calculations of solutes with small molecular weight, provided by using eq.(6.40), do not (physically) describe the simultaneous diffusive and convective mass transport processes. Therefore, the solute clearance has to be calculated from the local solute flux (eq.(6.4)) along the hemodialyzer length [1,14,15]. In order to determine the convective and diffusive clearance (designated here as Cl_c and Cl_d respectively), we define the convective and diffusive components as in eq.(5.38) and eq.(5.39) respectively:

$$Cl_c = \frac{S}{2 L_f C_{wi}} \int_o^{L_f} J_v (C_w + C_d)\, dx \tag{6.43}$$

$$Cl_d = \frac{SK_d}{L_f C_{wi}} \int_o^{L_f} (C_w - C_d)\, dx \tag{6.44}$$

In eq.(6.44), the product SK_d is the permeation coefficient or diffusive performance capacity in ml/min. Given the solute clearance by eq.(6.40), the overall mass transfer coefficient (K_o) in eqs.(6.30-6.31) is determined from $Cl \approx Cl_D$ [12,13]. At theoretical zero ultrafiltration (J_v=0, consequently Q_f=0), as applied in intermittent hemodialysis, the mass transfer coefficient can be obtained by solving SK_o at the boundary values of eq.(6.30) and eq.(6.31) at x=L_f:

$$K_o = \frac{\ln\left[(\frac{Cl_D - Q_{wi}}{Cl_D - Q_{di}})(\frac{Q_{di}}{Q_{wi}}) \right]}{S(\frac{1}{Q_{di}} - \frac{1}{Q_{wi}})} \tag{6.45}$$

As a measure of diffusive performance of the dialyzer, the product SK_o [ml/min] is termed the permeation coefficient or diffusive performance capacity in ml/min at zero ultrafiltration [13]. In case of Q_{wi}=Q_{di}, eq.(6.45) may be approximated by using l'Hôpital's rule:

$$\frac{1}{K_o} \approx S(\frac{1}{Cl_D} - \frac{1}{Q_{di}}) \tag{6.46}$$

Using eq.(6.45), clearance (Cl_D) of a dialyzer with an overall diffusive mass transfer coefficient or permeability (K_o in µm/min), including boundary layer effects, in counter-current operation at zero ultrafiltration, may be predicted:

$$\frac{Cl_D}{Q_{wi}} = \frac{1 - e^{\frac{SK_o}{Q_{wi}}(\frac{Q_{wi}}{Q_{di}} - 1)}}{1 - \frac{Q_{wi}}{Q_{di}} e^{\frac{SK_o}{Q_{wi}}(\frac{Q_{wi}}{Q_{di}} - 1)}} \tag{6.47}$$

Eqs.(6.45-6.47) correspond to the formula's used for intermittent hemodialysis [4].To determine the mass transfer coefficient K_d for an ultrafiltration flux profile J_v=α+βx, we solve eq.(6.20) for K_d at the boundary condition (x=L_f) and write it in terms of K_o:

$$K_d = \frac{SK_o(\dfrac{Q_{wi} - Q_{di}}{Q_{di}Q_{wi}}) + \dfrac{1}{2}\ln(\dfrac{Q_{wo}Q_{di}}{Q_{wi}Q_{do}})}{I_1(L_f) - I_2(L_f)} \tag{6.48}$$

in which $I_1(L)$ and $I_2(L)$ are calculated from eqs.(6.22-6.23) at $x=L_f$. For $J_v=0$, $K_d/K_o=1$. As can be seen from eq.(6.48), the term $I_1(L_f)-I_2(L_f)$ is not explicitly determined in terms of measurable flow rates and solute concentrations.

With J_a as given by eq.(6.32), the flow profiles from eqs.(6.14-6.15) become equal to the flow profiles from eqs.(6.33-6.34). Using eq.(6.33) and eq.(6.34) for Q_w and Q_d respectively in eq.(6.22) and in eq.(6.23), the term $I_1(L)-I_2(L)$ in eq.(6.48) can be written as:

$$I_1(L) - I_2(L) = \frac{S}{Q_f}\ln(\frac{Q_{wo}Q_{do}}{Q_{wi}Q_{di}}) \tag{6.49}$$

On substitution of eq.(6.49) in eq.(6.48), one obtains the diffusive mass transfer coefficient K_a for a mean, constant volume flux J_a:

$$K_a = \frac{SK_o(\dfrac{Q_{wi} - Q_{di}}{Q_{di}Q_{wi}}) + \dfrac{1}{2}\ln(\dfrac{Q_{wo}Q_{di}}{Q_{wi}Q_{do}})}{\dfrac{S}{Q_f}\ln(\dfrac{Q_{wo}Q_{do}}{Q_{wi}Q_{di}})} \tag{6.50}$$

which may also be obtained by solving K_a from the boundary value of eq.(6.35) at $x=L_f$. When the overall diffusive mass transfer coefficient (K_a) for a given ultrafiltration flow rate is known, one may predict the solute clearance, by writing eq.(6.50) in terms of clearance from eq.(6.39):

$$\frac{Cl}{Q_{wi}} = \frac{1 - (\dfrac{Q_{do}Q_{wo}}{Q_{di}Q_{wi}})^{S\frac{K_a}{Q_f} + \frac{1}{2}}}{1 - \dfrac{Q_{wi}}{Q_{do}}(\dfrac{Q_{do}Q_{wo}}{Q_{di}Q_{wi}})^{S\frac{K_a}{Q_f} + \frac{1}{2}}} \tag{6.51}$$

Eq.(6.45) is valid for $J_v=0$. Eq.(6.48) is valid for $J_v=\alpha+\beta x$. Eq.(6.50) is valid for $J_v=J_a=Q_f/S$ and not valid for $Q_{wi}\le Q_{di}+Q_f$. Using l'Hôpital's rule it can be seen that, at zero ultrafiltration, eq.(6.48) and eq.(6.50) become equal to eq.(6.45).

Boundary values

The flow rate of plasma water (Q_{wi}) at the blood inlet is calculated from the arterial blood flow rate (Q_{ba}), taking into account the hematocrit (Ht_a), the plasma protein concentration (C_{pa}) and the rate of substitution fluid infusion (Q_{pred}) according to:

$$Q_{wi} = Q_{ba}(1 - Ht_a)(1 - \sigma \, C_{pa}) + fHt_a \, Q_{ba} + Q_{pred} \tag{6.52}$$

where $\sigma = 0.00107$ l/g [6] is a factor to calculate the protocrit from plasma protein concentration, f is the fractional volume distribution of solute in blood cells ($f=0.8$ for urea and $f=0$ for other uraemic solutes and drugs [17]). A patient treated by CAVHD, will loose a certain amount of ultra filtrate (plasma water) which must be replaced by an almost equal amount of sterile substitution fluid. In CAVHD, one injects this fluid into the blood line before the hemofilter (predilution) or after the hemofilter (postdilution). In this study, the predilution mode is used. The rate of substitution fluid (Q_{pred}) depends on the overall fluid balance and desired weight loss of the patient [18]:

$$Q_{pred} = Q_f + Q_{ul} - Q_h - Q_{dra} - Q_{efm} \tag{6.53}$$

where Q_f is the rate of ultrafiltration flow (400-600 ml/h), Q_{ul} is the rate of urine, insensible and GI losses (50 ml/h), Q_h is the hyperal (hyper alimentation fluid) rate (up to 100 ml/h), Q_{dra} is the fluid of drug administration rate (40 ml/h) and Q_{efm} is the necessary rate of excessive fluid removal from the patient's body (100-150 ml/h). The solute concentration in plasma water at the blood inlet (C_{wi}) is calculated from the solute concentration in arterial plasma (C_{pl}) as:

$$C_{wi} = \frac{C_{pl} \, F_f}{1 - \sigma \, C_{pa}} (1 - \frac{Q_{pred}}{Q_{wi}}) \tag{6.54}$$

The solute concentration in arterial plasma (C_{pl}) has to be corrected for unbound free fraction (F_f) if the solute in question is bound to plasma proteins, because only unbound solutes in plasma water participate in the process of diffusion and convection. Solute concentration in plasma water (C_{wo}) at the blood outlet can be calculated from eq.(5.10) at $x=L_f$. Solute concentration at the dialysate inlet is $C_{di}=0$ and that at the dialysate outlet (C_{do}) is measured from a collection bag. Plasma water flow rate (Q_{wo}) at the blood outlet equals $Q_{wi} - Q_f$ with Q_f the net rate of ultrafiltration flow. The flow rate of dialysate (Q_{do}) at the dialysate outlet equals $Q_{di} + Q_f$, with Q_{di} the dialysate inlet flow rate.

6.4 DISCUSSION AND COMMENTS

Eqs.(6.39-6.42) are used for conventional intermittent hemodialysis, where the ultrafiltration flow rate Q_f is almost zero and the clearance is mainly due to diffusive mass transport. With the help of eqs.(6.41-6.42), eq.(6.40) may be interpreted as the sum of diffusive clearance (Cl_D) when the ultrafiltration is zero and the convective clearance (Cl_C) when the dialysate flow is zero. In conventional hemodialysis, since the convective component Cl_C is practically zero, the interpretation of eq.(6.40) as separate contributions to total measured solute clearance

may not be wrong. However, as we mentioned earlier in Chapter 5, we are interested in CAVHD where the volume flux (J_v) decreases along the membrane length as given by eq.(6. 10). This means that the condition of zero net ultrafiltration $Q_f=0$ is not necessarily combined with the condition of $J_v=0$, but with the case of $J_v>0$ in the first half and $J_v<0$ in the second half (back filtration) of the hemofilter. In CAVHD, a theoretical zero local ultrafiltration is not realistic. To some extend, by equalizing the pressure on dialysate side to the total pressure on the blood side of the hemofilter, a net zero ultrafiltration can be achieved. Without such a pressure equalizing system (as it is in the clinical applications of CAVHD), a local zero ultrafiltration is not likely because there is a decreasing pressure drop along the hemofilter length on the blood side of the membrane.

When the effective surface area of dialyzing membrane is calculated (or known), flow rates and solute concentrations are measured, one can calculate the overall diffusive mass transfer coefficients (K_o for $J_v=0$, K_a for $J_a=Q_f/S$ and K_d for $J_v=\alpha+\beta x$).

The numerical values of the overall mass transfer coefficients, as defined in the equations (6.45), (6.48) and (6.50) may hardly be interpreted in terms of the real mass transfer coefficient of the hemofilter, since they are all based on the assumptions we made. Separate *in vitro* studies, using membrane characterization (permeability measurements) techniques, such as differential scanning calorimetry and inverse size exclusion chromatography might be helpful in providing the real mass transfer coefficient [16]. So far, such techniques are not used to provide the real mass transfer coefficient of the hemofilters or dialyzers under clinical conditions.

6.5 APPENDIX

We assume that the transmembrane pressure difference is given by:

$$TMP = P_b^e - P_d \tag{6.55}$$

in which P_b^e is an effective blood pressure on the blood side and P_d is that on the dialysate side of the membrane. The P_b^e and P_d may be determined by Poiseuille's law in differential form as:

$$\frac{dP_b^e}{dx} = -\frac{R_f}{L_f} Q_b \eta_b \tag{6.57}$$

$$\frac{dP_d}{dx} = -\frac{R_{fd}}{L_f} Q_d \eta_d \tag{6.56}$$

where η_b (η_d) is the apparent blood (dialysate) viscosity and R_f (R_{fd}) is the resistance to the

blood (dialysate) flow. Q_b and Q_d are local blood and dialysate flow rates respectively. We assume also that the viscosities are constant along the x-direction. We integrate eq.(6.55) from 0 to x:

$$TMP = TMP_i - \frac{R_f \eta_b}{L_f} \int_o^x Q_b(y)dy + \frac{R_{fd}\eta_d}{L_f} \int_o^x Q_d(y)dy \qquad (6.58)$$

where

$$TMP_i = P_b^e(x=0) - P_d(x=0) = P_{bi} - P_{do} - \Pi_{pi} \qquad (6.59)$$

is the TMP at the hemofilter blood inlet (x=0) with P_{bi}, P_{do} and Π_{pi}, each representing the hydraulic blood pressure, dialysate pressure and oncotic pressure respectively at the hemofilter blood inlet (x=0). By making use of eq.(5.1) for the blood (Q_b) and the dialysate flow rates (Q_d), eq.(6.58) can be written as:

$$TMP - TMP_i = (\delta P_d - \delta P_b^e)x + G \int_o^x (\int_o^y w J_v(z)dz)dy \qquad (6.60)$$

with

$$\delta P_b^e = \eta_b Q_{bi} \frac{R_f}{L_f} = \frac{\Delta P_b^e}{L_f} = \frac{P_{bi} - P_{bo} - \Pi_{pi} + \Pi_{po}}{L_f} \qquad (6.61)$$

$$\delta P_d = \eta_d R_{fd} \frac{Q_{do}}{L_f} = \frac{\Delta P_d}{L_f} = \frac{P_{do} - P_{di}}{L_f} \qquad (6.62)$$

$$G = \frac{\eta_b R_f - \eta_d R_{fd}}{L_f} = \frac{1}{L_f}(\frac{\Delta P_b^e}{Q_{bi}} - \frac{\Delta P_d}{Q_{do}}) \qquad (6.63)$$

in which ΔP_b^e is the pressure drop along the hemofilter length on the blood side of the membrane, ΔP_d is the pressure drop along the hemofilter length on the dialysate side of the membrane, Q_{bi} and Q_{do} represent the blood flow rate at the blood inlet and the dialysate flow rate at the dialysate outlet respectively. P_{bo} and Π_{po} are hydrostatic blood pressure and oncotic pressure at the blood outlet (x=L_f). Derivation of eq.(6.60) with respect to x yields:

$$\frac{dTMP}{dx} = \delta P_d - \delta P_b^e + wG \int_o^x J_v(y)dy \qquad (6.64)$$

and again derivation of eq.(6.64) with respect to x yields:

$$\frac{d^2 TMP}{dx^2} = wGJ_v(x) \qquad (6.65)$$

Eq.(6.65) may be rewritten as:

$$k^2 TMP(x) = wJ_v(x) \qquad (6.66)$$

where k is a constant. The second order derivation of eq.(6.66) yields the following differential equation:

$$\frac{d^2 J_v(x)}{dx^2} = \frac{k^2}{w} G J_v(x) = a_1^2 J_v(x) \tag{6.67}$$

where a_1 is a constant. From eq.(6.67) follows that

$$\frac{k^2}{w} G = a_1^2 \tag{6.68}$$

Eq.(6.67) has the solution:

$$J_v(x) = a e^{a_1 x} + b e^{-a_1 x} \tag{6.69}$$

in which a and b are constants. Derivation of eq.(6.69) with respect to x yields:

$$\frac{d J_v(x)}{dx} = a a_1 e^{a_1 x} - b a_1 e^{-a_1 x} \tag{6.70}$$

At x=0 (blood inlet), eq.(6.66), eq.(6.69) and eq.(6.70) become:

$$J_v(0) = a + b = a_1^2 \frac{TMP_i}{G} \tag{6.71}$$

$$\frac{d J_v(x)}{dx}\Big|_{x=0} = (a-b)a_1 = \frac{a_1^2}{G}(\delta P_d - \delta P_b^e) \tag{6.72}$$

From eqs.(6.71) and eq.(6.72) follows that:

$$b = \frac{a_1}{2G}(a_1 TMP_i - \delta P_d + \delta P_b^e) \tag{6.73}$$

$$a = a_1^2 \frac{TMP_i}{G} - \frac{a_1}{2G}(a_1 TMP_i - \delta P_d + \delta P_b^e) \tag{6.74}$$

Using eq.(6.66), a length average TMP can be defined as:

$$\overline{TMP} = \frac{1}{L_f} \int_0^{L_f} TMP(x)\,dx = \frac{w}{k^2 L_f} \int_0^{L_f} J_v(x)\,dx \tag{6.75}$$

where

$$w \int_0^{L_f} J_v(x)\,dx = Q_f \tag{6.76}$$

is the net ultrafiltration flow rate. Eq.(6.75) may be rewritten as:

$$\overline{TMP} = \frac{Q_f}{k^2 L_f} \tag{6.77}$$

From eq.(6.77) follows that:

$$k^2 = \frac{Q_f}{L_f \overline{TMP}} \tag{6.78}$$

Substitution of eq.(6.78) in eq.(6.68) yields:

$$a_1^2 = \frac{Q_f}{S \cdot \overline{TMP}} G = L_p \cdot G \tag{6.79}$$

in which L_p is the hydraulic permeability (See also eq.(3.22) in Chapter 3):

$$\frac{Q_f}{S \cdot \overline{TMP}} = L_p \tag{6.80}$$

Substitution of eq.(6.73) and eq.(6.74) in eq.(6.69) gives:

$$J_v = L_p \, TMP_i \, Cosh(x a_1) + \frac{a_1}{G} (\delta P_d - \delta P_b^e) \, Sinh(x a_1) \tag{6.81}$$

Substitution of eq.(6.61), eq.(6.62), eq.(6.79) in eq.(6.81) gives:

$$J_v = L_p \, TMP_i \, Cosh(x a_1) - \sqrt{\frac{L_p}{a_2}} \frac{(\Delta P_d - \Delta P_b)}{L_f} \, Sinh(x a_1) \tag{6.82}$$

where a_1 and a_2 represent:

$$a_1 = \mp \sqrt{L_p a_2} \tag{6.83}$$

$$a_2 = \frac{1}{L_f} (\frac{\Delta P_b}{Q_{bi}} - \frac{\Delta P_d}{Q_{do}}) \tag{6.84}$$

For small a_1's the first term on the right hand side of eq.(6.82) becomes

$$L_p \, TMP_i \, Cosh(x a_1) \rightarrow L_p TMP_i \tag{6.85}$$

and the second term becomes:

$$\sqrt{\frac{L_p}{a_2}} \frac{(\Delta P_d - \Delta P_b)}{L_f} \, Sinh(x a_1) \rightarrow L_p (\Delta P_b^e - \Delta P_d) \frac{x}{L_f} \tag{6.86}$$

From eq.(6.85) and eq.(6.86) follows that

$$J_v(x) \approx L_p \cdot [TMP_i - (\Delta P_b^e - \Delta P_d) \frac{x}{L}] \tag{6.87}$$

6.6 REFERENCES

[1]. Pallone TL, Hyver S, Peterson J. The simulation of continuous arteriovenous hemodialysis with a mathematical model. Kidney Int 1989; 35: 125-33.

[2]. Jaffrin MY, Ding L, Laurent JM. Simultaneous convective and diffusive mass transfer in a hemodialyser. Journal of Biomedical Engineering, (1990) Vol:112 pp.212-219.

[3]. Zydney LA, Bulk Mass Transport Limitations during High-Flux Hemodialysis, Artif. Organs. (1993) Vol. 17, No: 11, pp. 919 - 924.

[4]. Sigdell J.E., Calculation of Diffusive and Convective Mass Transfer, The International Journal of Artificial Organs, (1982) Vol:5 pp.361-372.

[5]. Landis EM, Pappenheimer JR. Exchange of substances through the capillary wall, in: Handbook of Physiology. Circulation. Washington, Am Physiol Soc 1963, sect 2, vol II, chapt 29, p 962-1034.

[6]. Colton CK, Henderson LW, Ford CA, Lysaght MJ. Kinetics of hemodiafiltration I. In vitro transport characteristics of a hollow-fiber blood ultrafilter. J Lab Clin Invest 1975; 85: 355-371.

[7]. Abramomitz M, Stegun JA, eds., 'Handbook of Mathematical Functions' Dover Publ. Inc, New York, (1965).

[8]. Akcahuseyin E, van Duyl WA, Vos MC, Vincent HH. An analytical solution to solute transport in continuous arterio-venous hemodiafiltration (CAVHD). Med. Eng. Phys.(1996) Vol:18 No:1, pp.26-35.

[9]. Akcahuseyin E, Vincent HH, van Ittersum FJ, van Duyl WA, Schalekamp MADH. A Mathematical Model of Continuous Arterio-Venous Hemodiafiltration (CAVHD), Computer Methods and Programs in Biomedicine, (1990) Vol:31 pp.215-224.

[10]. Vincent HH, van Ittersum FJ, Akcahuseyin E, Vos MC, van Duyl WA, Schalekamp MADH. Solute Transport in Continuous Arteriovenous Hemodiafiltration: A New Mathematical Model Applied to Clinical Data, Blood Purif., (1990) Vol:8 pp.149-159.

[11]. Sigler MH, Teehan BP. Solute transport in continuous hemodialysis: A new treatment for acute renal failure. Kidney International 1987; 32: 562-571.

[12]. Sargent JA, Gotch FA. Principles and biophysics of dialysis. In: Drukker W, Parsons FM, Maher JF. Replacement of renal function by dialysis. Martinus Nijhoff Medical Division Publ, The Hague, 1978.

[13]. Colton CK, Lowrie EG. Hemodialysis,: Physical principles and technical considerations, in: The Kidney, second edition 1981; 2: 2425-2489.

[14]. Jaffrin MY, Gupta BB, Malbrancq JM. A one-dimensional hemodialysis and ultrafiltration with highly permeable membranes. Journal of Biomedical Engineering, (1981) Vol:103 pp.261-266.

[15]. Rose SM, Uvelli DA, Babb AL. A one dimensional mathematical model of transmembrane diffusional and convective mass transfer in a hemodialyser. ASME paper no. 73-WA/510-514.

[16]. Broek A. Characterization of hemodialysis membranes: Membrane structure and function. Phd thesis. (1993) Druk: Alfa, Enschede, The Netherlands.

[17]. Colton CK, Smith KA, Merrill EW, Reece JM. Diffusion of organic solutes in stagnant plasma and red cell suspensions. Chem Eng Progr Symp Ser no 66, 1970; 99: 85-100.

[18].   Golper T.A.: Continuous Arterio-Venous Hemofiltration in Acute Renal Failure. American Journal of Kidney Diseases, (1985), Vol VI, No 6, pp. 373-386.

[19].   Akcahuseyin E, Vincent HH, van Duyl WA, Vos MC, Schalekamp MADH. Bulk mass transport during continuous arterio-venous hemodiafiltration (CAVHD): Analysis of resistance to diffusion. Medical Biol Engineering & Computing (1996) (submitted).

ANALYTICAL MODEL APPLICATION TO *IN VIVO* UREA DATA IN CAVHD

7.1 INTRODUCTION

Continuous arterio-venous hemodiafiltration (CAVHD) differs from conventional hemofiltration and dialysis by the interaction of convection and diffusion, the use of very low dialysate flow rates and by the deterioration of membrane conditions during the treatment. To study the impact of these phenomena on diffusive transport, an analytical mathematical model of CAVHD was presented, by which the overall diffusive mass transfer coefficient (K_d) for a solute may be calculated from blood, filtrate and dialysate flow rates and solute concentrations that can be measured in the clinical setting. The model was set up as a one-dimensional analysis of solute transport from plasma water to dialysate by simultaneous diffusion and convection. Within both the blood and the dialysate compartment, the solute concentration was assumed to vary in the axial direction but not in the radial direction, i.e., calculations are based on local "mixing cup" concentrations. Thus, diffusive solute transport results from a concentration gradient between plasma water and dialysate only. Furthermore, the membrane permeability for ultrafiltration and for diffusion was assumed to be constant over the entire membrane length. The sieving coefficient of the solute, i.e. the ratio of its concentration in ultrafiltrate to that in plasma water, was taken to be one. The dialysate solute concentration at the dialysate side inlet was taken to be zero. The model concerns the countercurrent mode of blood and dialysate flows. A detailed description of the mathematical derivation is given in Chapter 6.

Our model is the first detailed mathematical description of solute transport in CAVHD. It was meant as a tool to study the impact of variables such as blood, dialysate, ultrafiltration flow rates and the deterioration of membrane conditions with continued use of the hemofilter on solute transport [1]. In clinical practice, as ultrafiltration rate has to be monitored, convective clearance is easily determined. There is, however, a need for methods to estimate diffusive (and therefore total) solute transport. Hence we focused on the parameter K_d, which represents the mass transfer coefficient of the hemofilter membrane for diffusion.

In this chapter, the model is applied to clinical data obtained with 0.6 m² AN-69 capillary hemofilters. This was carried out to analyze the influence of dialysate flow rates and of the deterioration of membrane conditions with prolonged use of the hemofilter on the hemofilter performance. Further, the model equations governing the overall mass transfer coefficients (K_o, K_d and K_a) are evaluated by applying them to data of urea clearance measurements.

7.2 METHODS

Clinical conditions

To evaluate the mathematical model equations (6.45, 6.48 and 6.50), data were obtained from clearance measurements of the urea under various clinical circumstances. Patients were treated with CAVHD for acute renal failure and either sepsis, circulatory, respiratory or neurological instability or a combination of these, using the AN-69 0.6 m^2 capillary dialyser (Multiflow 60[R], Hospal, France). In all cases blood access was via 8F CAVH catheters in the femoral artery and vein. Our clinical routine is to infuse the substitution fluid into the arterial line ("predilution"), to prevent excessive hemoconcentration in case of a sudden decrease in the blood flow rate. Heparin was given at a dose of 500 U/h unless clinically contraindicated. Dialysate, heated to 38 °C, was run counter currently at a rate of 0.5 to 3.0 l/h using a roller pump (Bellco BL758, Mirandola, Italy). Measurements were performed according to a special protocol on 15 occasions up to 5 days of hemofilter use.

Measurements and calculations

We measured pre- and postfilter hydrostatic blood pressures (P_{bi} and P_{bo}) in the arterial and venous tubing. We calculated dialysate pressure (P_d) from the ultrafiltrate column height (0.74x column height in centimeters). Following the displacement of an air bubble we measured arterial blood flow rate (Q_{ba}) over a length of tubing, containing a volume of 13 ml. Arterial hematocrit (Ht_a) and arterial plasma protein concentration (C_{pa}) were measured to calculate the inlet (C_{pi}) and outlet (C_{po}) plasma protein concentrations from protein mass balance equations, eqs.(3.16, 3.18). The pre- (Π_{pi}) and postfilter (Π_{po}) oncotic pressures were calculated according to eq.(3.25) by a third order polynomial from the inlet and outlet plasma protein concentrations respectively. Dialysate flow rate (Q_{di}) and infusion rate of the substitution fluid (Q_{pred}) 'predilution' were determined by means of an electronic weighing device. The net ultrafiltration rate (Q_f) was determined by timed collection. The infusion rate of the subtitution fluid (Q_{pred}) was determined according to the overall fluid balance. At the dialysate inlet, Q_{di} was set at 1.0, 0.5, 2.0, and 3.0 l/h, and after a suitable period for equilibration urea concentration was measured in the mixture of ultrafiltrate plus spent dialysate (C_{do}) as well as in arterial blood plasma (C_{pi}). Plasma water flow rate (Q_{wi}) and urea concentration (C_{wi}) at the hemofilter inlet were calculated according to eqs.(6.52) and (6.54) respectively.

Statistics

Data were examined by regression analyses. Regression equations are given only when statistically significant ($p<0.01$). The goodness of curve-fitting is given by the corresponding correlation coefficients (R^2-values), or by the coefficient of variation (COV) of the values predicted by the regression equation.

7.3 RESULTS

Model equations

The model equations have been evaluated for clinical data of urea clearance. Within the limits of operating conditions by CAVHD (see Table 7.1), urea clearance was measured with the same type of hemofilters (Multiflow AN-69 Hospal with $S=0.6$ m^2 and $L_f=0.13$ m). For each measurement the hydraulic permeability and the mass transfer coefficients (or the overall permeation coefficients), the diffusive and convective urea clearance were calculated.

Table 7.1: The ranges of measured values during clinical measuring of urea clearance.

Variables	Range of values	Variables	Range of values
Q_{ba} [ml/min]	80 - 345	P_{bi} [mmHg]	37 - 88
Q_{di} [ml/min]	7 - 56	P_{bo} [mmHg]	12 - 42
Q_f [ml/min]	3 - 18	- P_d [mmHg]	1 - 65
Q_{pred} [ml/min]	0 - 17	Ht_a	0.18 - 0.38
C_{pa} [g/l]	37 - 85	C_{do} [mmol/l]	6 - 39
C_{pl} [mmol/l]	9 - 40	C_{di} [mmol/l]	0

Table 7.2: Urea clearance and overall diffusive mass transfer coefficients for two different sets of measurements (See Text). The flow rates, clearance and overall permeation coefficients (SK_d, SK_a, SK_o) are in units of ml/min.

	Q_{di}	C_{do}/C_{wi}	Cl	Cl$_D$	Cl$_C$	Cl$_d$	Cl$_c$	SK$_d$	SK$_a$	SK$_o$
Data	7.3	0.93	23.6	6.8	16.8	7.8	15.8	29.1	31.0	20.0
set	18.0	0.92	33.1	16.6	16.6	17.9	15.2	58.4	60.6	47.8
I	35.5	0.87	46.7	31.0	15.7	32.4	14.4	88.7	90.8	80.0
	51.0	0.80	55.4	40.9	14.4	41.9	13.4	97.7	99.5	92.5
Data	8.8	0.81	11.9	6.9	5.1	7.0	4.9	15.2	15.5	14.1
set	18.0	0.70	17.2	12.6	4.6	12.7	4.5	24.5	24.8	24.0
II	35.6	0.57	24.2	20.5	3.7	20.2	4.0	35.1	35.3	35.7
	53.0	0.51	30.5	27.1	3.3	26.7	3.7	46.1	46.3	47.2

Data set I: Q_{wi}=250.4 ml/min, Q_f=18 ml/min, TMP$_m$=78.4 mmHg, MI=13.8 ml/(h·mmHg)
Data set II: Q_{wi}=81.5 ml/min, Q_f=6.5, ml/min, TMP$_m$=52.6 mmHg, MI=7.4 ml/(h· mmHg)

Analytical model application to in vivo urea data in CAVHD

In Table 7.2, the results of urea clearance measurements and calculations are shown for two set of measurements with different filtration fractions (Q_f/Q_{wi}). Data of the first set of measurements were obtained with a new hemofilter characterized by a relatively high rate of ultrafiltrate production. The second one was obtained with a hemofilter used for three days. Deterioration of the hemofilter conditions is reflected in both a lower value of the hydraulic permeability index MI and lower values of SK_d. The diffusive and convective components of the urea clearance were calculated both from the boundary values using eq.(6.41) and eq.(6.42) and from the concentration and volume flux profiles using eq.(6.43) and eq.(6.44). The calculated diffusive (Cl_D and Cl_d) and convective (Cl_C and Cl_c) components of urea clearance are slightly different. The relative difference, $(Cl_d-Cl_D)/Cl_d$ [%], between the values of Cl_d and Cl_D depends on the values of both dialysate and ultrafiltration flow rate. It varied from 2.4% at Q_{di}=3 l/h to 13% at Q_{di}=0.5 l/h for Q_f=18 ml/min and from -1.45% at Q_{di}=3 l/h to 1.42% at Q_{di}=0.5 l/h for Q_f=6.5 ml/min. The diffusive clearance increases with increasing rate of dialysate flow while the convective component decreases slightly. Despite those small differences, the sum of Cl_D and Cl_C equals the sum of Cl_d and Cl_c.
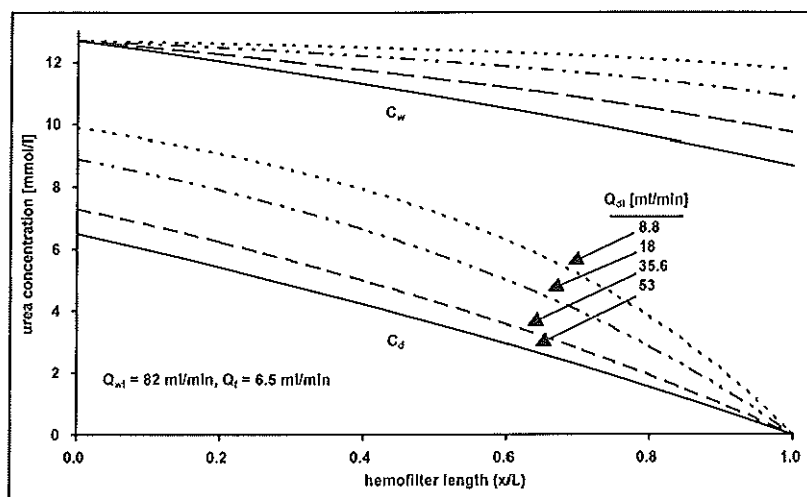
Concentration profiles

The concentration profiles (C_w for the local urea concentration in plasma water and C_d for the local urea concentration in the dialysate compartment) were calculated using eq.(6.28) and eq.(6.29), assuming that the ultrafiltration volume flux decreases linearly with the distance along the hemofilter length. The concentration difference $\Delta C=C_w-C_d$ is responsible for the diffusive urea removal. The urea concentration that is dragged by plasma water by convection from blood into the dialysate compartment is given by $C_m=(C_w+C_d)/2$. In Figure 7.1, the urea concentration profiles are shown as a function of the distance along with the hemofilter length for an ultrafiltrate flow rate of Q_f=18 ml/min and the plasma water flow rate of Q_{wi}=250 ml/min at different dialysate flow rates of Q_{di}=7.3, 18, 35.5 and 51 ml/min.

In Figure 7.2, the urea concentration profiles are shown for a relative low rate of ultrafiltration and blood flow, namely Q_f=6.5 ml/min and Q_{wi}=81.5 ml/min at different dialysate flow rates of Q_{di}=8.8, 18, 35.6 and 53 ml/min. As can be seen from Figures 7.1 and 7.2, the urea concentration at the dialysate inlet of the hemofilter (C_{di}) is zero. The removed urea concentration (C_{do}) at x=0 equals the sum of the urea concentration removed by diffusion and that by convection. Evidently, the high rates of dialysate flow favor the concentration gradient. At relative low rates of ultrafiltration and blood flow and at relative high rates of dialysate flow, the concentration profiles seem as those in the conventional hemodialysis where the concentration profiles develop almost linearly along the hemofilter length.
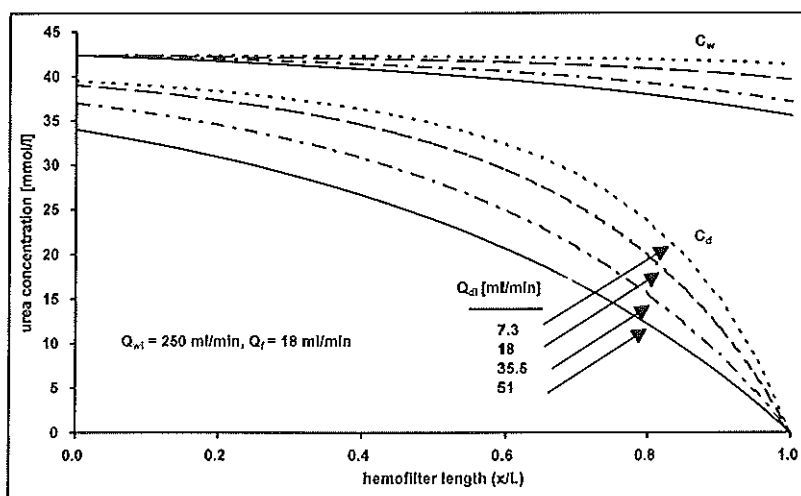
Figure 7.1: Urea concentration profiles in blood (C_w) and in dialysate (C_d) compartment as a function of hemofilter length (x/L_f) for Q_{di}=7.3, 18, 35.5 and 51 ml/min with Q_{wi}=250 ml/min and Q_f=18 ml/min [8].

Figure 7.2: Urea concentration profiles in blood (C_w) and in dialysate (C_d) compartment as a function of the hemofilter length (x/L_f) for Q_{di}=8.8, 18, 35.6 and 53 ml/min with Q_{wi}=82 ml/min and Q_f=6.5 ml/min.

The overall diffusive permeation coefficients (SK_d, SK_a and SK_o)

Under the same conditions the overall permeation coefficients SK_o, SK_a and SK_d were

calculated from eq.(6.45), eq.(6.50) and eq.(6.48) respectively. The expressions for the overall permeation coefficients SK_o, SK_a and SK_d were derived from the overall mass balance equations, depending on the profile of ultrafiltration volume flux, namely $J_v=0$, $J_v=Q_f/S$ and $J_v=\alpha+\beta x$. To demonstrate the influence of the ultrafiltration (volume flux profile) on the overall permeation coefficient SK_d, the ratio K_o/K_d as well as the ratio K_a/K_d are illustrated in Figure 7.3 in relation to the dialysate flow rates at 3 different ultrafiltration flow rates (or filtration fractions). The trend lines show that at high rates of dialysate flow and low rates of ultrafiltration, the ratio K_d/K_o approaches to 1 where the value of $K_d=K_o$ is independent from the ultrafiltration flow rate and it represents the permeation coefficient of the dialyzer in a conventional hemodialysis. At flow rates for $Q_f \ll Q_{vi} \ll Q_{di}$, the effect of ultrafiltration on the overall permeation coefficient is negligible, as almost the case in conventional hemodialysis. When the dialysate flow rates are low as compared with the rates of ultrafiltration flow, the effect of ultrafiltration on the overall permeation coefficient becomes significant.
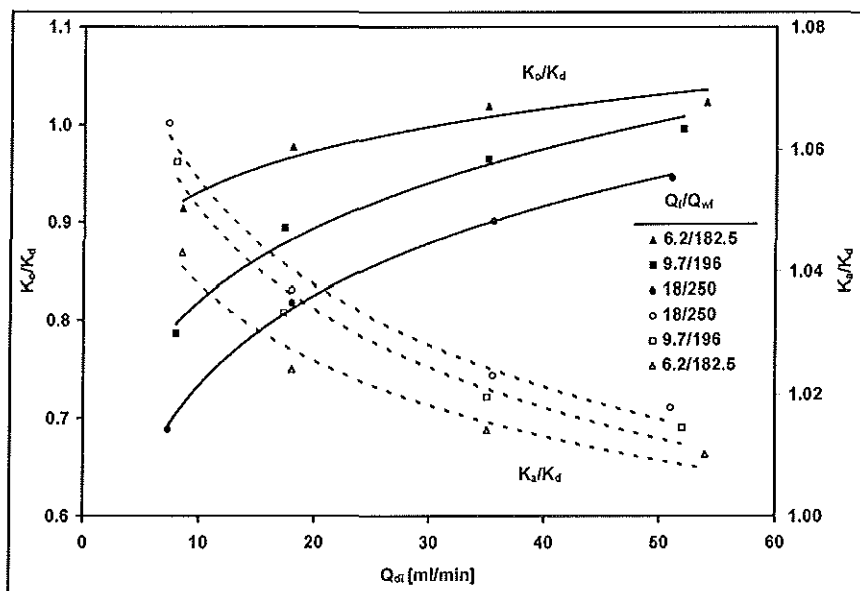

Figure 7.3: Ratio of the mass transfer coefficient K_o to the mass transfer coefficient K_d in relation to dialysate flow rate for the filtration fractions $Q_f/Q_{vi}=6.2/182.5$, 9.7/196 and 18/250. The broken lines show the relation between K_a/K_d and the dialysate flow rate Q_{di} [8].

In order to show the general trend, the ratio K_o/K_d in relation to the ratio Q_f/Q_{di} is shown in Figure 7.4 for 67 different sets of the urea clearance measurements. The trend line shows the best fit to the experimental data points with the following regression equation:

$$\frac{K_o}{K_d} = 1.01 - 0.16\frac{Q_f}{Q_{di}} \tag{7.1}$$

with R^2=0.85 and n=67. The K_d increases with the decreasing rate of ultrafiltration flow (Q_f). As can be seen from eq.(7.1), at Q_f=0, K_d becomes equal to K_o. The ultrafiltration flow reduces the overall mass transfer coefficient due to the reduction of the concentration gradient [3]. At flow rates for $Q_{di} \ll Q_f \ll Q_{wi}$, the total mass removal will be dominated by ultrafiltration, especially at the first half of the hemofilter. For the diffusive transport, the second half part of the hemofilter will be important. Lowering the dialysate flow rate rather than the rate of ultrafiltration can cause dialysate saturation ($C_{do}/C_{wi} \to 1$) or diffusion equilibrium. As can be seen from Figure 7.4, the big departures from K_d/K_o=1 come out at high values of Q_f and low values of Q_{di} where the convection dominates the clearance process. The clearance becomes equal to the ultrafiltration flow ($Cl=Q_f$, only water transport) when conditions Q_{di}=0 and C_{do}/C_{wi}=1 are fulfilled (See further Chapter 8).
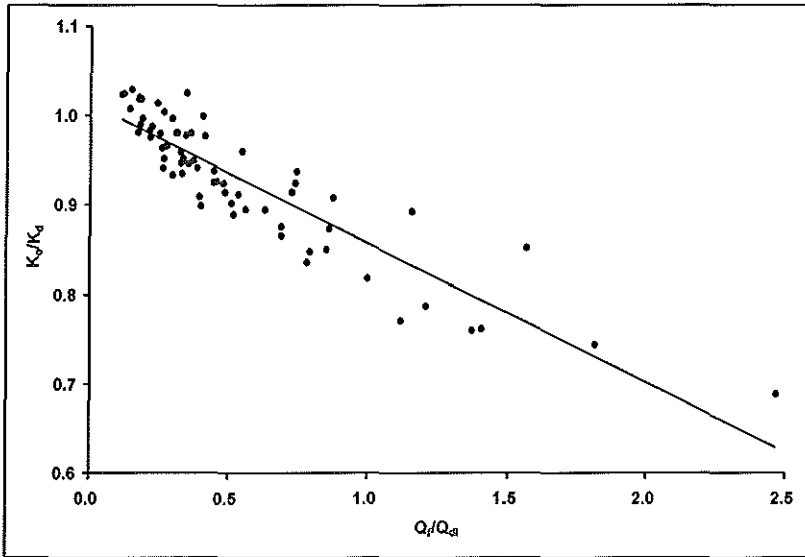

Figure 7.4: The ratio K_o/K_d in relation to the ratio of the ultrafiltration flow rate to the dialysate flow rate (Q_f/Q_{di}) for different filtration fractions [8].

In Figure 7.3, the ratio K_a/K_d is illustrated in relation to the dialysate flow rates. The differences between the values of K_a and K_d at different dialysate and ultrafiltration flow rates are relatively small. However, one important condition of using the constant volume flux model ($J_a=Q_f/S$) is that within the hemofilter there is no back filtration from dialysate into the blood compartment. If the transmembrane pressure gradient becomes negative somewhere in the hemofilter, the assumption of constant volume flux is not valid any longer.

SK$_d$max - Wilson's plot

As can be seen from Table 7.2, the overall permeation coefficient (SK$_d$) increases with the increasing rate of the dialysate flow. In Figure 7.5 the SK$_d$ is shown as a function of the dialysate flow rate (Q$_{di}$). This curvilinear increase in the SK$_d$ is a result of the fact that with the increasing rate of dialysate flow the dialysate concentration will be better distributed over the whole membrane surface area and the dialysate resistance to diffusive mass transfer will be smaller.
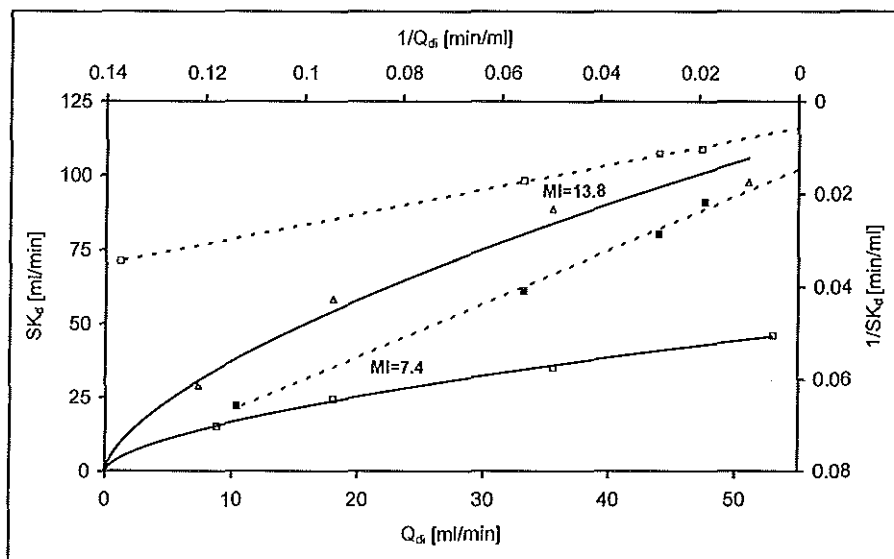
Figure 7.5: Wilson's plot represents the relation between 1/SK$_d$ and 1/Q$_{di}$ for urea. The linear regression lines show the Wilson's plot at two different values of membrane index, namely MI=7.4 and MI=13.8 ml/(h mmHg).

The overall permeability coefficient (SK$_d$) reaches its maximal value at an infinite dialysate flow rate. This maximal value, designated as "SK$_d$max", can be obtained by extrapolation. In Figure 7.5, the reciprocal of SK$_d$ is shown as a function of the reciprocal of Q$_{di}$. The value of 1/SK$_d$max is the intercept of the corresponding regression line with the 1/SK$_d$-axis. The value of 1/K$_d$max equals the sum of the resistance to diffusion of the blood boundary layer (R$_b$) and the resistance to diffusion of the membrane (R$_m$) according to Wilson's plot [2]. The maximal value of SK$_d$ depends also on the membrane hydraulic permeability index (MI). In Figure 7.5, the (dashed) trend lines represent the following regression equations (with R^2=0.99 and n=4):

$$\frac{1}{SK_d} = \frac{0.45}{Q_{di}} + \frac{1}{68} \quad for \ MI=7.4 \tag{7.1}$$

$$\frac{1}{SK_d} = \frac{0.21}{Q_{di}} + \frac{1}{175} \quad for \ MI=13.8 \tag{7.2}$$

On perfusing a new hemofilter ($S=0.6$ m^2) with a dialysate flow rate of 5 l/h, the maximum value of SK_d was 120 ml/min, which was determined by extrapolation from urea clearance data[1]. See Chapter 9 for a detailed explanation of Wilson's plot.

Linear decreasing versus a constant volume flux profile

Using the data from Table 7.4, the urea flux profiles are shown in Figure 7.6 for a constant ultrafiltration volume flux model ($J_v=J_a=Q_f/S$) and for a linear decreasing ultrafiltration volume flux ($J_v=\alpha+\beta x$) model.

Table 7.4: The urea clearance is separated into the convective and diffusive components according to the ultrafiltration volume flux models: $J_v=0$, $J_v=J_a=Q_f/S$ and $J_v=\alpha+\beta x$.

clearance [ml/min] and overall permeation coefficients [ml/min]	standard eq.(6.40)	depending on volume flux J_v		
		$J_v = 0$	$J_v = J_a = Q_f/S$	$J_v = \alpha+\beta x$
Cl	15.7	15.7	15.7	15.7
Cl$_C$	13.1	0		
Cl$_D$	2.6	15.7		
Cl$_c$			4.4	6.4
Cl$_d$			11.3	9.3
SK$_o$		18.4		
SK$_a$			15.2	
SK$_d$				10.4

With: $P_d= -1$ mmHg, $P_{bi}=73$ mmHg, $P_{bo}=25$ mmHg, $C_{pa}=85$ g/l, $Q_{ba}=60$ ml/min, $Q_f=8$ ml/min, $Q_{di}=40$ ml/min, $C_{do}=12.3$ mmol/l, $Ht_a=0.39$, $C_{pl}=32.2$ mmol/l, $Q_{pred}=0$ ml/min.

The total urea flux, calculated from the data in Table 7.4 is separated into the convective (J_vC_m) and the diffusive ($K_d\Delta C$) components by calculating the local solute flux (J_s) using eq.(6.4), the local volume flux (J_v) using eq.(6.10) and the overall mass transfer coefficient (K_d) using eq.(6.48). The concentration $C_m=0.5(C_w+C_d)$ represents the local solute concentration, which is dragged by plasma water into the dialysate region. The $\Delta C=C_w-C_d$ represents the local concentration difference (gradient). The same total urea flux is also separated into the convective (J_aC_m) and the diffusive ($K_a\Delta C$) components by calculating the local solute flux (J_s) using eq.(6.4), the J_a using eq.(6.32) and the K_a using eq.(6.50). In Figure 7.6, the local convective solute flux (J_aC_m) and the local diffusive solute flux ($K_a\Delta C$) are shown with dashed (broken) lines. The corresponding cumulative values of the same urea clearance are shown

Figure 7.7. The measured total urea clearance, calculated from the urea flux profiles in Figure 7.6 is separated into the convective (Cl_c) and the diffusive (Cl_d) components by using eqs.(6.43) and (6.44) respectively.
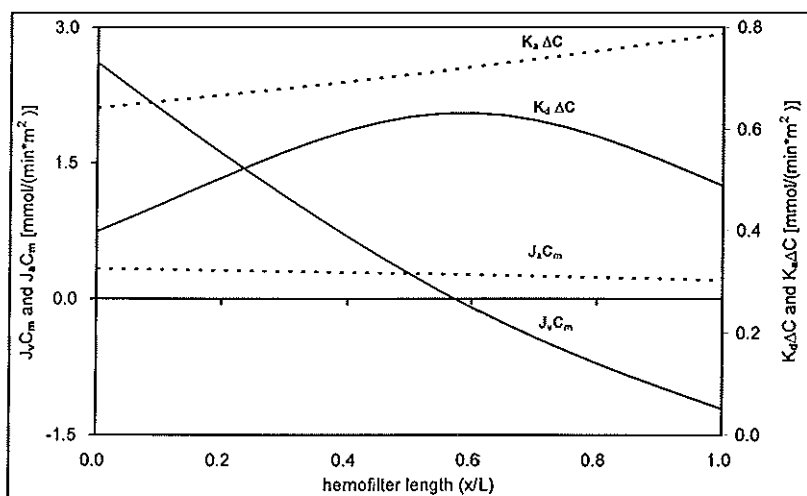

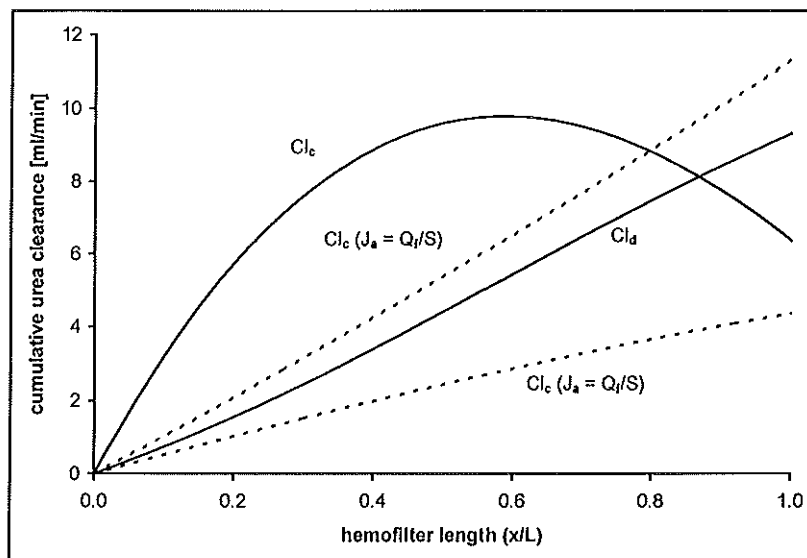**Figure 7.6:** Urea flux profiles as a function of the hemofilter length (x/L_f). $L_f=0.13m$ [8].

Figure 7.7: The cumulative urea clearance as a function of the hemofilter length (x/L_f) [8].

In Figure 7.7, the same components for $J_v=J_a=Q_f/S$ are shown by dashed lines. According to the linear decreasing volume flux model, the transmembrane pressure difference is zero at about $x/L_f=0.58$ where ($J_v=0$ and $K_d=K_o$) the diffusive flux ($K_d\Delta C$) and the cumulative convective clearances reach their maximal values. From $x/L_f>0.58$ to $x/L_f=1$ where $J_v<0$, the diffusive flux and cumulative convective clearance decrease with the length because of backwards convective flux. According to the urea flux profiles (J_aC_m and $K_a\Delta C$, shown by broken lines) of the constant volume flux model, the effect of back filtration on the diffusive urea flux will not be observed. The backwards dialysate fluid (volume flux) reduces the concentration gradient from blood into the dialysate side, resulting in a reduced overall permeation coefficient.

7.4 DISCUSSION

Previous models
Our model differs from previous models of diffusive solute transport in several respects. The anticipated differences between CAVHD and conventional hemodialysis and hemodiafiltration are borne out, first, by the demonstration of the curvilinear solute concentration profiles in the blood and dialysate compartments (Figures 7.1 and 7.2). Second, the hemofilter performance had indeed decreased appreciably after three days of use (Table 7.2). It must be remembered that the K_d cannot be measured directly, but is calculated from the resulting solute transport, assuming a constant membrane surface area. A decrease in K_d may therefore result either from a decrease in the (effective) membrane permeabilityor from a decrease in the (effective) membrane surface area. The latter may be due to clotting of fibers. It might also be due to unequal distribution of the dialysate over the dialysate compartment, which is likely to occur at very low dialysate flow rates. This influence of dialysate flow rates on K_d was not recognized by Pallone et al [4]. In a recent publication Pallone et al [4] give a detailed description of solute transport in CAVHD. In that article the curvilinear changes in blood and dialysate solute concentration along the length of the dialyser are demonstrated. However, the authors apparently lack a mathematical expression to calculate K_d. In their article they assume that K_d does not depend on the dialysate flow rate. Our experiments show that, for the range of dialysate flow rates used in CAVHD, we cannot safely make that assumption. Indeed, also for the particular plate hemodialyzer that is described in ref. [4], we found that K_d increases with Q_{di} [11,12]. Furthermore, a similar finding had already been reported by Babb et al [13], who also studied solute transport through the parallel plate dialyzer.

In the classical model of dialysis, as described by Sargent and Gotch [7], the influence of ultrafiltration is not taken into account. Furthermore, their model is based on the assumption that there is a linear increase in blood and dialysate solute concentrations along the length of

the dialyzer. This assumption clearly is invalid in CAVHD [1,4,8,9]. The model developed by Jaffrin et al [5,6] is a description of pump-driven hemodiafiltration. In that model, however, changes in blood and dialysate solute concentrations are not considered and, hence, that model does not provide a means to estimate the diffusive mass transfer coefficient. The same applies to the model by Van Geelen [10].

Overall diffusive mass transfer coefficient

The mass transfer coefficient (K_d) represents the overall (apparent) permeation coefficient or diffusive performance capacity of the hemofilter. Its value depends on the flow rates, ultrafiltration, concentration gradient, membrane permeability, the solute molecular weight, deteriorating conditions such as clotting and other physical conditions such as temperature. It represents the overall mass transfer coefficient of a flowing system, from which the lifetime is limited by some unfortunate deteriorating conditions (MI). Therefore, it cannot be considered as a constant during the whole operation time of the hemofilter. In conventional intermittent hemodialysis, where the dialysate flow rate is 5 to 6 times larger than that of CAVHD and the ultrafiltration flow is practically zero, the mass transfer coefficient (K_o), calculated by using eq.(6.45), will not be affected by the dialysate and ultrafiltration flows. When the dialysate flow rates are low as compared to the ultrafiltration flow rates, the mass transfer coefficient (K_d) of a CAVHD hemofilter has to be determined in the presence of ultrafiltration. By using eq.(6.50), one can calculate the mass transfer coefficient (K_d) when the ultrafiltration volume flux (J_v) is given by $J_v = \alpha + \beta x$. The calculated values of K_d and K_o show that the departure of K_o/K_d from one occurs at high values of Q_f/Q_{di}. For $Q_f/Q_{di} \ll 1$, the mass transfer coefficient K_d equals the mass transfer coefficient K_o calculated at zero-ultrafiltration. Values of the overall permeation coefficient depend not only on the rate of ultrafiltration flow but also on its direction.

The calculated mass transfer coefficient K_d shows that at high values of dialysate flow and low value of ultrafiltration, the overall mass transfer coefficient (K_d) of a CAVHD hemofilter equals the mass transfer coefficient (K_o) of a dialyzer in conventional intermittent hemodialysis. Also, the calculated mass transfer coefficient K_d shows no significant differences when the ultrafiltration volume flux is assumed to be constant along the length of the hemofilter if no back filtration occurs in the hemofilter. Unfortunately, it is not possible to show the effect of different rates of ultrafiltration flow on the overall permeation coefficient at a constant rate of dialysate flow, since the way of ultrafiltrate production in CAVHD differs from that of the pump-driven intermittent hemodiafiltration. In the intermittent hemodiafiltration, one can adjust the rate of ultrafiltration flow to a certain value while in CAVHD it is limited by the spontaneous transmembrane pressure. For the mathematical simplicity, the diffusive mass transfer coefficient can be calculated from eq.(6.50) which is valid for a constant volume flux model $(J_v = J_a = Q_f/S)$. Considering a constant ultrafiltration along

the membrane length will have minor influence on the calculated convective transport, due to a relatively small decrease of solute concentration in the blood compartment. A similar conclusion was reached by Jaffrin et al [5,6]. If there is no back filtration in the hemofilter, the use of K_a in place of K_d is preferable. Nevertheless, assuming a constant volume flux is risky concerning monitoring the pressure distributions along the hemofilter length, because, from a clinical point of view, back filtration needs to be avoided. When the dialysate fluid is filtered back into the blood of the patient, the back filtration can cause potentially unsterile dialysis fluid or pyrogen to enter the blood of the patient.

Shortcomings
This model is based on a linear decreasing volume flux model. A linear decreasing volume flux model is not always correct, especially at very high transmembrane pressure differences. The model equations apply to solutes with a sieving coefficient of one. This condition is likely to be met for most solutes, which are considered to contribute to the uraemic state. K_d will depend on solute parameters, of which the molecular weight or diameter is likely to be most important. The difference in molecular weight may fully account for the finding (See Chapter 8) that under equal circumstances the value of K_d for creatinine was 0.75 times that of urea. For phosphate, the value of K_d is likely to be decreased also by its polarity, which will increase apparent molecular weight by the binding of many of water molecules, while it will be increased by its negative charge, which increases the sieving coefficient. Such considerations are especially relevant when our model is used to analyze the clearance of other clinically relevant solutes, like drugs, by CAVHD. So far, our analytical model does not apply to solutes with a sieving coefficient of less than one. According to the specifications of the manufacturer, with the AN-69 membrane, solutes up to at least 1000 Daltons may be expected to have a sieving coefficient of one. When applying our model to the kinetics of still larger solutes, we should bear this limitation of our model in mind. Also, when considering drugs, protein binding and its influence on sieving would have to be taken into account. In those cases, the K_d derived from eqs.(6.48 and 6.50) can be used as an estimator.

7.5 CONCLUSION

Considering some simplifying conditions, the mathematical analysis shows that the diffusive mass transfer coefficient K_d can be calculated from the clinical data of CAVHD. The diffusive mass transfer coefficient proved to depend on the dialysate flow rate. The calculated mass transfer coefficient K_d shows that at high values of dialysate flow and low values of ultrafiltration, the overall mass transfer coefficient (K_d) of a CAVHD hemofilter equals the mass transfer coefficient (K_o) of a dialyzer in conventional intermittent hemodialysis. Also, the calculated mass transfer coefficient K_d shows no significant differences when the ultrafiltration volume flux is assumed to be constant along the length of the hemofilter if no back filtration

occurs in the hemofilter. We conclude that our model is a useful addition to the existing models of hemodiafiltration, especially since it allows calculation of the diffusive mass transfer coefficient. It may be used both as a means to further our insight in the determinants of solute transport in CAVHD and to adjust clinical settings, e.g. dialysate flow rate, based on the predicted clearance of uraemic solutes.

7.6 REFERENCES

[1]. Vincent HH, van Ittersum FJ, Akcahuseyin E, Vos MC, van Duyl WA, Schalekamp MADH. Solute Transport in Continuous Arteriovenous Hemodiafiltration: A New Mathematical Model Applied to Clinical Data, Blood Purif., (1990) Vol:8 pp.149-159.

[2]. Colton CK, Lowrie EG. Hemodialysis,: Physical principles and technical considerations, in: The Kidney, second edition 1981; 2: 2425-2489.

[3]. Sigdell J.E., Calculation of Diffusive and Convective Mass Transfer, The International Journal of Artificial Organs, (1982) Vol:5 pp.361-372.

[4]. Pallone TL, Hyver S, Peterson J. The simulation of continuous arteriovenous hemodialysis with a mathematical model. Kidney Int 1989; 35: 125-33.

[5]. Jaffrin MY, Ding L, Laurent JM. Simultaneous convective and diffusive mass transfer in a hemodialyser. Journal of Biomedical Engineering, (1990) Vol:112 pp.212-219.

[6]. Jaffrin MY, Gupta BB, Malbrancq JM. A one-dimensional hemodialysis and ultrafiltration with highly permeable membranes. Journal of Biomedical Engineering, (1981) Vol:103 pp.261-266.

[7]. Sargent JA, Gotch FA. Principles and biophysics of dialysis. In: Drukker W, Parsons FM, Maher JF. Replacement of renal function by dialysis. Martinus Nijhoff Medical Division Publ, The Hague, 1978.

[8]. Akcahuseyin E, van Duyl WA, Vos MC, Vincent HH. An analytical solution to solute transport in continuous arterio-venous hemodiafiltration (CAVHD). Med. Eng. Phys.(1996) Vol:18 No:1, pp.26-35.

[9]. Akcahuseyin E, Vincent HH, van Ittersum FJ, van Duyl WA, Schalekamp MADH.A Mathematical Model of Continuous Arterio-Venous Hemodiafiltration (CAVHD), Computer Methods and Programs in Biomedicine, (1990) Vol:31 pp.215-224.

[10]. van Geelen JA. Hemodiafiltration, simultaneous application of hemodialysis and hemofiltration.Thesis,1983. University of Limburg, Maastricht, the Netherlands.

[11]. Vincent HH, Akcahuseyin E, Vos MC, van Duyl WA, Schalekamp MADH: Continuous arteriovenous hemodiafiltration: Filter Design and Blood Flow Rate, Contrib Nephrol, (1991), 93, pp.196-198.

[12]. Vincent HH, Vos MC, van Duyl WA, Schalekamp MADH: Solute Transport in hemodiafiltration:A New Mathematical Model to Analyse Dialyzer Performance, Contrib Nephrol, (1991), 93, pp.199-201.

[13]. Babb LA, Maurer CJ, Fry DL, Popovich RP, McKee RE. The determination of membrane permeabilities and solute diffusivities with applications to hemodialysis. Chem Eng Progr Symp Ser no 84, 1968; 64: 59-68.

A SENSITIVITY ANALYSIS OF THE MODEL TO PARAMETERS AT LOW DIALYSATE FLOW RATES IN CAVHD

8.1 INTRODUCTION

In continuous arterio-venous hemodiafiltration (CAVHD), the removal of excess water is administered by using continuous arterio-venous hemofiltration (CAVH) while the removal of uraemic solutes is achieved by continuous slow dialysis, allowing manipulation of extracellular volume and solute concentration. Since the solute transport in CAVHD occurs by simultaneous convection and diffusion, it is necessary to make a clinical protocol prescribing the amount and with which flow rate the solute will be withdrawn, coupled with the removal of excess water simultaneously. As we have mentioned earlier, the ultrafiltration flow rate (Q_f) and the solute clearance (Cl) are used as measures of the removal rate of excess water and the removal rate of solute respectively. In CAVHD the solute clearance is determined by the dialysate flow rate (Q_{di}), the overall diffusive permeability coefficient (SK_d) of the hemofilter, the plasma water flow rate (Q_{wi}) at the blood inlet and the ultrafiltration flow rate (Q_f):

- Its relative low rates of dialysate flow make the CAVHD a unique treatment method, especially for the acute dialysis patients [1,2]. In CAVHD, the patient is mostly hemodynamically unstable [2]. Therefore, controlling the patient's uraemic state with dialysis as slow as possible is important. In the previous chapters, we have demonstrated that the dialysate flow rate is the main determinant for controlling the rate of solute removal by diffusion. However, how slow or how fast the dialysate flow rate will be is usually not known, since the administration of dialysate flow depends on the patient's uraemic state. According to the clinical experience, a dialysate flow rate of 1 l/h is enough to control the patient's uraemic state [3].

- The rate of solute removal by diffusion depends on the solute concentration driving force (concentration gradient) and on the overall diffusive permeability coefficient $(K_s=SK_d)$. In Chapter 7, we have demonstrated that the overall diffusive permeability coefficient $(K_s=SK_d)$ is an important parameter allowing us to manipulate the diffusive solute removal in the presence of ultrafiltration [4]. It includes the flow rates, the solute concentrations and the membrane surface area, which may be obtained from clinical measurements and manufacturers' specifications.

- In intermittent hemodialysis, the patient's blood is dialyzed with pump-driven blood and dialysate flow rates by adjusting them to their standard values, namely 200 and 500 ml/min respectively. The ultrafiltration flow rate is negligibly small. In CAVHD, however, the blood flows spontaneous (not routinely measured in the clinic) and depends on the patient's cardiac output and the resistance of the extracorporeal circuit. The ultrafiltration flow rate (Q_f) is also spontaneous. As we have studied in

Chapter 3 the ultrafiltration flow rate decreases over the treatment time because of the deterioration of the hemofilter membrane. With prolonged use of the hemofilter, deterioration of the hemofilter membrane is likely not only to decrease the rate of ultrafiltrate production but also to impair the diffusive solute transport [4].

In this chapter we studied the determinants of uraemic solute clearance in CAVHD. First, on considering the spontaneous blood and ultrafiltration flows, we analyzed the clearance of uraemic solutes such as urea, creatinine and phosphate in the region of relative low dialysate flow rates. Second, by analyzing the effect of the dialysate, blood and ultrafiltration flow rates on the uraemic solute clearance we investigated the degree of conditions in which blood-dialysate solute equilibrium can be achieved. Third, we investigated the diffusive component of solute clearance in relation to the overall diffusive permeability coefficient (SK_d). Fourth, the diffusive permeability coefficients of urea and phosphate were related to diffusive permeability coefficient of creatinine. Further, by running a simple sensitivity analysis on the overall diffusive permeability coefficient ($SK_d = K_s$), we analyzed the dependence of K_s on the flow rates and on the strength of concentration driving force at the blood inlet of the hemofilter (C_{do}/C_{wi}). The sensitivity analysis provides information about the reliability of predicting the K_s from flow rates and solute concentrations.

8.2 METHODS

Solute clearance (Cl) and the overall diffusive permeation coefficient ($K_s = SK_d$)
In CAVHD, solute clearance (Cl) is a measure of the rate of solute removal by simultaneous convection (Cl_c) and diffusion (Cl_d). Both mechanisms have effect on each other. Usually, the solute clearance (dialysance) is calculated from the mass balance equations of either the blood side or the dialysate side of the hemofilter membrane. Since the inlet dialysate uraemic solute concentration (C_{di}) is zero, the uraemic solute clearance may be calculated from eq.(6.39). In Chapter 6, we derived an expression of solute clearance, which may be calculated from the flow rates and the overall diffusive permeability coefficient ($K_s = SK_d$) in the presence of ultrafiltration. The solute clearance per unit rate of ultrafiltration is given (See eq.(6.51)) by:

$$\frac{Cl}{Q_f} = \frac{Q_{wi}}{Q_f} \frac{1 - (\frac{Q_{do} Q_{wo}}{Q_{di} Q_{wi}})^{S\frac{K_d}{Q_f} + \frac{1}{2}}}{1 - \frac{Q_{wi}}{Q_{do}} (\frac{Q_{do} Q_{wo}}{Q_{di} Q_{wi}})^{S\frac{K_d}{Q_f} + \frac{1}{2}}} \tag{8.1}$$

where Q_{wi} is the inlet flow rate of plasma water, Q_{di} is the inlet dialysate flow rate, $Q_{wo} = Q_{wi} + Q_f$ is the flow rate of outlet plasma water, $Q_{do} = Q_{di} + Q_f$ is the outlet dialysate flow rate, Q_f is the net flow rate of ultrafiltration, S is the total surface area of the hemofilter membrane and finally K_d is the overall diffusive mass transfer coefficient. To calculate the solute clearance from eq.(8.1) one needs the overall diffusive permeability coefficient ($K_s = SK_d$). Using eq.(8.1)

and eq.(6.39), the overall diffusive permeability coefficient ($K_s=SK_d$) per unit rate of the ultrafiltration flow (Q_f) can be reformulated as:

$$\frac{SK_d}{Q_f} = \frac{\ln\left[\dfrac{Q_{do}\,C_{do} - Q_{wi}C_{wi}}{Q_{wi}\,(C_{do} - C_{wi})}\right]}{\ln\left(\dfrac{Q_{wo}\,Q_{do}}{Q_{wi}\,Q_{di}}\right)} - \frac{1}{2} \tag{8.2}$$

where C_{do} is the solute concentration at the dialysate/ultrafiltrate outlet, C_{wi} is the solute concentration at the blood inlet. The overall diffusive permeability coefficient ($K_s=SK_d$) per unit rate of the ultrafiltration flow (Q_f) represents the relative importance of solute removal to the removal rate of excess water. This expression is valid only for solutes with sieving coefficient $\gamma=1$ and for a constant profile of ultrafiltration volume flux along the hemofilter length. In previous chapters, we used K_a to represent the overall mass transfer coefficient for a constant profile of ultrafiltration. We have proved in Chapter 7 that assuming a constant profile for the local ultrafiltration volume flux has negligible effect on the numerical values of K_d. In this text, therefore, the notation "K_a" is simply replaced by the notation "K_d".

Sensitivity analysis of K_s

In eq.(8.2), solute concentrations and flow rates are variables and measured clinically. The considered values of C_{wi}, C_{do}, Q_{wi}, Q_{di} and Q_f are within the range of clinically measured values during CAVHD treatment. The variation in each data point, namely ΔC_{wi} in C_{wi}, ΔC_{do} in C_{do}, ΔQ_{wi} in Q_{wi}, ΔQ_{di} in Q_{di} and ΔQ_f in Q_f, will contribute a variation ΔK_s in the calculated value of K_s. The variation ΔK_s can be estimated by using the following expression:

$$(\Delta K_s)^2 \approx (\Delta C_{wi}\frac{\partial K_s}{\partial C_{wi}})^2 + (\Delta C_{do}\frac{\partial K_s}{\partial C_{do}})^2 + (\Delta Q_{wi}\frac{\partial K_s}{\partial Q_{wi}})^2 + (\Delta Q_{di}\frac{\partial K_s}{\partial Q_{di}})^2 + (\Delta Q_f\frac{\partial K_s}{\partial Q_f})^2 \tag{8.3}$$

where the derivatives on the right are partial derivatives, each representing the differentiation of K_s with respect to one variable (C_{wi}, C_{do}, Q_{wi}, Q_{di} and Q_f) while the other variables are supposed to be constant. All the variations in eq.(8.3) are estimated experimental variations in measuring the related variable and supposed to be independent of each others. From eq.(8.2) one can derive the partial derivatives needed in eq.(8.3). The variations of K_s with respect to solute concentrations C_{wi} and C_{do} are given by:

$$\frac{\partial K_s}{\partial C_{wi}} = \frac{Q_f}{k_1}\frac{C_{do}\,(Q_{do} - Q_{wi})}{k_2\,(C_{wi} - C_{do})} \tag{8.4}$$

$$\frac{\partial K_s}{\partial C_{do}} = \frac{Q_f}{k_1}\frac{C_{wi}\,(Q_{wi} - Q_{do})}{k_2\,(C_{wi} - C_{do})} \tag{8.5}$$

where k_1 and k_2 are defined as:

$$k_1 = \ln(\frac{Q_{wo} Q_{do}}{Q_{wi} Q_{di}}) \tag{8.6}$$

$$k_2 = Q_{wi} C_{wi} - Q_{do} C_{do} \tag{8.7}$$

The variations of K_s with respect to the flow rates Q_{wi}, Q_{do} and Q_f are given by:

$$\frac{\partial K_s}{\partial Q_{wi}} = \frac{Q_f}{k_1}[\frac{Q_{do} C_{do}}{Q_{wi} k_2} - (\frac{k_3}{k_1})(\frac{Q_f}{Q_{wo} Q_{wi}})] \tag{8.8}$$

$$\frac{\partial K_s}{\partial Q_{di}} = \frac{Q_f}{k_1}[(\frac{k_3}{k_1})(\frac{Q_f}{Q_{do} Q_{di}}) - \frac{C_{do}}{k_2}] \tag{8.9}$$

$$\frac{\partial K_s}{\partial Q_f} = \frac{K_s}{Q_f} - \frac{Q_f}{k_1}[\frac{C_{do}}{k_2} + (\frac{k_3}{k_1})(\frac{1}{Q_{do}} - \frac{1}{Q_{wo}})] \tag{8.10}$$

$$k_3 = \ln[\frac{k_2}{Q_{wi}(C_{wi} - C_{do})}] \tag{8.11}$$

Experimental evaluation

The sensitivity analysis of the model to the parameters at low dialysate flow rates was performed using clearance data of uraemic solutes such as urea (MW:60 Daltons), creatinine (113 Daltons) and phosphate (174 Daltons), obtained from different patients who were treated with CAVHD for acute renal failure, using the AN-69 capillary hemofilters (Multiflow 60, Hospal, France, $S=0.6$ m^2 and $L_f=0.13$ m) [5]. Blood and ultrafiltration flows were spontaneous. Arterial blood flow rates (Q_{ba}) were determined by the displacement of an air bubble over a length of tubing, with a relative variation of $\Delta Q_{ba}/Q_{ba}=10\%$. The range of blood flow varied from 82 ml/min to 345 ml/min. An electronic weighing device determined dialysate flow rates (Q_{di}), with a relative variation of $\Delta Q_{di}/Q_{di}=5\%$. For each blood flow rate, the dialysate flow rate was varied with $Q_{di}=0.5, 1, 2$ and 3 l/h. The net ultrafiltration rate (Q_f) at each set of blood and dialysate flow rate was determined by timed collection with a relative variation of $\Delta Q_f/Q_f=5\%$. The measured net ultrafiltration rate varied from 3 to 18 ml/min. Accordingly, solute concentration (C_{wi}) in the inlet plasma water and the removed solute concentration (C_{do}) were determined with a relative variation of $\Delta C_{wi}/C_{wi}=\Delta C_{do}/C_{do}=3\%$.

8.3 RESULTS

In Table 8.1, the operational and clinical conditions and also the results of model calculations (MI, K_s, Cl, etc.) for the measurement of urea, creatinine and phosphate clearance are shown in average values within their ranges.
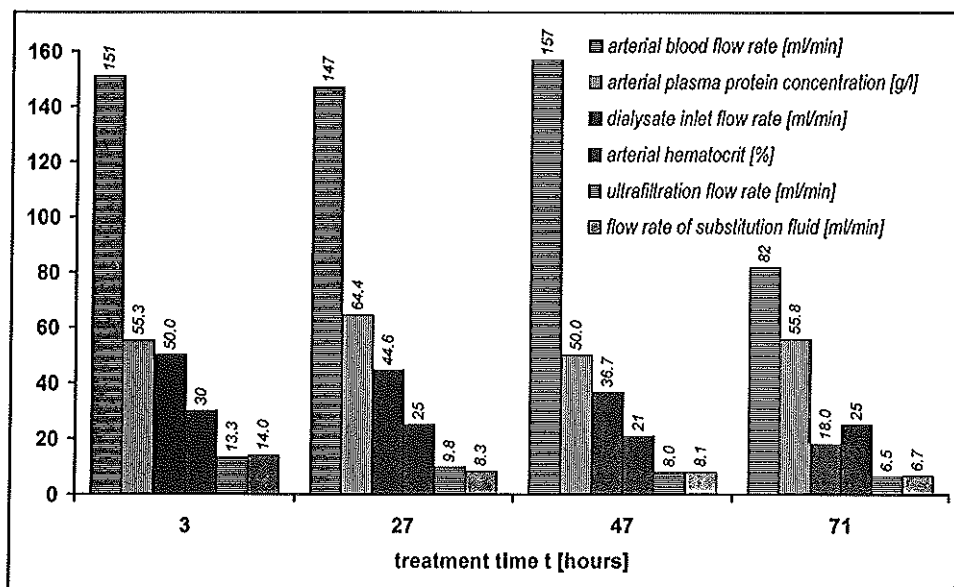
Figure 8.1: Blood, dialysate, ultrafiltration, substitution fluid flow rate, arterial plasma protein concentration and hematocrit of a patient during a CAVHD treatment of 3 days.
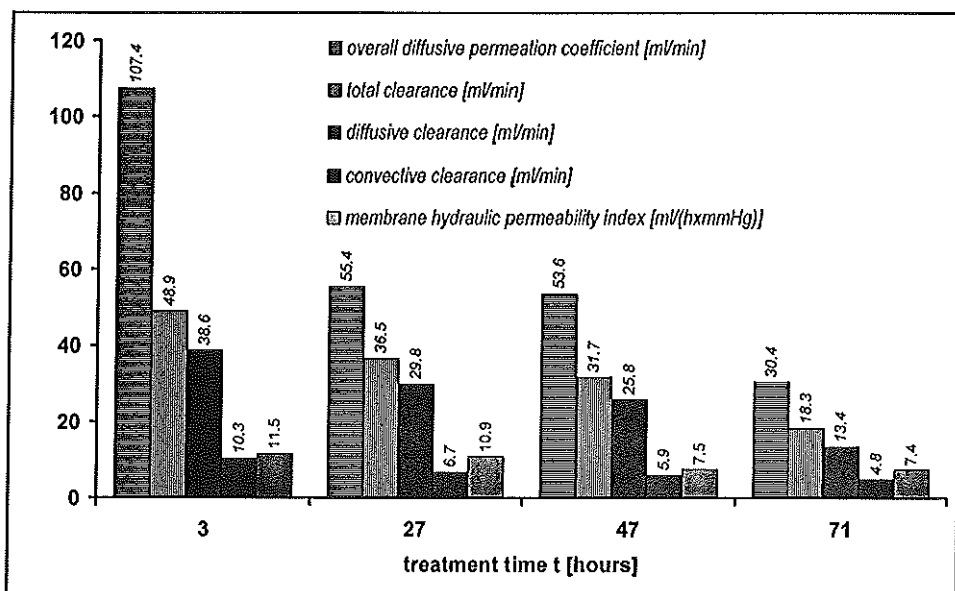
Figure 8.2: Overall, diffusive and convective urea clearance of a patient and the hydraulic (MI) and diffusive (SK_d) performance of an AN-69 capillary hemofilter during a CAVHD treatment of 3 days

Figures 8.1 and 8.2 show an example of blood (Q_{ba}), dialysate (Q_{di}), ultrafiltration (Q_f), flow

rate of substitution fluid (Q_{pred}), arterial plasma protein concentration (C_{pa}), hematocrit (Ht_a), the overall (Cl), diffusive (Cl_d) and convective (Cl_c) urea clearance and the hydraulic (MI) and diffusive (SK_d) performance of an AN-69 capillary hemofilter during a patient treatment of 3 days with CAVHD.

Table 8.1: Urea, creatinine and phosphate clearance under different clinical and operational conditions measured with Multiflow-60 AN-69 capillary hemofilters and special CAVH catheters (M8CAVHD4, 11.4 long with an internal diameter of 2.7 mm) for both arterial and venous access.

| average [range] value (n=51)		average [range] value (n=51)	
C_{pa} [g/l]	60.4 [37.6 - 85.3]	K_s -urea [ml/min]	51.1 [7.5 - 111.6]
Q_{ba} [ml/min]	187.2 [82 - 345]	K_s - creatinine [ml/min]	42.3 [7.2 - 108.4]
Ht_a	0.27 [0.18 - 0.32]	K_s - phosphate [ml/min]	31.2 [7.2 - 60.1]
Q_{di} [ml/min]	27.9 [8 - 56]	Cl -urea [ml/min]	28.1 [7.3 - 55]
Q_f [ml/min]	9 [3 - 18]	Cl -creatinine [ml/min]	25.7 [7.1 - 49.6]
Q_{pred} [ml/min]	8.3 [1.7 - 17]	Cl -phosphate [ml/min]	22.9 [6.4 - 42.1]
TMP_m [mmHg]	67 [24 - 107]	R_f [mmHg/mlmin]	0.24 [0.04 - 0.53]
T (°C)	37	MI [ml/hmmHg]	8.3 [2.5 - 18.7]

URAEMIC SOLUTE CLEARANCE

Dialysate flow rate (Q_{di})

For conventional intermittent hemodialysis, where the ultrafiltration flow rate (Q_f) is almost zero [6,7,8,9], the solute clearance is mainly due to diffusive mass transfer. In CAVHD however, solute removal occurs by simultaneous convection and diffusion. Since the rate of ultrafiltrate production limits the solute convective clearance, higher rates of solute diffusive clearance are achieved by increasing the dialysate flow rate. Depending on the patient's uraemic state, it varies between 0.5 and 3 l/h. In Figure 8.3, the urea clearance measured under the conditions in Table 8.1 is shown in relation to the dialysate flow rate at two different rates of blood flow, e.g. an averaged blood inlet flow rate of 295 ml/min and 160 ml/min. The corresponding average ultrafiltration flow rates were 12.6 and 9 ml/min respectively. The values obtained by extrapolating the clearance (dashed lines) at Q_{di}=0 are the convective contributions (Cl_c) to the overall urea clearance. The average contribution of convective clearance was 11.5 for Q_{bi}=295 and 7.8 ml/min for Q_{bi}=160 ml/min.
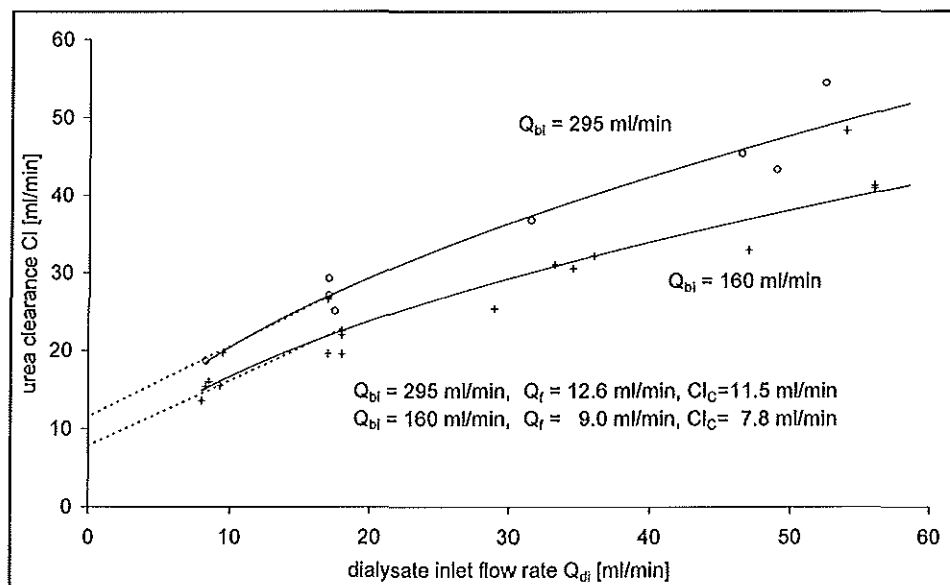
Figure 8.3: Urea clearance in relation to the dialysate flow rate (Q_{di}) for two different rates of the blood inlet flow (Q_{bi}) and the ultrafiltration flow (Q_f) [10].
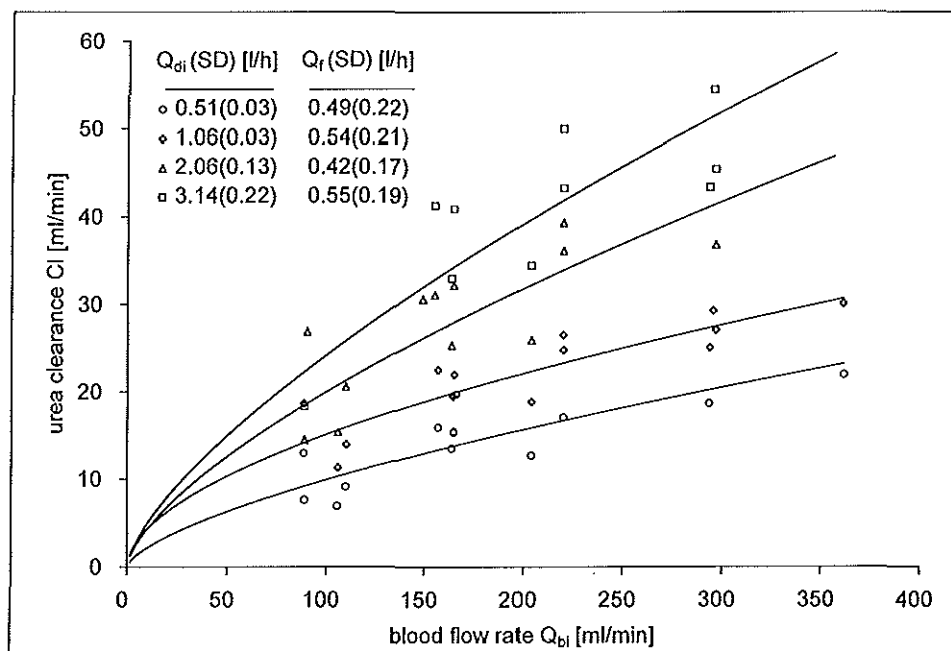
Figure 8.4: Urea clearance as a function of the blood inlet flow rate (Q_{bi}) for dialysate flow rates of 0.5, 1, 2 and 3 l/h and for an ultrafiltration flow rate of approximately Q_f=0.5 l/h.

Blood flow rate (Q_{bi})

In CAVHD, the blood (Q_{bi}=50-350 ml/min) and ultrafiltrate (Q_f=5-20 ml/min) flows are spontaneous. Since the blood flow depends on the patient's cardiac output and the resistance of extracorporeal circuit, high rates of blood flow may be difficult to achieve. The urea clearance measured at different blood flow rates is shown in Figure 8.4 for the dialysate flow rates of 0.5, 1, 2 and 3 l/h. The trend lines show a curvilinear increase in urea clearance with Q_{bi} at relative high rates of the dialysate flow. High blood flow rates favor high rates of solute removal. The fluctuations in the clearance data in Figure 8.4 are due to the fluctuations in the ultrafiltration flow rate. The blood flow rate is strongly dependent on the resistance of the extracorporeal circuit to the blood flow (R_f). Data of uraemic solute clearance for R_f>0.4 mmHg/(ml/min) were disregarded. For R_f>0.4 mmHg/(ml/min) the hemofilter was assumed to be clotted.

Ultrafiltration flow rate (Q_f)

Values of the same urea clearance data corresponding to the different ultrafiltration rates are illustrated in Figure 8.5
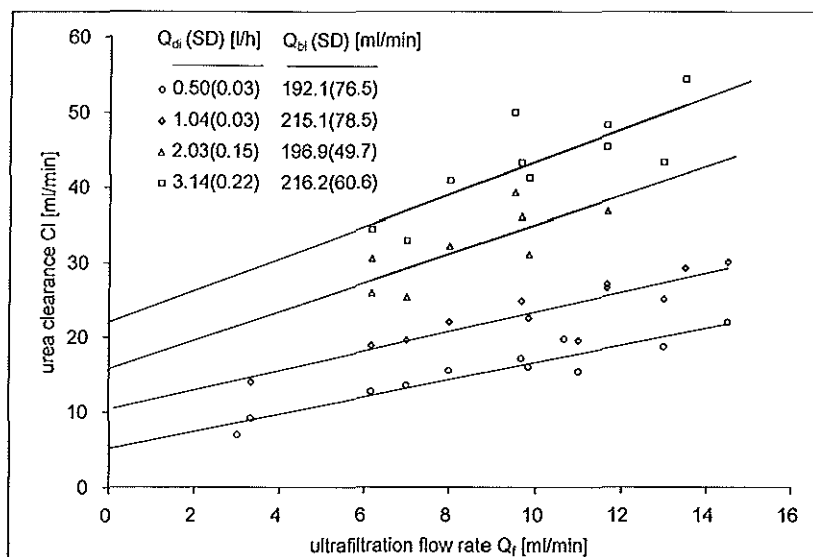
Figure 8.5: Urea clearance as a function of the ultrafiltration flow rate (Q_f) for dialysate flow rates of 0.5, 1, 2 and 3 l/h [10].

Evidently, increasing the rate of ultrafiltration (Q_f) will result in an increased urea clearance since the convective contribution to total urea clearance is proportional to the rate of ultrafiltration. To some extend the ultrafiltration flow rate can easily be controlled by adjusting the hemofilter position with respect to the patient's bed. Furthermore, the hemofilter

characteristics may change with time due to the binding of plasma proteins to the membrane or due to clotting. With CAVHD, effectiveness of therapy rests in large part on low solute clearance continuously maintained over a prolonged period of time. Hence the effect of deteriorating conditions over time on the hemofilter performance is important. The ultrafiltration flow rate rapidly decreases with the treatment time. After a variable time span, ultrafiltration flow rate falls below the level necessary for fluid removal and the hemofilter must be changed. The fall in the ultrafiltration flow rate over time results in a decrease in solute clearance primarily due to a decline in the convective component. The trend lines in Figure 8.5 show that as ultrafiltration is increased the overall (total) urea clearance increases linearly. Since the sieving coefficient of urea (and of other uraemic solutes) for the AN-69 membrane is 1, the convective clearance is essentially the same as the ultrafiltration flow rate. According to eq.(6.39), the intercepts of the trend lines with the clearance (Cl)- axis at Q_f=0 ml/min correspond to the pure diffusive contributions to the overall urea clearance. In Figure 8.5, the data of urea clearance corresponding to the ultrafiltration flow rates less than 3 ml/min were not taken into account.
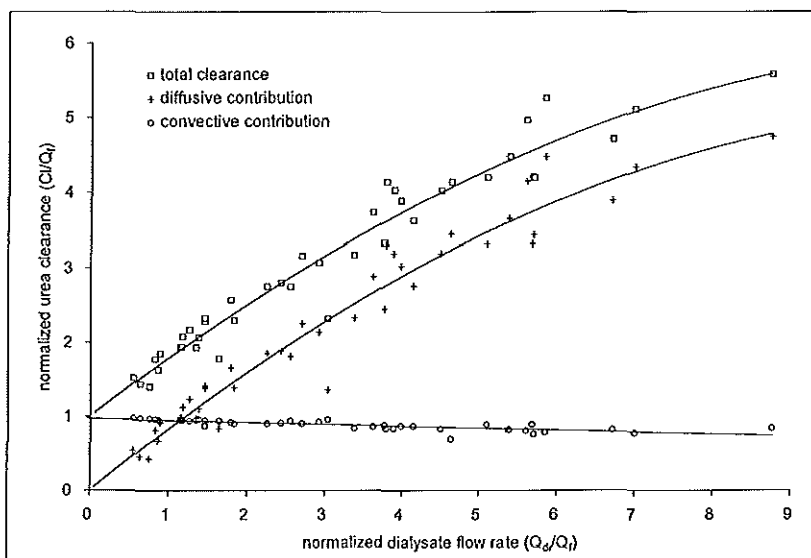
Figure 8.6: The normalized diffusive and convective contributions of urea clearance in relation to the dialysate flow rate, normalized with respect to (Q_{di}/Q_f).[10].

Diffusive and convective contributions to the uraemic solute clearance

As we have stated earlier in Chapter 5, the division of solute clearance (Cl) into separate convective (Cl_C) and diffusive (Cl_D) contributions as in eq.(6.41) and eq.(6.42) is somewhat misleading since the convective flow alters the concentration profiles because of the inter-

action between the convective and diffusive components. Therefore, model predictions of the diffusive (Cl_d) and convective (Cl_c) contributions to the total (overall) urea clearance were calculated according to eq.(6.44) and eq.(6.43) respectively. The overall urea clearance normalized to the ultrafiltration flow rate (Cl/Q_f) calculated according to eq.(8.1), the diffusive component normalized to the ultrafiltration flow rate (Cl_d/Q_f) calculated according to eq.(6.44) and the convective component normalized with respect to the ultrafiltration flow rate (Cl_c/Q_f) calculated according to eq.(6.43) are shown in Figure 8.6 in relation to the dialysate inlet flow rate normalized with respect to the ultrafiltration flow rate (Q_{di}/Q_f). In the analysis of regression lines representing the relation between Cl/Q_f and Q_{di}/Q_f, the blood flow rate varied from 82 to 345 ml/min, yielding an averaged value of 213 ml/min. The lines in Figure 8.6 represent thus the general trends for an average blood flow rate of Q_{ba}=213 ml/min.

In CAVHD, the dialysate flow is administered in the presence of ultrafiltration. Therefore, in the analysis of solute clearance from the 'dialysate flow' point of view, the presence of ultrafiltration flow has to be taken into account. As can be seen from Table 7.2 and Figure 8.6, the convective component of the overall urea clearance decreases (slightly) with the increasing rate of the dialysate flow. One of the differences between CAVHD and conventional intermittent hemodialysis is the effect of increasing dialysate flow rate (Q_{di}) on ultrafiltration flow rate (Q_f). In intermittent hemodialysis systems increases in Q_{di} results in decreases in Q_f because of the increased hydrostatic pressure in the dialysate compartment, which decreases the net transmembrane pressure difference. However, in CAVHD, increases in dialysate flow rate do not decrease Q_f because the dialysate flow rate is so small in size and compliance of the dialysate compartment. As can be seen from Figure 8.6, the urea clearance per ultrafiltration flow rate (Cl/Q_f) increases with increasing rates of the normalized dialysate flow (Q_{di}/Q_f) in a quadratic form. Figure 8.6 shows a linear relation between the normalized urea clearance and the dialysate flow rate for $Q_{di}/Q_f \leq 3$. Lowering the dialysate flow rate faster than the rate of ultrafiltration weakens the concentration driving force and eventually dialysate saturation (diffusion equilibrium) takes place. At Q_{di}=0, solute removal occurs only by convection ($Cl=Q_f$), resulting in the solute concentration in the blood inlet (C_{wi}) becoming equal to the solute concentration in the dialysate/ultrafiltrate outlet (C_{do}) if there is no clotting in the hemofilter.

Dialysate-blood equilibrium (saturation)
In contrast to the conventional intermittent hemodialysis, in CAVHD an excellent dialysate-blood equilibration is achieved. To determine the degree to which blood and dialysate achieve equilibrium of urea concentration during CAVHD, we analyzed the normalized dialysate flow rate in relation to the ratio (C_{do}/C_{wi}) with C_{do} the uraemic solute concentration at the dialysate/ultrafiltrate outlet and C_{wi} the uraemic solute concentration at the blood inlet of the hemofilter.
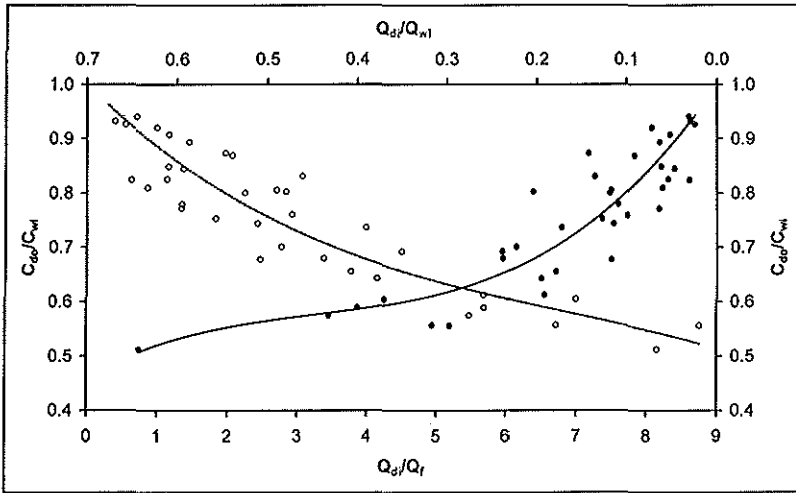
Figure 8.7: The ratio of solute concentration at the blood inlet to that at the dialysate outlet (C_{do}/C_{wi}) as a function of the dialysate flow administered per ultrafiltration flow rate (Q_{di}/Q_f) (dashed line) and as a function of the ratio of dialysate flow rate to the blood inlet flow rate (Q_{di}/Q_{wi}) [10].

In Figure 8.7, the ratio (C_{do}/C_{wi}) is related to the normalized dialysate flow rate (Q_{di}/Q_f) and to the ratio of dialysate-to-plasma water inflow (Q_{di}/Q_{wi}). From Figure 8.7 it can be seen that for approximately $Q_{di}/Q_f \leq 3$ and $Q_{di}/Q_{wi} \leq 0.2$, the ratio C_{do}/C_{wi} increases from 0.7 up to 1 where complete blood-dialysate equilibration for urea is achieved. Sigler et al [2] assigned the reduction of the dialysate-to-blood-urea concentration ratio (C_{do}/C_{wi}) below 1 to an early sign of hemofilter clotting. When $C_{do}/C_{wi} < 0.6$ complete clotting can be anticipated within next 3 to 4 hours. They stated this for a dialysate flow rate of 1l/h. In fact, the term C_{do}/C_{wi} represents the strength of the concentration driving force at the hemofilter blood inlet. The smaller the ratio C_{do}/C_{wi} (thus $C_{do}/C_{wi} \ll 1$), the stronger the concentration driving force. Also in the absence of clotting, by relative high dialysate flow rates, as can be seen From 8.7, values ≤ 0.6 for C_{do}/C_{wi} may be achieved, leading to a solute clearance more by diffusion than that by convection.

In the region of low dialysate flow rates, where the dialysate-blood equilibrium occurs, the ultrafiltration may improve the dialysis. It is, in fact, a prediction of our mathematical model that at low dialysate flow rates and low overall diffusive permeability, the diffusive component of solute clearance may increase as ultrafiltration flow rate rises. During simultaneous convection and diffusion, the ultrafiltrate formed across the hemofilter membrane carries solute at a concentration (C_m, see eq.(5.15)) that is less than that in the plasma water. By that, true convective clearance must be less than the rate of ultrafiltration. If the ultrafiltrate so

formed, particularly near the hemofilter blood outlet where the solute concentration in blood is least (See Figures 7.1 and 7.2), is to leave the hemofilter at the dialysate/ultrafiltrate outlet in equilibrium with the blood side, prior to exit of that ultrafiltrate from the hemofilter, some additional solute from the blood side must be transported by diffusion. From Figure 7.1 can be seen that as the dialysate flow rate decreases, nearly complete equilibrium can exist in the first half of the hemofilter length, while diffusion transports solute in the second half from the blood side. For conditions of perfect blood-dialysate equilibration at the blood inlet of the hemofilter, the entire solute carried by the dialysate flow must be transported by diffusion (in the second half of the hemofilter) so that the total rate of diffusive solute removal will exceed the rate of dialysate flow ($Cl > Q_{di}$). Nevertheless, Sigdell [9] and other authors [12] have suggested that, due to solvent drag, increasing rates of ultrafiltration may diminish the diffusive component of solute clearance by reducing the blood-dialysate concentration gradient.
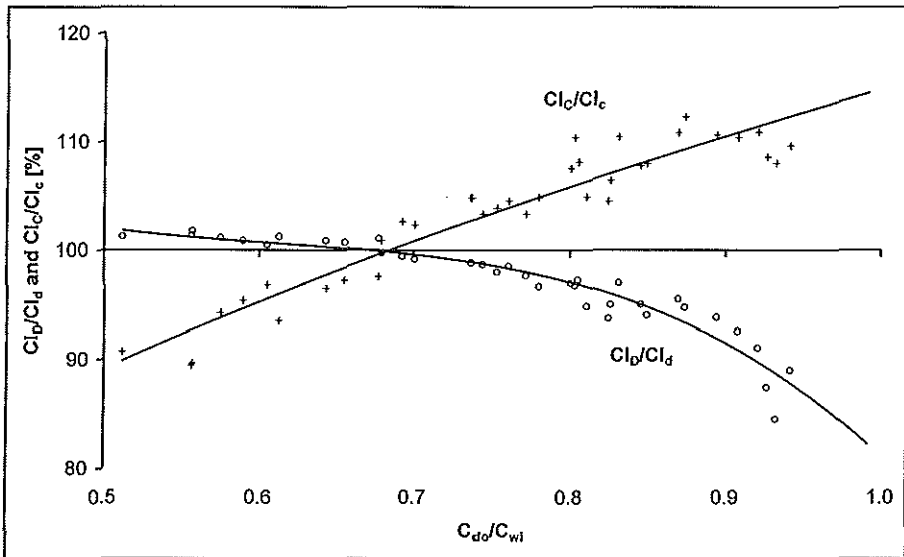
Figure 8.8: The calculated diffusive and convective urea clearance as a function of the ratio (C_{do}/C_{wi}). The Cl_D and Cl_C represent the diffusive and convective contributions to the solute clearance respectively in the manner used by Sigler et al [2].

In the analysis of solute transport the fact that $C_{do}/C_{wi} \approx 1$ allows the diffusive and convective components to be computed as separate components of solute clearance. Justification of this assertion rests on the fact that when there is dialysate saturation (or equilibrium) where $C_{do} = C_{wi}$, the diffusive transport will always be the one value that is the upper limit for a given solute concentration and volume flow rate. The explicit upper limit is numerically equal to

the dialysate flow rate (Cl=Q_{di}), where $Q_{wi} \gg Q_{di}$. As Q_{wi} falls or becomes equal to Q_{di} there are progressive deviations from complete dialysate-blood urea saturation. In intermittent hemodialysis, dialysate saturation does not occur and it is not possible to accurately compute the separate diffusive (Cl_D) and convective (Cl_C) components from eq.(6.41) and eq.(6.42).

Model predictions of the diffusive (Cl_D) and convective (Cl_C) contributions to the total (overall) urea clearance were also calculated in the manner used by Sigler et al [2] according to eq.(6.41) and eq.(6.42) respectively. In Figure 8.8, the ratio of diffusive clearance according to eq.(6.41) to the diffusive clearance according to eq.(6.44) (Cl_D/Cl_d) and the ratio of convective clearance according to eq.(6.42) to the convective clearance according to eq.(6.43) (Cl_C/Cl_c) are shown for various values of the ratio C_{do}/C_{wi}.

At about $C_{do}/C_{wi}=0.7$, Cl_D becomes equal to Cl_d and the Cl_C becomes equal to Cl_c. For $C_{do}/C_{wi} \geq 0.7$, the fraction of urea clearance due to diffusion, as determined by eq.(6.44) was underestimated by eq.(6.41). As is shown in Table 7.2 this underestimation corresponds to the values of low dialysate flow rates at relative high rates of ultrafiltration flow. From $C_{do}/C_{wi}=0.7$ up to $C_{do}/C_{wi}=1$, the underestimation rises up to 20%. For $C_{do}/C_{wi} \leq 0.7$, the diffusive clearance by eq.(6.41) with respect to the diffusive clearance by eq.(6.44) is overestimated by no more than 5%. In contrast to the diffusive clearance, from $C_{do}/C_{wi}=0.7$ up to $C_{do}/C_{wi}=1$, the fraction of urea clearance due to convection as determined by eq.(6.43) is overestimated by eq.(6.42). According to eq.(6.41) and eq.(6.42), the dialysate flow rate normalized with respect to the rate of ultrafiltration flow (Q_{di}/Q_f) equals the ratio Cl_D/Cl_C. According to the trend lines in Figures 8.6 and 8.7, we may hardly prove the existence of the relation $Cl_D/Cl_C=Q_{di}/Q_f$ in CAVHD, since the definition of diffusive contribution (Cl_D) (or clearance) according to Sigler et al [2] is a hypothetical clearance that would produce the same concentration at the dialysate outlet without ultrafiltration.

Overall diffusive permeability coefficient

According to eq.(6.44) the diffusive urea transport (clearance) is proportional to the overall diffusive permeability coefficient ($K_s = SK_d$) and to the existing concentration gradient. An increase in the overall diffusive permeability will lead consequently to an increase in the diffusive solute clearance. The size of this increase depends strongly on the dialysate flow rate, noting that the overall diffusive permeability coefficient itself depends also on the dialysate flow rate [5]. In Chapter 7, the effect of dialysate flow rates on the overall diffusive permeability was demonstrated in Figure 7.5.

In Figure 8.9, the relation between the diffusive urea clearance and the overall diffusive permeability coefficient is illustrated for the dialysate flow rates of 0.5, 1, 2, and 3 l/min, showing the curvilinear increase of the diffusive urea clearance with the increasing values of

the diffusive permeability. To calculate solute clearance from eq.(8.1), the overall diffusive permeability coefficient ($SK_d=K_s$) has to be determined in the presence of ultrafiltration, noting the fact that we derived the overall diffusive permeability coefficient as normalized with respect to the ultrafiltration flow rate (SK_d/Q_f) from the expression of the normalized urea clearance (Cl/Q_f) according to eq.(8.1). The overall diffusive permeability coefficient (SK_d/Q_f) is a measure of the relative importance of solute removal by diffusion with regard to that by ultrafiltration (convection). At $SK_d/Q_f=0$, the solute clearance becomes equal to the ultrafiltration flow rate ($Cl=Q_f$).
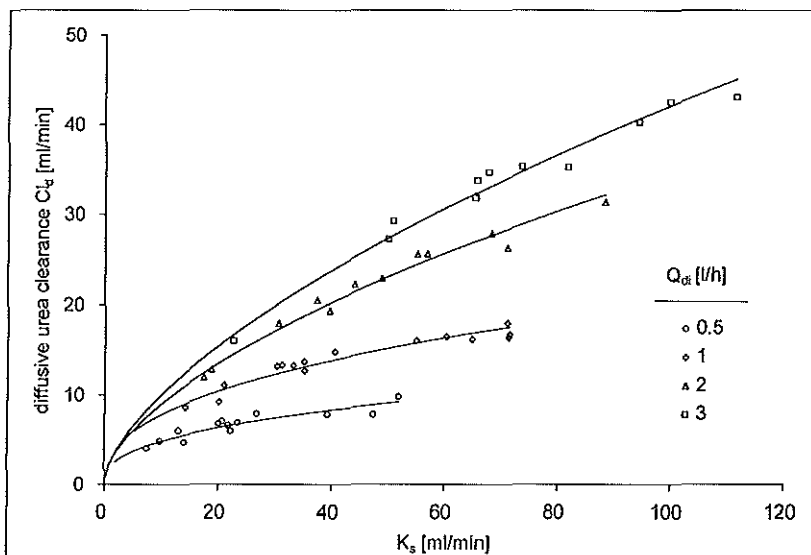
Figure 8.9: Diffusive urea clearance (Cl_d) as a function of the overall diffusive permeability coefficient (K_s) at different rates of dialysate inlet flow (Q_{di}) [10].

Clearance of different uraemic solutes

As can be seen from Table 8.1, uraemic solutes such as urea, creatinine and phosphate were cleansed from blood with different rates of removal under the same operational conditions, with the flow rates ranging from $Q_{ba}=82$ to 345 ml/min, $Q_{di}=0.5$ to 3 l/h and $Q_f=3$ to 18 ml/min. It is evident that the difference in the clearance of uraemic solutes is caused by the overall diffusive permeability of the hemofilter membrane. Under the same operational conditions and hemofilter characteristics we calculated the overall diffusive permeability coefficients ($K_s=SK_d$) for urea, creatinine and phosphate. In Figure 8.10, the K_s's of urea and that of the phosphate are shown in comparison to the K_s of creatinine, all under the same operational conditions and hemofilter characteristics. The regression lines, representing the following regression equations,

$$K_s(urea) = 1.32 K_s(creatinine) \quad R^2 = 0.94 \quad n = 36 \tag{8.12}$$

$$K_s(phosphate) = 0.75 K_s(creatinine) \quad R^2 = 0.88 \quad n = 36 \tag{8.13}$$

show that the K_s of urea is 32% greater and that of the phosphate is 25% smaller than the K_s of creatinine. With increasing molecular size (weight) of solutes, the overall diffusive permeability coefficient was observed to decrease. The data regarding the overall permeability coefficients of these solutes were obtained under the conditions where the hemofilter resistance to blood flow varied between 0.04 en 0.4 mmHg/(ml/min) as we mentioned earlier. The overall diffusive permeability coefficient (K_s) for urea, creatinine, phosphate and other solutes (some antibiotic drugs) up to 1500 Daltons are shown in relation to the hemofilter hydraulic condition (MI) and the dialysate flow rate (Q_{di}) in Chapter 9.
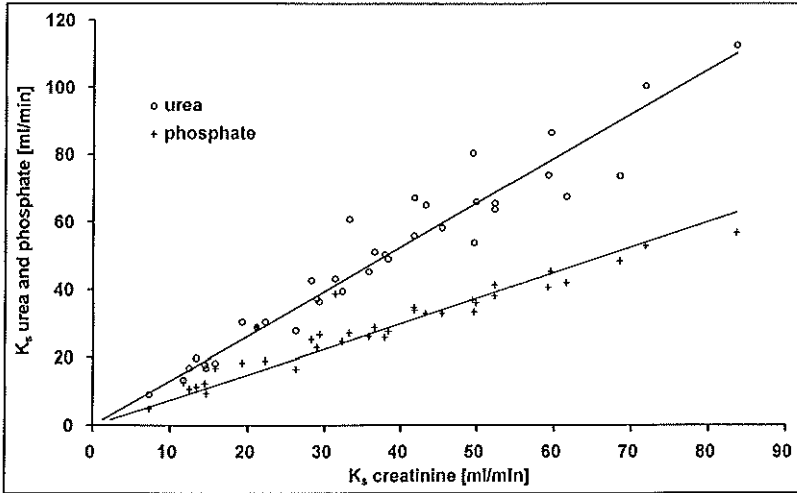
Figure 8.10: The overall diffusive permeability coefficients of creatinine and phosphate in relation to the overall diffusive permeability coefficient of urea. The permeability coefficients were obtained under the same operational conditions.

SENSITIVITY OF K_s AT LOW DIALYSATE FLOW RATES

As mentioned before, the CAVHD is a unique treatment method with its very slow dialysis that is mostly provided by keeping the dialysate flow at relative low rates. In order to determine the effect of flow rates and concentration gradients on predicting the values of diffusive permeation coefficient from clearance data, a simple sensitivity analysis is performed by calculating the relative variations of the overall diffusive permeability coefficient ($\Delta K_s/K_s$) due to the relative variations of flow rates and solute concentrations, according to eq.(8.3).

The relative variation of the overall diffusive permeability coefficient ($\Delta K_s/K_s$) due to the concentration gradient (C_{do}/C_{wi}), is illustrated in Figure 8.11. As can be seen from Figure 8.11, the $\Delta K_s/K_s$ remains constant (unchanged) up to $C_{do}/C_{wi}=0.7$, probably due to the fact that the K_s reaches its maximal value ($K_d$max) where the concentration driving force at that moment is the strongest. From $C_{do}/C_{wi}=0.7$ up to 1 (dialysate saturation), the $\Delta K_s/K_s$ shows a sharp increase of up to more than 30%, resulting from a sharp decrease in K_s due to blood-dialysate equilibrium. In Chapter 7, see for example Figure 7.5, we have demonstrated that the K_s increased with increasing rates of the dialysate flow up to its limiting (maximal) value in a quadratic form. By comparing Figure 8.7 with Figure 8.11, it can be seen that the value $C_{do}/C_{wi}=0.7$ corresponds to the value $Q_{di}/Q_f{\approx}3$ and $Q_{di}/Q_{wi}{\approx}0.2$. This value may be interpreted as the limiting value of the dialysate flow rate to get rid of the trouble of ultrafiltration in manipulating the diffusive solute removal safely.
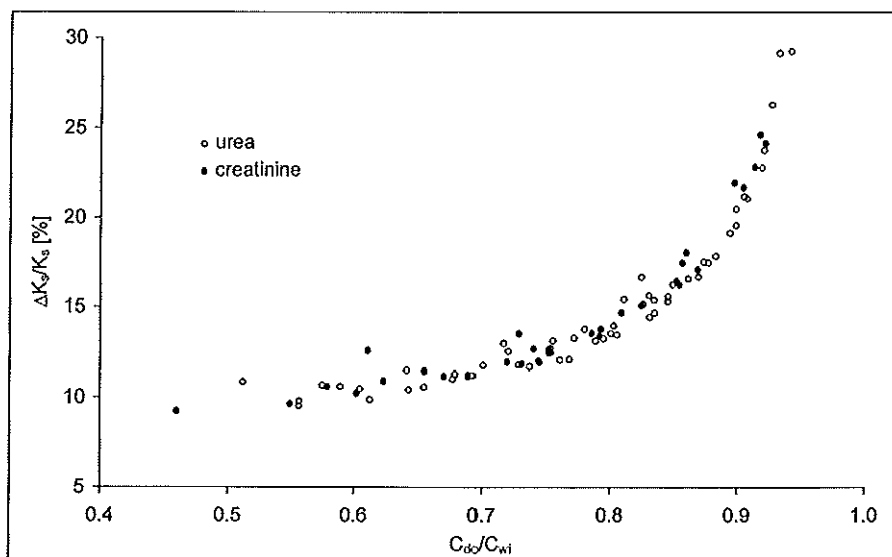
Figure 8.11: Relative variation of K_s in relation to the ratio of solute concentrations (C_{do}/C_{wi}) for varying values of flow rates. ($Q_{di}=0.5$-3 l/h, $Q_{ba}=82$ -345 ml/min and $Q_f=6$-18 ml/min) [10].

A dialysate flow rate slower than the ultrafiltration flow has consequences for the solute clearance: As the dialysate flow decreases, the concentration gradient between the blood and dialysate compartments on each side of the hemofilter membrane, which takes care of the diffusive solute removal, will be less or not effective on the first half of the hemofilter length [4,11]. Gradually, the dialysate outlet solute concentration (C_{do}) becomes almost equal to the incoming blood solute concentration (C_{wi}). At $C_{do}{\approx}C_{wi}$, clearance reaches a critical cut-off and equals the sum of rates of dialysate and ultrafiltration flows only. As the dialysate flow rate

becomes lower than the ultrafiltration flow, diffusive solute removal in the first half of the hemofilter will eventually stop as a result of dialysate saturation or diffusion equilibrium. The ultrafiltration alone reduces the concentration gradient [2]. Reducing the concentration gradient will reduce the overall permeability coefficient (K_s) [9]. Consequently, the solute removal by diffusion stops while the removal of excess water continues. In Figure 8.12, the $\Delta K_s/K_s$ resulting from the variation of dialysate flow rates (Q_{di}) is shown for comparison at different rates of the ultrafiltration flow (Q_f). The $\Delta K_s/K_s$ reaches his limiting (minimal) value at the highest dialysate and at the lowest ultrafiltration flow rate. This can also be seen from Figure 8.13 where $\Delta K_s/K_s$ due to the variation of ultrafiltration flow rates (Q_f) is shown for comparison at different rates of dialysate flow (Q_{di}).
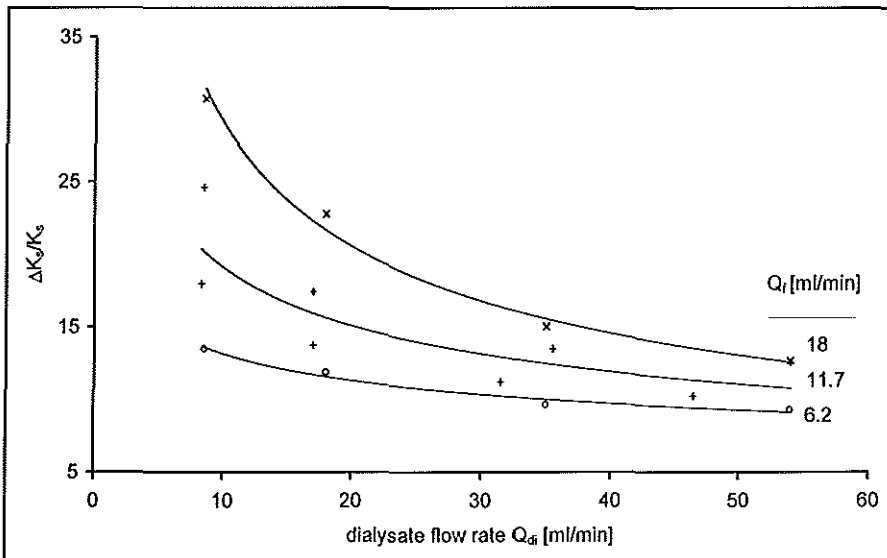
Figure 8.12: Relative variation of K_s in relation to the dialysate flow rate (Q_{di}) for different values of the ultrafiltration flow rate (Q_f) [10].

Concern that concomitant ultrafiltration flow might markedly interfere with the dialysis process was unfounded by other investigators so far [3]. Figures 8.12 and 8.13 show that the ultrafiltration flow rate may interfere with the dialysis process by affecting the diffusive permeability, depending on the dialysate flow rate. The relative variations of K_s decrease with the increasing values of Q_{di}/Q_f. The higher the dialysate flow rates, the smaller the relative variations of K_s. At relative high rates of dialysate flow, one can predict a maximal value of K_s (SK_dmax) with relative small variations. This may be attributed to the fact that on high dialysate flow rates, the thickness of the dialysate boundary layer will be smaller and the dialysate fluid will be better distributed over the whole bundle of fibers in the hemofilter, resulting consequently in a better diffusive performance. At low dialysate flow rates on the

contrary, the ultrafiltration affects the K_s resulting in a poor diffusive performance.
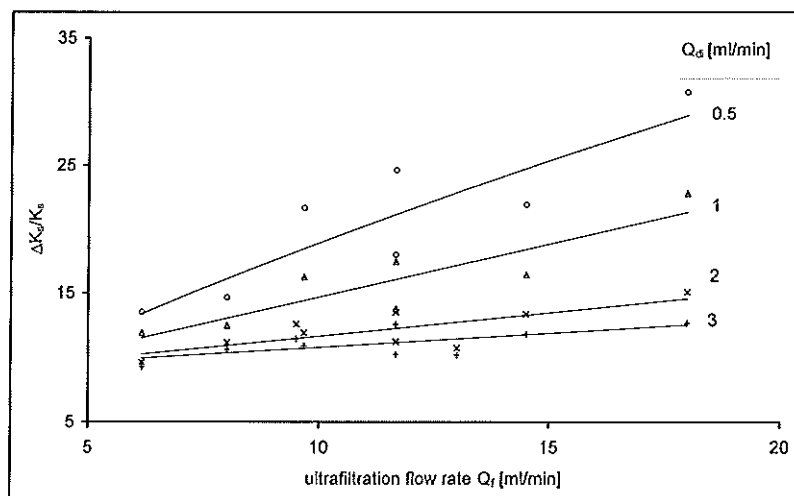
Figure 8.13: Relative variation of K_s in relation to the rate of the ultrafiltration flow (Q_f) [10].
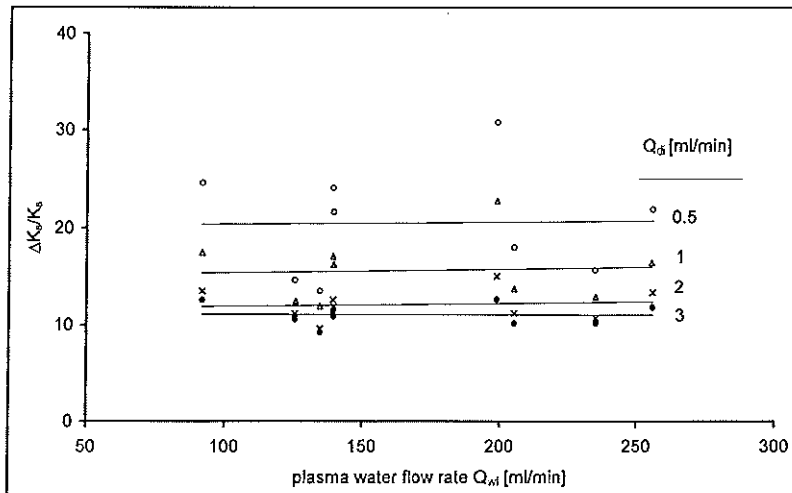
Figure 8.14: Relative variation of K_s in relation to the inlet plasma water flow rate (Q_{wi}) [10].

In Figure 8.14, the $\Delta K_s/K_s$ as a function of the blood flow rate is shown for comparison at different dialysate flow rates. Blood flow rate apparently does not affect the $\Delta K_s/K_s$. In a laboratory setting we have studied the effect of blood flow rates on the overall diffusive permeation coefficient [1]. Also from the results of that study, we could not observe any

relation between the blood flow rate and the overall diffusive permeability coefficient (K_s).

8.4 DISCUSSION AND CONCLUSION

In the previous chapters, we introduced mathematical models to analyze the clinical clearance data in terms of the overall diffusive permeability coefficient ($K_s = SK_d$) as a measure of the solute removal by diffusion in the presence of ultrafiltration. In this chapter, we analyzed the determinants of uraemic solute clearance in CAVHD, especially at low dialysate flow rates. Further, by applying a simple sensitivity analysis to the clinical data of uraemic solutes such as urea and creatinine, we analyzed the dependence of K_s on the flow rates and concentration gradient.

In CAVHD, the ultrafiltrate (Q_f=5-20 ml/min) flow is spontaneous. Evidently, increasing the rate of ultrafiltration (Q_f) will result in an increased uraemic solute clearance since the convective contribution to total urea clearance is proportional to the rate of ultrafiltration. Our results show a curvilinear increase in urea clearance with Q_f at relative high rates of the dialysate flow. Since the rate of ultrafiltrate production limits the solute convective clearance, higher rates of solute diffusive clearance are achieved by increasing the dialysate flow rate. Depending on the patient's uraemic state, it varies between 0.5 and 3 l/h. In CAVHD, the slow dialysis occurs in the presence of ultrafiltration and may be manipulated by adjusting the dialysate flow rate to a certain level to control the patient's uraemic state. Low rates of dialysate flow provide slow dialysis of small uraemic solutes such as urea and creatinine. In CAVHD, the blood (Q_{ba}=50-350 ml/min) flows are spontaneous. High blood flow rates favor high rates of solute removal. Our results show a curvilinear increase in urea clearance with Q_{bi} at relative high rates of the dialysate flow. Since the blood flow depends on the patient's cardiac output, the type of vascular access and the hemofilter characteristics, an adequate blood flow rate may be difficult to achieve. If the resistance of an AN-69 capillary hemofilter to blood flow (R_f) is higher than 0.4 mmHg/(ml/min), the hemofilter may be assumed to start clotting.

Model predictions of the diffusive and convective contributions to the total (overall) urea clearance were calculated in the manner used by Sigler et al [2] (See eq.(6.41) and eq.(6.42)) and also calculated according to eq.(6.43) and eq.(6.44). In cases with the relative high ultrafiltration flow rates, the fraction of urea clearance due to diffusion, as determined by eq.(6.44) was underestimated by eq.(6.41). The convective contribution to urea clearance decreases (slightly) with the increasing rate of the dialysate flow. The diffusive clearance on the other hand increases with increasing rates of the normalized dialysate flow (Q_{di}/Q_f) in a quadratic form. A linear relation between the normalized urea clearance and the dialysate flow rate was observed for $Q_{di}/Q_f \leq 3$.

In contrast to the conventional intermittent hemodialysis, in CAVHD an excellent dialysate-blood equilibration is achieved. Lowering the dialysate flow rate faster than the rate of ultrafiltration weakens the concentration driving force and eventually dialysate saturation (diffusion equilibrium) takes place in the first half of the hemofilter length. At $Q_{di}=0$, solute removal occurs only by convection (Cl=Q_f), resulting in the solute concentration in the blood inlet (C_{vi}) becoming equal to the solute concentration in the dialysate outlet (C_{do}).

Results of our measurements show a curvilinear increase of the diffusive urea clearance with the increasing values of the overall diffusive permeability. The size of this increase depends strongly on the dialysate flow rate, noting that the overall diffusive permeability coefficient itself depends also on the dialysate flow rate [5,11]. The overall diffusive permeability coefficient may be calculated from clinical data. In contrast to the intermittent hemodialysis, this must be calculated in the presence of ultrafiltration, since the diffusive clearance in CAVHD is a combined clearance process with ultrafiltration rather than a pure diffusion process. With increasing molecular size (weight) of solutes, the overall diffusive permeability coefficient was observed to decrease. Under the same operational conditions and hemofilter characteristics, we found that the K_s of creatinine is 25% and the K_s of phosphate is 45% smaller than the K_s of urea.

In contrast to the conventional intermittent hemodialysis, in CAVHD excellent dialysate-blood equilibration may be achieved. The concentration profiles depicted in Figure 7.1 and Figure 7.2 (See Chapter 7), show apparently that adjusting the dialysate flow can manipulate the concentration gradient to a certain degree in the presence of ultrafiltration, to control the diffusive removal rate of (uraemic) solutes. By setting the dialysate flow to a certain rate and by considering the blood and ultrafiltration flow rates, one can predict the rate of solute removal by simultaneous convection and diffusion on the hand of the nomograms from Figures 8.3, 8.4, 8.5, 8.6, and 8.9. From the relation between C_{do}/C_{vi} and Q_{di}/Q_f and the relation between C_{do}/C_{vi} and Q_{di}/Q_{vi} from Figure 8.7 one can estimate the necessary rate of dialysate flow to achieve a certain rate of solute removal coupled with the simultaneous removal of excess water.

Sensitivity analysis
On one side, this sensitivity analysis of K_s shows that calculating the K_s at relative low rates of the dialysate flow in presence of ultrafiltration is not reliable, especially near or at complete blood-dialysate equilibrium. The higher the dialysate flow rates and the lower the ultrafiltration flow rates, the smaller the variations in K_s. Calculating the overall permeability coefficient at relative high rates of dialysate flow is therefore important, for example by extrapolation ($K_d$max, see further Chapter 9). On the other side, the relative low rates of dialysate flow make the CAVHD unique for the treatment of hemodynamically unstable

acute dialysis patients. Within the operational limits of CAVHD, with the upper values of Q_f=20 ml/min and Q_{di}=60 ml/min, the effect of ultrafiltration on the predicted value of the permeation coefficient is negligible if the condition $Q_{di}/Q_f \geq 3$ is fulfilled. In intermittent hemodialysis this problem does not exist (Q_{di}=200 ml/min and Q_f<5 ml/min). With slow and continuous dialysis, dialysate saturation can occur, especially at dialysate flow rates less than ultrafiltration flow rates. In that region of flows, the relative variations in the predicted values of the permeation coefficient are considerably high (up to 35%), especially for $Q_{di} \leq 3Q_f$. Keeping this controversial fact and the results of this sensitivity analysis in mind, a dialysate flow rate at least 3 times the ultrafiltration flow rate is enough to manipulate the solute removal by diffusion without considering the ultrafiltration. Both mechanisms of solute removal by simultaneous convection and diffusion are subject to the same blood flow.

Two important parameters indicating the hemofilter performance

In therapies such as CAVHD, the membrane hydraulic permeability index (MI) and the overall diffusive permeation coefficient (SK_d) strongly determine the hydraulic and diffusive performance of the hemofilter. These two parameters are the decisive parameters in estimating the rate of ultrafiltration flow and diffusive solute removal in the presence of ultrafiltration. Both parameters decline over time, independently from the hemofilter resistance (We investigated data of declining of K_d in time in a different study.).

8.5 REFERENCES

[1].   Vos MC. Continuous Arteriovenous Hemodiafiltration. Rotterdam, the Netherlands: Erasmus University Rotterdam, (1992), PhD Thesis.

[2].   Sigler MH and Teehan BP. Solute transport in continuous hemodialysis. A new treatment for acute renal failure, Kidney Int. 32 (1987) 562-571.

[3].   Vincent HH, Vos MC. The use of continuous arteriovenous hemodiafiltration in multiple organ failure patients. Applied Cardiopulmonary pathophysiology, (1991), 4, pp.109-116.

[4].   Akcahuseyin E, Vincent HH, van Ittersum FJ, van Duyl WA, Schalekamp MADH. A Mathematical Model of Continuous Arterio-Venous Hemodiafiltration (CAVHD), Computer Methods and Programs in Biomedicine. 31 (1990) 215-224.

[5].   Vincent HH, van Ittersum FJ, Akcahuseyin E, Vos MC, van Duyl WA, Schalekamp MADH. Solute Transport in Continuous Arteriovenous Hemodiafiltration: A New Mathematical Model Applied to Clinical Data, Blood Purif. 8 (1990) 149-159.

[6].   Sargent JA, Gotch FA. Principles and biophysics of dialysis. In: W. Drukker, F.M. Parsons, J.F. Maher, Replacement of Renal Function of Dialysis. The Hague: Martines Nijhorf Medical Divison Publ, (1978).

[7].   Pallone TL, Petersen J. Continuous arteriovenous hemofiltration: An in vitro simulation and mathematical model. Kidney International, 33 (1988) 685-698.

[8].   Jaffrin MJ, Gupta BB, Malbrancq JM. A One-dimensional Model of Simultaneous Hemodialysis and Ultrafiltration with Highly Permeable Membranes, Journal of Biomechanical Engineering, (103) (1981), 261-266.

[9].   Sigdell JE. Calculation of combined diffusive and convective mass transfer, The International Journal of Artificial Organs. Vol. 5. No. 6 (1982) 361-372.pp.26-35.

[10].   Akcahuseyin E, van Duyl WA, Vincent HH, Vos MC, Schalekamp MADH. A sensitivity analysis of uraemic solute clearance and diffusive permeability coefficient at low dialysate flows in CAVHD. Med. Eng. Phys.(1996) (submitted).

[11].   Akcahuseyin E, van Duyl WA, Vos MC, Vincent HH. An analytical solution to solute transport in continuous arterio-venous hemodiafiltration (CAVHD). Med. Eng. Phys.(1996) Vol:18 No:1,

[12].   Husted FC, Nolph KD, Vitale FC, Maher JF. Detrimental effects of ultrafiltration on diffusion in coils. J Lab Clin Med (1976) 87; 435-442.

ANALYSIS OF RESISTANCE TO DIFFUSION DURING BULK MASS TRANSPORT IN CAVHD: A prediction model for antibiotic drug clearance

9.1 INTRODUCTION

In Chapter 5, on allowing for bulk mass transport limitations under the combined effects of solute convection and diffusion, we developed a one-dimensional mathematical model to analyze the removal rate of solutes in continuous arterio-venous hemodiafiltration (CAVHD). The analysis of the combined effects of mass transport by simultaneous convection and diffusion owing to bulk mass transport is limited to the knowledge of the relative weighting factors (f_b) and (f_d) for the convective part and to some extend to the knowledge of the overall diffusive mass transfer coefficient (K_d) for the diffusive part of solute transport. The factors (f_b) and (f_d) describe the relative weighting of the bulk solute concentration in blood (C_w) and in the dialysate (C_d) compartments to the concentration $C_m = f_b C_w + f_d C_d$ that is dragged by plasma water during the solute removal by convection. The K_d is regarded as the reciprocal of the sum of the resistance to diffusion exerted by the blood concentration boundary layer (R_b) and the resistance exerted by the dialysate concentration boundary layer (R_d) and the resistance exerted by the membrane (R_m).

In Chapter 6 we were able to develop an analytical mathematical model for the solute and volume transport in CAVHD by assuming that the solute concentrations within both the blood and the dialysate compartments are 'mixing cup' concentrations. By virtue of this assumption (and some other assumptions of course) we could analytically solve the transport equations so as to yield an expression of the overall diffusive permeability coefficient $(K_s = SK_d)$ as a function of the membrane surface area, the blood, filtrate and dialysate flow rates and solute concentrations [1,2,3]. When we applied our model to data obtained during CAVHD [4], the data showed that we cannot take the value of K_d as a constant because of the following reasons: 1) The K_d of a solute decreases in time. In our interpretation this reflects an increase of the resistance $(R_b + R_m)$ to diffusion because of ongoing protein adsorption and gradual clotting. 2) The K_d of a solute increases with the increasing rates of dialysate flow. This may be explained by a fall in the resistance to diffusion (R_d) due to thinning of the dialysate concentration boundary layer. In simple terms, the improved mixing within the dialysate compartment lowers the concentration of the solute near the membrane and by that promotes diffusion [5]. These observations show that the assumption regarding the "mixing-cup" concentrations may not be valid in the low rates of dialysate flow as far as the dialysate compartment is concerned. Consequently, when our model is used for the prediction of solute transport rates, the influence of the membrane condition and that of the dialysate flow rate have to be taken into account.

In this chapter we described a numerical computational method for solving the equations governing the mass balance. The method was applied to the clearance data of uraemic solutes and some antibiotic drugs up to 1500 Daltons and to the data of hemofilter hydraulic condition measured during CAVHD, so as to determine the convective concentration factors (f_b and f_d) and the resistances (R_b+R_m and R_d) to diffusion from the overall diffusive mass transfer coefficient (K_d) within the operational limits of CAVHD. Depending on the hemofilter hydraulic condition (MI) and the dialysate flow rates (Q_{di}), the resistance (R_b+R_m) of blood and membrane and the resistance (R_d) of dialysate to diffusion were determined by Wilson's plots. Further, by making use of the capillary pore theory, the diffusive permeation coefficients (K_s) of some antibiotic drugs were related to that of the creatinine so as to predict the clearance of antibiotic drugs from the clearance of creatinine under the same operational conditions and hemofilter characteristics (a prediction model). By this, it was demonstrated how, by using the results of this analysis, our one-dimensional analytical model may be applied to predict transport rates of different solutes under different operational conditions and membrane characteristics.

9.2 METHODS

The model description and equations describing the overall mass balance are given in Chapter 5. In Table 5.1, the boundary definitions and variables are shown.

Computational methods for local flow and mass balance
Calling Δx a length element on which all variables are considered to be constant, all the first order differential equations governing the local flow rates, pressure and solute mass balance along the length of hemofilter membrane are solved by the Euler method [16]. The local blood pressure is computed from the following difference equation:

$$P_b(x+\Delta x) = P_b(x) - \frac{R_{f,p}}{L_f} \eta_b(x) Q_b(x) \Delta x \tag{9.1}$$

with its starting value at x=0:

$$P_b(x=0) = P_{bi} = P_{la} - R_{aa}Q_{ba} \tag{9.2}$$

Solution of eq.(9.1) at $x=L_f$ results in the postfilter blood pressure $P_b(L_f)=P_{bo}$. Local blood viscosity (η_b) is related to the local protein concentration (C_p) and to the local hematocrit (Ht), according to eq.(3.12). The local blood flow rate (Q_b) is computed from:

$$Q_b(x + \Delta x) = Q_b(x) - Q_f(x, x + \Delta x) \tag{9.3}$$

with its value $Q_{bi}=Q_{ba}+Q_{pred}$ at x=0, with Q_{pred} the flow rate of substitution fluid [8]. In eq.(9.3), the term $Q_f(x,x+\Delta x)$ represents the cumulative rate of ultrafiltration flow:

$$Q_f(x, x + \Delta x) = \frac{S}{L_f} L_p [P_b(x) - P_d - \Pi_p(x)] \Delta x \qquad (9.4)$$

Eq.(9.4) at x=L_f results in the net rate of ultrafiltration flow. In the previous equations governing the local blood flow and pressure, the rate of blood flow entering the extracorporeal circuit (Q_{ba}) is assumed to be measured. As we mentioned earlier in Chapter 3, the resistance of blood access components could reasonably be predicted from their geometry, but the measured resistance of hemofilter to the blood flow was 3 times higher than its predicted value. We, therefore, determine the blood flow rate (Q_{ba}) with the condition that the blood pressure at the venous access, P_{iv}, calculated by means of eq.(3.1), becomes equal to the measured value of mean venous pressure (MVP). The equations are then solved with successive adjustments of Q_{ba} until the following condition is satisfied:

$$MVP - [P_b(L_f) - \frac{128 L_{va}}{\pi \, d_{va}^4} \eta_b(L_f) \, Q_b(L_f)] \leq 10^{-4} \qquad (9.5)$$

where $P_b(L_f)$, $\eta_b(L_f)$ and $Q_b(L_f)$ are values of hydrostatic blood pressure, blood viscosity and blood flow rate at x=L_f, which result from eq.(9.1), eq.(3.12) and eq.(9.3) respectively. In order to compute the local flow rates and solute concentration profiles on both side of the membrane, which are needed for the conservation of local mass balance, the solute mass transfer rates ($Q_w C_w$) and ($Q_d C_d$) are solved numerically by using the measured or calculated boundary values as initials. In the blood compartment the solute mass transfer rate is calculated as:

$$C_w(x+\Delta x) Q_w(x+\Delta x) = Q_w(x) \, C_w(x) - \frac{S}{L_f} \Delta x \, J_s(x) \qquad (9.6)$$

with the initial value $Q_w(0)C_w(0)=Q_{wi}C_{wi}$ at x=0 and J_s, the transmembrane solute flux, is given by eq.(5.33):

$$J_s = \gamma \, J_v (f_b C_w + f_d C_d) + K_d (C_w - C_d) \qquad (9.7)$$

with the convective concentration factors f_b and f_d and the overall diffusive mass transfer coefficient (K_d). The local flow rate of plasma water (Q_w) is computed from:

$$Q_w(x + \Delta x) = Q_w(x) - Q_f(x, x + \Delta x) \qquad (9.8)$$

with its value $Q_w(0)=Q_{wi}$ at x=0. The rate of solute mass transfer in terms of dialysate variables is calculated as:

$$C_d(x+\Delta x) Q_d(x+\Delta x) = \frac{S}{L} \Delta x \, J_s(x) - C_d(x) Q_d(x) \qquad (9.9)$$

with the initial value $Q_d(0)C_d(0)=Q_{do}C_{do}$ at x=0. The local dialysate flow rate (Q_d) is computed from:

$$Q_d(x + \Delta x) = Q_f(x, x + \Delta x) - Q_d(x) \qquad (9.10)$$

with its initial value $-Q_{di}(0)=Q_{do}$ at x=0. In all points along the hemofilter length, eq.(9.6) and eq.(9.9) obey eq.(5.10) conserving the overall mass balance.

In calculating the local mass balance, the overall diffusive mass transfer coefficient (K_d) is determined from the solution of analytical model [3,4,17] (See Chapter 6). For solutes with sieving coefficient $\gamma=1$ and for a constant profile of ultrafiltration volume flux, the overall mass transfer coefficient can be predicted from eq.(6.50). In other cases, the overall diffusive permeability coefficient is calculated by iterative adjustment techniques using eq.(6.48) as its initial value. All the equations governing the mass transfer rate are solved by adjusting the K_d successively with the condition that mass transfer rate, $Q_{di}(L_f)C_d(L_f)$ at the dialysate inlet, which results from eq.(9.9) at x=L_f, must equal the measured or known value of $Q_{di}C_{di}=0$. With the condition met all governing equations are then solved with successive adjustments of K_d until the following condition is obtained:

$$Q_d(L_f) C_d(L_f) - Q_{di} C_{di} \leq 10^{-4} \tag{9.11}$$

As the condition defined by eq.(9.11) is provided at x=L_f, eq.(9.6) and eq.(9.9) obey eq.(5.10) conserving the overall mass balance in all points along the hemofilter length.

The convective concentration factors f_b and f_d

In Chapter 5, the net solute flux across the membrane was expressed in terms of the solute concentration (C_{wm}) at the blood-membrane interface and the solute concentration (C_{md}) at the dialysate-membrane interface [6]. See Figure 5.2. Then, by using thin-film theory [7] the solute interface concentrations were corrected for the bulk mass limitations, namely for the bulk solute concentrations (C_w and C_d). Eventually, the net solute flux was expressed by eq.(9.7) including the relative weighting (convective concentration) factors (f_b and f_d). The convective concentration factors, describing the relative weighting of blood (C_w) and dialysate concentrations (C_d) in the evaluation of the concentration of solute ($C_m=f_bC_w+f_dC_d$) that is dragged by plasma water into the dialysate region or by dialysate fluid into the blood region in case of back filtration, were given by eq.(5.34) and eq.(5.35) [8]:

$$f_b = \frac{e^{\theta_t}}{(1-\gamma)e^{\theta_d}(e^{\theta_m}-1)+\gamma(e^{\theta_t}-1)} - \frac{K_d}{\gamma J_v} \tag{9.12}$$

$$f_d = -\frac{1}{(1-\gamma)e^{\theta_d}(e^{\theta_m}-1)+\gamma(e^{\theta_t}-1)} + \frac{K_d}{\gamma J_v} \tag{9.13}$$

where J_v is the local ultrafiltration volume flux (density) as given by eq.(5.3) or by eq.(6.5) used also by Sigdell [9]. θ_t represents the sum of the Péclet numbers for the blood (θ_b), the membrane (θ_m) and the dialysate region (θ_d):

$$\theta_t = \theta_b + \theta_m + \theta_d = J_v \left(\frac{d_b}{D_b} + \gamma \frac{d_m}{D_m} + \frac{d_d}{D_d} \right) \tag{9.14}$$

where d_b, d_m and d_d are the thicknesses of the blood concentration boundary layer, the physical membrane and the dialysate concentration boundary layer (See Figure 5.2) respectively. The D_b, D_m and D_d represent the effective diffusion coefficients in blood, membrane and dialysate respectively. In Figure 5.2, the convective concentration factors were theoretically demonstrated for two different solutes with sieving coefficient $\gamma=1$ and $\gamma=0.4$ as a function of the total observed Péclet number ($\gamma J_v / K_d$).

Analysis of the overall diffusive mass transfer coefficient
The overall mass transfer coefficient (K_d) is to be regarded as the reciprocal of the sum of the resistances to diffusion exerted by the blood side (R_b), the membrane ($R_m = 1/P_m$) and the dialysate side (R_d) of the hemofilter:

$$\frac{1}{K_d} = R_{td} = R_b + \frac{1}{P_m} + R_d \tag{9.15}$$

According to Colton [5], there is a linear relationship between R_d and Q_{di}^{-m}, with the value of m ranging between 0.5 and 1.0, depending on hemofilter geometry. For the overall resistance to diffusion, we used eq.(9.15) as:

$$\frac{1}{K_d} = \frac{1}{K_d\text{max}} + \frac{b}{Q_{di}^m} \tag{9.16}$$

where bQ_{di}^{-m} corresponds to R_d. At infinite dialysate flow rate, the resistance to diffusion of the dialysate compartment will be zero and the maximum value of K_d, $K_d\text{max}$, is obtained. Therefore, the term $R_b + 1/P_m$ in eq.(9.15) corresponds to the reciprocal of $K_d\text{max}$. See further Chapter 8 for the sensitivity analysis of $K_s = SK_d$ on the blood, ultrafiltration and dialysate flow rates [10]. In CAVHD, the maximum value of K_d has to be related to the hemofilter condition (membrane index MI) because K_d of a solute decreases in time. In accordance with eq.(9.16), a linear regression analysis of $1/K_d$ as a function of $1/Q_{di}$ ('Wilson's plots') yields the value of $K_d\text{max}$ that is the reciprocal of the y-intercept of the corresponding regression line and the value of b, which is the slope of the regression line. The value of m is obtained by using the curve fitting procedure.

Mass transfer coefficient of solutes of different molecular weights
The rate of diffusion through the membrane is influenced by the size, the shape and the electrical charge of the molecule. The influence of the size, i.e. the molecular radius (r_s) of the solute, may be theoretically predicted from "capillary pore model". For a rigid non-adsorbing spherical solute diffusing through a cylindrical pore (radius r_p), the effective diffusion coefficient (D_m) is related to the free diffusion coefficient (D) in water according to [11]:

$$\frac{D_m}{D} = (1 - \frac{r_s}{r_p})^2 \frac{[1 - 2.1\frac{r_s}{r_p} + 2.09(\frac{r_s}{r_p})^3 - 1.71(\frac{r_s}{r_p})^5 + 0.73(\frac{r_s}{r_p})^6]}{1 - 0.76(\frac{r_s}{r_p})^5} \tag{9.17}$$

where solute radius (r_s, [Å]) may be approximated from published data [12]:

$$r_s = 0.51 MW^{0.375} \tag{9.18}$$

with MW [Daltons] the molecular weight of solute. Eq.(9.17) is known as the Haberman and Sayre equation. For practical clinical purposes, if the overall mass transfer coefficient (K_{dc}) for creatinine is known, the corresponding values for other solutes may be estimated:

$$\frac{K_{dc}}{K_d} = d_b \frac{r_s}{r_c} + d_m \frac{r_s}{r_c} [\frac{D_m}{D}]_c \frac{D}{D_m} + d_d \frac{r_s}{r_c} \tag{9.19}$$

where the subscript c represents creatinine. However, the boundary layer thickness (d_b) of blood side and that (d_d) for the dialysate side are not known. The d_b and d_d may be calculated from inner and outer diameters of the hemofilter fibers as described by Sigdell [9]. However, Sigdell's expressions are related to the dry or wet state condition of membrane only, not to the operating hemofilter membrane index (MI), which declines over time. Therefore, depending on the membrane condition (MI) and the dialysate flow rate (Q_{di}), the membrane resistance ($R_m = 1/P_m$) has to be estimated in relation to the total resistance to diffusion using eq.(9.16) for a known pore radius.

Clinical conditions
Patients were treated with CAVHD for acute renal failure and sepsis and/or circulatory or neurological instability [13]. For vascular access we used special 11 cm CAVH-catheters (Medcomp, 8 F) in the femoral vessels. Hemofilters were prepared by rinsing the dialysate and blood compartment respectively with 2 l of saline containing heparin 5000 U/l. Filters were placed in the upright position with the ultrafiltrate outlet up. Standard anticoagulation consisted of heparin 500 U/h into the arterial line of the hemofilter. No loading dose of heparin was given. No protamine was used. For fluid substitution Ringer's lactate or saline was infused into the arterial line (predilution). The amount of substitution fluid was adjusted hourly to the net ultrafiltration rate. Reasons for hemofilter replacement were clotting of the filter or an ultrafiltration flow rate <200 ml/h. For dialysate a commercially available hemofiltration substitution fluid was used (HF-21, Fresenius). Dialysate was heated to 38 °C. It was run counter currently at a rate of 0.5 to 3.0 l/h using a roller pump (Bellco BL758, Mirandola, Italy). The flow rate was adjusted to blood chemistry if necessary. Antibiotic drugs were given as clinically indicated.

Measurements and study protocol

The hemofilter we used is the 0.6 m^2 AN-69 capillary hemofilter (Multiflow-60^R, Hospal, France). AN-69 is a symmetrical high-flux membrane. The hemofilter contains 6000 fibers, 15 cm long including 1 cm length of potting at both ends. The inner diameter of the fibers is 220-240 μm [14]). The pre-and postfilter blood pressure (P_{bi} and P_{bo}) were measured from the arterial and venous tubing using an electronic pressure monitor. The pressure in the dialysate compartment (P_d) was calculated from the ultrafiltrate column height (h_c). Oncotic pressure (Π_p) was calculated from the average plasma protein concentration (C_{pm}) according to Landis-Pappenheimer equation [15]. The arterial blood flow rate (Q_{ba}) was measured by air bubble displacement over a length of arterial tubing, containing a volume of 13 ml or by using an electronic flowmeter with a clamp-on probe around the blood line. The net ultrafiltration flow rate (Q_f) was measured by timed collection. Dialysate (Q_{di}) and substitution fluid (Q_{pred}) flow rates were determined by an electronic weighing device. First, the infusion pumps of dialysate and substitution fluid were turned off. We measured the hemofilter resistance (R_f) to blood flow and the hydraulic permeability index (MI) to determine the hemofilter condition. Samples of arterial blood plasma (C_{pl}) and ultrafiltrate (C_f) were taken to determine the apparent sieving coefficient. Then, the infusion pump of substitution fluid was turned on and the sieving coefficient was again determined. After that, the dialysate flow rate was set to $Q_{di}=1$ l/h. Dialysate samples (C_{do}) were taken from the collection bag to determine the solute and drug clearance and the overall mass transfer coefficient (K_d) from eq.(9.2) and numerical iterations [16] provided that the condition defined in eq.(9.11) is fulfilled. Finally, the dialysate pump was turned off and MI and R_f were determined again to control the hemofilter condition according to eq.(3.21) and eq.(3.3) respectively. Hemofilters had been used for up to 3-5 days. If the value of R_f was higher than 0.4 mmHg·min/ml, clotting of fibers was assumed and the data were discarded. The same procedure was repeated at dialysate flow rates of 0.5, 2 and 3 l/h.

9.3 RESULTS

Relative weighting factors f_b and f_d

In order to determine the effect of relative weighting (convective concentration) factors (f_b and f_d) on the convective solute removal, the local creatinine concentrations (C_w and C_d) along the hemofilter length were calculated from the data of creatinine clearance, which was obtained with $Q_{ba}=199$ ml/min, $Q_f=6.2$ ml/min, $Q_{pred}=5$ ml/min, $Q_{di}=8.5$ ml/min, $Ht_a=0.3$, $C_{pa}=80$ g/l, $P_{bi}=60$, $P_{bo}=20$ and $P_d=-3$ mmHg, $C_{pl}=229$ and $C_{do}=193$ mmol/l. The overall diffusive mass transport coefficient was calculated as $K_{dc}=21.2$ μm/min (21.6 μm/min according to eq.(6.50)). The creatinine clearance by combined convection and diffusion was Cl=11.8 ml/min (eq.(5.26)) and the convective clearance $Cl_c=5.9$ ml/min (eq.(5.27)). The relative importance of removal of plasma water to that of creatinine was $\theta_o \approx Q_f/SK_d=49\%$. The

contribution of convention to the creatinine clearance was $Cl_c/Cl= 50\%$.
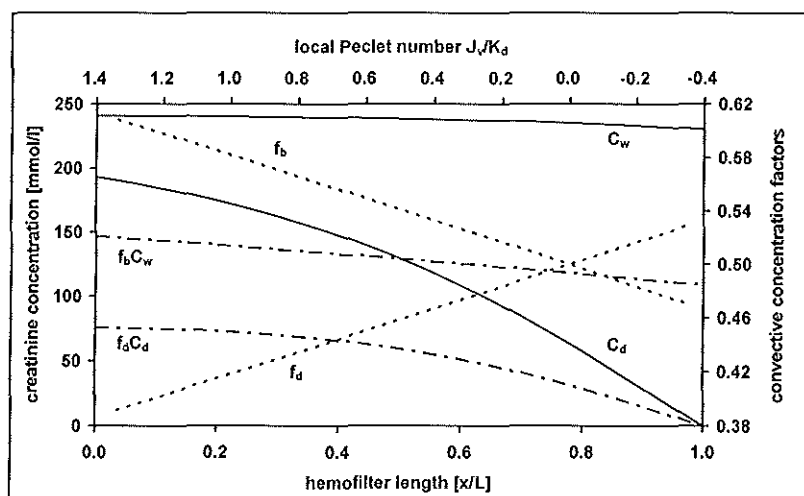
Figure 9.1: Creatinine concentration profiles and the concentration factors f_b and f_d in relation to distance along the length of hemofilter and in relation to the local Péclet number (J_v/K_d) [18].
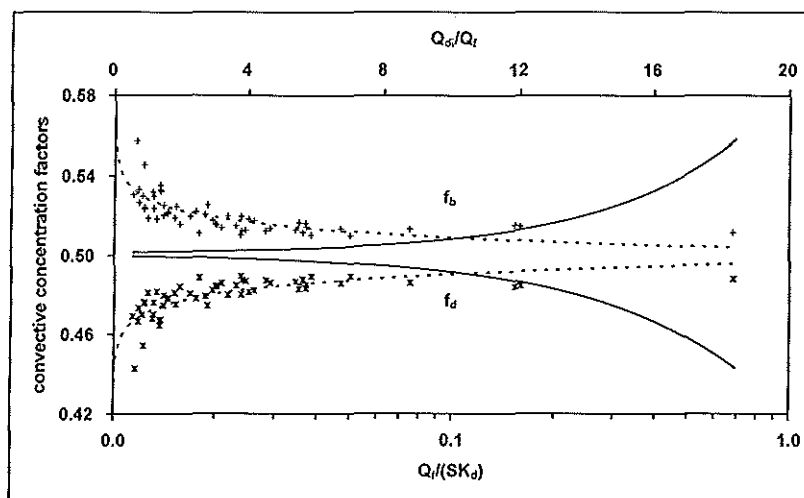
Figure 9.2: Length averaged convective concentration factors f_b and f_d in relation to the overall Péclet number (Q_f/SK_d) and to the ratio (Q_{di}/Q_f) (dashed lines) [18].

In Figure 9.1, solute concentrations contributing to diffusive $(C_w\text{-}C_d)$ and convective $(f_bC_w+f_dC_d)$ creatinine clearance are shown as a function of the distance along the length of the hemofilter and as a function of the local Péclet number (J_v/K_d). The average contribution

of blood side to the convective creatinine removal was $f_b = 54\%$ and that of the dialysate side was $f_d = 46\%$. In calculating the factors f_b and f_d, we used $R_b : R_m : R_d = 10:50:40$. In fact, as can be seen from eq.(9.12) and eq.(9.13), the factors f_b and f_d depend on the local Péclet number (J_v/K_d), not on the ratio $R_b : R_m : R_d$. In Figure 9.1, the f_b and f_d are shown as a function of J_v/K_d and as a function of the distance along the hemofilter length. The factors f_b and f_d equal 0.5 at $J_v = 0$. At $J_v < 0$, where the filtration takes place from dialysate into blood (back filtration), the concentration factors become $f_b < 0.5$ and $f_d > 0.5$. Within the conventional ranges of operational conditions ($Q_{ba} = 50\text{-}345$ ml/min, $Q_f = 5\text{-}20$ ml/min, $Q_{pred} = 0\text{-}15$ ml/min and $Q_{di} = 5\text{-}60$ ml/min), we calculated the length averaged values of f_b and f_d in relation to the overall Péclet numbers (Q_f/SK_d) and in relation to the ratio of dialysate flow rate to the rate of ultrafiltration flow (Q_{di}/Q_f). As can be seen from Figure 9.2, the length averaged values of f_b and f_d depart from 0.5 up to 10% with increasing values of (Q_f/SK_d) and with decreasing values of (Q_{di}/Q_f).
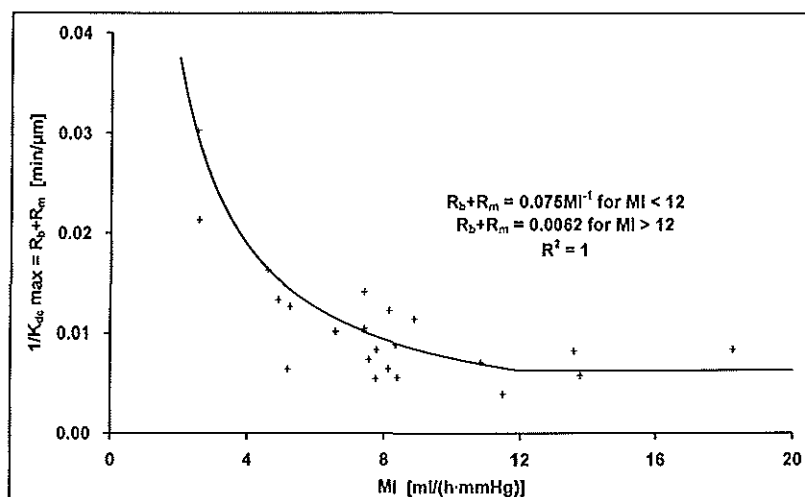
Figure 9.3: Relationship between extrapolated value of $R_b + R_m$ and membrane hydraulic permeability, as expressed by the value of MI. The drawn curve represents prediction of $R_b + R_m$ according to the equation: $R_b + R_m = 0.075/MI$ for MI < 12 and $R_b + R_m = 1/160$ for MI > 12 [18].

Predicting the overall mass transfer coefficient and solute clearance

Under different operational conditions, we calculated the overall mass transfer coefficient (K_{dc}) for creatinine. For the calculation of $R_b + 1/P_m$ from eq.(9.16), 16 times regression analyses were performed. With our data, a linear relationship was best approached when we substituted 1.0 for the value of m, where dialysate flow rate was varied between $Q_{di} = 0.5$ and 3 l/h. The average slope of the regression equations, which indicates the influence of Q_{di} on K_d, was $b = 0.15$ (s.e.m. 0.05). For each data set, $K_d$max was determined by taking the

reciprocal of the y-intercept of the corresponding regression equation. Further, $1/K_d max$ of creatinine was calculated at different values of the membrane permeability index (MI). The relation between R_b+R_d and MI is shown in Figure 9.3. The relationship was then described by the following simple empirical equation for MI<12 ml/(h·mmHg):

$$\frac{1}{K_{dc}} = \frac{0.075}{MI} + \frac{0.15}{Q_{di}}$$
(9.20)

and for MI>12 ml/(h·mmHg):

$$\frac{1}{K_{dc}} = \frac{1}{160} + \frac{0.15}{Q_{di}}$$
(9.21)

By combining eqs.(9.20) and (9.21), we estimated the SK_d for creatinine. We then compared them with the observed SK_d values, which were calculated by using eq.(9.11) at different values of Q_{di} and MI. The value of Q_{di} varied from 0.5 to 3 l/h.
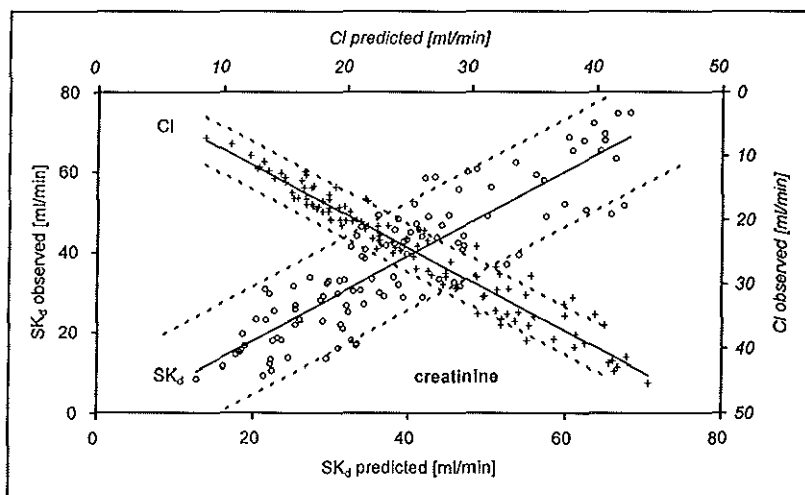
Figure 9.4: The observed diffusive permeability coefficient (SK_d) and the observed clearance of creatinine in relation to the values calculated by prediction. The broken lines show the 95% reliability intervals [18].

In Figure 9.4, the observed SK_d is shown versus the predicted SK_d for creatinine. The average difference between observed and predicted values was 5% according to the regression equation: SK_{dc} (observed)=$1.05 \cdot SK_{dc}$ (predicted) -3.02 with $R^2=0.77$ and n=112. Using both the observed and predicted values of K_{dc}, we calculated the observed and predicted creatinine clearance by eq.(6.51) and compared to each other in Figure 9.4. The average difference between observed and predicted values was 3% according to the regression equation: Cl (observed)=1.03Cl (predicted)-1.25 with $R^2=94$ and n=112.

Table 9.1: Observed values of the ratio K_d/K_{dc} for different uraemic solutes and antibiotic drugs with their free fractions in plasma water measured with an AN-69 membrane [2].

solute	MW [Daltons]	K_d/K_{dc}	n	free fraction	n
urea	60	1.32	109		
lactate	90	0.93	2		
creatinine	113	1	109		
uric acid	168	0.93	123		
phosphate	174	0.75	125		
vitamin B_{12}	1355	0.24	5		
imipenem	317	0.68	20	1.00	22
ciprofloxacin	331	0.85	2	1.02	6
cilastatin	384	0.56	21	0.68	20
cefuroxime	424	0.72	21	0.80	21
cefotaxime	455	0.37	11	0.76	14
tobramycin	468	0.72	26	0.82	19
ceftazidine	547	0.66	22	0.92	12
vancomycin	1449	0.37	5	0.67	5

Mass transfer coefficient of solutes of different molecular weights

Further, by calculating the overall mass transfer coefficients of other uraemic solutes and antibiotic drugs (See Table 9.1) up to 1500 Daltons, a fixed relationship was found from the following regression equation:

$$\frac{K_d}{K_{dc}} = (\frac{MW}{113})^{-0.42} \tag{9.22}$$

In Figure 9.5, the ratio K_d/K_{dc} is shown in relation to the solute molecular weight (MW, [Daltons]). Using Wilson's plots, we estimated the contribution of membrane resistance (R_m/R_{td}) to the total resistance from our data.

Table 9.2: Membrane resistance as a percentage of the total resistance to diffusion for different dialysate flow rates and membrane hydraulic permeability index (MI, [ml/h·mmHg]).

Q_{di} [l/h]	membrane resistance to diffusion, R_m [% of R_{td}]		
	for MI=4	for MI=8	for MI=12
0.5	34 -51	29 -34	26
1	45 -68	43 -51	41
2	54 -81	56 -68	58
3	57 -96	63 -76	68

As shown in Table 9.2, the R_m may vary between 26% and 86% of the total resistance, depending on MI and Q_{di}. At MI=8 ml/(h·mmHg) and Q_{di}=1.0 l/h, a realistic estimation of

R_m/R_{td} would seem to be 50%. Using eq.(9.20), the contributions of R_b and R_d to the total resistance (R_{td}) were estimated by adjusting the parameters d_m, d_b and d_d in eq.(9.19) so that the values of K_d/K_{dc} according to eq.(9.19) become equal to the values of K_d/K_{dc} from eq.(9.22).
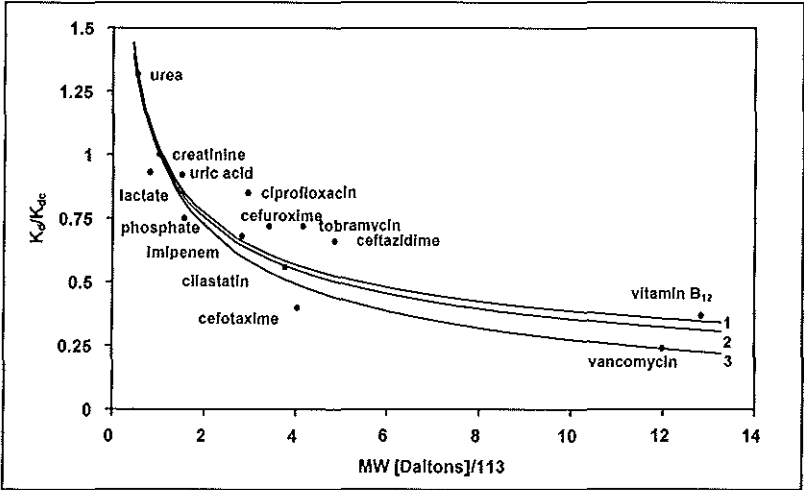
Figure 9.5: Relationship between observed values of K_d/K_{dc} of different uraemic solutes and antibiotic drugs and their molecular weight. See text. Data were obtained with the 0.6 m² AN-69 capillary hemofilter (Multiflow-60^R, Hospal, France) [18].
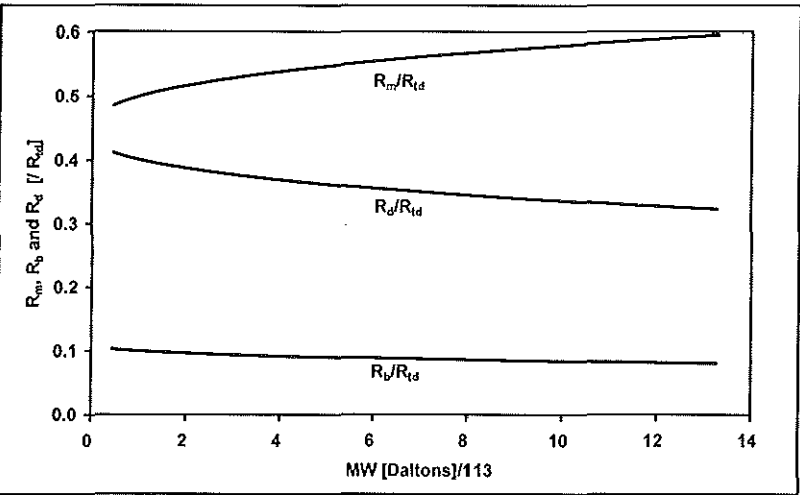
Figure 9.6: Nomogram for the estimation of resistances R_b, R_m and R_d of solutes up to 1500 Daltons [18].

In Figure 9.5, the calculated values of K_d/K_{dc} from eq.(9.19) are shown for pore radii $r_p=30$ Å and $r_p=60$ Å. With the AN-69 membrane, the pore radius is approximately 60 Å. From Figure 9.5, we estimated that for creatinine, with an average membrane index (MI=8 ml/(h·mmHg)) and at a dialysate flow rate of 1 l/h, the resistances R_b, R_m and R_d are related to each other as $R_b:R_m:R_d=10:50:40$. In Figure 9.5, the curve 1 represents the regression curve: $K_d/K_{dc}=(MW/113)^{-0.42}$ with $R^2=0.76$ and n=15, the curve 2 represents the K_d/K_{dc} curve according to Haberman and Sayre equation for pore radius $r_p=60$ Å with $R_b:R_m:R_d=10:50:40$ and the curve 3 represents the curve 2 for r =30 Å. In Figure 9.6 a nomogram is shown for estimating the relative values of the blood (R_b), the membrane (R_m) and the dialysate (R_d) in relation to molecular weight up to 1500 Daltons.

Predicting the antibiotic drug clearance

Clearances of some antibiotic drugs were measured during CAVHD at the dialysate flow rates of 1 and 3 l/h (See Table 9.3). The clearance data were obtained with the AN-69 capillary hemofilters at different operational conditions.

Table 9.3: Range of antibiotic drug clearance during CAVHD at two different rates of dialysate flow. Data obtained with the AN-69 capillary hemofilter [2].

Drugs	Q_F [ml/h]	Cl [ml/min] $Q_{di}=1$ l/h	Cl [ml/min] $Q_{di}=3$ l/h	n
imipenem	180-720	8-34	17-49	23
ciprofloxacin	410-490	18-23	24-39	4
cilastatin	200-720	6-20	7-24	24
cefuroxime	270-990	7-26	10-42	22
cefotaxime	380-990	9-20	17-25	13
tobramycin	240-880	13-24	17-32	30
ceftazidine	240-890	13-30	17-38	24
vancomycin	330-740	8-20	11-20	6

The overall diffusive permeation coefficients of drugs were calculated using the iterative adjustment techniques with the condition described in eq.(9.11). The overall permeation coefficients calculated on this way we call "SK_d observed". From the relation between the SK_d of creatinine and the SK_d of other solutes, as described by eq.(9.22), we predicted the overall diffusive permeation coefficient of drugs, which we call "SK_d predicted". Using the predicted values of the overall diffusive permeation coefficients, we predicted the clearance of antibiotic drugs from eq.(6.51). In Figure 9.7, the observed values of SK_d and drug clearance are shown in relation to their predicted values. The average difference between the

observed and predicted values of SK_d was 4% according to the regression equation: SK_d (observed)=$1.04 \cdot SK_{dc}$ (predicted) -1.72 with R^2=0.65 and n=106. The average difference between the observed and predicted values of clearance was 7% according to the regression equation: Cl (observed)=0.93Cl (predicted)+1.89 with R^2=86 and n=112.
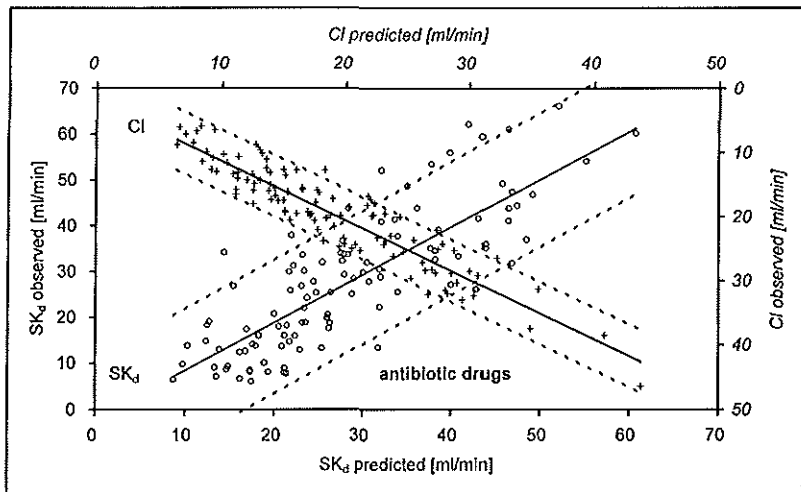
Figure 9.7: The observed diffusive permeability coefficient (SK_d) and the observed clearance of antibiotic drugs (See Tables 9.1 and 9.3) in relation to the values calculated by prediction. The broken lines show the 95% reliability intervals [18]

9.4 DISCUSSION AND CONCLUSION

Within the conventional ranges of operational conditions, the factors f_b and f_d contributing to the convective clearance for uraemic solutes can be best taken to be equal to 0.5 with a variation of maximal 10%, so that the condition "$f_b=f_d=0.5$" for the validation of eq.(6.4) is fulfilled. The empirical equations, eq.(9.20) and eq.(9.21), in which the resistances R_b+R_m and R_d are related to the ultrafiltration coefficient (MI) and to the dialysate flow rate (Q_{di}) respectively, are aimed not to gain a true physical picture of resistance to the diffusive solute transport in each region of the hemofilter, but rather to show the impact of the dialysate and the ultrafiltration flow rate on estimating the creatinine clearance by combined effect of diffusion and convection. The 'Wilson's plots' allowed us both to determine R_b+R_m and R_d separately and to quantify the influence of dialysate flow rate on R_d. This analysis serves three purposes: First, the estimation of K_d allows our model to be applied in the prediction of solute transport under different operating conditions. Second, quantitative information about the effect of the dialysate flow rate on the overall diffusive permeation coefficient (SK_d), i.e. the slope of the regression line. Third, if the contribution of R_m is determined within certain limits,

the Haberman and Sayre equation may be applied so as to predict the transport rate of solutes of different molecular weight. The actual results showed that, in CAVHD, the precise determination of R_b, R_m and R_d is of little importance. The method allows a crude estimation of the relative contribution of R_b, R_m and R_d to the overall hemofilter resistance to diffusion. The latter may be of importance when one attempts to extrapolate to transport rates of solutes of different molecular weights. We previously reported on our one-dimensional analytical model of continuous arteriovenous hemodiafiltration (CAVHD) [3, 4, 10, 17]. In that model, the possible effect of bulk-mass limitations (the 'unstirred layer effect') was not taken into account. Unfortunately, as in CAVHD the dialysate flow rates are low and variable, the influence of dialysate flow rate on the resistance to diffusion cannot be disregarded. Therefore, this mathematical model can be used to take the effect of bulk-mass limitations into account. This is, however, a numerical model that requires time consuming iterative calculations. Moreover, it takes for input a number of variables (R_b, R_d and R_m), the value of which can be estimated by using Haberman and Sayre equation, as it is demonstrated in Figure 9.5 and in Figure 9.6. But, in our view, a more practical solution is to separately analyze the determinants of the resistance to diffusion, and incorporate the relevant regression equations (9.20, 9.21 and 9.22) into the analytical model.

So far, the overall diffusive permeability coefficient ($K_s=SK_d$) were calculated by using eq.(6.50) as an initial value of numerical iterations so as to provide the condition given by eq.(9.11) is fulfilled. Eq.(6.50) was derived from the analytical solutions of the overall mass balance equations as we earlier described in Chapter 6. The overall diffusive permeability coefficients calculated by both computation techniques were compared to each other. For urea, creatinine and phosphate, we found that the K_s on the hand of analytical model was calculated with an average (n=65) difference of maximal 5% in respect to the K_s calculated according to the numerical adjustment techniques. The use of the predicting the overall diffusive permeability coefficients on the hand of the relation between the overall diffusive permeability coefficient of creatinine and other solutes, depending on the solute molecular weight as given by eq.(9.22) resulted in a fairly accurate estimation of the clearance of drugs. Furthermore, this prediction model can be used to estimate the clearance of other drugs of solutes used in case of self-poisoning.

9.5 REFERENCES

[1]. Sigler MH, Teehan BP, Van Valkenburg D. Solute transport in continuous hemodialysis: A new treatment for acute renal failure, Kidney International, 1987; 32; 562-571.

[2]. Vos MC: 'Continuous Arteriovenous Hemodiafiltration', Uitgeverij Eburn, Delft, 1993 (Erasmus University Rotterdam PhD Thesis).

[3]. Akcahuseyin E, Vincent J¹H, van Ittersum FJ, van Duyl WA, Schalekamp MADH. A

Mathematical Model of Continuous Arterio-Venous Hemodiafiltration (CAVHD), Computer Methods and Programs in Biomedicine, 1990; 31; 215-224.

[4]. Vincent HH, van Ittersum FJ, Akcahuseyin E, Vos MC, van Duyl WA, Schalekamp MADH. Solute Transport in Continuous Arteriovenous Hemodiafiltration: A New Mathematical Model Applied to Clinical Data, Blood Purif., 1990; 8; 149-159.

[5]. Colton CK, Lowrie EG: Hemodialysis. Physical principles and technical considerations; in: Brenner, Rector, The Kidney; 2nd ed., vol. 2, p. 2425-2489. (Saunders, New York 1981).

[6]. Villarroel F, Klein E, Holland F. Solute Flux in Hemodialysis and Hemofiltration Membranes, Trans. Am. Soc. Artif. Intern. Organs., 1977; 22; 225-233.

[7]. Jaffrin MJ, Ding L and Laurent JM. Simultaneous Convective and Diffusive Mass Transfer in a Hemodialyser, J of Biomedical Engineering, 1990; 112; 212-219.

[8]. Zydney AL. Bulk Mass Transport Limitations during High-Flux Hemodialysis, Artificial Organs, 1993; 17; 11; 919-924.

[9]. Sigdell JE. Calculation of diffusive and convective mass transfer, Int J Art Organs, 1982; 52; 5; 361-372.

[10]. Akcahuseyin E, van Duyl WA, Vincent HH, Vos MC, Schalekamp MADH. A sensitivity analysis of uraemic solute clearance and diffusive permeability coefficient at low dialysate flows in CAVHD. Med. Eng. Phys.(1996) (submitted).

[11]. Verniory A, Du Bois R, Decoodt P, Gassee JP and Lambert PP. Measurement of the permeability of biological membranes. J. Gen. Physiol. 1973;62; 489-507.

[12]. Hobbie RK. Transport through membranes. in: Intermediate physics for medicine and biology, p 132. J Wiley & Sons Inc, New York, 1978.

[13]. Vincent HH, Vos MC. The use of arteriovenous hemodiafiltration in multiple organ failure patients. Applied Cardiopulmonary Pathophysiology, 1991; 4; 109-116.

[14]. Vincent HH, Akcahuseyin E, Vos MC, van Ittersum FJ, van Duyl WA, Schalekamp MADH. Determinants of blood flow and ultrafiltration in continuous arteriovenous hemodiafiltration: Theoretical predictions and laboratory and clinical observations. Nephrology Dialysis Transplantation, 1990; 5; 1031-1037.

[15]. Landis EM and Pappenheimer JR. Exchange of Substances Through the Capillary Wall, in: 'Handbook of Physiology', Sect.2 Vol.2, Circulation, Chapt.29, pp.962-1034. (American Physiologic Society, Washington DC, 1963).

[16]. Gear CW: Numerical Initial Value Problems in Ordinary Differential Equations. Englewood Cliffs, New Jersey, Printice-Hall, (1971).

[17]. Akcahuseyin E, van Duyl WA, Vos MC, Vincent HH. An analytical solution to solute transport in continuous arterio-venous hemodiafiltration (CAVHD). Med. Eng. Phys.(1996) Vol:18 No:1, pp.26-35.

[18]. Akcahuseyin E, Vincent HH, van Duyl WA, Vos MC, Schalekamp MADH. Bulk mass transport during continuous arterio-venous hemodiafiltration (CAVHD): Analysis of resistance to diffusion. Medical Biol Engineering & Computing (1996) (submitted).

EFFECT OF ULTRAFILTRATION, DIALYSATE SODIUM CONCENTRATION, TREATMENT TIME AND UREA CLEARANCE ON THE TRANSCELLULAR FLUID SHIFT: A simulation study of sodium therapy

Chapter 10

10.1 INTRODUCTION

As we have mentioned in Chapter 2, the most frequent complication of conventional intermittent hemodialysis and hemodiafiltration therapy is the dialysis-induced hypotension [1]. An important factor in the development of hypotension during hemodialysis is a decrease in blood (plasma) volume, due to ultrafiltration and an insufficient refilling the intravascular volume. The (rate of) plasma volume refilling, a measure of the fluid transport from interstitium to the intravascular space during ultrafiltration, is one of the major determinants of vascular stability during conventional hemodialysis [2]. Previous reports pointed out a transcellular fluid shift from the extracellular volume (V_e) compartment to the intracellular volume (V_i) compartment during conventional (low dialysate sodium) hemodialysis, leading to a decrease in V_e that might interfere with the process of repleting the intravascular volume. This insufficient refilling might be caused by a transcellular fluid shift from the V_e compartment to the V_i compartment [3]. It has been stated that the rapid fall in plasma osmolality during dialysis causes a fluid shift from the V_e into the V_i, so called disequilibrium syndrome [2,4,5]. This internal fluid shift together with external fluid removal by ultrafiltration results in a decreased intravascular volume and hypotension [3,6]. Plasma refilling is one of the major determinants of vascular stability during hemodialysis. It has been shown that the magnitude of hypovolemia and resultant intra dialytic hypotension is dependent upon the rate of fluid removal and vascular stability [7,8,9]. It has also been demonstrated that dialysate fluid with a high sodium concentration can induce a transcellular fluid shift from V_i compartment to the V_e compartment [3,8,10,11,12]. The reduction in the incidence of hypotension [2,13], disequilibrium syndrome [10], and muscle cramps [14] by high-sodium hemodialysis may therefore be related to changes in fluid balance between the V_i and V_e compartments.

In this chapter, we introduced a mathematical simulation model of sodium kinetic which may be useful for the clinical practice. The simulation is based on a 2-pool sodium kinetic model. By means of such a simulation model, the changes in the concentration, the volume, and the osmolality in both the intracellular and the extracellular compartments can be predicted during modeled dialysis sessions. We analyzed the influence of dialysate sodium concentration and the rate of ultrafiltration and dialysis duration on the transcellular fluid shift during treatment with modeled dialysis sessions of 1 to 8 hours. The simulation results show that the magnitude of fluid shift from V_e to V_i decreases with slow dialysis, high sodium concentration

in the dialysate fluid and low rate and amount of ultrafiltration. Refilling of the intravascular volume is faster at high than at low rates of the ultrafiltration flow. To some extend, this reduces the fluid shift from the V_e into the V_i compartment. Increasing the dialysate sodium concentration has therefore the greatest effect on the transcellular fluid shift at low rates of ultrafiltration flow.

10.2 MATHEMATICAL MODEL

Previous models

Previous investigators have developed mathematical models to calculate sodium mass balance [15, 16, 17] and to predict the volume changes in extracellular and intracellular space that occur during hemodialysis [18,19,20,21,22,23]. These models have made important contributions to the understanding of sodium therapy. However, these models do not include the effect of transcellular urea gradients on fluid shift; these models also assume that this fluid shift occurs instantaneously, so that osmotic equilibrium exists between V_e and V_i at all times during a dialysis session. These assumptions may be invalid for short-time, high-efficiency dialysis, where the difference between transcellular urea and nonurea osmolar gradients may be large and time insufficient for equilibrium to occur. In their mathematical model, Heineken et al [24] have included the effects of urea osmolar gradient, and osmotic disequilibrium and were able to successfully simulate the high- and low-sodium dialysis experiments and calculate a whole body ultrafiltration coefficient. However, in this model the correction factor for plasma water (F_w), Donnan ratio (α_{Na}) of dialyzer plasma water sodium, transcellular reflection coefficient (σ_u) for urea, and hematocrit (Ht_a) dependence of sodium dialysance (D_{Na}) were not included. Furthermore, the convective transport of urea from V_i to V_e was incorrectly calculated. By accounting these factors in their model, Pastan et al [25] were able to calculate the changes in osmolality, fluid shift and sodium and urea mass balance during dialysis. In their model, however, the changes in hematocrit and plasma protein concentration during a dialysis session were not included and the Donnan ratio was taken to be constant. In fact, the Donnan ratio is dependent on the plasma protein concentration which may also change due to ultrafiltration. Since sodium removal occurs from plasma water only, the changes in plasma water as a result of changes in hematocrit and plasma proteins have to be taken into account. These factors were accounted for in our model. Our model incorporates differential equations describing the mass balance of intra- and extracellular urea, nonurea and plasma water as a function of treatment time (t_d). Our model formulation is similar to that of Pastan et al [25], but not identical.

Model description

We assumed a 2-compartment model consisting of V_e and V_i. Urea is constantly generated in the liver and assumed to directly enter to extracellular volume (V_e) [26]. During dialysis,

urea transport between V_i and V_e and its removal across the dialyzer membrane occur by diffusion and convection. For the purpose of the mathematical model, all impermeant nonurea solutes (NaCl, KCl, mannitol, etc.) are lumped together as a single nonurea solute. The only other additional extracellular osmotically active solute is assumed to be sodium (Na^+) at a total (free plus bound) concentration $C_{e,Na}$. Between the V_i and V_e compartments ion exchange occurs by diffusion and plasma water is transported with an ultrafiltration coefficient (K_F). The Donnan-ratio is taken to be dependent on the plasma protein concentration. We assumed that the changes in the plasma protein concentration and hematocrit depend on the changes in the extracellular volume.

Intracellular water, urea and Na^+ mass balance
The rate of volume flow between V_e and V_i equals the change in the V_i during dialysis and is taken to be proportional to the difference between the osmotic pressure in these spaces:

$$\frac{dV_i}{dt} = -K_F RT \Delta Osm. \tag{10.1}$$

where $K_F = 149.4$ l·Atm/mmol°K is the whole body ultrafiltration coefficient [24], that is, how quickly water enters or leaves the plasma volume from the interstitial space, R is the gas constant, T is the temperature. The magnitude of the net osmolar driving force is defined as:

$$\Delta Osm. = \kappa_{Na}(C_{e,Na} - C_i) + \sigma_u(C_{e,u} - C_{i,u}) \tag{10.2}$$

where $\kappa_{Na} = 1.846$ is a factor that converts the molar concentration of Na^+ and its accompanying anions into its osmotically equivalent osmolar concentration [27], $C_{e,Na}$ is the extracellular Na^+ concentration, C_i is the intracellular concentration of osmotically active nonurea, $\sigma_u = 0.95$ is the transcellular urea reflection coefficient [28], $C_{e,u}$ is the extracelluar urea concentration and $C_{i,u}$ is the intracellular urea concentration. The rate of nonurea solute mass transport is assumed to be constant:

$$\frac{d(V_i C_i)}{dt} = 0 \tag{10.3}$$

The rate of intracellular urea mass transport is due to the sum of diffusive and convective transport from V_i into the V_e:

$$\frac{d(V_i C_{i,u})}{dt} = -K_u(C_{i,u} - C_{e,u}) + s C_{i,u}\frac{dV_i}{dt} \tag{10.4}$$

where $K_u = 800$ ml/min is the diffusion coefficient of urea [24,29,30], s=1 is the urea trans-cellular sieving coefficient [25].

Extracellular water, urea and Na^+ mass balance
The change in the extracelluar volume (V_e) during dialysis equals the sum of the rate of volume flows from or into V_i and that from dialyzer:

$$\frac{dV_e}{dt} = -\frac{dV_i}{dt} - Q_f \tag{10.5}$$

in which Q_f is the net rate of ultrafiltration flow through the dialyzer. The mass balance of extracellular Na^+ is given by:

$$\frac{d(V_e C_{e,Na})}{dt} = D_{Na}(1 - \frac{Q_f}{Q_{wi}})(C_{di,Na} - \alpha_{Na} C_{e,Na}) - Q_f \alpha_{Na} C_{e,Na} \tag{10.6}$$

in which $C_{di,Na}$ is inlet dialysate Na^+ concentration, Q_{wi} is the inlet plasma water flow rate, α_{Na} is Donnan ratio [15, 31] and D_{Na} is the dialyzer sodium dialysance [15].The terms on the right-hand side of eq.(10.6) includes the rate of Na^+ mass transport by diffusion as well as by ultrafiltration through the dialyzer membrane. The Na^+ concentration in plasma water $(C_{wi,Na})$ at the dialysate blood inlet equals the Na^+ concentration in the extracellular volume $(C_{e,Na})$. Plasma water flow rate (Q_{wi}) is calculated from the inlet blood flow rate (Q_{ba}) as:

$$Q_{wi} = Q_{ba} \frac{(1 - 0.96\, Ht_a)}{F_w} \tag{10.7}$$

in which $F_w = 0.927$ is a correction factor for plasma water [31,32] and Ht_a is the arterial hematocrit. The rate of extracellular urea mass transport is given by:

$$\frac{d(V_e C_{e,u})}{dt} = K_u(C_{i,u} - C_{e,u}) - sC_{i,u}\frac{dV_i}{dt} + G_u - [D_u(1 - \frac{Q_f}{Q_{ba}}) + Q_f] C_{e,u} \tag{10.8}$$

where the first term on the right-hand side is the rate of diffusive and the second term is the rate of convective urea transport, the third term ($G_u = 0.083$ mmol/min) is the urea generation rate [15,33] and the last term is the rate of urea removal by diffusion and convection through the dialyzer membrane with D_u representing the dialyzer urea dialysance (clearance). Since the dialysate inlet urea concentration ($C_{di,u}$) is zero, the urea dialysance is the same as the urea clearance [15]. The urea clearance can be calculated from eqs.(6.45-6.47) using the flow rate of blood in place of plasma water. According to Pastan et al [25], the Na^+ dialysance may be derived from the urea dialysance as:

$$D_{Na} = D_u(1 - 0.96\, Ht_a) \tag{10.9}$$

because Na^+ is removed only from plasma water.

Donnan factor α_{Na}

The impermeability of the dialyzer membrane for charged proteins causes a Donnan-effect. The so-called Donnan-factor is defined as the concentration (measured by flame photometry) ratio of electrolyte ions between plasma and dialysate after reaching an equilibrium. The Donnan-factor (ratio) is calculated according to the NCE "net cation equivalency" of proteins. Part of the sodium in plasma water is covalently bound or "complexed" to proteins. This

amounts to no more than 1% according to Van Leeuwen [34], and 1.37 mmol per 100 gram of hydrated proteins according to Bosch et al [35]. Depending on the plasma protein concentration, the Donnan-factor for Na^+ varies up to 1.0. According to Bosch et al [35], the Donnan factor has to be calculated as the ratio of Na^+ concentration in ultrafiltrate to that in plasma water both measured by ion selective electrode (ISE). In this way, for sodium plasma concentrations within the range of 136-146 mmol/l, Man et al [36] has calculated the Donnan ratio from the ratio plasma-to-dialysate concentration at equilibrium and found to be $\alpha_{Na}=0.954$. According to Stiller et al [31] and Sargent et al [15], the Donnan ratio amounts to 0.94. Shaldon et al [37] derivated an empirical formula to calculate the Donnan ratio from the plasma protein concentration:

$$\alpha_{Na} = 1.007 - 9 \cdot 10^{-4} \frac{C_{pi} + C_{po}}{2} \qquad (10.10)$$

with C_{pi} and C_{po}, each representing the plasma protein concentration at the dialyzer blood inlet and at the blood outlet respectively. C_{pi} and C_{po} are calculated according to eq.(3.16) and eq.(3.18) respectively, with $Q_{pred}=0$, noting that C_{pi} becomes equal to C_{pa}.

Hematocrit and plasma protein mass balance

The arterial plasma protein concentration and arterial blood hematocrit are conserved with the following protein and hematocrit balance:

$$C_{pa} = \frac{C_{pa}(0) V_e(0)}{V_e} \qquad (10.11)$$

$$Ht_a = \frac{Ht_a(0) V_e(0)}{V_e} \qquad (10.12)$$

in which $C_{pa}(0)$, $Ht_a(0)$ and $V_e(0)$ represent the predialysis (at t=0) values of arterial plasma protein concentration, arterial hematocrit and extracellular volume respectively.

Dialysis efficiency index

The delivery of a dialysis treatment is highly dependent on adequate solute removal, adequate fluid removal and the stability of the patient's treatment. The quantity of urea removed during dialysis is the product of dialyzer clearance (D_u, [l/min]) and the treatment time (t_d,[min]). An adequate dialysis treatment is achieved if the total amount of urea clearance per treatment approximates the predialysis volume of urea distribution ($V_o=V_e(t=0)+V_i(t=0)$, [l]) in patients who have negligible residual renal function. This statement is characterized by an efficiency index (DP) as:

$$DP = \frac{D_u t_d}{V_o} = \ln\frac{C_{e,u}(0)}{C_{e,u}(t_d)} = \ln\frac{1}{1 - FRU_e} \qquad (10.13)$$

where $C_{e,u}(0)$ and $C_{e,u}(t_d)$ are the pre- (t=0) and postdialysis (t=t_d) extracellular urea concentrations respectively and FRU_e represents the removed fraction of urea (urea reduction ratio) from extracellular volume:

$$FRU_e[\%] = \frac{C_{e,u}(0) - C_{e,u}(t_d)}{C_{e,u}(0)} \times 100 \qquad (10.14)$$

DP index is used as a measure of the effective dialyzer performance and also as a measure of the amount of dialysis (dose of dialysis), a fractional volume which is cleared per dialysis session. When the efficiency index (DP) is grater than 1, the treatment is considered adequate. An efficiency index of DP=1 corresponds to an urea reduction ratio of 60 to 65%. To remove 60 to 65% of the predialysis urea in a given patient, a dialyzer with a low urea clearance will require a longer treatment time than a dialyzer with a high urea clearance.

10.3 SIMULATION RESULTS

All equations governing the urea and sodium mass balance are numerically integrated by using the Runge-Kutta-Merson method [38] in the simulation programme Psi/e [39]. See Appendix for the Psi/e listing of simulation. The computation times were short enough to perform the simulations. In Table 10.1 the constants and variables used for this simulation work are shown.

Table 10.1: Values of parameters used for the mathematical simulation of Na^+ and urea transport.

Parameter	Value	Units	Parameter	Value	Units
$C_{di,Na}$	variable	mmol/l	Q_{ba}	0.3 or 0.2	l/min
$C_{di,u}$	0	mmol/l	Q_f	V_{UF}/t_d	l/min
$C_i(0)$	140	mmol/l plasma	V_{UF}	1 - 3	l
$C_{e,Na}(0)$	140	mmol/l plasma	$V_e(0)$	16.4	l
$C_{e,u}(0)$	40	mmol/l plasma	$V_i(0)$	28.0	l
$C_{i,u}(0)$	40	mmol/l plasma	V_o	44.4	l
Ht_a (t=0)	0.3		σ_u	0.95	
$C_{pa}(t=0)$	70	g/l	R	0.08206	lAtm/(°Kmmol)
T	310	°K	K_F	149.4	ml/(minAtm)
K_u	800	ml/min	G_u	0.083	mmol/min
κ_{Na}	1.846		s	1	
F_w	0.927		DP	0.5 - 1.5	

The simulations were performed for an ideal 72 Kg patient, with an initial value of V_e(t=0)=16.4 l and V_i(t=0)=28 l prior to dialysis. Initial values of $C_{e,Na}$ and C_i were 140

mmol/l in plasma. In calculations, the urea and nonurea plasma concentrations were used in units of mmol/l in plasma water on dividing plasma concentrations by $F_w=0.927$. Initial urea concentrations $C_{i,u}$ and $C_{e,u}$ were 40 mmol/l. Throughout each dialysis session we used

$Q_{ba}=0.2$-0.3 l/min, $Ht_a(0)=0.3$ and $C_{pa}(0)=70$ g/l. The modeled urea dialysance (clearance) was calculated from different values of dialysis performance index, eq.(10.13), namely DP=0.5, 0.75, 1, 1.25 and 1.5 for varying treatment durations ($t_d=1$ to 8 hours). The predialysis volume of urea distribution was $V_o=44.4$ l. For each dialysis session, the ultra-filtration flow rate ($Q_f=V_{UF}/t_d$, V_{UF} represents the amount of ultrafiltration in liters) was adjusted so that $V_{UF}=2.4$ l plasma water was ultra filtered from the V_e compartment.
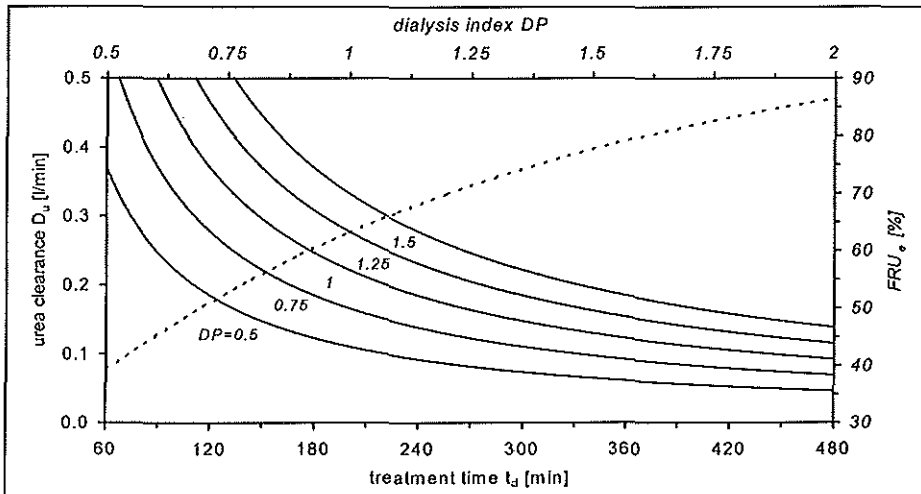
Figure 10.1: Theoretical urea dialysance (clearance) for modeled dialysis sessions from 1 to 8 hours at different values of dialysis performance index (DP). An achievable urea clearance even with short, high efficiency treatments is maximal 0.33 l/min. The dashed line represents the urea reduction ratio (FRU$_e$) versus the dialysis index.

In Figure 10.1, the urea clearance for values of different dialysis index is shown as a function of modeled dialysis sessions from 1 to 8 hours. Figure 10.1 shows how a "short-time, high-efficiency dialysis" may be modeled from the parameters of dialysis performance index (DP), the patient volume of urea distribution (V_o) and treatment time (t_d) under the condition that the same amount of urea and the same amount of water are removed at the end of each dialysis session. The dialysis indexes DP=0.5, 0.75, 1, 1.25 and 1.5 correspond to an urea reduction of 40%, 53%, 63%, 71% and 83% of the predialysis volume of urea distribution (V_o) at the end of dialysis session respectively. In short, high efficiency treatments ($t_d<240$ minutes), an urea clearance of 0.26 l/min can be achieved with a blood flow rate of 0.3

l/min, dialysate flow rate of 0.5 l/min and a dialyzer with an overall diffusive permeation coefficient of SK_o=1.0 l/min (K_o : overall diffusive mass transfer coefficient and S : membrane surface area, see eq.(6.45)). With a blood flow rate of 0.4 l/min and dialysate flow rate of 1.0 l/min and a dialyzer with SK_o=1.0 l/min, an urea clearance of 0.33 l/min can be achieved. For urea clearance of D_u>0.33 l/min, higher blood flow rate than 0.4 l/min and higher dialysate flow rate than 1.0 l/min are needed. In conventional intermittent hemodialysis, an urea clearance of 0.12-0.18 l/min is achieved with a dialysis session of 3-4 hours.

Effect of urea clearance on the fluid shift
In the simulations, the ultrafiltration rate (Q_f) was adjusted so that at the end of each treatment session 2.4 liters of plasma water was ultrafiltered. The dialysate sodium concentration was $C_{di,Na}$=140 mol/l. The urea clearance was adjusted so that for each dialysis session of a period of t_d=4 hours, the dialysis index DP=0.5, 0.75, 1, 1.25 and 1.5 is obtained. Further, we calculated the time courses of transcellular urea osmolar gradient, $(C_{e,u}-C_{i,u})$, the nonurea osmolar gradient, $\kappa_{Na}(C_{e,Na}-C_i)$, and resultant (net) osmolar driving force, $\Delta Osm.=\sigma_u(C_{e,u}-C_{i,u})+\kappa_{Na}(C_{e,Na}-C_i)$, the changes in the intracellular volume, $\Delta V_i=V_i-V_i(0)$, the changes in the extracellular volume, $\Delta V_e=V_e-V_e(0)$, for different values of DP index. In Figure 10.2 and Figure 10.3, these time courses are shown.
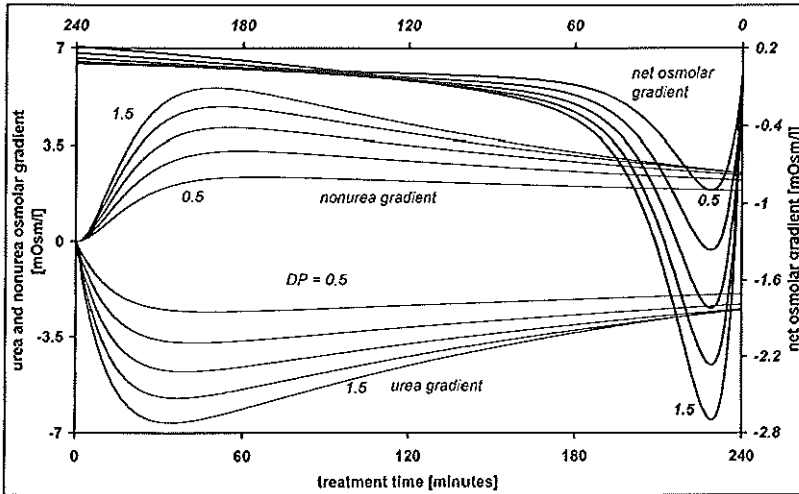
Figure 10.2: Time courses of urea, nonurea and net osmolar gradients for modeled dialysis sessions of 4 hours with $C_{di,NA}$=140 mmol/l and Q_f=0.01 l/min.

Figure 10.2 shows that almost always in the first hour of each dialysis session, the nonurea (positive) and the urea (negative) osmolar gradients result in a (negative) net osmolar gradient. Urea osmolar gradient causes the water to move from V_e to V_i while the nonurea osmolar

gradient works in the opposite direction. As water flows from V_e to V_i, the plasma sodium concentration rises slightly. This results in a nonurea osmolar gradient that is of the same magnitude as the urea gradient, but of opposing direction. A small water shift results in a relatively large increase in extracellular sodium concentration because the extracellular sodium mass is so large. This small degree of water shift is also a result of the dialysate sodium concentration $C_{di,Na}=140$ mmol/l (See the following section "Effect of sodium concentration on the fluid shift".). As the magnitude of the net (negative) osmolar gradient (driving force) increases with the increasing rate of urea removal as a result of the fact that the nonurea gradient develops slower than its counter part, towards the end of dialysis time the net osmolar gradient reaches a zero value resulting in equilibrium or a positive value resulting in water movement from V_i to V_e. The faster the urea is removed, the faster the (negative) osmolar urea gradient develops. The time delay in developing both osmolar gradients results from barriers to solute diffusion (noting the fact that the equilibration rate is less than infinite) and from a decrease of extracellular osmolality more quickly than the intracellular osmolality with increasing rates of urea removal. Since the amount of ultrafiltration (and ultrafiltration flow rate) is the same for each dialysis session, the changes in V_i with urea clearance may be attributed to the urea clearance by diffusion through the hemodialyzer membrane.
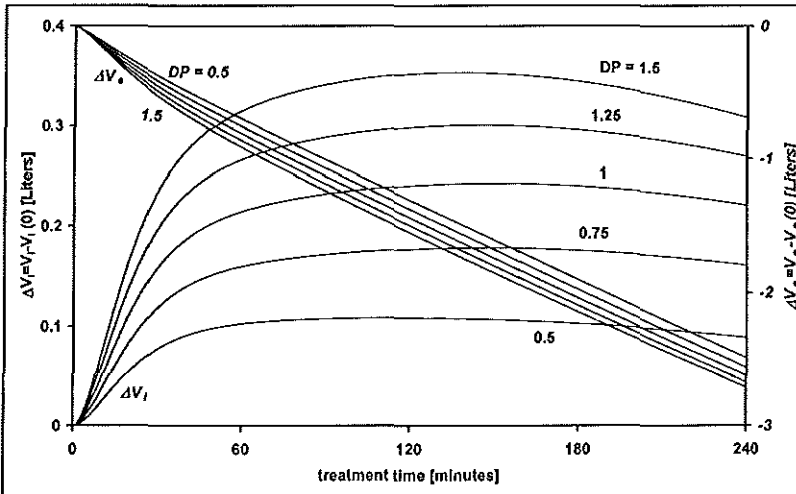
Figure 10.3: Changes in ΔV_i and ΔV_e in time for modeled dialysis sessions of 4 hours with DP=0.5, 0.75, 1, 1.25 and 1.5.

The time courses of the changes in V_e and V_i due to the net osmolar gradient and ultra-filtration are shown in Figure 10.3. The magnitude of fluid shift from V_e to V_i, $\Delta V_i=V_i-V_i(0)$, is determined from the increase in V_i. The sum of postdialysis values of ΔV_i and ΔV_e reaches the predefined amount of ultrafiltration volume, $V_i(t_d)+\Delta V_e(t_d)=-V_{UF}=2.4\ l$ of water, which

means that at the end of each modeled dialysis session, 2.4 liters of plasma water is filtered. The size of fluid shift increases with increasing rates of urea removal. An increase in the rate of urea removal steepens the osmolar gradient between V_i and V_e compartments, resulting in a fluid shift into cells, thus contributing hypotension.

Table 10.2: The relative changes in V_i and V_e compartments as a result of different rate of urea removal at the end of a dialysis session of t_d=4 hours with a fixed Q_f=0.01 l/min.

DP	D_u [l/min]	$\Delta V_i(t_d)/V_i(0)$ [%]	$\Delta V_e(t_d)/V_e(0)$ [%]	$t_{eq.}$ [min] after start
0.5	0.093	0.32	-15.18	113
0.75	0.139	0.58	-15.62	145
1	0.185	0.79	-15.98	148.5
1.25	0.231	0.96	-16.28	143.6
1.5	0.278	1.1	-16.51	136

In Table 10.2, the relative changes in V_i and V_e as a result of different rates of urea removal at the end of a dialysis session of t_d=4 hours with $\Delta V_i (t_d)=V_i (t_d)-V_i (0)$ and $\Delta V_e (t_d)=V_e (t_d)-V_e (0)$. As the urea clearance increases, the V_i volume increases and the V_e volume decreases. However, the relative changes in size of both compartments because of different rates of urea removal are small. The time at which an osmolar equilibrium occurs does change with the increasing urea clearance. In Table 10.2, $t_{eq.}$ represents the time of reaching equilibrium (zero net osmolar gradient) after starting the dialysis session. Model predictions show for example with an urea clearance of D_u=0.139 l/min, water movement from V_e to V_i stops at $t(=t_{eq})=$ 145th minute and from that time to the end ($t=t_d$=240 min.) of the dialysis treatment time water removes from V_i to V_e.

Effect of treatment time on the fluid shift
We modeled dialysis sessions in which the same amount of urea and the same amount of water are withdrawn in different treatment durations. The urea clearance and ultrafiltration flow rate were adjusted so that the dialysis performance index DP=1 is obtained and 2.4 liters of ultrafiltration volume is filtered during and at the end of each dialysis session respectively. In Figure 10.4, the time courses of the osmolar gradients are shown for DP=1, $C_{di,Na}$=140 mmol/l and Q_f=2.4/t_d during dialysis session from t_d=1 to 4 hours. During a dialysis session with the longest treatment time, the net (negative) osmolar driving force is the lowest, e.g., the rate of fluid shift from V_e to V_i is the slowest with the longest treatment time. The time courses of the changes in V_e and V_i due to the net osmolar gradient and ultrafiltration are shown in Figure 10.5. It is evident that as the duration of dialysis treatment increases, the size of transcellular fluid shift decreases, noting that a zero or relatively more positive net osmolar

gradient is achieved earlier in short than in long duration of dialysis treatment. In Table 10.3, the relative changes in V_i and in V_e at the end of each dialysis session are listed for $C_{di,Na}=140$ mmol/l, $V_{UF}=2.4$ l, DP=1, $V_i(0)=28$ l and $V_e(0)=16.4$ l. From both Table 10.3 and Figure 10.5 it can be seen that the magnitude of water shift from V_e to V_i is relatively small. This magnitude becomes smaller with longer duration of dialysis treatment and smaller dialysis performance index, namely with slower dialysis. The shorter the dialysis duration, the longer time is needed to achieve osmolar equilibrium.
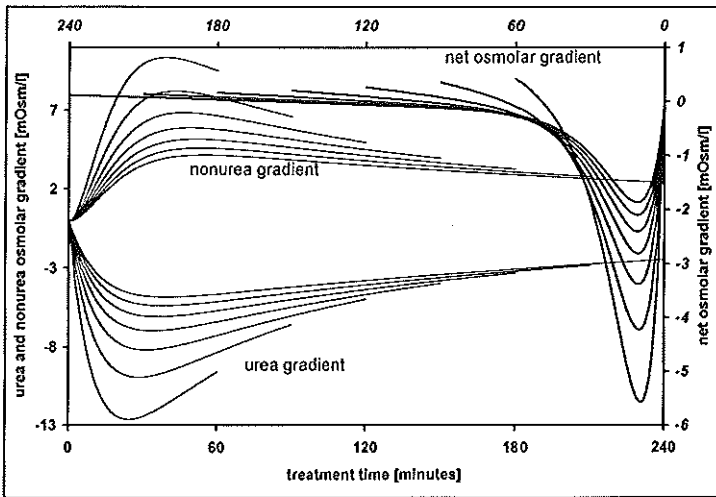
Figure 10.4: Changes in nonurea, urea and net transcellular osmolar driving force ΔOsm. in time for modeled dialysis sessions from 1 to 4 hours.

Table 10.3: The relative changes in V_i, $\Delta V_i(t_d)=V_i(t_d)-V_i(0)$ and in V_e, $\Delta V_e(t_d)=V_e(t_d)-V_e(0)$ as a result of varying treatment times with a fixed DP=1.

t_d [minutes]	D_u [ml/min]	Q_f [ml/min]	$\Delta V_i(t_d)/V_i(0)$ [%]	$\Delta V_e(t_d)/V_e(0)$ [%]	$t_{eq.}$ [min] after start
60	740	40	1.4	-17.03	49.9
90	493.3	26.7	1.27	-16.80	64.8
120	370	20	1.12	-16.54	80
150	296	16	1.0	-16.34	97.5
180	246.7	13.3	0.91	-16.19	116.8
210	211.4	11.4	0.84	-16.07	137.3
240	185	10	0.79	-15.98	158.5

In Figure 10.6, the magnitude of fluid shift from V_e to V_i is shown in relation to varying dialysis duration and dialysis performance index. Dialyzing the patient in the shortest duration of treatment with obtainable highest urea clearance results in the greatest magnitude of fluid shift.
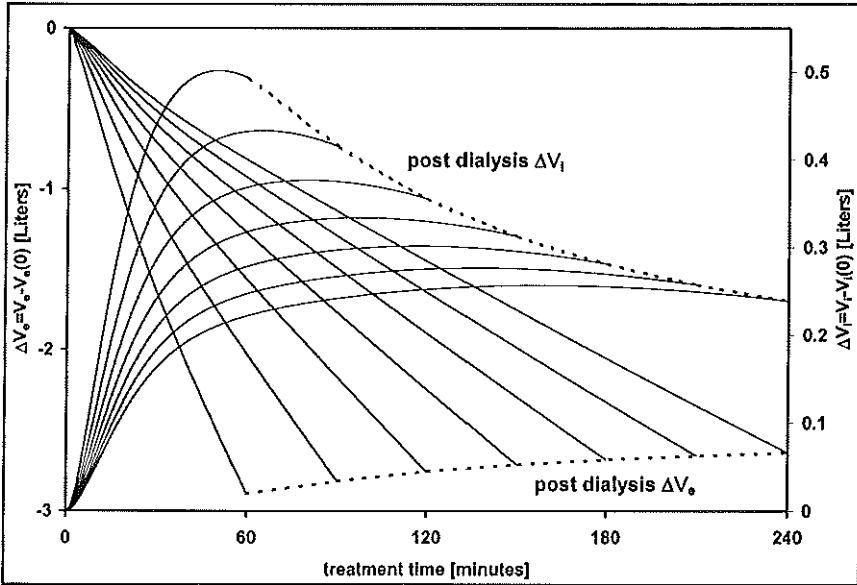
Figure 10.5: Time courses of changes in ΔV_i and ΔV_e. The dashed lines represent the postdialysis values of ΔV_i and ΔV_e.
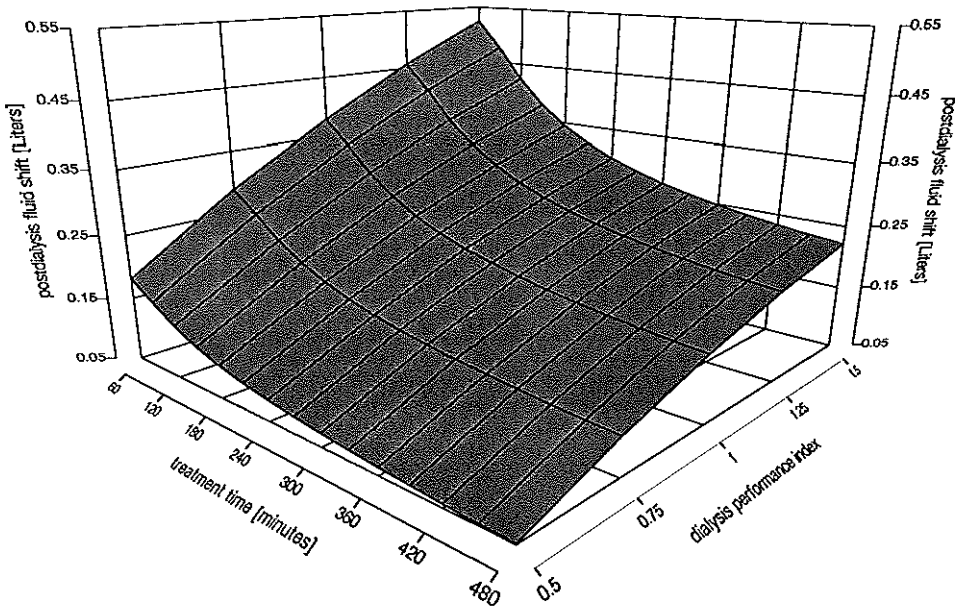
Figure 10.6: Fluid shift at the end of dialysis sessions modeled for 1 to 8 hours at different values of DP= $D_u t_d / V_o$ with $V_o = 44.4\, l$.

Effect of dialysate sodium concentration on fluid shift

The main effect of sodium in dialysis therapy is the regulation of the water distribution between the intra- and extracellular space. To demonstrate the effect of dialysate sodium concentration on the transcellular fluid shift, we simulated dialysis schedules for a 4 hours treatment, keeping the rate (Q_f=0.01 l/min) and amount (V_{UF} = 2.4 l) of ultrafiltration and urea clearance (D_u = 0.185 l/min) constant and varying the dialysate Na$^+$ concentration ($C_{di,Na}$) from 120 to 150 mmol/l. In Figures 10.7a and 10.7b time courses of the osmolar gradients areshown.

From the time courses of the transcellular urea, nonurea and net osmolar gradients in Figures 10.7a and 10.7b, it is evident that an increased Na$^+$ concentration leads to an increased nonurea (positive) osmolar gradient while the urea (negative) osmolar gradient was almost unchanged. An increased sodium concentration in the dialysate fluid leads to an increased net osmolar gradient, but in the early hours or minutes of dialysis treatment this net osmolar gradient is more negative at low than at high dialysate sodium concentration. Not only the size of nonurea osmolar gradient is increased with increasing values of Na$^+$ concentration, but also the time necessary for equilibrium (t_{eq}) is shortened. A zero or relatively more positive net osmolar gradient is achieved earlier with a high than with a low dialysate Na$^+$ concentration.

The time courses of the changes due to varying dialysate Na$^+$ concentration in the fluid shift are shown in Figure 10.8. Lower dialysate sodium concentration results in much larger transcellular volume shift from V_e to V_i while higher dialysate sodium concentration show reversal with shift occurring from V_i to V_e.In Table 10.4, the relative changes in V_i and in V_e due to varying dialysate sodium concentration are listed. Up to almost $C_{di,Na}$=140 mmol/l, the fluid shift occurs from V_e to V_i. The equilibrium time is sensitive to the dialysate Na$^+$ concentration. The higher the dialysate sodium concentration, the shorter the equilibrium time is. It is evident that in the very early minutes of treatment, lesser amount of fluid is shifted from V_e and to V_i at higher than at lower concentration of dialysate sodium, therefore relatively lesser time is needed to diminish the fluid shift. With highest $C_{di,Na}$, where the size of water shift from V_e to V_i reaches its minimal value, the shortest time is needed to refill the V_e compartment. This may indicate that with high dialysate sodium concentration water is shifted earlier from interstitium to V_i than from plasma volume to V_i. The lower the dialysate sodium concentration, the lower the rate of refilling the V_e compartment. For example with this particular setting of modeled dialysis session, if $C_{di,Na}$=120 mmol/l, one deals with an insufficient refill. As the amount of water shifted from V_e to V_i together with the amount of water withdrawn from V_e to the dialyzer outlet reaches its maximal value at the end of treatment, the maximal size of decrease in plasma volume is reached.
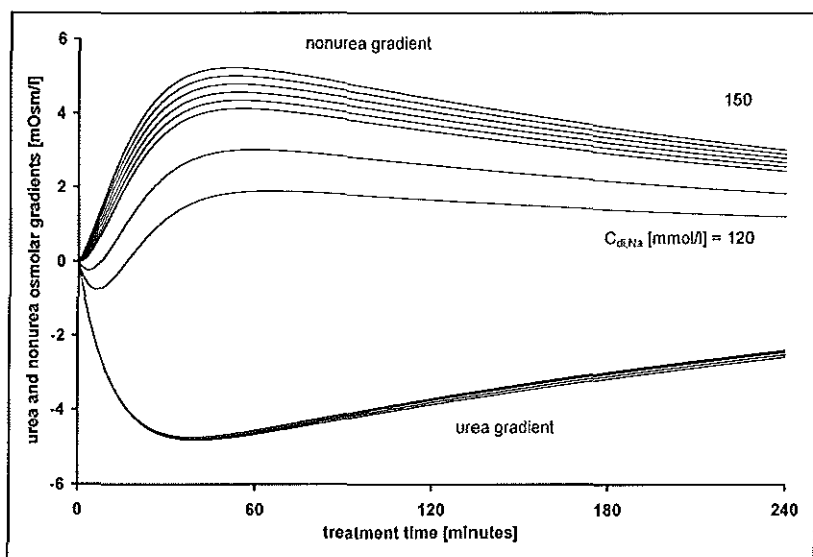
Figure 10.7a: Effect of dialysate Na$^+$concentration on the urea and nonurea osmolar gradients for a modeled dialysis session of 4 h with a fixed Q_f=0.01 l/min and a fixed D_u=0.185 l/min.
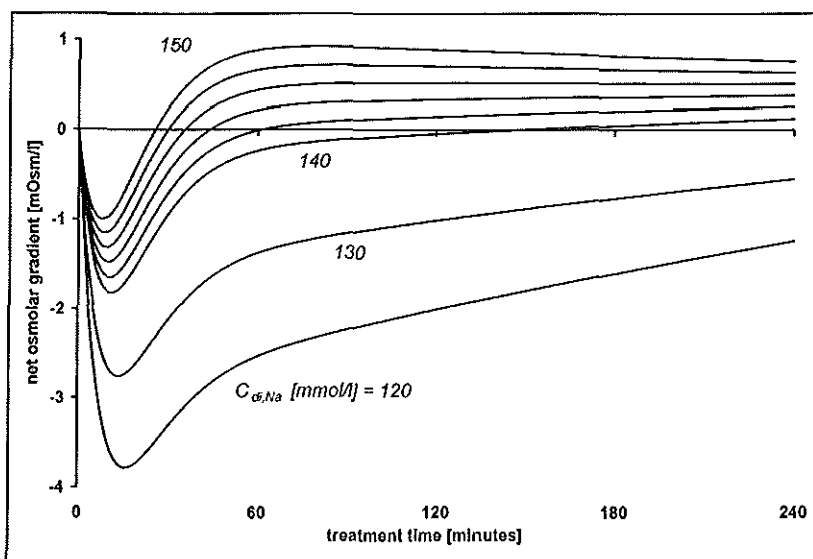
Figure 10.7b Effect of dialysate Na$^+$concentration on the net transcellular osmolar gradients.
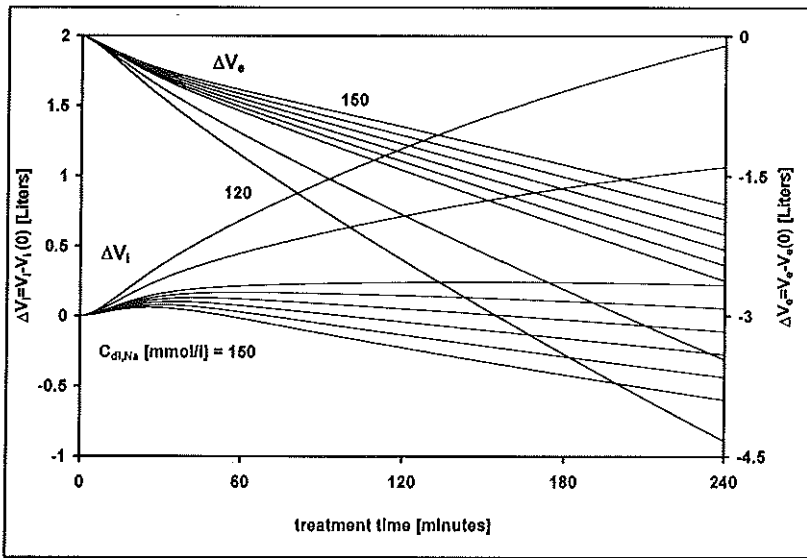
Figure 10.8: Effect of dialysate Na$^+$concentration on the fluid shift for a modeled dialysis session of 4 hours with a fixed ultrafiltration flow rate Q$_f$=0.01 l/min and a fixed dialyzer urea dialysance of D$_u$=0.185 l/min.

A fluid shift from the interstitium toward the intravascular space forms the only compensatory mechanism to overcome or diminish hypovolemia. It is evident that dialysate sodium with high concentration prevents the fluid shift from V$_e$ to V$_i$ and further improves it from V$_i$ to V$_e$

Table 10.4: The relative changes in V$_i$ and in V$_e$ at the end of dialysis session due to the changes in the dialysate sodium concentration. t$_d$=4 h, Q$_f$=0.01 l/min.

C$_{di,Na}$ [mmol/l]	$\Delta V_i(t_d)/V_i(0)$ [%]	$\Delta V_e(t_d)/V_e(0)$ [%]	t$_{eq.}$ [min] after start
120	6.90	-26.42	insufficient
125	5.35	-23.76	insufficient
130	3.81	-21.13	insufficient
135	2.29	-18.54	insufficient
140	0.79	-15.98	149
142	0.19	-14.97	62
144	-0.39	-13.96	44
145	-0.69	-13.46	39
146	-0.98	-12.96	36
148	-1.56	-11.97	30
150	-2.14	-10.98	26

Hypotension is more likely to occur with lower dialysate sodium concentration. If the dialysate sodium concentration is lower than the plasma sodium concentration, the effects of osmotic

transcellular fluid shift consequent on the removal of urea will be exaggerated because the plasma will become even hypoosmolar relative to the cells as the result of movement of sodium from plasma to dialysate compartment. A high dialysate sodium concentration is, therefore, particularly important at the beginning of dialysis treatment when osmolar gradient between V_i and V_e compartments is greatest as is shown in Figures 10.7a and 10.7b.

Consequently, a high plasma sodium concentration will counterbalance the effects of transcellular fluid shift. As can be seen from Figure 10.7b, the sodium concentration may better be decreased slowly towards the end of dialysis, by taking care of time which is necessary for the refill. After being reached a critical rate of sufficient refilling, the sodium concentration may later be increased again. But administration of too high sodium concentration may lead to an excessive water intake as a result of thirst, which may cause further problems for the next dialysis sessions.

Effect of ultrafiltration on the fluid shift

During the course of a single dialysis session of 3-4 hours, an ultrafiltration volume in magnitude equal to the entire plasma volume (several liters of fluid) are removed by ultrafiltration. The effects of the amount of ultrafiltration or flow rate on the fluid shift were investigated by simulating dialysis sessions of 4 hours. Hereby the urea dialysance was fixed to 0.185 l/min and the ultrafiltration flow rates were varied from 0 to 0.04 l/min. The postdialysis volume of ultrafiltration was modeled 2.4 liters ultrafiltrate per 0.01 ml/min (9.6 liters ultrafiltrate with Q_f=0.04 l/min). Further, the $C_{di,Na}$ was fixed to 120 mmol/l for low, 140 mmol/l for normal and 150 mmol/l for high dialysate sodium concentration. In Figures 10.9a, 10.9b and 10.9c, the effect of varying ultrafiltration flow rate on the changes of nonurea, urea and net transcellular osmolar gradient is shown for high, normal and low dialysate sodium concentration respectively. The time courses of the changes in both V_i and V_e, due to varying ultrafiltration flow rates are shown in Figures 10.10a, 10.10b and 10.10c for high, normal and low dialysate sodium concentration respectively. With high and normal dialysate sodium concentration, ultrafiltration has effect on the urea gradient in the early hours and on the nonurea gradient in the late hours of treatment. In the first hour of treatment, the nonurea gradients were almost unchanged. With the low dialysate concentration, the nonurea osmolar gradient decreases in the early minutes and increases again within the first half hour. As the magnitude of osmolar urea gradient decreases with the increasing rate of ultrafiltration flow, the osmolar nonurea gradient increases in the opposite direction. The relative change in the magnitude of osmolar urea gradient with increasing ultrafiltration flow rate did not alter with the dialysate sodium concentration. The equilibrium time is also sensitive to the ultrafiltration flow rate. The higher the rate of ultrafiltration flow, the shorter the equilibrium time is. It is evident that the equilibrium time is shorter with higher dialysate sodium concentration.
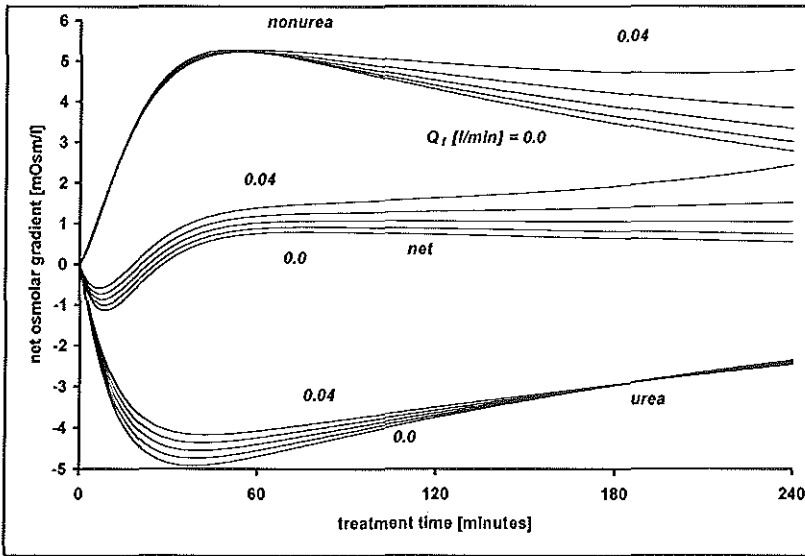
Figure 10.9a: Effect of ultrafiltration flow rate on the transcellular osmolar gradients at high dialysate sodium concentration. $C_{di,Na}=150$ mmol/l.
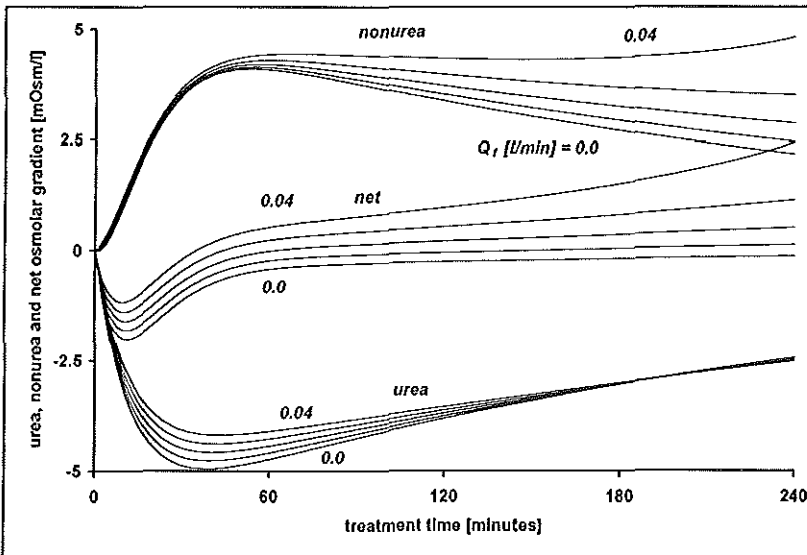
Figure 10.9b: Effect of ultrafiltration flow rate on the transcellular osmolar gradients at normal dialysate sodium concentration. $C_{di,Na}=140$ mmol/l.
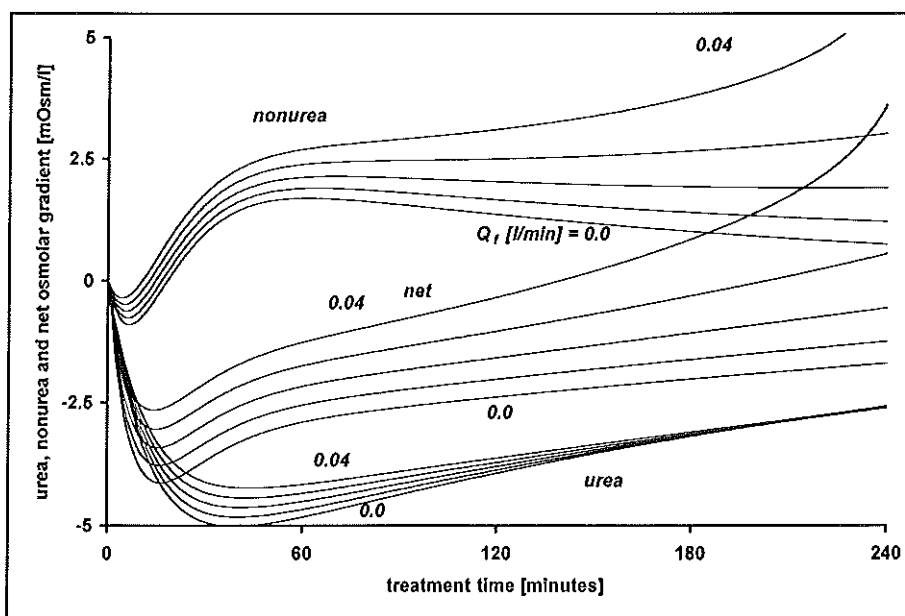
Figure 10.9c: Effect of ultrafiltration flow rate on the transcellular osmolar gradients at low dialysate sodium concentration $C_{di,Na}$=120 mmol/l.
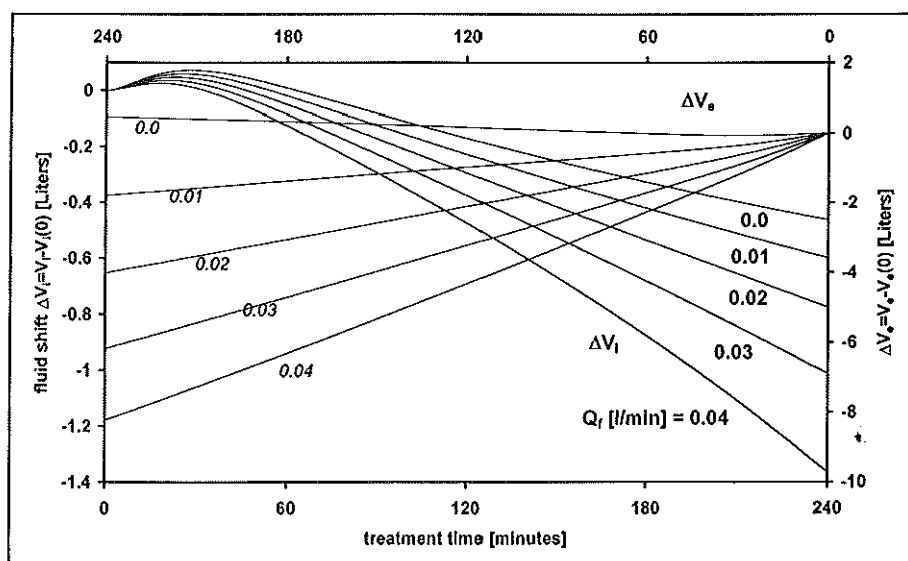
Figure 10.10a: Effect of ultrafiltration on the fluid shift at high dialysate sodium concentration. $C_{di,Na}$=150 mmol/l.
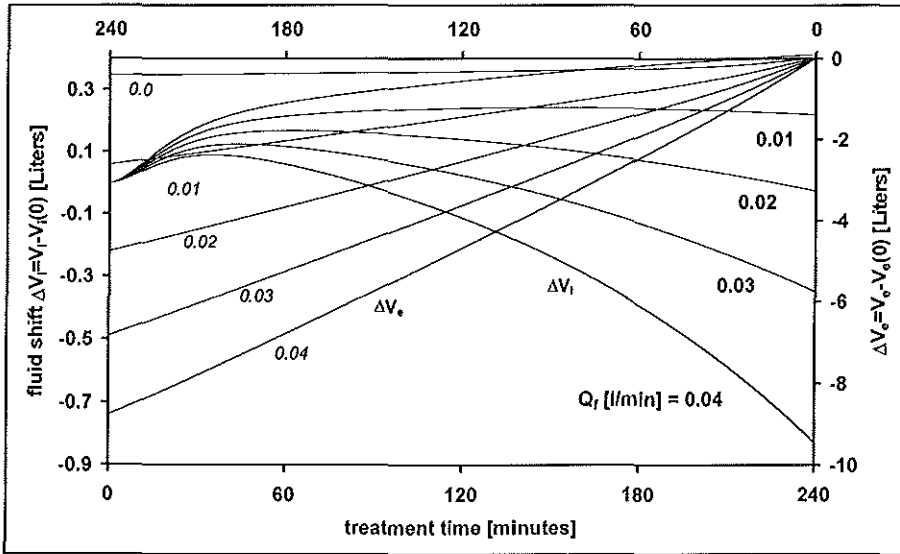
Figure 10.10b: Effect of ultrafiltration on the fluid shift at normal dialysate sodium concentration $C_{di,Na} = 140$ mmol/l.
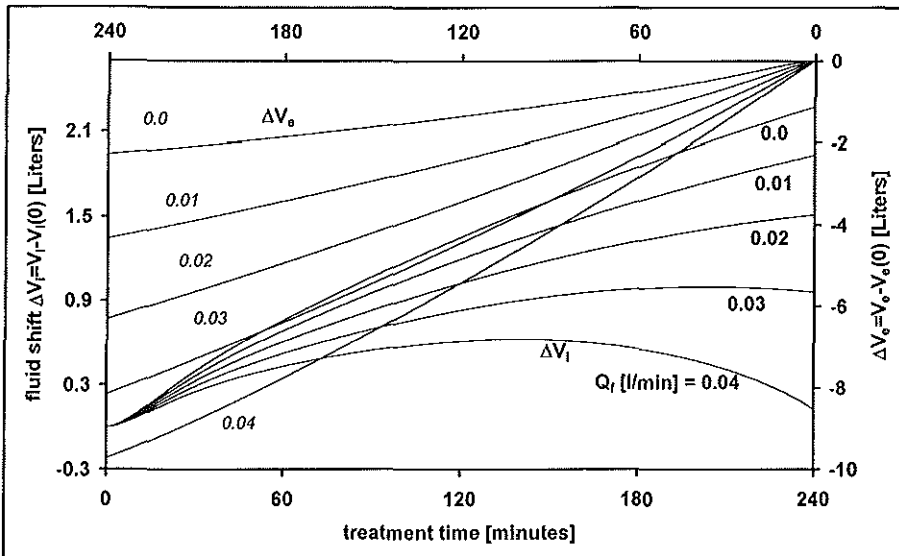
Figure 10.10c: Effect of ultrafiltration on the fluid shift at normal dialysate sodium concentration $C_{di,Na} = 120$ mmol/l.

Table 10.5: The relative changes in V_i, V_e, arterial hematocrit Ht_a or plasma protein concentration C_{pa}, and oncotic pressure Π_p. Dialysis duration t_d=4h. $\Delta Ht_a(t_d)=Ht_a(0)-Ht_a(t_d)$, $\Delta\Pi_p(t_d)=\Pi_p(0)-\Pi_p(t_d)$ with $Ht_a(0)=0.3$ and $C_{pa}(0)=70$ g/l, $\Pi_p(0)=25.63$ mmHg

Q_f [l/min]	$\Delta V_i(t_d)/V_i(0)$ [%]	$\Delta V_e(t_d)/V_e(0)$ [%]	$\Delta Ht_a(t_d)/Ht_a(0)$ [%]	$\Delta\Pi_p(t_d)/\Pi_p(o)$ [%]	$t_{eq.}$ [min] after start
Dialysate sodium concentration $C_{di,Na}$=140 mmol/l				
0	1.48	-2.52	2.59	4.04	insufficient
0.01	0.79	-15.98	19.02	31.91	149
0.02	-0.09	-29.12	41.08	75.65	62
0.03	-1.25	-41.77	71.74	149.77	44
0.04	-2.96	-53.49	115.01	284.51	36
Dialysate sodium concentration $C_{di,Na}$=120 mmol/l				
0	8.11	-13.85	16.08	26.65	insufficient
0.01	6.9	-26.42	35.91	64.71	insufficient
0.02	5.4	-38.48	62.56	125.83	insufficient
0.03	3.4	-49.77	99.07	230.46	202
0.04	0.47	-59.33	145.89	405.08	139
Dialysate sodium concentration $C_{di,Na}$=150 mmol/l				
0	-1.65	2.82	-2.74	-4.19	28
0.01	-2.14	-10.98	12.34	20.13	25
0.02	-2.77	-24.55	32.53	57.79	23
0.03	-3.61	-37.73	60.59	120.89	21
0.04	-4.88	-50.21	100.83	236.15	18

In Table 10.5, the relative changes in V_i, V_e, arterial hematocrit Ht_a or plasma protein concentration C_{pa}, and the colloid osmotic pressure Π_p due to varying rates of ultrafiltration are listed for high, normal and low dialysate sodium concentration. With high dialysate sodium concentration, the fluid shift occurs from V_i to V_e. The size of this fluid shift from V_i to V_e increases as the ultrafiltration flow rates increase. At the same time the intracellular volume decreases more with the higher ultrafiltration flow rates. At zero ultrafiltration, however, fluid shift occurs from V_i to V_e due to high sodium concentration in the plasma. At low dialysate sodium concentration, fluid shift occurs from V_e to V_i. Higher ultrafiltration flow rates result in more decrease in the size of fluid shift from V_e to V_i on one side and more decrease in the plasma volume on the other side. With a normal dialysate sodium concentration, the fluid shift occurs from V_e to V_i at zero ultrafiltration and at a rate of 0.01 l/min. At even larger ultrafiltration flow rates, the fluid shift occurs in the reverse direction.

Arterial hematocrit, plasma protein concentration and oncotic (calculated according to eq.(3.20), Landis-Pappenheimer formula) pressure increase as the ultrafiltration flow rate rises. Our simulations showed that the removal of 2.4 l of ultrafiltrate over a 4 hours of period causes about 16% decrease in the extracellular volume with normal, 11% with high and 26% with low dialysate sodium concentration. In spite of a relative decrease up to above 50% in V_e, sessions with the ultrafiltration flow rates higher than 0.01 l/min may not be tolerated because of high levels in the changes of hematocrit and oncotic pressure. Removal of such ultrafiltration volumes greater than 2.4 l should be better realized with sessions in longer time (slow dialysis).

The hydraulic pressure of the interstitial fluid and the oncotic pressure in the plasma volume are important determinants of the rate of change of plasma volume. The interstitial fluid hydraulic pressure may decrease and even may become more negative if the interstitial volume falls below normal. This may further result in a decreased water shift from interstitial volume to the vascular volume. On the other hand, as the plasma volume decreases, the colloid osmotic pressure increases due to the increased plasma protein concentration retained in the plasma volume. According to Starling's law, the transvascular (and transcellular) pressure difference decreases as the colloid osmotic pressure increases [53], which will result in an increased refilling rate of plasma volume by extravascular fluid because of reverse osmosis. When refilling of the intravascular (plasma) compartment by extravascular fluid does not keep pace with the rate of ultrafiltration flow, a variety of compensatory mechanisms (as acute stimulation of the sympathetic nervous system) come into play to maintain blood pressure.

Our simulations showed that the fluid shift depends on both ultrafiltration flow rate and dialysate sodium concentration. For a specific setting of dialysis session of 4 hours with an urea clearance of $D_u=0.185$ l/min, we calculated the "critical" dialysate sodium concentrations which are necessary for diminishing the fluid shift (zero fluid shift) at different rates of ultrafiltration flow. From Figure 10.11, which suggests a control mechanism that could account for the limitation of dialysis-induced fluid shift, we derived a correlation between the rate of ultrafiltration and the dialysate sodium concentration. In Figure 10.12, these "critical" dialysate sodium concentrations are depicted in relation to the ultrafiltration flow rates. It is very evident that the higher the dialysate sodium concentration, and the lower the rate of ultrafiltration, the smaller the magnitude of fluid shift from V_e to V_i.
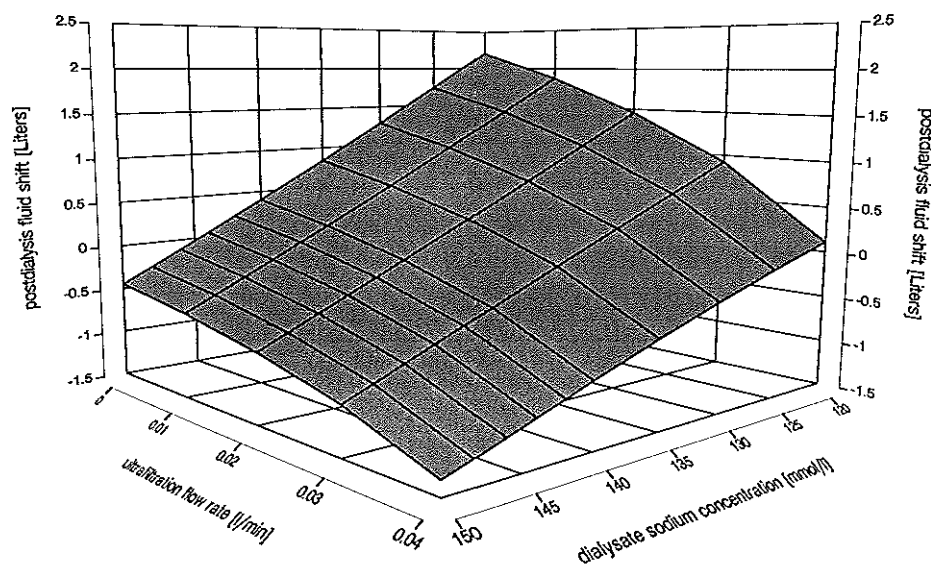
Figure 10.11: Effect of ultrafiltration flow rate Q_f on the changes in ΔV_i at the end (postdialysis) of a modeled dialysis session of 4 hours as a function of different dialysate Na^+ concentration with a fixed urea clearance of 0.185 l/min.
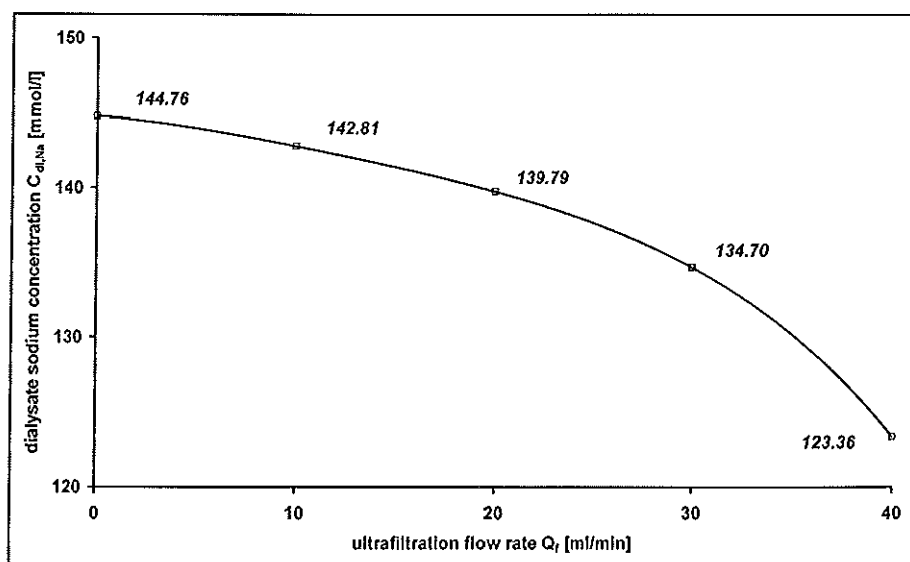
Figure 10.12: Relation between the rate of ultrafiltration flow (Q_f) and the "critical" dialysate Na^+ concentration ($C_{di,Na}$) for minimizing the transcellular fluid shift (See Figure 10.11), for a modeled dialysis session of 4 hours with a fixed dialyzer urea dialysance of 0.185 l/min.

110.4 DISCUSSION AND COMMENTS

Strategies

In particular the dialysis doctor is interested in the question "How can we prevent the conditions which cause a serious fall in the blood pressure during the dialysis ?". This question may be formulated as "How and with which means the dialysis-induced hypotension can be prevented ?" Further, the following questions may form the basic of understanding the sodium and ultrafiltration characteristics towards the improvement of hypotension:

- How (with which model and measurements) can the transport of urea and sodium be accurately predicted during a dialysis treatment ?
- How can the sodium concentration be varied in the dialysate fluid during a dialysis session ?
- How can the effect of varying the sodium concentration in the dialysate on the course of the body volume and the blood pressure be evaluated ?

Many clinical studies have demonstrated the benefits of high sodium concentration in the dialysate fluid [3,10,11,12]. But, it is still not clear, in which measure and to which pattern the sodium concentration has to be administered. In the recent literature, there are lot of examples of different patterns of varying high and low rate of ultrafiltration and sodium concentrations which might be optimal for the individual patients [21,40-48].

Examples of different strategies of sodium administrations are according to De Vries et al [49]:

1. normal sodium concentration of 140 mmol/l,
2. sodium concentration profile between 140 and 150 mmol/l,
3. sodium concentration profile (140-150) and ultrafiltration flow profile from high to low rates.

according to Raja et al [50]:

1. constant ultrafiltration flow rate and constant dialysate sodium concentration (140 mmol/l),
2. sequentially decreasing ultrafiltration flow rates (50%, 30% and 20% in the first, second and third hour of treatment) and constant dialysate sodium concentration,
3. sequentially decreasing ultrafiltration flow rates (50%, 30% and 20% in the first, second and third hour of treatment) and sequentially decreasing dialysate sodium concentration (from 150 to 140 mmol/l),

and according to Acchiardo et al [51] for high-flux dialysis:

1. constant sodium concentration (140 mmol/l),
2. linear decreasing sodium concentration 9% (149 mmol/l),
3. step drop sodium concentration,
4. exponential drop sodium concentration,

with volumetric ultrafiltration control and bicarbonate dialysis fluid.

Refining the sodium modeling

So far, the mathematical description of the mass balance of urea, plasma water and non-urea between body fluid volume and dialyzer was based on a 2-pool volume model where the plasma volume (PV) and interstitial space were lumped together as a single volume, the so called extracellular space. In such models, the transport barriers between interstitium and plasma volume such as vascular wall are not taken into account. From a 2-pool model considering the plasma volume as one (separate) pool and the rest of body fluid volume as the second one, and including transcapillar filtration, Ahrenholz et al [52] was able to calculate the time courses for plasma sodium, total protein concentration and hematocrit during hemodialysis. However, in this model, the osmotic gradient through the cell-membrane which is caused by the decrease of urea concentration was not taken into account. By assuming a 3-pool model of intracellular volume, interstitial space and plasma volume, we have simulated also the sodium and urea kinetic. According to 3-pool model, the plasma volume is taken as a single compartment and the trancapillar pressure difference is taken into account so that the effect of colloid osmotic pressure and hematocrit on the fluid shift is better modeled. (The simulation results are not shown).

Evaluation and atomized controlling the blood volume during a dialysis session

The predictions may be tested by measuring the osmolality and by determining the exact mass balance of both urea and sodium from the hemodialysis patients. The predicted values with regard to the mass balance of urea en sodium may be evaluated by an apparatus which can measure the exact volumes and by continuous sampling the dialysate fluid. An electronic counter may be connected to a balance unit of dialyzing machine and mixing unit of dialysate fluid which 6 ml/min in a 2 liters bag is recycled. The diffusive gradient of sodium may be determined by measuring the concentrations of sodium ions in plasma water and in the dialysate fluid. To measure those concentrations, an ion-selective electrode may be used. Further, the technical requirements for sodium modeling are in principle available [54-64]. Nowadays, all dialyzing machines offer the possibility of adjusting the mixing-pump to achieve different levels of sodium concentration in the dialysate fluid. In the modern machines it is also possible to choose a sodium concentration which changes further during the dialysis time according to a certain pattern. So, by means of measuring the conductivity of blood or dialysate, indirectly the sodium concentration can be measured. The signals representing the sodium concentration can then be feed-backed to the mixing-pump of the dialyzing machine.

Conclusion

We analyzed the influence of dialysate sodium concentration, the rate or amount of ultrafiltration, dialysis duration and urea clearance on the transcellular fluid shift during treatment with modeled dialysis sessions of 1 to 8 hours. The simulation results showed that the magnitude of fluid shift from V_e to V_i decreases with slow dialysis, high sodium

concentration in the dialysate fluid, low rate and amount of ultrafiltration and low rates of urea removal. Refilling of the intravascular volume is faster at high than at low rates of the ultrafiltration flow. To some extend, this reduces the fluid shift from the extracellular into the intracellular fluid compartment. Increasing the dialysate sodium concentration has therefore the greatest effect on the transcellular fluid shift at low rates of ultrafiltration flow. Use of the conventional hemodialysis even with a better sodium modeling is contraindicated for the treatment of patients of serious hemodynamic instability. With slow dialysis, the size of fluid shift decreases. Manipulating the sodium and ultrafiltration profiles during a long duration of treatment (such us CAVHD) is easier than the shorter one. This means that the continuous arterio-venous hemodialysis is a good alternative for patients with serious hemodynamic instability.

10.5 REFERENCES

[1].   Rosa AA, Fryd DS, Kjellstrand CM. Dialysis symptoms and stabilization in long-term dialysis. Arch Int Med 1980; 140: 804-807.

[2].   Henrich WL, Woodard TD, Blachley JD, Gomez-Sanches C, Pettinger W, Cronin RE. Role of osmolality in blood pressure stability after dialysis and ultrafiltration. Kidney Int 1980; 18: 480-488.

[3].   van Stone, Bauer J, Carey J. The effect of dialysate sodium concentration on body fluid distribution during hemodialysis. Trans Am Soc Artif Intern Organs 1980; 26: 383-386.

[4].   Bergström J. Ultrafiltration without dialysis for removal of fluid and solutes in uremia. Clinical Nephrology 1978; 4: 156-164.

[5].   Sherman RA. The pathophysiologic basis for hemodialysis-related hypotension. Seminars in dialysis 1988; 1: 136-142.

[6].   Keshaviah P, Shapiro FL. A critical examination of dialysis-induced hypotension. Am J Kidney Dis 1982; 2: 290-301.

[7].   Daugirdas JT. Dialysis hypotension: A hemodynamic analysis. Kidney Int (1991); 39: 233-246.

[8].   Whele B, Asaba H, Castenfors J, et al Hemodynamic changes during sequential ultrafiltration and dialysis. Kidney Int (1979); 15: 411-418.

[9].   Kooman JP, Gladwuza U, Bocker G, et al Role of the venous system in hemodynamic during ultrafiltration and bicarbonate dialysis. Kidney Int (1992); 42: 718-726.

[10].   Port FK, Johnson WJ, Klass DW. Prevention of dialysis disequilibrium syndrome by use of high sodium concentration in the dialysate. Kidney Int 1973; 3: 327-333.

[11].   Fleming SJ, Wilkinson JS, Greenwood RN, Aldridge C, Baker LRI, Cattell WR. Effect of dialysate composition on intercompartmental fluid shift. Kidney Int 1987; 32: 267-273.

[12].   De Vries PMJM, Kouw PM, Olthof CG, Solf A, Schuenemann B, Oe LP, Quellhorst E, Donker AJM. The influence of dialysate sodium and variable ultrafiltration on fluid balance during hemodialysis. Trans ASAIO 1990; 36: 821-824.

[13].   Kjellstrand C, Rosa A, Shideman J. Hypotension during hemodialysis: Osmolality fall is an important pathogenetic factor. J ASAIO 1980; 3: 11-19.

[14].   Steward WK, Fleming LW, Manuel MA. Benefits obtained by the use of high dialysate

sodium during maintenance haemodialysis. Proc Eur Dial Transplant Assoc 1972; 9: 211-214.

[15].   Sargent JA and Goth FA. Principles and biophysics of dialysis, in Maher JF (ed), Replacement of Renal Function by Dialysis (3rd edition), The Netherlands, Kluwer Academic Publishers, 1989, pp.124-126.

[16].   Sargent JA and Goth FA. Mathematical modeling of dialysis therapy. Kidney Int 1980; 18(suppl 10): 2-10.

[17].   Sancipriano GP, Negro A, Amateis C et al Optimizing Sodium Balance in Hemodialysis. Blood Purif 1996; 14: 115-127.

[18].   Kimura G, Satani M, Kojima S, Kuroda K, Itoh K, Ikeda M. A computerized model to analyze transcellular fluid shift during hemofiltration. Trans ASAIO 1982; 6: 31-36.

[19].   Kimura G, Van Stone JC, Bauer JH, Keshaviah PR. A simulation study on transcellular fluid shifts induced by hemodialysis. Kidney Int 1983; 24: 542-548.

[20].   Kimura G, Van Stone JC, Bauer JH. Prediction of postdialysis serum sodium concentration and transcellular fluid shift without measuring body fluid volumes. Artif Organs 1983; 7: 410-415.

[21].   Kimura G. Quantitative assessment of sodium and water metabolism in hemodialyzed patients. Int J Artif Organs 1989; 12: 744-748.

[22].   Petitclerc T, Man NK, Funck-Brentano LJ. Sodium modeling during hemodialysis. Artif Organs 1984; 8(4): 418-422.

[23].   Locatelli F, Ponti R, Pedrini L, Di Filippo S. Adequate sodium balance and cardiovascular stability. Nephrol Dial Transplant 1990; 5 (suppl 1): 141-143.

[24].   Heineken FG, Evans MC, Keen ML, Gotch FA. Intercompartmental fluid shift in hemodialysis patients. Biotechnology Progress 1987; 3: 69-73.

[25].   Pastan S, Colton C. Transcellular urea gradients cause minimal depletion of extracellular volume during hemodialysis. Trans ASAIO 1989; 35: 247-250.

[26].   Guyton AC. Textbook of Medical Physiology (6th ed). Philadelphia, W.B. Saunders. 1981, p.866.

[27].   Katz MA, Bresler EH. Osmosis, in Staub NA, Taylor AE (eds), Edema, New York, Raven Press, 1984, pp.39-46.

[28].   Levitt DG, Mlekoday HJ. Reflection coefficient and permeability of urea and ethylene glycol in the human red cell membrane. J Gen Physiol 1983; 81: 239-253.

[29].   Schindhelm K, Farrell PC. Patient-hemodialyzer interactions. Trans ASAIO 1978; 24: 357-366.

[30].   Popovich RP, Hlavinka DJ, Bomar JB, Moncrief JW, Decherd JF. The consequence of physiological resistances on metabolite removal from the patient-artificial kidney system. Trans ASAIO 1975; 21: 108-116.

[31].   Stiller S, Mann H. The Donnan effect in artificial kidney therapy. Life Support Systems. 1986; 4: 305-318.

[32].   Colton CK, Henderson LW, ford CA, Lysaght MJ. Kinetics of hemodiafiltration. I. In vitro transport characteristics of a hollow-fiber blood ultrafilter. J Lab Clin Med 1975; 85: 355-370.

[33].   Colton CK, Lowrie EG. Hemodialysis: Physical principles and technical considerations, in Brenner BM, Rector FC (eds). The Kidney (2nd edition), Philadelphia, W.B. Saunders Company, 1981, pp.2465-2471.

[34].   Van Leeuwen, AM. Net cation equivalency ('Base Binding Power') of the plasma proteins. Acta Med Scand 1964; 176 (suppl):922-928.

[35].   Bosch J, Ponti R, Glabman S and Lauer A. Sodium fluxes during hemodialysis. Nephron

1987; 45: 86-92.

[36].   Man NK, Petitclerc T, Tien NQ, Jehenne G, Funck-Brentano JL. Clinical validation of a predictive modeling equation for sodium. Artif Organs 1985; 9: 150-154.

[37]   Shaldon S, Baldamus CA, Beau MC, Koch KM, Mion CM and Lysaght MJ. Acute and chronic studies of the relationship between sodium flux in hemodialysis and hemofiltration. ASAIO Transactions 1983; XXIX: 641-644.

[38].   Gear CW. Numerical initial value problems in ordinary differential equations. Englewood Cliffs. New Jersey, Printice-Hall. 1971.

[39].   Van den Bosch PPJ, Butler H, Soeterboek ARM (eds). Modeling and simulation with Psi/e. Version 1.0. Delft University of Technology, (1989). Boza Automatisering BV, Pijnacker, The Netherlands.

[40].   Dumler f, Grondin G, Levin NW. Sequential high/low sodium hemodialysis: an alternative to ultrafiltration. Trans ASAIO 1979; 25: 351-353.

[41].   Raja RM, Kramer MS, Barber K et al Sequential changes in dialysate sodium during hemodialysis. Trans ASAIO 1983; 29: 649-652.

[42].   Daugirdas JT, Al Kudsi PR, Ing TS et al A double-blind evaluation of sodium gradient hemodialysis. Am J Nephrol 1985; 5: 163-168.

[43].   Chen WT, Ing TS, Daugirdas JT et al Hydrostatic ultrafiltration during hemodialysis using decreasing sodium dialysate. Artif Organs 1980; 4: 187-191.

[44].   Stefoni S, Coli L, Zaca F, Bombardini T, Feliciangeli G, Stagni B, Puddu G, Cianciolo G, Puddu P, Bonomini V. The CMS 08 modulated dialysis. Optimization of dialysis treatment. Contrib Nephrol 1989; 74: 221-230.

[45].   Deuber HJ, Schulz W, Ohrisch G. Clinical application of the sodium modeling computation with CMS 08. Contrib Nephrol 1989; 74: 159-164.

[46].   Van Kuijk WHM, Wirtz JJJM, Grave W, de Heer F, Menheere PPCA, van Hooff JP and Leunissen KML. Vascular reactivity during combined ultrafiltration-haemodialysis: Influence of dialysate sodium. Neprol Dial Transplant (1996) 11: 323-328.

[47].   Mann H, Ernst E, Gladziwa U, Schallenberg U and Stiller S. Changes in blood volume during dialysis are dependent upon the rate and amount of ultrafiltrate. ASAIO Transactions 1989; 35: 250-252.

[48].   Locatelli F, Ponti R, Pedrini L and Di Filippo S. Adequate sodium balance and cardiovascular stabiliy. Nephrol Dial Transplant.Suppl 1. 1990; 141-143.

[49].   De Vries PMJM, Kouw PM, Olthof CG, Solf A, Schuenemann B, Oe LP, Quellhorst E, Donker AJM. The influence of dialysate sodium and variable ultrafiltration on fluid balance during hemodialysis. Trans ASAIO 1990; 36: 821-824.

[50].   Raja RM, Cristoper LP. Plasma refilling during hemodialysis with decreasing ultrafiltration. Influence of dialysate sodium. ASAIO Journal 1994; 40: M423-M425.

[51].   Acchiardo SR, Hayden AJ. Is Na+ modeling necessary in high flux dialysis ? ASAIO Transactions 1991; 37: M135-M137.

[52].   Ahrenholz P, Falkenhagen D, Haeling D, Sitarek U, Foerster J, Nonnemann M, Holtz M, Ernst B, Brown GS, Klinkmann H. Measurements of plasma colloid osmotic pressure, total protein and sodium concentration during hemodialysis: Can single-pool sodium modelling explain the results? Blood Purif 1990; 8: 199-207.

[53].   Dorhout Mees EJ, Koomans HA. Understanding the nephrotic syndrome: What's new in a

decade ? Nephron 1995; 70: 1-10.

[54].   Mann H, Stiller S, Gladziwa U and Konigs f. Kinetic modelling and continuous on line blood volume measurement during dialysis therapy. Nephrol Dial Transplant.Suppl 1. 1990; 144-146.

[55].   De Vries PMJM. Fluid balance during haemodialysis and haemofiltration. The effect of dialysate sodium. Nephrol Dial Transplant.Suppl 1. 1990; 158-161.

[56].   Biasioli S, Petrosino L, Cavallini L, Cesaro A, Fazion S, Zambello A, Foroni R and Mazzali. Cardiovascular stability during the haemodialysis session: Relationship between modelling and impedance parameters. Nephrol Dial Transplant.Suppl 1. 1990; 137-140.

[57].   Sturniolo A, Costanzi S, Barbare G, Ruffini MP, Passalacqua S, Fulignati P and Splendiani G. Computerised Monitoring of sodium and fluid during haemodialysis. Nephrol Dial Transplant.Suppl 1. 1990; 162-164.

[58].   Sanciprinao GP, Negro A, Amateis C, Calitri V, Cantone F, Deabate MC, Della Casa M, Fidelio T, Iacono G, Licata C, Serra A, Sussa I. Optimizing sodium balance in hemodialysis. Blood Purif 1996; 14; 115-127.

[59].   Gotch F, Evans M and Keen ML. Measurement of the effective dialyzer Na diffusive gradient in vitro and in vivo. Trans ASAIO 1985; XXXI: 354-358.

[60].   Gotch F, Evans M, Metzner K, Westphal D, Polaschegg H. An on-line monitor of dialyzer Na and K flux in hemodialysis. Trans ASAIO 1990; 36: M359-M361.

[61].   Goureau Y, Petitclerc T, Man NK. Evaluation of plasma sodium concentration during hemodialysis by computerization of dialysate conductivity. Trans ASAIO 1990; 36: M444-M447.

[62].   De Vries PMJM, Kouw PM, Meijer JH, Oe LP, Schneider H and Donker AJM. Changes in blood parameters during hemodialysis as determined by conductivity measurements. ASAIO Transactions 1988; XXXIV: 623-626.

[63].   Mann H, Stiller S, Schallenberg U, Thoemmes A. Optimizing dialysis by variation of ultrafiltration rate and sodium concentration controlled by continuous measurement of circulating blood volume. Contrib Nephrol 1989; 74: 172-190.

[64].   R Verheij, CSM Veenman, JV den Bakker, WA van Duyl. Comments on the interpretation of tissue impedance measurements during hemodialysis. Blood Purification (1996); 14; 8-14.

10.6 APPENDIX: LISTING OF THE PSI/E MODEL SIMULATION

$C_{e,Na}$	INT	$C_{e,Na}'$	151.1	{V_e sodium concentration}
$C_{e,u}$	INT	$C_{e,u}'$	43.15	{V_e urea concentration}
C_i	INT	C_i'	151.1	{V_i nonurea concentration}
$C_{i,u}$	INT	$C_{i,u}'$	43.15	{V_i urea concentration}
V_e	INT	V_e'	16.40	{extracellular volume}
V_i	INT	V_i'	28.00	{intracellular volume}
$C_{di,Na}$	PAR		140	{dialysate sodium concentration}
C_{pao}	PAR		70	{plasma protein concentration at t=0}
F_w	PAR		0.927	
DP	PAR		1	{dialysis performance index}
G_u	PAR		0.083	
Ht_{ao}	PAR		0.3	{arterial hematocrit at t=0}
K_F	PAR		0.1494	
κ_{Na}'	PAR		1.846	
K_U	PAR		0.800	
Q_{ba}	PAR		0.2 or 0.3	{arterial blood flow rate}
R	PAR		0.00008206	
s	PAR		1.0	
σ_u	PAR		0.95	
T	PAR		310	{temperature}
t_d	PAR		240	{duration of dialysis treatment}
V_{uf}	PAR		2.4	{ultrafiltration volume}
V_{eo}	PAR		16.4	{extracellular volume at t=0}
V_{io}	PAR		28	{intracellular volume at t=0}
α_{Na}	VAR		$1.007-0.0009\cdot(C_{pi}+C_{po})/2$	
$C_{e,Na}'$	VAR		$(D_{Na}\cdot(1-Q_f/Q_w)\cdot(C_{di,Na}-F2)-Q_f\cdot F2)/V_e-V_e'\cdot C_{e,Na}/V_e$	
$C_{e,u}'$	VAR		$(-C_{e,u}\cdot V_e'+F3-V_i'\cdot s\cdot C_{i,u}-F4+G_u)/V_e$	
C_i'	VAR		$(-V_i'/V_i)\cdot C_i$	
$C_{i,u}'$	VAR		$(-K_u/V_i)\cdot(C_{i,u}-C_{e,u})+(s-1)\cdot C_{i,u}\cdot V_i'/V_i$	
C_{pa}	VAR		$C_{pao}\cdot V_{eo}/V_e$	
C_{pi}	VAR		$C_{pa}\cdot Q_{ba}\cdot(1-Ht_a)/(Q_{ba}\cdot(1-Ht_a))$	
C_{pi}	VAR		$C_{pa}\cdot Q_{ba}\cdot(1-Ht_a)/(Q_{ba}\cdot(1-Ht_a)-Q_f)$	
ΔOsm	VAR		$\kappa_{Na}\cdot(C_{e,Na}-C_i)+\sigma_u\cdot(C_{e,u}-C_{i,u})$	{net osmolar gradient}
ΔV_e	VAR		V_e-V_{eo}	{changes in V_e}
ΔV_i	VAR		V_i-V_{io}	{changes in V_i = fluid shift}
D_{Na}	VAR		$D_u\cdot(1-0.96\cdot Ht_a)$	
D_u	VAR		$DP\cdot V_o/t_d$	{urea dialysance}

F2	VAR	$\alpha_{Na} \cdot C_{e,Na}$	
F3	VAR	$K_u \cdot (C_{i,u} - C_{e,u})$	
F4	VAR	$C_{e,u} \cdot (D_u \cdot (1 - Q_f/Q_{ba}) + Q_f)$	
Ht_a	VAR	$Ht_{ao} \cdot V_{eo}/V_e$	
NUgradient	VAR	$\kappa_{Na} \cdot (C_{e,Na} - C_i)$	{nonurea osmolar gradient}
Q_v	VAR	$Q_{ba} \cdot (1 - 0.96 \cdot Ht_a)/F_w$	
Q_f	VAR	V_{uf}/t_d	{ultrafiltration flow rate}
Ugradient	VAR	$C_{e,u} - C_{i,u}$	{urea gradient}
V_e'	VAR	$-V_i' - Q_f$	
V_i'	VAR	$-K_F \cdot R \cdot T \cdot (\kappa_{Na} \cdot (C_{e,Na} - C_i) + \sigma_u \cdot (C_{e,u} - C_{i,u}))$	
V_o	VAR	$V_{io} + V_{eo}$ {patient's volume of urea distribution at=0}	

INT: integral, PAR: parameter, VAR: variable

SUMMARY

Chapter 1:

In this chapter, a short historical background and physical principles of continuous arterio-venous hemofiltration (CAVH), intermittent hemodialysis (IHD) and continuous arterio-venous hemodiafiltration (CAVHD) are viewed. CAVHD was first introduced in the Dijkzigt University Hospital in 1984 by Van Geelen and Vincent. The aims of this thesis are to describe the physical transport processes in CAVHD, to investigate the determinants of blood, ultrafiltration and dialysate flow rates and their influences on the uraemic solute and drugs clearance during CAVHD, to formulate the physical relationships between the hemofilter characteristics and operational quantities, and to access the efficacy of CAVHD compared to intermittent hemodialysis or hemodiafiltration for the treatment of patients with hemodynamic instability.

Chapter 2:

In this chapter, a short overview is given of the clinical problems encountered with conventional intermittent hemodialysis or hemodiafiltration. The indications and contra-indications of CAVHD are outlined. Further in this chapter, the clinical equipment and the guidelines for priming the hemofilter and initiating the CAVHD are reviewed. The most frequent complication is the dialysis-induced hypotension. The most important indication of treatment by CAVHD is the combination of renal failure and circulatory instability. If the extracorporeal circuit interferes with the mobilization of the patient, the CAVHD is contraindicated.

Chapter 3:

In this chapter, the results of feasibility of predicting the hemofilter performance are given. The feasibility of predicting the hemofilter performance was studied by examining the determinants of blood and ultrafiltration flow rates under clinical conditions. In patients who were treated with CAVHD, serial measurements of blood flow rate, blood pressure and ultrafiltration rate were performed, so as to determine the hemofilter resistance (R_f) to blood flow and its hydraulic permeability index (MI). Further, we predicted the blood flow rate circulating the extracorporeal circuit of CAVHD from the manufacturer specifications of the circuit components and from the blood viscosity in each circuit component depending on patient's arterial hematocrit, plasma protein concentration and temperature. During continuous treatments the net ultrafiltrate production was measured at least once every hour and the substitution infusion rate was adjusted accordingly.

Observed hemofilter resistance to blood flow was two to three times higher than the predicted value. To explain this discrepancy we considered clotting of fibers, underestimation of blood viscosity, turbulent flow, additional pressure losses due to the sudden changes in the blood path diameter and deviations of the internal diameter of the fibers. Comparison of the actual blood viscosity with the predicted value showed that blood viscosity was grossly underestimated. Herewith, part (43%) of the discrepancy between measured and predicted values of blood flow rates could be explained. Further the discrepancy between the observed and predicted hemofilter resistance could be explained if the fiber diameter would be 8-10% less than the value given by the manufacturer (See Chapter 4). We observed a logarithmic fall of the ultrafiltration flow rate (Q_f) in time. The fall in Q_f over time may be explained both by changes in the membrane permeability, presumably resulting from protein

adsorption to the membrane, and by a fall in the available membrane surface area, e.g. due to unsuspected clotting of fibers. Under clinical conditions unsuspected clotting of fibers is unlikely to occur during the treatment. Indeed, the hemofilter was clotted just toward the end of the treatment. Therefore, the decrease in membrane permeability with time is more likely to be due to ongoing protein adsorption. Estimating the blood flow rate from patients output such as arterio-venous pressure difference, protein concentration, hematocrit and hemofilter manufacturer specification, is not reliable as far as the hemofilter is concerned.

Chapter 4:
This chapter gives the results of resistance to blood flow and membrane permeability index (MI) measured in a laboratory setting. In laboratory setting, for some of the CAVH(D) capillary hemofilters the resistance to flow was measured with fluid solutions of different viscosity. The hemofilters were perfused with saline, sucrose solution, pig blood and human blood as perfusion fluid. The effect of hemofilter resistance on the hydraulic performance (ultrafiltration) was investigated by measuring the membrane permeability index (MI) and the resistance to (human) blood flow simultaneously over a survival time of about 220 hours.

The resistance of the hemofilter, perfused with saline or a sucrose solution, was 40% higher than expected. Furthermore, it was to some extent flow dependent, suggesting that turbulence does occur, most likely at the hemofilter inlet. When we applied Bernouilli's law to estimate the pressure drop that results from the sudden changes in diameter at the filter inlet and outlet, we calculated a pressure drop of far less than 1 mmHg. On the other hand, a 40% increase in resistance would be explained if the fiber diameter would be a mere 8-10% lower than the given value. With pig blood, the hemofilter resistance to blood flow was 156% higher than expected and it seemed no longer flow dependent, probably indicating that turbulence is diminished by the higher viscosity of blood. Comparison of the actual (pig) blood flow with the value calculated, confirmed our suspicion that we had grossly measured the pig blood viscosity with a (Viscomat) viscometer. The measured average resistance (R_f) to blood flow was 0.16 mmHg/(ml/min) when the hemofilter was perfused with human blood. On considering a fiber diameter 8-10% less than the manufacturer specification (for the AN-69 capillary hemofilter) and using the actual blood viscosity (1.43 times the calculated blood viscosity, see Chapter 3) we overestimated the effective blood flow rate by no more than 20%. With human blood as have observed in the clinic, we observed also a logarithmic fall of the membrane permeability index (MI) in time. According to some investigators the hemofilter hydraulic permeability may fall even after contact with water alone. To our knowledge, however, this finding has not been reproduced by others. For the AN-69 capillary hemofilter we did not observe a fall in hydraulic permeability between 1 and 150 hours of saline perfusion. The resistance to flow of the hemofilters studied was low enough to ensure an adequate blood flow rate in most cases. By using laboratory data on the hemofilter resistance and a more accurate estimation of blood viscosity, a reasonably accurate prediction of blood flow rate under clinical conditions is feasible.

Chapter 5:
In this chapter, a mathematical model of solute and volume transport during CAVHD is introduced. Existing models of conventional hemodialysis are not likely to be useful for the analysis of solute

transport in CAVHD, since solute transport in CAVHD differs from that in intermittent hemodialysis or hemodiafiltration in several respects. The most important differences are 1) With CAVHD, solute transport occurs in the presence of simultaneous diffusion and convection. 2) Dialysate (Q_{di}=10-60 ml/min) and blood (Q_{ba}=50-350 ml/min) flow rates are relative low compared to those in conventional hemodialysis (Q_{di}=500 ml/min and Q_{ba}≥200 ml/min). 3) Ultrafiltration flow rate is not negligible small (Q_f=5-15 ml/min) compared to that in conventional hemodialysis (Q_f≤5 ml/min) and small compared to that in intermittent hemodiafiltration (Q_f= up to 60 ml/min). 4) CAVHD is a continuous technique. With prolonged use of the hemofilter, deterioration of the hemofilter membrane is likely not only to decrease the rate of ultrafiltration flow, but also to impair diffusive permeability.

In view of the shortcomings of previous models, we developed a new mathematical model of CAVHD. We made the following assumptions: 1) All of the hollow fibers in the hemofilter behave as a single capillary tube. 2) The permeability coefficients are constant along the hemofilter length. 3) The flow rates and concentrations are time-independent for a given set of measurements (steady-state). The overall solute mass balance is based on the solute flux (J_s) equation: $J_s=\gamma J_v(f_bC_w+f_dC_d)+K_d(C_w-C_d)$. This model takes into account the local variation of concentration (C_w) in the blood plasma water and dialysate fluid (C_d) as well as the concentration inside the membrane ($f_bC_w+f_dC_d$) in the presence of simultaneous diffusive and convective solute transports, depending on the local ultrafiltration volume flux profile (J_v). In calculating the weighting factors (f_b and f_d) and the overall diffusive mass transfer coefficient (K_d), this model requires an estimation of the resistance of blood (R_b), the resistance of dialysate (R_d), and the resistance of membrane ($R_m=1/P_m$) to diffusion and the solute sieving coefficient (γ), so as to determine the solute clearance in CAVHD. Precise values of the resistance to diffusion of blood, membrane and dialysate can hardly be obtained from clinical data. Therefore, depending on the membrane condition (MI) and the dialysate flow rate (Q_{di}) the precise values of R_b, R_d and $1/P_m$ have to be determined in *in vitro* studies. We therefore made some simplifications (See Chapter 6) in the modeling of solute transport in CAVHD, so as to obtain the overall diffusive mass transfer coefficient (K_d) from clinical data at first and then to analyze the resistances R_b, R_d and $1/P_m$ under different operational and clinical conditions (See Chapter 9).

Chapter 6:
In this chapter, analytical solutions to solute and volume transport in CAVHD are presented in order to calculate the diffusive mass transfer coefficient (K_d) for a solute when blood, filtrate and dialysate flow rates and solute concentrations are known. Next to the assumption we made in Chapter 5, we made the following major assumptions: 4) The solute concentration in the blood (C_w) and in the dialysate (C_d) are 'mixing-cup' concentrations: in radial direction the solute concentrations in blood and dialysate are homogeneously distributed over the respective compartments. 5) The sieving coefficient is 1 (for small solutes such as urea, creatinine and phosphate). Following the assumptions, first we made some simplifications of the ultrafiltration volume flux (J_v) and solute mass flux (J_s) equations. Then, we introduced analytical solutions to solute and volume transport in CAVHD, so as to obtain expressions of the overall diffusive mass transfer coefficient, depending on the ultrafiltration volume flux profile under the following conditions: K_o for zero ultrafiltration volume flux (J_v=0), K_a for a constant (mean) volume flux ($J_v=J_a=Q_f/S$) and K_d for a linear decreasing volume flux ($J_v=\alpha+\beta x$). The relative weighting (convective concentration) factors for blood (f_b) and for dialysate (f_d) equal 0.5.

Summary

The overall mass transfer coefficients are derived from the concentration profiles along the length of hemofilter. Further we derived expressions of solute clearance in relation to the overall mass transfer coefficients K_o, K_a and K_d. By virtue of the expressions of the overall mass transfer coefficients related to solute clearance, the model is well suited for the analysis of diffusive transport in CAVHD. This model can easily be implemented in any spreadsheet.

Chapter 7:

In this chapter, the analytical model is applied to clinical data obtained with 0.6 m² AN-69 capillary hemofilters. The model equations, governing the overall mass transfer coefficients (K_o, K_d and K_a) are evaluated by applying them to data of urea clearance measurements.

The K_d proved to depend on the dialysate flow rate (Q_{di}). As the dialysate flow rate rises from 0.5 l/h to 3 l/h, the overall mass transfer coefficient (K_d) increases curvilinearly. At a dialysate flow rate of about 5 l/h, the K_d reaches a maximal value ($K_d$max). The $K_d$max, obtained by extrapolation, is not dependent on Q_{di}. At relative high values of Q_{fi} and low rates of ultrafiltration flow (Q_f), the overall mass transfer coefficient (K_d) becomes equal to the K_o, which is used for the overall mass transfer coefficient for a dialyzer in intermittent hemodialysis. At relatively high values of Q_{di} and low values of Q_f, the solute concentration profiles along the length of hemofilter seem to be the same as those in the conventional hemodialysis. Also, the calculated mass transfer coefficient K_d shows no significant differences when the ultrafiltration volume flux is assumed to be constant along the length of hemofilter if no back filtration occurs in the hemofilter. With a linear decreasing volume flux model, one can observe the occurrence of back filtration, which with a constant volume flux model is not possible. Our model is a useful addition to the existing models of hemodiafiltration, especially because it allows calculation of the diffusive mass transfer coefficient from the clinical data of CAVHD. It may be used both as a means to further our insight in the determinants of solute transport in CAVHD and to adjust clinical settings, e.g. dialysate flow rate, based on the predicted clearance of uraemic solutes.

Chapter 8:

In this chapter we studied the determinants of uraemic solute clearance in CAVHD. Clearance and its diffusive and convective components of uraemic solutes such as urea, creatinine and phosphate were determined in the region of relative low dialysate flow rates (Q_{di}) at varying blood (Q_{bi}) and ultra-filtration flow rates (Q_f). The degree of conditions in which blood-dialysate solute equilibrium can be achieved was investigated. The diffusive permeability coefficients ($K_s=SK_d$) of urea and phosphate were related to diffusive permeability coefficient of creatinine. Further, by running a simple sensitivity analysis on the overall diffusive permeability coefficient, we analyzed the dependence of K_s on the flow rates and on the strength of concentration driving force at the blood inlet of the hemofilter. The sensitivity analysis provides information about the reliability of predicting the K_s from flow rates and solute concentrations.

Urea clearance increases curvilinearly with ultrafiltration and blood flow rates at relative high rates of the dialysate flow. The convective contribution to urea clearance decreases (slightly) with the increasing rate of the dialysate flow. The diffusive clearance on the other hand increases with increasing rates of the normalized dialysate flow (Q_{di}/Q_f) in a quadratic form. There is a linear relation

between the normalized urea clearance (Cl/Q_f) and the normalized dialysate flow rate (Q_{di}/Q_f) for $Q_{di}/Q_f \leq 3$. This indicates that the removal of urea is only due to the ultrafiltration when blood-dialysate equilibrium is achieved. In contrast to the conventional intermittent hemodialysis, in CAVHD an excellent dialysate-blood equilibration may be achieved by manipulating the dialysate and ultra-filtration flow rates for $Q_{di}/Q_f \leq 3$. Results of our measurements show a curvilinear increase of the diffusive urea clearance with the increasing values of the overall diffusive permeability (K_s). The size of this increase depends strongly on the dialysate flow rate, noting that the overall diffusive permeability coefficient itself depends also on the dialysate flow rate. Under the same operational conditions and hemofilter characteristics, the K_s of urea is 32% greater and the K_s of phosphate is 25% smaller than the K_s of creatinine. Within the operational limits of CAVHD, with the upper values of Q_f=20 ml/min and Q_{di}=60 ml/min, the effect of ultrafiltration on the predicted value of the permeation coefficient is negligible if the condition $Q_{di}/Q_f \geq 3$ is fulfilled. In the region of flows where blood-dialysate saturation occurs (especially for $Q_{di} \leq 3Q_f$), the relative variations in the predicted values of K_s are considerably high (up to 35%). On one side, the sensitivity analysis of K_s shows that calculating the K_s at relative low rates of the dialysate flow in presence of ultrafiltration is not reliable, especially near or at complete blood-dialysate equilibrium. On the other side, the relative low rates of dialysate flow make the CAVHD unique for the treatment of hemodynamically unstable acute dialysis patients. Keeping this controversial fact and the results of this sensitivity analysis in mind, a dialysate flow rate at least 3 times the ultrafiltration flow rate is enough to manipulate the solute removal by diffusion without considering the ultrafiltration.

Chapter 9:

In this chapter we described a numerical computational method for solving the equations governing the mass balance in Chapter 5. The method was applied to the clearance data of uraemic solutes and some antibiotic drugs up to 1500 Daltons and to the data of hemofilter hydraulic condition measured during CAVHD, so as to determine the relative weighting factors of blood (f_b) and dialysate (f_d) solute concentrations contributing the convective uraemic solute transport and the resistances $(R_b + R_m$ and $R_d)$ to diffusion from the overall diffusive mass transfer coefficient (K_d) within the operational limits of CAVHD. Depending on the hemofilter hydraulic condition (MI) and the dialysate flow rates (Q_{di}), the resistance $(R_b + R_m)$ of blood and membrane and the resistance (R_d) of dialysate to diffusion were determined by Wilson's plots. Further, by making use of the capillary pore theory, the diffusive permeation coefficients (K_s) of some antibiotic drugs were related to that of the creatinine so as to predict the clearance of antibiotic drugs from the clearance of creatinine under the same operational conditions and hemofilter characteristics (a prediction model).

Our results show that the length averaged values of factors f_b and f_d equal 0.5 with a variation of maximal 10%, so that the condition "$f_b=f_d=0.5$" for the validation of analytical model is fulfilled. The Wilson's plots allows us both to determine $R_b + R_m$ and R_d separately and to quantify the influence of dialysate flow rate on R_d. There is a fixed relation between the ratio of the K_d of drugs to that of creatinine and the molecular weight of the drugs: If the K_d of creatinine is known, the K_d of drugs can be predicted. This allows us further to predict the clearance of drugs from the clearance of creatinine. Predicting the clearance of drugs from the clearance of creatinine is accurate enough to be used in the clinic.

Summary

Chapter 10:

In this chapter, we introduced a mathematical simulation model of sodium kinetic. By means of such a simulation model, the changes in the concentration of both urea and sodium, the volume, and the osmolality in both the intracellular volume (V_i) and the extracellular volume (V_e) compartments can be predicted during modeled dialysis sessions. We analyzed the influence of dialysate sodium concentration, the rate of ultrafiltration flow, dialysis duration and urea clearance on the transcellular fluid shift during treatment with modeled dialysis sessions.

The simulation results show that the magnitude of intercompartmental fluid shift can be minimized by keeping either the rate and amount of ultrafiltration flow low or by keeping the sodium concentration in the dialysate high and either by prolonging the dialysis treatment time (slow dialysis) or by keeping the rate of urea removal low. Refilling of the intravascular volume is faster at high than at low rates of the ultrafiltration flow. To some extend, this reduces the fluid shift from the extracellular into the intracellular fluid compartment. Increasing the dialysate sodium concentration has therefore the greatest effect on the transcellular fluid shift at low rates of ultrafiltration flow. Use of the conventional hemodialysis even with a better sodium modeling is contraindicated for the treatment of patients of serious hemodynamic instability. With slow dialysis, the size of fluid shift decreases. Manipulating the sodium and ultrafiltration profiles during a long duration of treatment (such as CAVHD) is easier than the shorter one. This means that the continuous arterio-venous hemo-diafiltration is a good alternative for patients with serious hemodynamic instability.

Hoofdstuk 1:

In dit hoofdstuk wordt een overzicht gegeven van de historische achtergrond en de beginselen van continue arterio-veneuze hemofiltratie (CAVH), intermitterende hemodialyse (IHD) en continue arterio-veneuze hemodiafiltratie (CAVHD). CAVHD is in 1984 geïntroduceerd in het Dijkzigt Academisch Ziekenhuis te Rotterdam door Van Geelen en Vincent. De doelstellingen van de onderhavige studie zijn de volgende: het beschrijven van de fysische transportverschijnselen in CAVHD, het bepalen van de determinanten van bloed-, dialysaat- en ultrafiltratiestroomsnelheden en de invloed daarvan op de klaringssnelheden van ureum, kreatinine, fosfaat en drugs tijdens CAVHD, het afleiden van wiskundige relaties tussen de hemofilter-karakteristieken en operationele grootheden, het bepalen van de efficiëntie van CAVHD voor de behandeling van patiënten met hemodynamische instabiliteit in vergelijking met intermitterende hemodialyse of intermitterende hemodiafiltratie.

Hoofdstuk 2:

In dit hoofdstuk is een kort overzicht gegeven van de problemen zoals die in de kliniek kunnen ontstaan tijdens de behandeling met conventionele intermitterende hemodialyse of hemodiafiltratie. De indicaties en contra-indicaties van CAVHD zijn samengevat. De klinische benodigdheden zijn opgesomd en een leidraad is gegeven voor het gebruik van CAVHD. De meest voorkomende complicatie tijdens de dialyse is de veroorzaakte hypotensie. De belangrijkste indicatie voor de behandeling met CAVHD is de combinatie van nierfalen en circulatoire instabiliteit. CAVHD is contra-geïndiceerd als het extracorporele circuit interfereert met de mobilisatie van de patiënt.

Hoofdstuk 3:

In dit hoofdstuk is de theoretische voorspelling gedaan van de prestatie van het hemofilter. De uitvoerbaarheid van continue technieken zoals CAVH en CAVHD hangt sterk af van de werking van het hemofilter welke kan falen door technische storingen of door te lage bloedstroomsnelheid (Q_{bs}). Lage bloedstroomsterkte kan leiden tot excessieve hemoconcentratie welke tot een toename van de bloedstromingsweerstand (R_f) kan leiden, met als gevolg een snelle stolling van het hemofilter. De theoretische voorspelling van de prestatie van het hemofilter is beschreven aan de hand van de bloedstroomsnelheid en ultrafiltratiestroomsnelheid (Q_f) onder klinische omstandigheden. Voor capillaire- en plaathemofilters kan de R_f worden voorspeld met behulp van de wet van Poiseuille en de door de fabrikant opgegeven specificaties. De bloedviscositeit is berekend uit de waarden van het arteriële hematocriet, de eiwitconcentratie en de temperatuur. Om de stromingsweerstand en de hydraulische permeabiliteitsindex (MI) van het hemofilter te kunnen bepalen zijn bij patiënten die werden behandeld met CAVHD metingen uitgevoerd van de bloedstroomsnelheid, de bloeddruk en de ultrafiltratiestroomsnelheid. Gedurende continue hemodialysebehandeling van patiënten is de netto ultrafiltratiestroomsnelheid gemeten over korte tijdsperioden. De infuusstroomsnelheid van de vervangende vloeistof was daarbij ingesteld rekening houdend met het waterverlies van de patiënt.

De waargenomen bloedstromingsweerstand was twee tot drie keer hoger dan de theoretisch voorspelde waarde. Als mogelijke oorzaken van deze discrepantie zijn verondersteld: bloedstolling, onderschatting

Samenvatting

van de bloedviscositeit, turbulentie in de bloedstroom, extra drukverliezen in het hemofilter en afwijkingen van de interne diameter van de vezels t.o.v. de specificaties. Vergelijking van de gemeten bloedviscositeit met de voorspelde waarde toonde aan dat de voorspelde bloedviscositeit veel te laag is. Een belangrijk deel (43%) van de discrepantie tussen de waargenomen en de berekende waarde van R_f kan hiermee worden verklaard. Een deel van de resterende discrepantie zou kunnen worden verklaard door aan te nemen dat de interne diameter van de capillaire vezels 8-10% lager is dan de door de fabrikant opgegeven waarde (Zie Hoofdstuk 4). De voorspelling van de bloedstroomsnelheid uit de gegevens van de patiënt (arterio-veneuze drukverschil, eiwitconcentratie, hematocriet) en uit de specificaties van de componenten van het dialyse circuit is niet betrouwbaar gebleken, voor zover dit het hemofilter zelf betreft. Ideaal voor een goede voorspelling is de continue meting van de bloedstroomsnelheid. Continue meting van Q_{ba} is uit te voeren met een echo-Doppler techniek. Helaas is deze apparatuur niet beschikbaar voor de routinematige klinische dialyse. Als alternatief is de Q_{ba} bepaald door de snelheid te meten van een luchtbelletje dat geïnjecteerd is in de arteriële bloedlijn. Zowel Q_f als MI vertonen als functie van de tijd een logaritmisch verloop. De daling van Q_f wordt veroorzaakt door de daling van de hydraulische permeabiliteit. Deze daling van de hydraulische permeabiliteit wordt waarschijnlijk veroorzaakt door de oplopende eiwitadhesie op het membraan en door de verkleining van het membraan oppervlak als gevolg van bloedstolling. Toch was het hemofilter pas geheel verstopt door bloedstolling tegen het eind van de behandelingsduur. Daarom is het waarschijnlijk dat de daling van MI veroorzaakt wordt door de toename van eiwitadhesie gedurende de behandelingsduur. Een voldoend hoog Q_f indiceert dat het systeem goed functioneert. Een te lage Q_f kan indiceren dat er bloedstolling aan de veneuze zijde van het hemofilter is opgetreden. Wanneer de Q_f onder 200 ml/h is gedaald dan moet het hemofilter worden vervangen.

Hoofdstuk 4:
In dit hoofdstuk worden de resultaten gegeven van de *in vitro* metingen aan het hemofilter betreffende de weerstand (R_f) en de hydraulische permeabiliteitsindex (MI). In een *in vitro* opstelling zijn de R_f-waarden van enkele CAVH(D) hemofilters gemeten. De hemofilters zijn geperfuseerd met oplossingen met verschillende viscositeit, namelijk zoutoplossing, sucroseoplossing, varkensbloed en mensenbloed. Het verloop is gemeten van de permeabiliteitindex (MI) en de weerstand (R_f) van het hemofilter voor mensenbloed gedurende de gebruiksduur van ongeveer 220 uren.

De gemeten weerstand (R_t) van een toevoerslang is in overeenstemming met de berekende waarde. Bij perfusie met een zout- of sucroseoplossing is de weerstand (R_f) van het hemofilter 40% hoger dan de berekende waarde. Bovendien bleek de R_f (eniger mate) afhankelijk te zijn van de stroomsnelheid. Vermoedelijk wordt dit veroorzaakt doordat in de bloedstroom bij de bloedingang van het hemofilter turbulenties optreden. Dit kan echter niet de enige verklaring zijn voor de grote afwijking met 40%. Op grond van de wet van Bernouilli, is uitgerekend hoe groot het drukverlies is bij een vernauwing of verwijding in de diameters van zowel bloed in- als uitgang van het hemofilter. Het berekende drukverlies is slechts in de orde van 1 mmHg. Als de diameter van een vezel 8-10% minder zou zijn dan volgens de door de fabrikant opgegeven waarde, dan voorspelt dit een grotere weerstand met 40%. De R_f van het hemofilter voor varkensbloed was hoger dan de R_f voor zout- of sucroseoplossing. Voor varkensbloed is de discrepantie tussen de gemeten en berekende hemofilter weerstand 156%. Vermoedelijk is de viscositeit van het varkensbloed gemeten met een (Viscomat) viscometer in

vergelijking met de bloedviscositeit in het hemofilter lager. De R_f voor varkensbloed is niet afhankelijk van de bloedstroomsnelheid zoals voor zout- of sucroseoplossing, waarschijnlijk doordat bij grote viscositeit de bloedstroom geen turbulentie vertoont. Bij toevoeging van een hoge dosis heparine aan het varkensbloed is de stromingsweerstand praktisch gelijk aan die voor mensenbloed zoals bepaald in de kliniek. Voor de gemiddelde weerstand van het hemofilter (AN-69 capillaire hemofilter) geperfuseerd met mensenbloed is 0.16 mmHg/(ml/min) gevonden. Wanneer R_f wordt berekend uit de gegevens van de fabrikant, waarbij rekening wordt gehouden met een 8-10% kleinere vezel diameter en de gemeten bloedviscositeit (die een factor 1.43 groter is dan de berekende waarde), dan wordt de Q_{ba} nog altijd met 20% overschat. Evenals in de kliniek verliepen in *de vitro* metingen met varkens- en mensenbloed zowel de Q_f als de MI logaritmisch dalend in de tijd. Voor het AN-69 hemofilter is bij perfusie met zoutoplossing gedurende een periode van 1 tot 150 uren geen vermindering van de hydraulische permeabiliteit gevonden. In de meeste gevallen was de R_f van de onderzochte hemofilters laag genoeg om een voldoend hoge bloedstroomsnelheid te verkrijgen. Uitgaande van de *in vitro* data van de stromingsweerstand en van een verbeterde predictie van de bloedviscositeit is een redelijk nauwkeurige predictie mogelijk van de bloedstroomsnelheid zoals die zich bij klinisch gebruik zal voordoen.

Hoofdstuk 5:

In dit hoofdstuk wordt een mathematisch model voor het massa- en watertransport in CAVHD beschreven. De reeds in de literatuur beschreven modellen van het massatransport voor intermitteren-de hemodialyse of hemodiafiltratie kunnen niet worden gebruikt voor de analyse van het massatrans-port voor CAVHD. Belangrijke verschillen tussen het massatransport bij CAVHD en conventionele hemodialyse zijn: 1) Bij CAVHD vindt het massatransport plaats door diffusie en convectie. 2) De stroomsnelheden van zowel bloed (Q_{ba}=50-350 ml/min) als van dialysaat (Q_{di}=10-60 ml/min) zijn laag in vergelijking met de stroomsnelheden ($Q_{bi}\geq$200 ml/min, Q_{di}=500 ml/min) in conventionele hemodialyse. 3) Bij CAVHD is de stroomsnelheid van ultrafiltratie niet verwaarloosbaar klein (Q_f=5-15 ml/min) zoals dat wel het geval is bij conventionele hemodialyse (Q_f<5 ml/min) terwijl deze klein is in vergelijking met die bij intermitterende hemodiafiltratie (Q_f= tot 60 ml/min). 4) CAVHD is een continue techniek. Door het langdurig gebruik van het membraan, zal, afhankelijk van de hydraulische membraan conditie (MI), de ultrafiltratie-stroomsnelheid (Q_f) in de tijd afnemen, als ook de permeabiliteit voor diffusie.

Voor het beschrijven van het massa- en watertranport bij CAVHD is een nieuw model ontwikkeld. Hierbij zijn de volgende aannamen gedaan: 1) T.a.v. transmembraan massatransport gedragen alle vezels van het capillaire hemofilter zich als een enkele capillaire buis. 2) De permeabiliteit voor zowel ultrafiltratie als voor diffusie is over de gehele lengte van het membraan constant. 3) De stroomsnelhe-den en concentraties zijn constant (steady state).

De totale massabalans is gebaseerd op de massaflux (J_s) vergelijking: $J_s = \gamma\, J_s(f_b C_w + f_d C_d) + K_d(C_w - C_d)$. Bij dit model wordt rekening gehouden met zowel de lokaal variërende concentraties in het bloed-plasmawater (C_w) en in het dialysaat (C_d) als ook de concentratie in het membraan ($f_b C_w + f_d C_d$). Voor de berekening van de gewichtsfactoren (f_b en f_d) en voor de totale massatransfercoëfficiënt (K_d) voor

diffusie dienen wij enerzijds de afzonderlijke waarden van de weerstanden (R_b, R_m en R_d) tegen diffusie en anderzijds de "solute" sievingscoëfficiënt (γ) te kennen. De R_b, R_m en R_d staan respectievelijk voor de weerstand van de bloedlaag, het membraan en de dialysaatlaag voor het massatransport door diffusie. De precieze waarden van R_b, R_m and R_d kunnen niet uit de klinische data worden verkregen. De waarden van R_b, R_d and R_m zijn bepaald in *in vivo* studies op basis van de membraanpermeabiliteits index (MI) en de dialysaatstroomsnelheid (Q_{di}). Eerst is een model ontwikkeld voor het massa- en volumetransport bij CAVHD (Hoofdstuk 6) waarbij de totale massatransportcoëfficiënt (K_d) kan worden bepaald uit de klinisch verkregen data. Later zijn de afzonderlijke waarden van R_b, R_d and R_m onder verschillende werk- en klinische condities bepaald (Hoofdstuk 9).

Hoofdstuk 6:

In dit hoofdstuk worden analytische oplossingen van het massatransport in CAVHD gepresenteerd om daaruit de massatransportcoëfficiënt (K_d) voor diffusie te kunnen afleiden op grond van de stroom-snelheden en concentraties in bloed, filtraat en dialysaat. Voor dat vereenvoudigde model zijn naast de hierboven genoemde aannamen nog de volgende extra aannamen gedaan: 4) De sievingscoëfficiënt is 1. 5) De berekeningen worden gebaseerd op lokale "mixing-cup" concentraties voor de concentratie in het bloed (C_w) en die in het dialysaat (C_d) zodat de radiale gradiënten zowel in het bloed als in het dialysaat niet in de beschouwing zijn betrokken. Teneinde de differentiaalvergelijkingen van het massatransport analytisch te kunnen oplossen en om de formules voor K_d te kunnen afleiden zijn de volgende condities gedefinieerd: K_o voor (zero) ultrafiltratie volumeflux (dichtheid), $J_v = 0$; K_a voor een constante (gemiddelde) volumeflux, $J_v = J_a = Q_f/S$; K_d voor een lineair afnemende volumeflux, $J = \alpha + \beta x$. De gewichtsfactoren voor de bloedconcentratie (f_b) en voor de dialysaatconcentratie (f_d) zijn gelijk aan 0.5. De coëfficiënten (K_o, K_a en K_d) zijn afgeleid uit de concentratieprofielen in de lengte richting van het membraan. Verder worden uit de analytische oplossingen relaties afgeleid tussen de klaringssnel-heid en de coëfficiënten K_o, K_a en K_d. Het model is geschikt voor de analyse van het massa- en water-transport in CAVHD en kan gemakkelijk worden geïmplementeerd in een werkblad voor klinisch gebruik.

Hoofdstuk 7:

In dit hoofdstuk wordt het analytische model toegepast op de klinische gegevens van ureumklaring, verkregen met 0.6 m² AN-69 capillaire hemofilters. De vergelijkingen, betreffende de coëfficiënten voor diffusie (K_o, K_d en K_a) zijn geëvalueerd aan de hand van de ureumklaringssnelheden.

K_d blijkt afhankelijk te zijn van de dialysaatstroomsnelheid (Q_{di}). Het neemt curvilineair toe met de toenemende Q_{di} (van 0.5 tot 4 l/h). De maximale waarde van K_d (dus $K_d$max) die door de waarde van K_d te extrapoleren op $Q_{di} = 5$ l/h is berekend, is niet langer afhankelijk van Q_{di}. Bij grotere Q_{di} is de totale permeabiliteit voor diffusie groter doordat de dialysaatweerstand voor de diffusie kleiner is en doordat het effectieve diffusie oppervlak groter is. Analyse van K_d toont aan dat bij hoge waarden van Q_{di} en bij lage waarden van de ultrafiltrate-stroomsnelheid (Q_f), de K_d van een CAVHD hemofilter overeenkomt met de K_o van een dialyzer in conventionele hemodialyse. Bij waarden van relatief hoge Q_{di}, lage Q_f en lage bloodstroomsnelheid (Q_{wi}) lijken de concentratieprofielen gelijk aan die bij inter-mitterende hemodialyse. Ook de berekende waarden van K_d vertonen geen significante verschillen indien de K_d op basis van een constante volumeflux berekend wordt onder de voorwaarde dat er geen

"back filtration" is. Met een lineair afnemende volumeflux wordt het optreden van "back filtration" uit de volumefluxgrafieken voorspeld. Wij concluderen dat het ontwikkelde model voor CAVHD klinisch bruikbaar is. Het maakt de berekening mogelijk van de massatransport- coëfficiënt (K_d) voor diffusie uit de klaringsdata onder verschillende klinische condities. Ons model vergroot het inzicht in de determinanten van het massatransport in CAVHD. Het biedt de mogelijkheid om de dialysaat- en ultrafiltratiestroomsnelheid in te stellen voor een gewenste ureumklaring.

Hoofdstuk 8:
Bij toepassing van CAVHD is de behandelde patiënt hemodynamisch instabiel. Het is daarom belangrijk het ureum- en waterniveau van de patiënt onder controle te houden door een zo laag mogelijke ureumklaring (Cl) en ultrafiltratiesnelheid (Q_f) in te stellen. In CAVHD vindt het massa-transport plaats door gelijktijdige diffusie en ultrafiltratie. Het manipuleren van het massatransport door diffusie hangt af van de concentraties aan de beide zijden van het hemofilter membraan en van de grootte van de permeabiliteitscoëfficiënt ($K_s = SK_d$) voor diffusie van het totale membraan. In de voorgaande hoofdstukken is aangetoond dat voor manipulatie van het massatransport door diffusie de dialysaatstroomsnelheid (Q_{di}) de belangrijkste factor is. De Q_{di} wordt ingesteld op basis van het ureum-niveau van de individuele patiënt. Toch is vaak niet bekend hoe groot de Q_{di} moet zijn. Volgens klinische ervaring met CAVHD is de snelheid van de dialysaatstroom van 1 1/u toereikend om het ureumniveau van de patiënt onder controle te houden. Bloedstroomsnelheid (Q_{vi}) en ultrafiltratie-stroomsnelheid (Q_f) hangen af van de patiënt en van het extracorporele circuit. De Q_f kan enigszins worden ingesteld door de positie van het hemofilter ten opzichte van het bed van de patiënt te veranderen.

In hit hoofdstuk worden de klaringssnelheden van ureum, kreatinine en fosfaat bestudeerd bij relatief lage dialysaatstroomsnelheden met variërende bloed- en ultrafiltratie-stroomsnelheid. Verder wordt de invloed van Q_{di} en Q_f op de afzonderlijke componenten van ureumklaring door convectie en diffusie beschreven. Ook de condities waaronder een "bloed-dialysaat saturatie" plaats kan vinden, wordt beschreven. De permeabiliteitscoëfficiënten (K_s's) voor diffusie van diverse toxische stoffen als ureum, creatinine en fosfaat worden bestudeerd. In dit hoofdstuk wordt ook een gevoeligheidsanalyse van K_s uitgevoerd voor de variaties in de stroomsnelheden en de concentratiegradiënt in het hemofilter.

Bij relatief hoge snelheden van de dialysaatstroom (Q_{di}) neemt de ureumklaringssnelheid curvilineair toe met toenemende bloed- en ultrafiltratiestroomsnelheid. Met een toename van de dialysaatstroom-snelheid ten opzichte van de ultrafiltratiestroomsnelheid (Q_{di}/Q_f) neemt de diffusiecomponent van ureumklaring curvilineair toe terwijl de convectiecomponent van de ureumklaring enigszins afneemt. Voor $Q_{di}/Q_f \leq 3$ is er een lineaire relatie tussen de genormaliseerde klaringssnelheid (Cl/Q_f) en de genormaliseerde dialysaatstroomsnelheid (Q_{di}/Q_f). Dit toont aan dat, wanneer een bloed-dialysaat evenwicht wordt bereikt, de ureumklaring plaatsvindt door alleen ultrafiltratie. Bij trage dialyse kan saturatie van bloed-dialysaat optreden, vooral bij waarden van Q_{di} dat lager zijn dan die van Q_f. In tegenstelling tot conventionele hemodialyse of hemodiafiltratie kan in CAVHD bloed-dialysaatsatura-tie worden bereikt door de dialysaatstroomsnelheid relatief laag te houden ten opzichte van de ultrafiltratiestroomsnelheid. Het massatransport door diffusie wordt niet alleen beïnvloed door de Q_{di} maar ook door de permeabiliteitscoëfficiënt (K_s) voor diffusie. Onder dezelfde omstandigheden (met

een hemofilterweer stand van 0.24 mmHg/(ml/min)) is de K_s voor ureum 32% groter en de K_s voor fosfaat 25% kleiner dan de K_s voor kreatinine. Volgens de resultaten van de gevoeligheidsanalyse is het berekenen van de permeabiliteitscoëfficiënt (K_s) voor diffusie in een gebied met een relatief lage dialysaatstroomsnelheid (Q_{di}) bij relatief hoge ultrafiltratie, onbetrouwbaar. Naarmate de Q_{di} ten opzichte van ultrafiltratie groter is, des te kleiner zijn de variaties in de K_s. De relatief lage Q_{di} bij de CAVHD maakt dit tot een unieke behandelingsmethode voor acute nierpatiënten die hemodynamisch instabiel zijn. Een dialysaatstroomsnelheid die 3 maal groter is dan de ultrafiltratiestroomsnelheid maakt het mogelijk om het massatransport door diffusie te manipuleren zonder dat met Q_f rekening behoeft te worden gehouden.

Hoofdstuk 9:
In dit hoofdstuk wordt een numeriek rekenmodel uitgewerkt om de vergelijkingen van massabalans in Hoofdstuk 5 op te lossen. De massatransportcoëfficiënten (K_d's) van verschillende stoffen (b.v. antibiotica tot 1500 Daltons) als ook de gewichtsfactoren f_b van bloed- en f_d van dialysaatconcentratie zijn berekend uit de klinisch verkregen data. De massatransportcoëfficiënt voor diffusie (K_d) is gerelateerd aan de membraanpermeabiliteitsindex (MI) en aan de dialysaatstroomsnelheid (Q_{di}). Vervolgens zijn de relatieve bijdragen van het membraan (R_m), het bloed (R_b) en het dialysaat (R_d) aan de totale weerstand ($1/K_d$) in afhankelijkheid van de diffusie berekend. Aan de hand van de zogenaamde Wilson-plots zijn de weerstandswaarde R_b+R_m en de weerstand R_d afzonderlijk bepaald en is de invloed van Q_{di} op R_d gekwantificeerd.

Binnen de grenzen van praktische waarden bij CAVHD wijken de gewichtsfactoren (f_b en f_d) maximaal 10% van hun gestelde waarde 0.5 af. Daarmee is de conditie "$f_b=f_d=0.5$" voor de analytische model-benadering gerechtvaardigd. Er blijkt een relatie te bestaan tussen de verhouding van de K_d van een antibioticum ten opzichte van de K_d van kreatinine en de verhouding van het molecuulgewicht van het antibioticum ten opzichte van het molecuulgewicht van kreatinine. Als de K_d van kreatinine bekend is, dan kunnen de waarden van de K_d van verschillende antibiotica dus worden voorspeld. Vervolgens kunnen de klaringssnelheden van de antibiotica worden voorspeld. Het gebruik van de voorspellingsformule van de K_d van kreatinine tesamen met de verhouding van de K_d van het antibioticum t.o.v. de K_d van kreatinine, levert een klinisch goed bruikbare voorspelling van de klaringssnelheden van de antibiotica op.

Hoofdstuk 10:
Hypotensie is één van de meest voorkomende complicaties tijdens intermitterende hemodialyse of hemodiafiltratie. Een belangrijke factor bij het ontstaan van hypotensie is de daling van het plasma-volume dat door zowel ultrafiltratie als door de ondervulling van het intravasculaire volume wordt veroorzaakt. De ondervulling van het intravasculaire volume wordt veroorzaakt door een waterverschuiving uit het extracellulaire compartiment naar het intracellulaire compartiment. In dit hoofdstuk wordt een model beschreven voor het effect van natriumbehandeling op de waterverschui-ving. Door simulatie met het model kunnen de tijdsveranderingen in volumes en concentraties, zowel van natrium als van ureum en de osmolaire gradiënten in zowel extracellulaire als intracellulaire compartimenten worden gevolgd. Met dit simulatiemodel wordt de invloed van de natriumconcentra-tie in het dialysaat, de ultrafiltratiestroomsnelheid, de klaringssnelheid van ureum en de dialyse

behandelingsduur op de intercompartimentele waterverschuiving onderzocht.

Bij hoge ultrafiltratiesnelheid ontstaat een snellere "refilling" van het intravasculair compartiment, waardoor de waterverschuiving naar intracellulair al enigszins wordt beperkt. Verhoging van de natriumconcentratie in het dialysaat heeft daarom bij een lage ultrafiltratiesnelheid grote invloed op de transcellulaire waterverschuiving. Resultaten met het simulatiemodel tonen aan dat de door de dialyse veroorzaakte intercompartimentele waterverschuiving kan worden geminimaliseerd door de ultrafiltratiestroomsnelheid laag of de natriumconcentratie in het dialysaat hoog te houden en door de dialyse behandelingsduur te verlengen of de ureumklaringssnelheid te verlagen. De conventionele intermitterende hemodialyse en intermitterende hemodiafiltratie worden contra-geïndiceerd als de patiënt hemodynamisch instabiel is. Door de dialyse behandelingsduur te verlengen ("slow dialysis") neemt de grootte van de waterverschuiving af. Om een gewenst profiel te handhaven is het manipuleren van de natriumconcentratie in het dialysaat en de ultrafiltratiesnelheid gemakkelijker bij een lange (zoals in CAVHD) dan bij een korte dialyse behandelingsduur. Dit betekent dat CAVHD een goed alternatief is voor de behandeling van patiënten met hemodynamische instabiliteit voor de intermitterende hemodialyse of hemodiafiltratie.

Abbreviations

Symbol	Explanation	Units
ARF	acute renal failure	
BWG	body weight-gain	[l] or [Kg]
BUN	blood urea nitrogen	
CAVH	continuous arterio-venous hemofiltration	
CAVHD	continuous arterio-venous hemodiafiltration	
C_d	local solute concentration in dialysate compartment	[mmol/l]
C_{di}	solute concentration at dialysate inlet	[mmol/l]
C_{do}	solute concentration at dialysate outlet	[mmol/l]
C_f	solute concentration in ultra filtrate	[mmol/l]
Cl	solute clearance in general	[ml/min]
Cl_c	convective component of solute clearance in CAVHD	[ml/min]
Cl_C	convective contribution to solute clearance in hemodialysis	[ml/min]
Cl_d	diffusive component of solute clearance in CAVHD	[ml/min]
$C_{di,Na}$	sodium concentration at the dialysate inlet	[mmol/l]
$C_{di,u}$	urea concentration at the dialysate inlet	[mmol/l]
$C_{do,Na}$	sodium concentration at the dialysate outlet	[mmol/l]
$C_{do,u}$	urea concentration at the dialysate outlet	[mmol/l]
Cl_D	pure diffusive clearance in the absence of ultrafiltration	[ml/min]
$C_{e,u}$	extracellular urea concentration	[mmol/l]
$C_{e,Na}$	extracellular sodium concentration	[mmol/l]
C_i	intracellular nonurea solute concentration	[mmol/l]
$C_{i,u}$	intracellular urea concentration	[mmol/l]
C_m	effective local solute concentration describing the convective contribution to total solute flux (in membrane)	[mmol/l]
C_{md}	local solute concentration at membrane-dialysate interface	[mmol/l]
C_p	local concentration of plasma proteins	[g/dl]
C_{pa}	concentration of arterial plasma proteins	[g/dl]
C_{pi}	blood inlet concentration of plasma proteins	[g/dl]
C_{pl}	solute concentration in arterial blood plasma	[mmol/l]
C_{pm}	mean concentration of plasma proteins	[g/dl]
C_{pn}	normalized plasma protein concentration	[g/dl]
C_{po}	blood outlet concentration of plasma proteins	[g/dl]
CRF	chronic renal failure	
C_w	local solute concentration in blood plasma water	[mmol/l]
C_{wi}	solute concentration in plasma water at blood inlet	[mmol/l]
C_{wm}	local solute concentration in plasma water at blood-membrane interface	[mmol/l]
C_{wo}	solute concentration in plasma water at blood outlet	[mmol/l]

Abbreviations

Symbol	Explanation	Units
d	internal diameter of any segment of the CAVHD circuit	[m]
d_{aa}	internal diameter of arterial access (catheter + tubing)	[m]
d_{ac}	internal diameter of arterial access catheter	[m]
d_{at}	internal diameter of arterial access tubing	[m]
d_b	thickness of blood concentration boundary layer	[μm]
d_d	thickness of dialysate concentration boundary layer	[μm]
d_m	thickness of membrane	[μm]
d_{vc}	internal diameter of venous catheter	[m]
d_{vt}	internal diameter of venous tubing	[m]
D	free diffusion coefficient in water	[m²/min]
D_b	effective diffusion coefficient in blood	[m²/min]
D_d	effective diffusion coefficient in dialysate	[m²/min]
d_f	internal diameter of a fiber	[μm]
d_i	internal diameter of the segment (i) of any circuit element	[m]
D_u	urea dialysance (clearance)	[l/min] or [ml/min]
D_{Na}	sodium dialysance	[l/min] or [ml/min]
d_m	thickness of membrane or fiber wall	[μm]
D_m	effective diffusion coefficient in membrane	[m²/min]
DP	dialysis (dialyzer) performance index	
d_{va}	diameter of venous access (tubing + catheter)	[m]
dx	differential length	[m]
dt	differential time	[min] or [hrs]
e_v	friction loss factor	
f	fractional volume distribution of solute in blood cells	
f_b	weighting factor of solute concentration in blood to convective transport	
f_d	weighting factor of solute concentration in dialysate to convective transport	
f_f	friction factor	
F_w	correction factor for plasma water	
G_u	urea generation rate	[mmol/min]
h	slope, variation coefficient	
h_{bc}	blood channel half-height	[m]
h_c	height of fluid column in ultrafiltration line	[cm]
HD	conventional hemodialysis	
Ht	local hematocrit	
Ht_a	arterial hematocrit	
Ht_i	hematocrit at blood inlet	
Ht_o	hematocrit at blood outlet	
IHD	Intermittent hemodialysis	

Abbreviations

Symbol	Explanation	Units
J_a	mean (constant) ultrafiltration volume flux (density)	[µm/min]
J_s	local transmembrane solute flux (density)	[µmol/(min·m^2)]
J_v	local ultrafiltration or transmembrane volume flux (density)	[µm/min]
K_a	overall mass transfer coefficient for a constant volume flux	[µm/min]
K_d	overall mass transfer coefficient or effective diffusive permeability	[µm/min]
K_{dc}	overall mass transfer coefficient for creatinine	[µm/min]
$K_d$max	maximum value of the overall mass transfer coefficient	[µm/min]
K_f	whole body ultrafiltration coefficient	[l·Atm/mmol°K]
K_o	overall mass transfer coefficient for $J_v = 0$	[µm/min]
K_s	diffusive permeability coefficient or index = SK_d	[ml/min]
K_u	urea transcellular diffusion coefficient	[ml/min]
L	length of any CAVHD circuit element	[m]
L_{aa}	length of arterial access components	[m]
L_{ac}	length of arterial access catheter	[m]
L_{at}	length of arterial access tubing	[m]
L_c	effective length of blood channels	[m]
L_f	effective length of hemofilter	[m]
L_i	length of i-th segment of extracorporeal circuit	[m]
L_p	membrane hydraulic permeability	[µm/(min·mmHg)]
L_{va}	length of venous access (tubing + catheter)	[m]
L_{vc}	length of venous access catheter	[m]
L_{vt}	length of venous access tubing	[m]
MAP	mean arterial blood pressure	[mmHg]
MI	hydraulic permeability index	[ml/(h·mmHg)]
MVP	mean venous blood pressure	[mmHg]
MW	molecular weight	[Daltons]
n	number of measurements or number of data points	
N	number of fibers	
N_c	number of blood channels	
P_b	local hydrostatic or hydraulic pressure in blood compartment	[mmHg]
P_b^e	effective blood pressure in blood compartment	[mmHg]
P_{bi}	prefilter hydrostatic or hydraulic blood pressure	[mmHg]
P_{bo}	postfilter hydrostatic or hydraulic pressure	[mmHg]
P_d	(average or mean) hydrostatic pressure on dialysate compartment	[mmHg]
P_{di}	dialysate pressure at dialysate inlet	[mmHg]
P_{do}	dialysate pressure at dialysate outlet	[mmHg]
P_{ia}	intra-arterial blood pressure	[mmHg]
P_{iv}	intra-venous blood pressure	[mmHg]

Abbreviations

Symbol	Explanation	Units
P_m	diffusive solute permeability of membrane	[μm/min]
Q_b	local blood flow rate	[ml/min]
Q_{ba}	measured arterial blood flow rate	[ml/min]
Q_{be}	effective blood flow rate circulating hemofilter	[ml/min]
Q_{bi}	blood flow rate at blood inlet = $(1-Ht_a)Q_{ba}+Q_{pred}$	[ml/min]
Q_{bo}	blood flow rate at blood outlet = $(1-Ht_a)Q_{ba}+Q_{pred}-Q_f$	[ml/min]
Q_d	local dialysate flow rate	[ml/min]
Q_{di}	flow rate of dialysate at dialysate inlet	[ml/min]
Q_{do}	flow rate of dialysate at dialysate outlet = $Q_{di}+Q_f$	[ml/min]
Q_{dra}	flow rate of drug administration	[ml/h]
Q_{dfm}	flow rate of desired fluid loss	[ml/h]
Q_f	(net) flow rate of ultra filtrate	[ml/min]
Q_h	flow rate of heparin administration	[ml/min]
q_k	discriminant	
Q_k	dummy flow rate (= Q_{vi} for k=1 and = Q_{do} for k=2)	[ml/min]
Q_{pred}	flow rate of substitution fluid (predilution)	[ml/min]
Q_{ul}	flow rate of urine loss	[ml/h]
Q_v	local flow rate of plasma water	[ml/min]
Q_{vi}	plasma water flow rate at blood inlet	[ml/min]
Q_{vo}	plasma water flow rate at blood outlet = $Q_{vi}-Q_f$	[ml/min]
R	gas constant	
R^2	square of the sum of residues	
R_{aa}	measured resistance of arterial access to blood flow	[mmHg·min/ml]
$R_{aa,p}$	predicted resistance of arterial access to blood flow	[mmHg·min/ml]
R_b	resistance of blood boundary layer to diffusion	[min/μm]
R_d	resistance of dialysate boundary layer to diffusion	[min/μm]
r	radial coordinate	[m]
r_f	inner radius of fiber	[μm]
r_c	molecular radius of creatinine	[Å]
R_e	Reynold number	
R_f	measured resistance of hemofilter to blood flow	[mmHg·min/ml]
$R_{f,p}$, $R_{f,p}$	predicted resistance of hemofilter to blood flow	[mmHg·min/ml]
R_i	resistance to blood flow of i-th segment of extracorporeal circuit	[mmHg·min/ml]
r_s	molecular radius	[Å]
R_m	resistance of membrane to diffusion = $1/P_m$	[min/μm]
$R_{n,aa}$	normalized resistance of arterial access to blood flow	[10^5/ml]
$R_{n,va}$	normalized resistance of venous access to blood flow	[10^5/ml]

Abbreviations

Symbol	Explanation	Units
$R_{n,f}$	normalized resistance of hemofilter to blood flow	$[10^5/\text{ml}]$
$R_{n,i}$	normalized resistance of segment (i) of dialysis circuit to blood flow	$[10^5/\text{ml}]$
r_p	radius of membrane pore	$[\text{Å}]$
$R_{t,p}$	predicted total resistance to blood flow	$[\text{mmHg·min/ml}]$
R_t	measured total resistance to blood flow	$[\text{mmHg·min/ml}]$
R_{td}	total resistance to diffusion $= 1/K_d$	$[\text{min}/\mu\text{m}]$
$R_{va,p}$	predicted resistance of venous access to blood flow	$[\text{mmHg·min/ml}]$
R_{va}	measured resistance of venous access to blood flow	$[\text{mmHg·min/ml}]$
s	urea transcellular sieving coefficient	
S	effective surface area of hemofilter	$[\text{m}^2]$
S_b	cross sectional area of wide part of a circuit element	$[\text{m}^2]$
SK_a	overall permeation coefficient for a constant $J_v = J_a = Q_f/S$	$[\text{ml/min}]$
SK_d	overall permeation coefficient for $J_v = \alpha + \beta x$	$[\text{ml/min}]$
SK_o	overall permeation coefficient for $J_v = 0$	$[\text{ml/min}]$
S_s	cross sectional area of narrow part of a circuit element	$[\text{m}^2]$
t	treatment time	[hour (h, hr)]
t_d	duration of dialysis treatment	[hour (h, hr)]
$t_{eq.}$	equilibrium time	[min]. or [h]
T	temperature	[°Celsius]
TMP	local transmembrane pressure difference or gradient	[mmHg]
TMP_i	transmembrane pressure difference at blood inlet	[mmHg]
TMP_m	mean transmembrane pressure difference	[mmHg]
v_e	friction loss factor	
V_i	intracellular volume	[l]
V_e	extracellular volume	[l]
V_o	predialysis patient's volume distribution of urea (at t=0)	[l]
v_m	average longitudinal fluid velocity	[m/s]
V_{UF}	ultrafiltration volume	[l]
w	membrane width (= S/L)	[m]
w_c	blood channel width	[m]
x	axial coordinate or position of hemofilter or dialyzer	[m]
y	dummy length variable or function	

Greek letters

α	ultrafiltration volume flux at blood inlet	$[\mu\text{m/min}]$
α_j	ratio of measured to the predicted resistance to blood flow	
α_{Na}	Donnan factor (ratio) for dialyzer plasma water sodium	

Abbreviations

Symbol	Explanation	Units
β	slope or dummy variable	
γ	apparent sieving coefficient	
$\Delta\Pi_P$	change in oncotic pressure	[mmHg]
$\Delta\Pi_P(t_d)$	postdialysis change in oncotic pressure	[mmHg]
ΔC	local concentration gradient = $C_w - C_d$	[mmol/l]
ΔHt_a	change in arterial hematocrit	
$\Delta Ht_a(t_d)$	postdialysis change in arterial hematocrit	
ΔK_s	variation, error in K_s	[ml/min]
$\Delta K_s/K_s$	relative variation of K_s or relative error in K_s	
ΔM	difference in mass transfer rate at blood inlet	[μmol/min]
$\Delta osm.$	net osmolar gradient	[mOsm/l]
ΔP	pressure loss	[mmHg]
ΔP_b	pressure drop in blood compartment	[mmHg]
δP_b^e	total pressure drop in blood compartment per unit length	[mmHg]
ΔP_b^e	total pressure drop in blood compartment	[mmHg]
δP_d	pressure drop in dialysate compartment per unit length	[mmHg]
ΔP_d	pressure drop in dialysate compartment	[mmHg]
ΔX	variation, error in X (X=Q_f, Q_{wi}, Q_{di}, C_{wi}, C_{do})	[ml/min]
ΔV_e	change in V_e	[l]
$\Delta V_e(t_d)$	postdialysis change in V_e	[l]
ΔV_i	fluid shift, change in V_i	[l]
$\Delta V_i(t_d)$	postdialysis fluid shift	[l]
Δx	difference length	[m]
η_{aa}	blood viscosity in arterial access	[mmHg·min]
η_b	local blood viscosity	[mmHg·min]
η_{bi}	blood viscosity at blood inlet	[mmHg·min]
η_{bo}	blood viscosity at blood outlet	[mmHg·min]
η_d	local dialysate viscosity	[mmHg·min]
η_i	blood viscosity of i-th segment of extracorporeal circuit	[mmHg·min]
η_p	local plasma viscosity	[mmHg·min]
η_{pn}	normal plasma viscosity = 1.54×10^{-7} mmHg min	[mmHg·min]
η_{va}	blood viscosity in venous access	[mmHg·min]
η_w	local plasma water viscosity	[mmHg·min]
θ_b	Péclet number for blood boundary layer	
θ_d	Péclet number for dialysate boundary layer	
θ_m	Péclet number for membrane	
θ_o	observed Péclet number	
θ_t	total Péclet number	

Abbreviations

Symbol	Explanation	Units
κ_{Na}	molar to osmolar concentration conversion factor	
λ	dummy variable	
Π_p	local colloid osmotic or oncotic pressure	[mmHg]
Π_{pi}	oncotic pressure at blood inlet	[mmHg]
Π_{pm}	mean oncotic pressure	[mmHg]
Π_{po}	oncotic pressure at blood outlet	[mmHg]
ρ	fluid density	[kg/m³]
σ	fractional volume distribution of solute in blood cells	[l/g]
σ_u	transcellular reflection coefficient for urea	
$\partial K_s/\partial X$	variation of K_s with respect to variable X	

1- HH Vincent, E Akcahuseyin, MC Vos, FJ van Ittersum, WA van Duyl, MADH Schalekamp. Determinants of blood flow and ultrafiltration in continuous arteriovenous haemodiafiltration: Theoretical predictions and laboratory and clinical observations. *Nephrology dialysis and Transplantation. (1990); 5: 1031-1037.*

2- HH Vincent, FJ van Ittersum, E. Akcahuseyin, MC Vos, W.A. van Duyl, MADH Schalekamp. Solute transport in continuous arteriovenous hemodiafiltration: A new mathematical model applied to clinical data. *Blood Purification. (1990); 8: 149-159.*

3- E Akcahuseyin, HH Vincent, FJ van Ittersum, WA van Duyl, MADH Schalekamp. A Mathematical model of continuous arteriovenous hemodiafiltration (CAVHD). *Computer Methods and Programs in Biomedics. (1990); 31: 215-224.*

4- E Akcahuseyin, HH Vincent, MC Vos, WA van Duyl. Continue arterio-veneuze Haemodiafiltratie (CAVHD). *Klinische Fysica. (1991); 93: 196-198.*

5- HH Vincent, E Akcahuseyin, MC Vos, WA van Duyl, MADH Schalekamp. Continuous arteriovenous hemodiafiltration: Filter design and blood flow rate. *Contribution to Nephrology. (1991); 93: 196-198.*

6- E Akcahuseyin, HH Vincent, MC Vos, WA van Duyl. Continuous arterio-venous hemodiafiltration (CAVHD): A mathematical model of solute transport. Commission of The European Comm. *1st European Conference on Biomedical Engineering.(1991); 13: 18-19.*

7- HH Vincent, MC Vos. The use of continuous arteriovenous hemodiafiltration in multiple organ failure patients. *Applied Cardiopulmonary Pathophysiology. (1991); 4: 109-116.*

8- HH Vincent, MC Vos, E Akcahuseyin, WA van Duyl, MADH Schalekamp. Blood flow, ultrafiltration and solute transport rate in continuous arteriovenous haemodiafiltration: The AN-69 Flat-Plate Haemofilter. *Nephrology Dialysis Transplantation. (1992) 7: 29-34.*

9- HH Vincent, MC Vos, E Akcahuseyin, WHF Goessens, WA van Duyl, MADH Schalekamp. Drug clearance by continuous arteriovenous hemodiafiltration (CAVHD). Analysis of sieving coefficients and mass transfer coefficients of diffusion. *Blood Purification (1993); 11: 99-109.*

10-   E Akcahuseyin, WA van Duyl, MC Vos, HH Vincent, MADH Schalekamp. Continuous arterio-venous hemodiafiltration (CAVHD): A sensitivity analysis of uraemic solute clearance and diffusive permeability coefficient at low dialysate flows. *Medical Biological Engineering & Computing. (1995); (submitted).*

11-   E Akcahuseyin, WA van Duyl, MC Vos, HH Vincent. An analytical solution to solute transport in continuous arterio-venous hemodiafiltration (CAVHD). *Biomedical Engineering and Physics (1996); 18 (1): 26-35.*

12-   R Verheij, CSM Veenman, JV den Bakker, WA van Duyl. Comments on the interpretation of tissue impedance measurements during hemodialysis. *Blood Purification (1996); 14: 8-14.*

13-   E Akcahuseyin, WA van Duyl, MC Vos, HH Vincent, MADH Schalekamp. Bulk mass transport during continuous arterio-venous hemodiafiltration (CAVHD): Analysis of resistance to diffusion. *Biomedical Engineering and Physics. (1996), (submitted).*

14-   E Akcahuseyin, WA van Duyl, MC Vos, HH Vincent, MADH Schalekamp. Hydraulic and diffusive permeability index of an "AN-69 Capillary hemofilter. *Medical Biological Engineering & Computing. (1996) (in press).*

15-   E Akcahuseyin, HH Vincent, WA van Duyl, MC Vos, MADH Schalekamp. A simulation study of the effect of ultrafiltration, dialysate sodium concentration, treatment time and urea clearance on the transcellular fluid shift. *Blood Purification. (1996), (in preparation).*

All published material has been used in this thesis with the permission of the original source.

Zonder iemand te kort te willen doen, zou ik graag de volgende personen danken voor hun commentaar en kritisch lezen, voor hun aandel, voor hun wetenschappelijke en niet-wetenschappelijke stuen en interesse bij het totstandkomen van dit proefschrift:

Prof. Dr. M.A.D.H. Schalekamp (Interne Geneeskunde I)
Dr. Ir. W.A. van Duyl (Opstetrie en Gynaecologie)
Prof. Dr. W. Weimar (Interne Geneeskunde I)
Prof. Dr. Ir. C. Ince (Experimentele Anesthesiologie, AMC Amsterdam)
Prof. Dr. R.M. Heethaar (Medische Fysica en Informatica, VU Amsterdam)

Dr. H.H. Vincent (Interne Geneeskunde, AZ Nieuwegein)
Prof. Dr. E.J. Dorhout Mees (Nefroloji Ana Bilim Dalı, Ege Üniversitesi İzmir)
Prof. Dr. H.A. Bruining (Algemene Heelkunde)
Prof. Dr. A.J. Man In T Veld (Interne Geneeskunde I)
Prof. Dr. A.C. Drogendijk (Opstetrie en Gynaecologie)

Dr. M.C. Vos (Bacteriologie)
Prof. Dr. Ir. C.J. Snijders (Biomedische Natuurkunde en Technologie)
Dr. H.M. Buyruk (Revalidatie)
Dr. M.W.J.A. Fieren (Interne Geneeskunde I)
Ing. J.V. de Bakker (Biomedische Natuurkunde en Technologie)
Mw. I. Buyruk-Burggraaf (Brussel, België)
Dr. J.N.A.L. Leijnse (Biomedische Natuurkunde en Technologie)

Dr. Ir. W.A. van Duyl, klinisch fysicus, was mijn co-promotor. Beste Wim, ik wil je bedanken voor jouw begeleiding in dit samenwerkingsproject. Je bent een co-promotor van onschatbare waarde geweest. Je hebt voorkeur voor het klinisch georienteerde fysisch onderzoek. Ondanks dat je van huis uit een elektrotechnicus bent, konden wij samen ook in medische transportfysica heleboel doen. Je hebt mij de smaak van toegepaste wetenschap in het medische gebeuren laten proeven. Voor de mogelijkheid die je mij gaf om zelfstandig onderzoek te kunnen doen en jouw aandacht voor ook niet-wetenschappelijk leven en in het bijzonder voor jouw geduld voor elk nieuw versienummer van mijn artikelen en hoofdstukken dank ik je van harte.

Dr. H.H. Vincent, nefroloog, is mijn projectleider van het klinisch onderdeel van dit onderzoek geweest. Beste Jeroen, je bent als initiator van dit onderzoek en als "de man" van CAVHD een leider geweest van onschatbare waarde. Toen ik op Wim's deur klopte en hem vroeg of ik misschien voor hem wat kon betekenen voor een biomedisch onderzoek, gaf hij mij een stuk papier met jouw "fysische" vragen er op aangetekend. Je tekende de concentratieprofielen in CAVHD en vroeg waarom ze niet dezelfde zijn als die in de hemodialyse, keurig met de formules erbij. Ik wist toen dat de fysica jou niet vreemd was, maar ik kon jouw handschrift moeilijk lezen. Zo zijn wij met het onderzoek begonnen. Vaak belde je mij op en

zei "Emin, luister eens, volgens Pallone is de K_d ...". Ik moest dan snel een antwoord geven. Als ik even naar de bibliotheek ging en je kon mij niet bereiken, dan zag ik je meteen in Wim's kamer naar mij vragen. Daarom moest ik van jou altijd een "pieper" dragen. Dankzij jouw disciplineaire aanpak en jouw wil om snel en nauwkeurig tot een resultaat te komen, is dit proefschrift totstandgekomen. Voor mijn wetenschappelijke en niet-wetenschappelijke problemen stond en sta je altijd klaar, ook als Stefanie even ziek was, waarvoor mijn dank van harte.

Dr. M.C. Vos, mijn arts collega was gedurende enige tijd belast met het klinische deel van het zelfde onderzoek. Beste en lieve Greet, net als stond in jouw dankwoord, waren de discussies over van alles en nog wat met jou wat mij betreft ook heerlijk. Meestal was het al zes uur geweest. Je kwam naar de 16de etage en bracht de slangen, injectienaalden, hemofilters of Lotus data diskettes mee en zei glimlachend "Hoi Emin ..." en begon je eerst even naar huis te bellen of Hans de aardappels wilde schillen zodat wij de transportfysica konden bestuderen. Jouw stimulerende harde werken en vooral gezellige collegiale sfeer waren de basis waarop wij allemaal in teamverband heel goed konden functioneren, waarvoor mijn dank van harte.

Collega's Ir. L.M. Kosterman (Martin), Ir.B.E. Westerhof (Berend), Drs. P. van Oss-Bossagh (Pury), stagiares en afstudeers van de MMD groep wil ik graag danken voor hun gezellige collegiale sfeer. Verder dank ik onze technicus Fons voor dat ik gebruik mog hebben van de dialyse apparatuur.

Tenslotte aan Elif, Hasan Ali, Yasemin, Ilhan, Monique, Necati en aan mijn ouders Gülsenin en Hasan, die mij gestimuleerd hebben om te studeren en vooral voor hun geestelijke en materiele steun, wil ik dit proefschrift opdragen.

CURRICULUM VITAE

The author was born on the 12th of March 1959 in Burdur-Guney (Turkey). After his secondary education at Nazilli Lyceum, he completed his first university physics education in Ankara and in KFA-Jülich (Germany) in 1981. From 1982 to 1988, he followed Dutch, Applied Physics and Computer courses at the Delft University of Technology in Delft, The Netherlands. After having graduated on the 31st of May 1988, he started to work as a scientific researcher at the Medical Faculty of the Erasmus University in Rotterdam, where he participated medical, clinical, biomedical physics and engineering courses. From 1989 until 1993, he was supervised by Dr. W.A. van Duyl at the department of Biomedical Physics and Technology (head: Prof. Dr. Ir. C.J. Snijders) and by Dr. H.H. Vincent at the department of Internal Medicine I (head: Prof. Dr. M.A.D.H. Schalekamp). This thesis was prepared at both departments. In 1993-94, he followed a post-doc course of clinical physics at the Eindhoven University of Technology. He is still participating the biomedical research with the Micro Motion Detection group at the department of Obstetrics and Gynaecology of the Academic Hospital Rotterdam (Dijkzigt Ziekenhuis).